A STUDY OF THE FLOW PERFORMANCE OF A SODIUM SILICATE FURNACE

PETER KNOTT

Ph.D. 1986

SUMMARY

The flow characteristics of neutral sodium silicate glass in an open hearth regenerative furnace have been studied using a one tenth scale physical model. The constraints of similarity have been investigated and discussed, and the use of sodium silicate liquor as a cold modelling solution has been developed. Methylene Blue and Sulphacid Brill Pink were used as delineators, and a technique for analysing the concentration of each even in a mixture has been developed. The residence time distributions from the model have been simulated using a mixed model computer program which identifies the nature and size of the most significant flow streams within the furnace.

The results clearly show that the model gives a true representation of the furnace and illustrates a number of options for operating or design changes which will lead to improved production efficiency.

Key Words: Sodium Silicate
Physical Model
Residence Time
Furnace

ACKNOWLEDGEMENTS

I wish to express my sincere thanks and gratitude to Professor G V Jeffreys for his invaluable advice, unending patience and helpful encouragement.

In addition I wish to thank the technicians and staff of the Department of Chemical Engineering for their helpful support and fruitful discussion, and J. Crosfield and Sons for their financial and technical input. Mrs Wendy Overton is entirely responsible for the lack of spelling mistakes, and I am most grateful for her meticulous typing.

Finally I wish to thank my wife Paula without whom this thesis would not have been possible.

DEDICATION

This work is dedicated to the memory of my father. His hard work and unique ability will encourage his family and those who admired him for many years to come.

CONTENTS

LIST OF FIGURES

LIST OF TABLES

CHAPTER 1

BACKGROUND INFORMATION

1.1 INTRODUCTION

One of the most important phenomena of glass manufacture in continuous tank reactors is the flow pattern of the melting glass in the tank. The nature and use of flow patterns has been under almost continual scrutiny since Siemens first introduced continuous glass production in the middle of the last century. It is much discussed whether currents are advantageous from the operational point of view. Homogenization of the glass melt was previously considered as the primary reason for encouraging glass flow. However it now appears (24) that this sort of flow has little influence on homogenization. It's influence on the distribution of heat may be of more importance.

In any case the optimisation of furnace design can only be brought about by a complete and thorough understanding of the flow system.

1.2 SODIUM SILICATE GLASS

Sodium Silicate is one of the oldest heavy inorganic chemicals and was certainly known to the Phoenicians. Much of the present day technology owes its beginnings to Professor Johann Von Fuchs who, as Professor of Mineralogy in Munich in 1818, carried out detailed investigations into the preparation and properties of these materials. His work led to the development of methods of industrial production and many uses including adhesives, cements and fire proof paints.

Sodium Silicates are basically combinations of sodium oxide (Na_2O) and silica (SiO_2) usually with some water. They are usually defined in terms of the molar or weight ratio, and the properties of the silicate can be varied over a wide range by varying the proportions of the three constituents. The products include powdered and lump glass, aqueous solutions (liquors) covering a wide concentration range, and soluble powders which are made by part drying solutions

to 85% solids. The total world production capacity is well in excess of 3 million tonnes, but the relatively low value of the product prohibits export and means that it is vital that any raw materials are indigenous.

There are two commercially viable routes for sodium silicate production. The most common is the fusion process using sand and soda ash at temperatures approaching 1400^{o}C, in open hearth regenerative tank furnaces or rotary furnaces. Oil, gas, or electric arc heating may be employed. Sodium silicate glass of almost any ratio may be produced by this technique according to the equation:

$$Na_2CO_3 + SiO_2 \rightarrow Na_2O \times SiO_2 + CO_2 \uparrow$$

An alternative approach is to dissolve sand in concentrated caustic soda Liquor at elevated temperatures and pressure. This process is considerably more cost effective than the traditional furnace route but is limited to the production of alkaline glass.

1.3 FURNACE DESIGN AND OPERATION

Furnace design and operating technology is common to most manufactured bottle and container glass. Sodium silicate furnaces have always been designed on the same principles but tend to operate with the liquid surface totally covered with feed or batch. There is no evidence to suggest that this basic furnace design is the most suitable for sodium silicate manufacture, although it is based on sound and logical theories for other types of glass production. Figure 1.1 illustrates a typical gas cross-fired regenerative type furnace. For container glass production a mixture of pre-mixed batch and cullet is fed into the furnace. Ram chargers or screw feeders are normally employed. As the batch moves along the length of the furnace the batch proceeds to melt and react, and this process is normally seen to be complete in less than half of the furnace length. The remaining furnace volume completes the process of sand dissolution and gas removal. Some furnaces have a

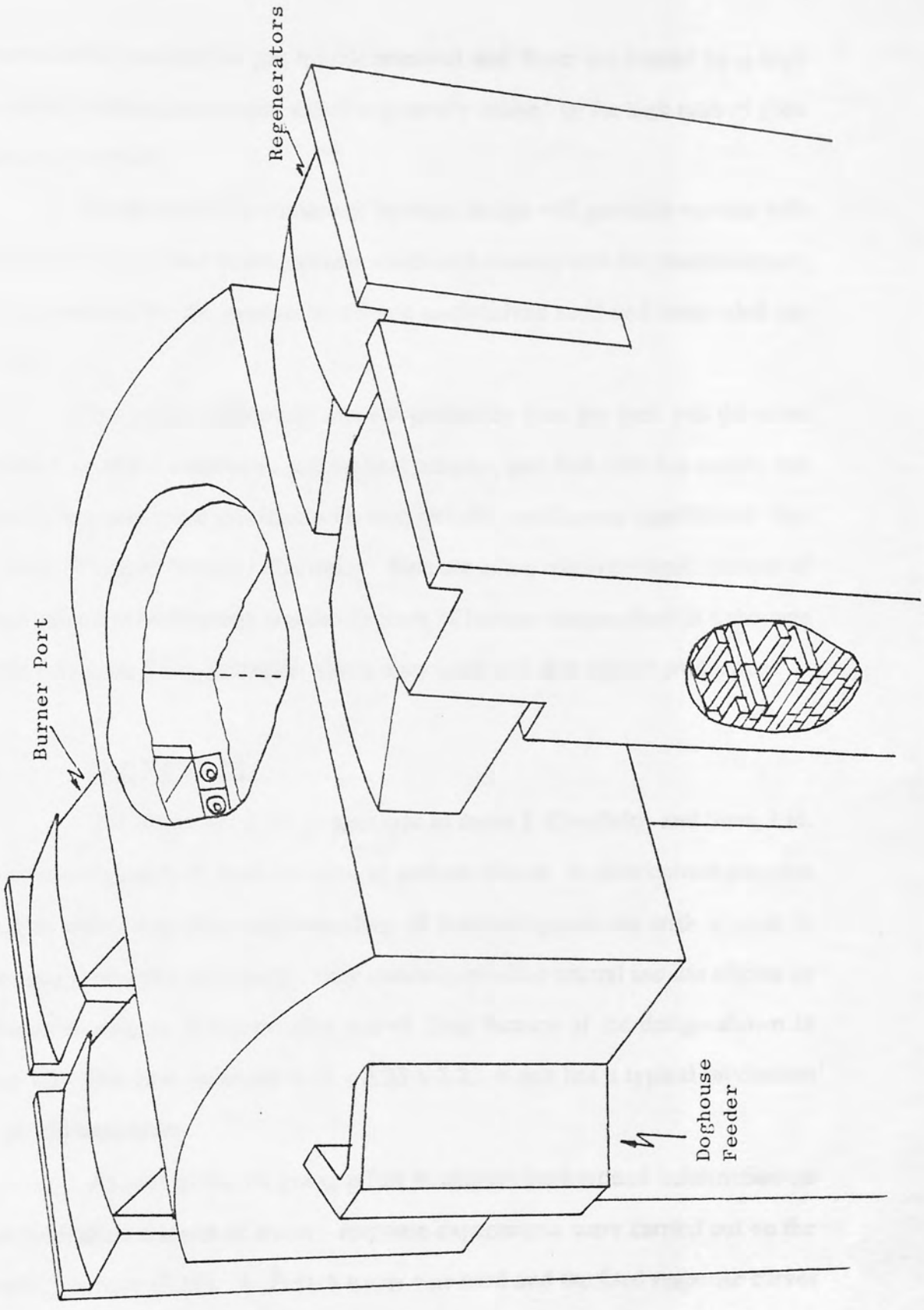

Figure 1.1: Typical gas cross fired glass furnace

further refining section for gas bubble removal and these are heated by a high temperature surface glass stream which is generally created by the high rates of glass withdrawal or 'pull'.

A sodium silicate furnace of identical design will generally operate with total batch cover. A weir block prevents solid batch leaving with the product stream, but it is common for the product to contain undissolved sand and suspended gas bubbles.

The batch surface has a lower emissivity than the melt and therefore provides a greater resistance to radiant heat transfer, and Jack (25) has shown that the batch is a very good insulator with heat transfer coefficients significantly less than those of typical furnace refractories. Because of the relatively small number of sodium silicate manufacturers and the diversity of furnace designs there is a shortage of information on the operating problems associated with this type of production.

1.4 THE PROJECT

The objective of the project was to assist J. Crosfields and Sons, Ltd, who are the biggest U.K. manufacturers of sodium silicate, in their current program aimed at increasing their understanding of furnace operations with a view to improving production efficiency. They currently produce neutral sodium silicate by the furnace route in a regenerative gas/oil fired furnace of the design shown in figure 1.2. The tank measures 9.45 x 5.33 x 2.22 m and has a typical production rate of 190 tonnes/day.

As part of the on going effort to acquire background information on glass production a series of tracer - response experiments were carried out on the operating furnace (9,26). A Potash tracer was used and the feed response curves were analysed using a mathematical model. A 'closest-fit' simulation curve was then obtained using a computer model and this gave an indication of the range of flow patterns within the furance melt. The simulation showed that the residence time

has little effect on glass composition, and that a significant improvement in throughput may be possible.

This project is designed to explore the nature of flow patterns and to identify changes which will lead to improved production efficiency.

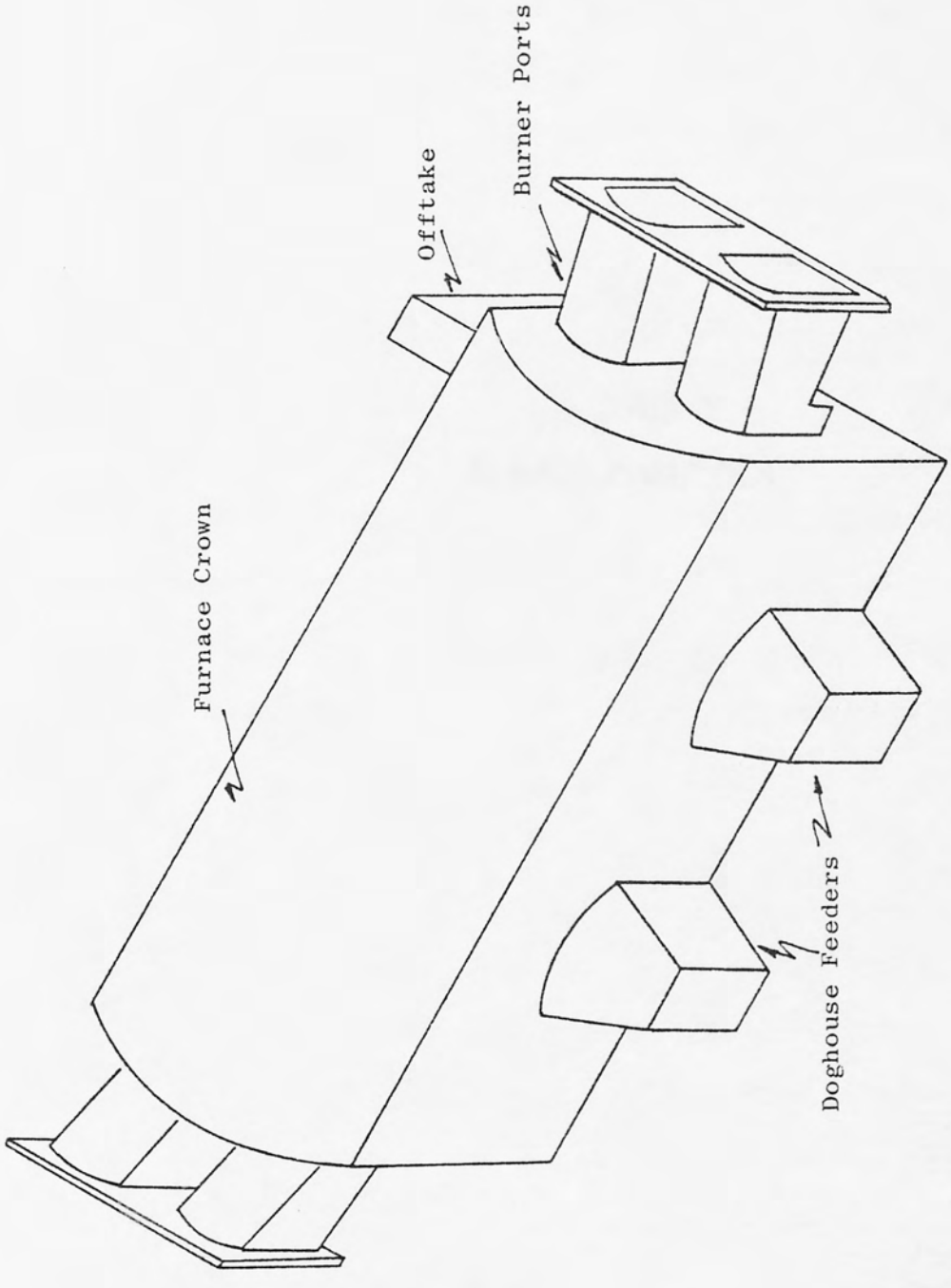

Figure 1.2: Crosfields Number 2 glass making furance

CHAPTER 2

FURNACE MODELS

2.1 INTRODUCTION

It has been frequently re-iterated by many authors that physical models have a limited use for evaluating flow patterns. The operating limits of a practical model mean that it cannot represent satisfactorily either the 'pull' factor, or the heat flow through the furnace walls. In addition most work has ignored the influence of batch cover and has utilised liquid feed only. However in stating the disadvantages it can also be noted that a considerable quantity of literature revolving around the use of models is still produced and the conclusions drawn from this work are frequently supported by direct observations of the operating furnace.

It is particularly difficult in the case of the Crosfield furnace to make direct observations because normal operation uses total batch cover, which therefore limits the work to the use of tracers such as Potash or Radioactive Isotopes. Because of this severe limitation it was decided that a physical model could play a vital role in obtaining information on flow patterns. The similarity analysis shown later will indicate the limitations of the model and how these can be taken into account.

2.2 PHYSICAL MODELS

A selective survey of model work up to 1956 was given by Michaels (12), where he outlines the criteria for similarity and pointed out the problems of physical models. Shortly after this two papers appeared in which detailed consideration is given to the validity of similarity conditions in model studies. That of Leger (13) gives an outline of dimensional analysis based on the ideas of Buckingham (14), and goes on to discuss the application of dimensional analysis to model studies of convection currents. Leger's equations are used by Duperroy (15) in the development of his model. According to Duperroy, the kinematic viscosity of the modelling liquid should be 90 times lower than that of glass, while the absolute viscosity should be 225 times lower. These values are obtained in the range

20-100°C by some slightly polymerised polyisobutylenes. Dupperroys tanks were made of glass and use methylene blue as a delineator.

Kruszewski (16) describes a study with perspex 1 : 20 scale models, heated by resistance elements (placed in the same way as ports) and with a liquid phenolic polymer to simulate glass. He acknowledges the limitations of the work, one of the most serious of which in his view was the absence of batch cover.

Hamilton, Rough and Silverman (17) presented an improved technique for model operation in which a plastic material is fed as solid and is melted, by the use of infra-red lamps, to represent the melting batch. They claim a significant improvement in the reliability of the results, but have not presented any data.

This technique together with the adoption of a rigerous similarity analysis seems to permit the greatest reliability and possible use of furnace models.

2.3 OTHER TECHNIQUES

2.3.1 Floater Experiments

It is common practice, when investigating furnaces with a refining or batch free section to utilise high temperature floaters. These devices are constructed with a stock or pole of pre-determined length such that they follow the flow of glass at a certain depth below the melt surface. A directional flag may also be included for ease of visability. Although the results cannot be regarded as completely reliable they can trace surface flow reasonably well and were used by Konig (18) and Jebsen (19) upto 60 years ago to illustrate surface flow away from the furnace 'hot-spot' at velocities of up to 12 m/h.

Unfortunately floaters cannot operate with the presence of any batch and are therefore of very limited use in this study.

2.3.2 Test Material Experiments

In order to identify glass movement in an operational tank a portion of batch can be replaced by a tracer material, the path of which may be more readily definable. This may be done by identifying the presence and movement of the tracer within the furnace itself or by analysing the product for the tracer and constructing a residence time distribution. It is vital in either case that the tracer should behave in exactly the same way as the glass batch and melt. Examples of test material are barium, cerium, phosphorous, strontium or scandium either as elements or as an oxide or as a radio-active substance. In the case of the Crosfield's furnace a tracer of potassium carbonate may also be used.

Some workers have suggested the use of dyes to introduce a colour change to the batch. However this technique must be utilised with care since any change in colour will bring about a change in the conditions controlling heat transfer and may therefore not represent normal operation.

These techniques are widely used and have allowed a considerable quantity of work to be carried out on operational furnaces, and consequently a complete picture of flow patterns within the more conventional furnace designs exists. Despite this the disruption of production schedules and the fact that new operating conditions and furnace designs cannot be easily investigated limit the application and exploitation of this technique.

2.3.3 Temperature Measurements

If the flow patterns within a furnace can be attributed to convection then the flow may be predicted by measuring the melt temperatures at a series of points within the furnace. This technique has been used by a number of workers but can be very expensive to introduce and the installation of temperature probes in the tank bottom may lead to errosion and eventual tank failure.

The other significant disadvantage is that the flow patterns predicted by this technique ignore the effects of feed impulse and product 'pull' which are undoubtedly significant in modern glass furnace operation.

2.3.4. Erosion Lines on Tank Blocks

In extinguished tanks it is often possible to see lines of erosion on the surface of the tank blocks. These lines are caused by the rapid flow of glass in this region. In some circumstances these lines can be analysed to predict glass flow within the furnace. However it is very difficult to identify the type of flow at the heart of the tank from what is observed at the walls, and in addition the continual improvement in block quality reduces erosion and therefore the available information.

2.3.5 Mathematical Methods

The significant technical problems associated with measuring glass currents suggest that a purely theoretical solution may be advantageous. The extremely complex processes occurring within the furnace require the solution of a number of interdependant mathematical expressions for a realistic model. Until fairly recently the computer capacity for this sort of situation was not readily available and oversimplifications and unreasonable assumptions were needed in order to solve the problem. More recently a number of workers in the field have had access to suitable computers and a number of realistic models have been developed. Moult (20) outlines a model using the finite difference method to analyse the flow in a three dimensional glass furnace. The convergence of the method and its applicability to non rectangular enclosures are examined. An improved model is presented by Mase (21) who uses a similar technique when examining the glass melt but also takes into account furnace heating and its influence of batch melting.

This technique presents the most versatile of all modelling methods and shows the most promise for the future.

2.4 SIMILARITY

If a model is to represent the furnace correctly, there must be dynamic similarity betwen them; that is to say, the model and the tank must be governed by the same physical laws acting in the same manner in both. Buckingham (22) published a definitive and detailed discussion of the conditions necessary for a model to be constructed so as to be dynamically similar to a tank furnace, and claimed to show that, even when reasonable simplifying assumptions were made, the necessary conditions were too stringent to be satisfied in practice. This conclusion seems inescapable on the data he assumed, but it will be shown that a satisfactory theory may be developed if two restrictions are accepted. They are:

i) The model does not represent the heat flow through the tank walls.

ii) Fluid impulse and pull are not totally similar.

Buckingham used a formal dimensional analysis to show that there are ten quantities which play a part in determining glass motion. These include, inter alia, the thermal conductivity of the tank walls, the difference between the mean temperature of the tank and its surroundings, and the rate of withdrawal of the glass. Subject to certain simplifying assumptions, these can be expressed in terms of six dimensions, hence no more than four independant dimensionless products may be formed from the variables, and, by ensuring that any set of four such independant products have identical values in the tank and in the model, dynamic similarity can be assured. The ten variables employed are given below:

Symbol	Significance	Dimensions
L	Linear dimension of tank	L

Symbol	Significance	Dimensions
Δ	Mean excess of surface temperature over outside air	ϑ
M	Time rate of withdrawal of mass	MT^{-1}
g	Gravitational constant	FM^{-1}
λ_T	Thermal conductivity of tank walls	$HL^{-1}T^{-1}\vartheta^{-1}$
ρ	Density of liquid	ML^{-3}
μ	Viscosity of liquid	$FL^{-2}T$
C	Specific heat of liquid	$HM^{-1}\vartheta^{-1}$
λ	Thermal conductivity of liquid	$HL^{-1}T^{-1}\vartheta^{-1}$
β	Coefficient of expansion of liquid	ϑ^{-1}

One significant problem which exists when modelling high temperature processes is that the flow of heat within the furnace is largely effected by radiation, while heat transfer in any model operating near to room temperature will be almost entirely by conduction and convection. To some extent it is possible to overcome this difficulty, by representing the temperature distribution over the glass-refractory boundary. This eliminates λ_T, reducing the number of independant variables to nine. Furthermore, Δ, is no longer relevant, and instead it is necessary to consider δT, any typical difference in temperature between two specified points in the liquid.

A model is used to supply information about the tank to be described and if it is to serve this purpose, the equations which govern the motion of fluid and the distribution of temperature in both tank and model must be identical. Flow in a viscous liquid conforms to the Navier-Stokes equation. For an incompressible liquid of constant viscosity this can be written in the form:

$$\rho \frac{\delta \vec{V}}{\delta t} + r(\vec{V}\,\text{grad})\vec{V} = \mu\,(\text{divgrad})\vec{V} + \vec{F} - \text{gradP} \qquad (2.1)$$

in which $\vec{V}$ represents the velocity of the liquid considered as a vector, F is the external force acting on unit volume of liquid, and P is the pressure. The boundary conditions are:

i) The components of $\vec{V}$ normal to the surface of the tank blocks is zero at that surface, and

ii) The pressure is equal to atmospheric pressure over the free surface of the liquid.

The fact that this equation can only be applied to a constant viscosity material is an over-simplification which is unacceptable and a refinement to allow for the variation of viscosity with temperature will be introduced later.

Consider the individual terms of equation (2.1) one at a time. The first term will vanish in the steady state. The second term represents inertial force per unit volume. The first term on the right-hand side represents the forces of viscosity per unit volume. The final two terms represent respectively the external forces acting on unit volume of liquid and the hydrostatic pressure. If the tank were at a uniform temperature, then:

$\vec{F}$ = rg and is a vector directed downwards

p = rg x depth below surface

$\therefore$ $\vec{F}$ - grad p = O;

all the other terms of the equation also vanish, $\vec{V}$ being everywhere zero. On the other hand, if any part of the liquid differs from the rest in temperature, and therefore, also in density, these two terms will no longer cancel, and there will be a net buoyancy force g.dr acting on unit volume. Then

$$\vec{F} - \text{gradp} = g.\delta\rho = g.\rho.B.\delta.T$$

The conditions which have been specified for the model and the requirement of similarity may be regarded as defining a set of scale factors S_L, S_μ etc by the equation:

$$L_i = S_L.L_o$$

$$\mu_i = S\mu.\mu_o \qquad (2.2)$$

$$V_i = S_V.V_o$$

etc., where the suffix 'o' refers to the tank and 'i' to the model. The term $\rho(\bar{V}\ \text{grad})\bar{V}$ when fully written out is:

$$\rho Vx\frac{\delta Vx}{\delta x} + \rho Vy\frac{\delta Vx}{\delta y} + \rho Vz\frac{\delta Vx}{\delta z}$$

$$+\ \rho Vx\frac{\delta Vy}{\delta x} + \rho Vy\frac{\delta Vy}{\delta y} + \rho Vz\frac{\delta Vy}{\delta z}$$

$$+\ \rho Vx\frac{\delta Vz}{\delta x} + \rho Vy\frac{\delta Vz}{\delta y} + \rho Vz\frac{\delta Vz}{\delta z}$$

and by applying equation (2.2), it can be seen that these quantities are all changed in the ratio:

$$\frac{S\rho.\ Sv^2}{S_L}$$

In other words, this term changes in passing from the tank to the model, in the same

ratio as ($\rho V^2/L$) and the two may be said to be dimensionally equivalent. Similarly, the viscous term is dimensionally equivalent to ($\mu V/L^2$). The buoyancy term remains as g.($\rho.\beta.\delta.T$). If the same equation is to govern both cases, the ratios of these quantities must remain unchanged.

The ratios derived from the inertial and viscous terms is:

$$\frac{\frac{\rho V^2}{L}}{\frac{\mu V}{L^2}} = \frac{\rho VL}{\mu}$$

and this is well known as the Reynolds number. The condition

$$\frac{\rho VL}{\mu} = \text{constant} \qquad (2.3)$$

must be satisfied if the relative magnitudes of inertial and viscous forces are to be preserved in passing from the original system to the model. Similarly, if the relative magnetudes of the viscous and buoyancy forces are to be preserved:

$$\frac{L.^2 g.\rho.\beta.\delta T}{V\mu} = \text{constant} \qquad (2.4)$$

In order to ensure full dynamic similarity between the tank and the model it is necessary to consider not only the flow of liquid, but also the transport of heat. The heat equation for a fluid in which flow is taking place is discussed by Klinkenberg and Mooy (23). If the fluid is incompressible and no heat is generated by chemical reaction or mixing, the equation takes the form:

$$\rho C \frac{\delta T}{\delta t} + \rho C V \text{ grad } T = \lambda \text{ divgrad } T \qquad (2.5)$$

dT/dt vanishes when steady state exists and ($\rho C\overline{V}$ grad T) represents the heat

transferred by convection and is dimensionally equivalent to ($\rho CVT/L$). The term (λdivgrad) T represents the heat flow into each unit by conduction and is dimensionally equivalent to ($\lambda T/L^2$). If the two systems are to be both dynamically and thermally similar, then the ratio of these two quantities must be preserved, so that:

$$\frac{\rho CVL}{\lambda} = \text{constant} \qquad (2.6)$$

writing K for ($\lambda/\rho c$), v for (μ/ρ) and inserting the value for V determined by equation (2.4) gives:

$$\frac{L^3 g}{Kv}\,\beta\delta T = \text{constant} \qquad (2.7)$$

for all systems in which dynamic and thermal similarity are preserved. This quantity is the product of the Prandtl and Grashof constants.

So far it has been assumed that inertial forces can be ignored. This may not be the case, but by ensuring that the same value of Reynolds number applies to the model and tank the relative magnitudes of viscous and inertial forces may be preserved. By substituting into the expression given for the Reynolds number (2.3) the appropriate expressions for the velocity derived from (2.4) and (2.6), there result the two conditions:

$$\frac{L^3.g.\rho^2.\beta\,\delta T}{\mu^2} = \text{constant} \qquad (2.8)$$

and

$$\frac{C\mu}{\lambda} = \text{constant} \qquad (2.9)$$

Thus where inertia cannot be ignored it is necessary that the Grashof and Prandtl numbers have the same value in the tank and the model, instead of this being necessary only for their product.

The analysis so far, based on equation (2.1), assumed that the viscosity of the liquid is a constant. This is not the case in a glass tank where the glass viscosity varies exponentially with temperature. Therefore it is not possible to apply equation (2.1) to the tank as a whole, but it could be applied to a region small enough to be able to consider the viscosity to be a constant. Therefore it is a requirement of similarity that the viscosity has the same scaled value in the glass tank and model at all corresponding points within the two systems.

It is also important to consider the variation of thermal diffusivity with temperature, as this quantity was also implicitly assumed to be a constant in writing (2.5). Where radiation plays an important role, the heat transfer is strongly temperature dependent, being governed by Stefan's Law. The thermal diffusivity of two clear glasses at high temperatures was measured by van Zee and Babcock (8), who found that it depended exponentially on temperature. Since the thermal diffusivity of all ordinary liquids near room temperature is practically independent of temperature it is impossible to attain full similarity between the tank and model in this respect.

The analysis so far has ignored the effect of 'pull' on similarity. If M is the time rate of withdrawal of mass, then mean velocity of flow due to pull alone will be dimensionally equivalent to $(M/\rho L^2)$. To preserve equivalence between the tank and the model, the ratio of this quantity to the glass velocity V at any point must be preserved ie:

$$\frac{M}{\rho V L^2} = \text{constant}$$

Combining this with equation (2.4) gives:

$$\frac{M\mu}{\rho^2.g.\beta\delta T.L^4} = \text{constant} \qquad (2.10)$$

which is the necessary condition.

In summary it is impossible to satisfy all the requirements of similarity, but it has been shown that a reasonable representation of flow due to convection and pull can be made, even though the transfer of heat cannot be represented at low temperatures.

The four dimensionless groups are:

Reynolds: $\frac{\rho VL}{\mu} = \text{constant}$

Grashof: $\frac{L^3.g.\rho^2.\beta.\delta T}{\mu^2} = \text{constant}$

Prandtl: $\frac{C\mu}{\lambda} = \text{constant}$

Pull: $\frac{M\mu}{\rho^2.g.\beta.\delta T\ L^4} = \text{constant}$

CHAPTER 3

MODEL DESIGN AND CONSTRUCTION

3.1 INTRODUCTION

The design and construction of physical models is generally limited by the practicalities of operation such as the materials of construction, space and services available. The analysis carried out in the previous chapter was based on two design principles (23):

i) For every point in one body there exists a corresponding point in the other - Geometric Similarity.

ii) Corresponding temperature differences bear a constant ratio to one another when the systems are kinematically similar - Thermal Similarity.

The first principle can be defined by the expression:

$$\frac{L_1}{L_o} = \text{constant}$$

and the second by:

$$\frac{(\delta T)_1}{(\delta T)_o} = \text{constant}$$

These two expressions together with the four dimensionless groups defined previously form the basis for both the design and operation of the model. In this instance it was decided that a model of one tenth linear dimensions would be constructed, and that, as far as possible, the model liquid and other variables would be changed in order to match the requirements of similarity.

3.2 TANK CONSTRUCTION

The model tank must be transparent, chemically resistant, shatter proof and durable. Glass was considered but was thought to be to difficult to work with and prone to damage. Acrylic, P.V.C., Polypropylene and Cellulose Acetate all have some good properties but some disadvantages. Polycarbonate was eventually

selected because of it s extraordinary strength and durability. It can also be heat welded and cemented and can withstand temperatures of up to 135°C. The model was designed to be geometrically similar to the real furnace in all respects and is shown in Figure 3.1. It measures 0.945 x 0.533 x 0.222 m and is constructed to one tenth scale. The walls are of 10 mm sheet which has sufficient strength to allow a direct view through the tank bottom. Combustion ports were included for the investigation of gas mixing and the effect of flame inpingement on glass batch. The depth of the skimmer block can be varied. In addition the lip height, and therefore the melt depth, can also be changed.

The real furnace generally operates with only one offtake, but a second offtake was added to the model to illustrate the effects this would have on the flow of glass melt.

3.3 HEATING SYSTEM

Heat supplied by lamps or by heating elements running at a high temperature will reach the liquid surface mainly in the form of infra-red radiation. Glass and glassbatch are opaque to the greater part of thermal radiation from the furnace crown, and it is desirable that the model liquid should be similarly opaque to the greater part of the radiation from the heating elements, which will be more easily achieved the lower the temperature of these elements. With this in mind four variable power 1 kw infra-red heaters were fitted above a mild steel plate bent to the same curvature as the furnace crown. The heat from the elements is absorbed by the steel plate and re-emitted with a different wave spectrum which will be more easily absorbed by the modelling solution.

The power for the elements is controlled by four variacs which enable temperature variations around the crown of the furnace to be taken into account.

FIGURE 3.1 Model Furnace

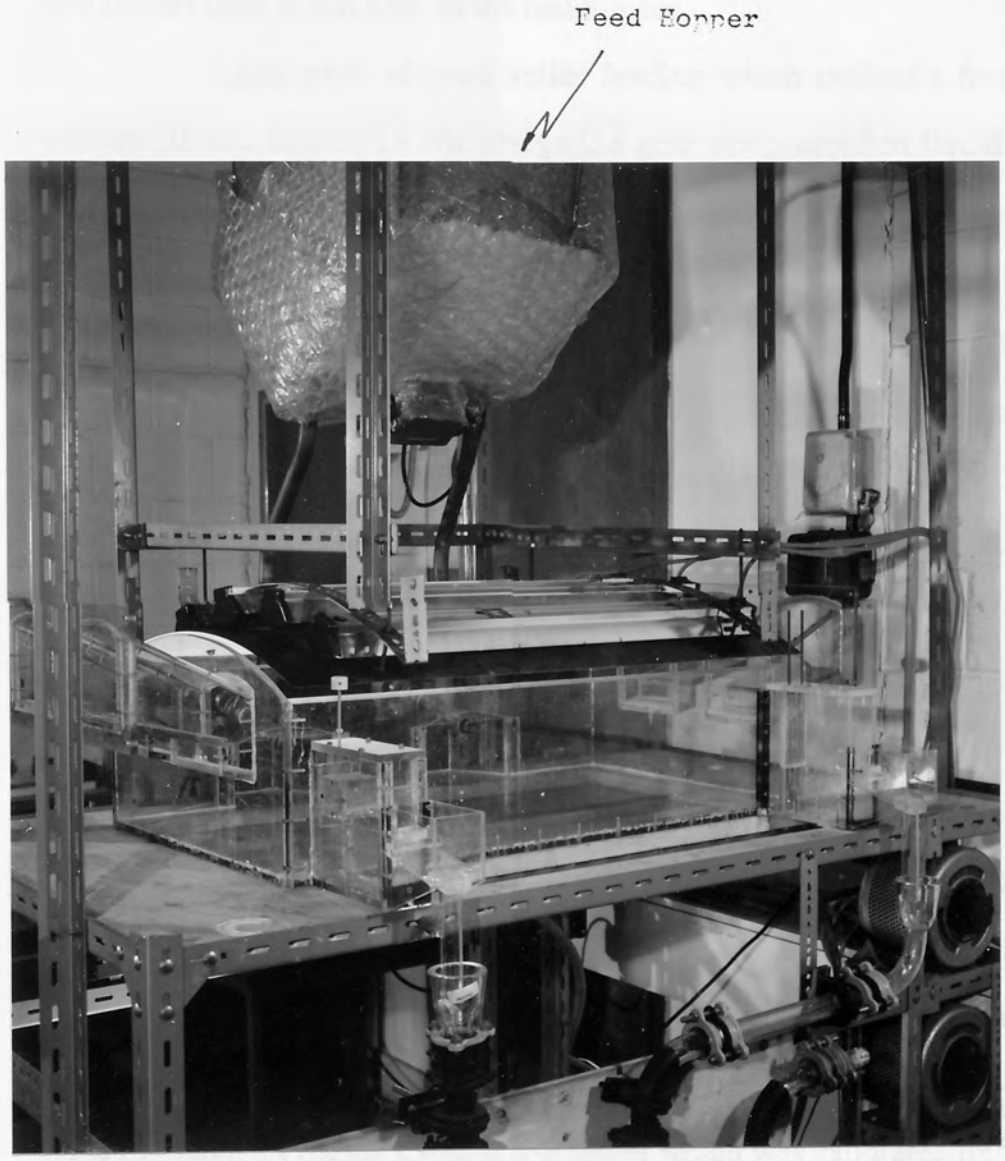

3.4 FEED SYSTEM

For commissioning of the rig a liquid modelling solution was fed to the model. A gear pump transferred the viscous liquid from a storage drum through calibrated rotameters and a temperature controller to one of two feed points. These feeders consisted of a rectangular channel of similar proportions to the face of the ram feeders used at that time on the real furnace.

Later work adopted solids feeding which utilised a frozen granular sodium silicate liquor. In this design the gear pump supplied liquid to a freezer assembly located above the model. Flow was calibrated by a direct pressure reading of the supply to the freezer. The freezer is shown in figure 3.2. This device operates using a chilled turntable assembly. A machined copper plate of 30 cm diameter is cooled to approximately - 35^{o}C using a secondary refrigerant. A scraper bar and liquid distributor rotate around this plate at approximately 1 R.P.M. The liquid distributor spreads drops of liquid sodium silicate evenly on the surface of the plate. During the time for one revolution these are frozen, and then pushed off the freezer plate by the scraper bar. They are collected in a cooled and insulated hopper.

The frozen liquor is fed from this hopper to the feed points through one of two 28 mm copper tubes. Blockages can occur but direct injection of a small quantity of liquid Nitrogen into the feed pipe was found to eleviate this problem. The tracer dye solutions were fed into this frozen liquor by means of a needle and syringe pump. Liquid Nitrogen could again be injected at this point to assist particle break-up and for final temperature control. The frozen grains were fed into the model through a variable speed screw feeder which was calibrated for flow against rotational speed. The essential features of the feeders are shown in figure 3.3.

3.5 DYE ANALYSIS AND DATA LOGGING

The solution which leaves the model passes through a dye concentration metering system shown in figure 3.4.

FIGURE 3.2 Freezer Assembly

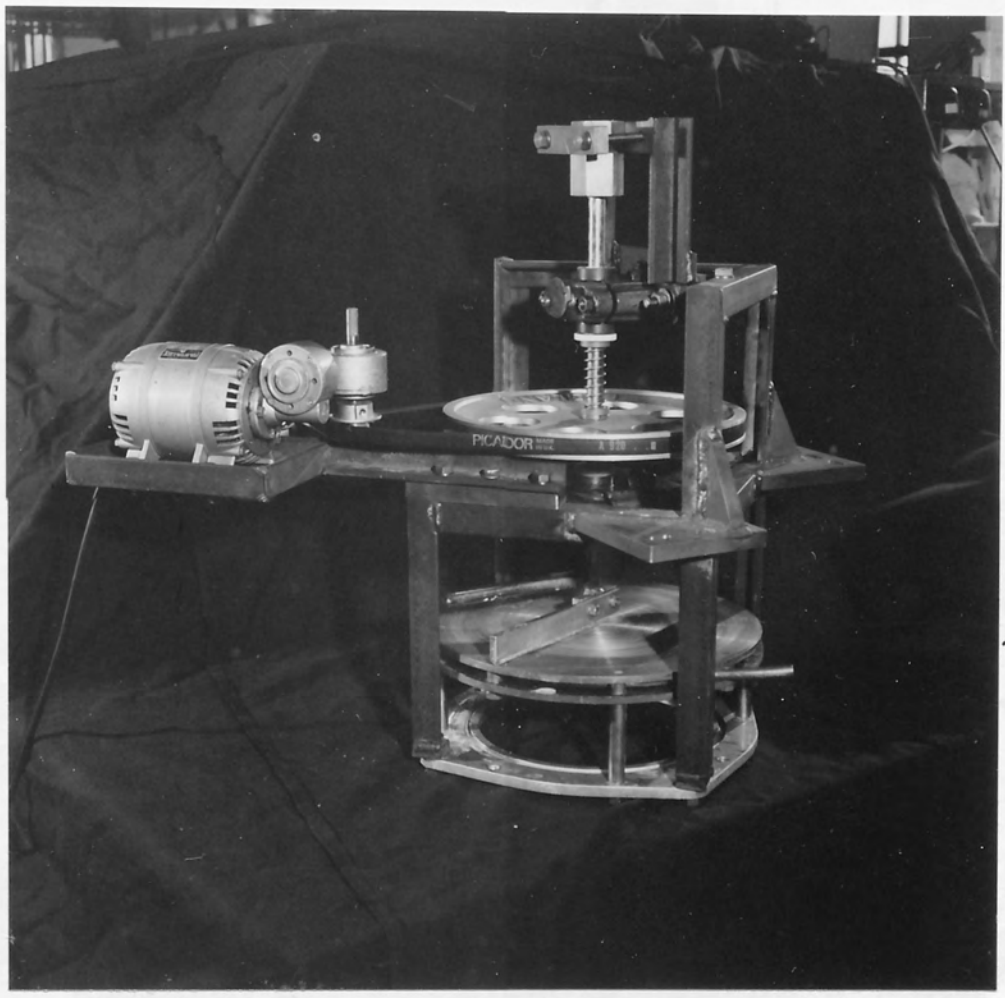

FIGURE 3.3 Screw Feeders

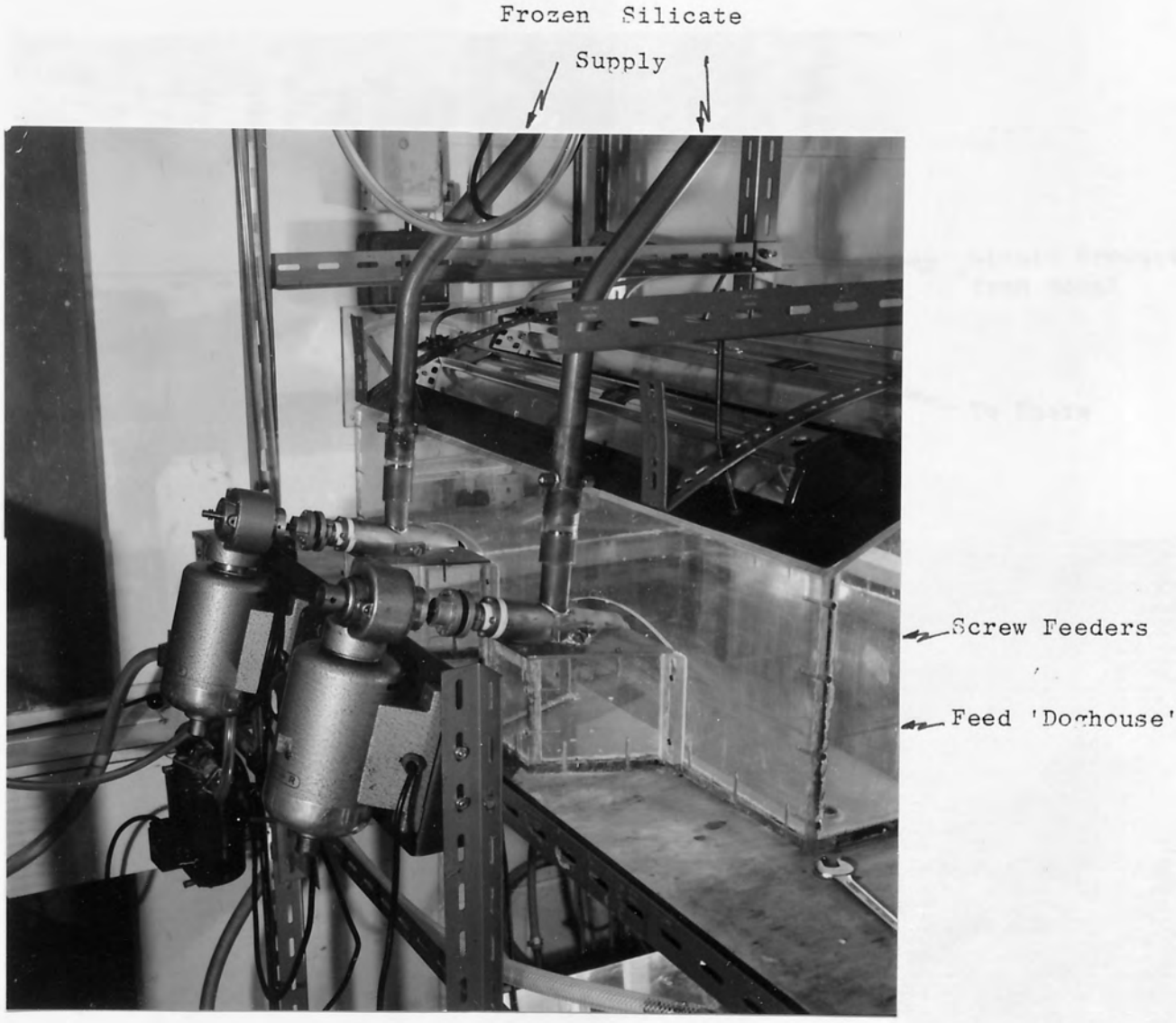

FIGURE 3.4 Dye Concentration Metering System

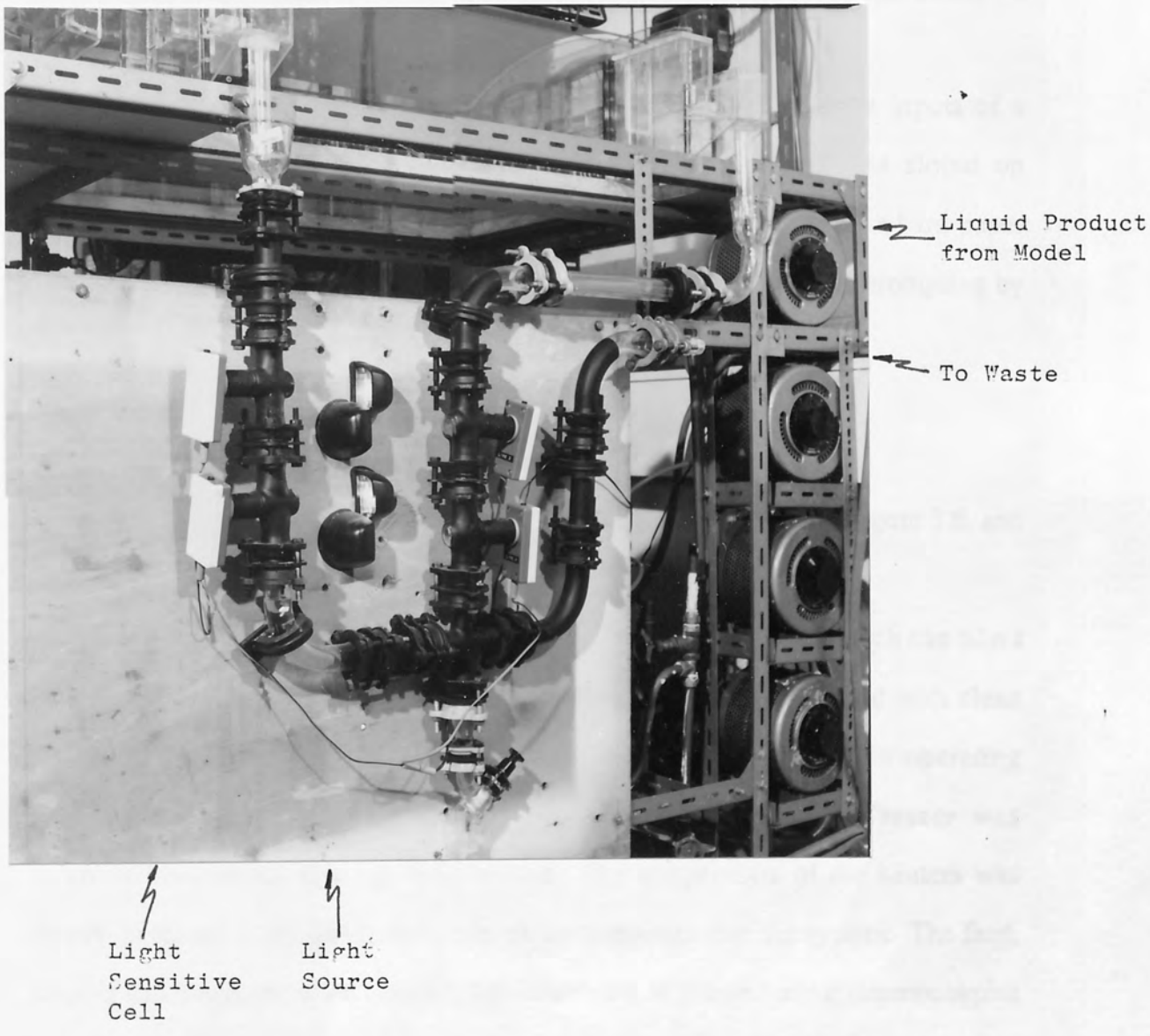

A light source emits light over all of the visible spectrum. This white light is filtered by a dye solution to give light of a particular waveform. This light then passes through the model solution and is partially absorbed. The concentration of light leaving the metering cell is measured using a light dependent resistor built into an electronic circuit, which gives a linear output in the range 0 to 1.8 volts depending on the incident light. In this way the dye concentration and hence its residence time distribution may be determined directly.

The 0 to 1.8 volt signal is fed to one of four analogue inputs of a B.B.C. micro-computer shown in figure 3.5. This signal may be stored on computer disc, plotted onto the screen for visual display or output as a hard paper copy. This system is fully automated and once initiated requires no prompting by the operator.

3.6 MODEL OPERATION AND CONTROL

A schematic flow diagram of the total system is given in figure 3.6, and figure 3.7 illustrates the experimental rig.

A run must be carried out under steady state conditions which can take a considerable time to be established. At start-up, the model was filled with clean silicate. The freezer was brought into operation, and cooled to its operating temperature before the introduction of any liquor. Once the freezer was commissioned solids feeding commenced. The temperature of the heaters was slowly increased as the solids feed reduces the temperature of the system. The feed, product and a number of boundary temperatures are monitored using thermocouples and a multipoint temperature readout. The heat input was carefully tuned to maintain the correct operating temperatures which can usually be obtained in approximately 2.5 x the average residence time. However the slow response of the system make it almost impossible to obtain a perfect steady state and continual monitoring of the system temperatures is essential.

Once a steady state has been achieved the dye metering system and computer data logger are introduced and the tracer is injected. Normally steady operating conditions are maintained for approximately 2 x the mean residence time, but this may vary according to the flow characteristics.

Once a run is complete the whole system is drained and cleaned thoroughly using warm water.

FIGURE 3.5 B.B.C. Micro-Computer and Ancilliary Equipment

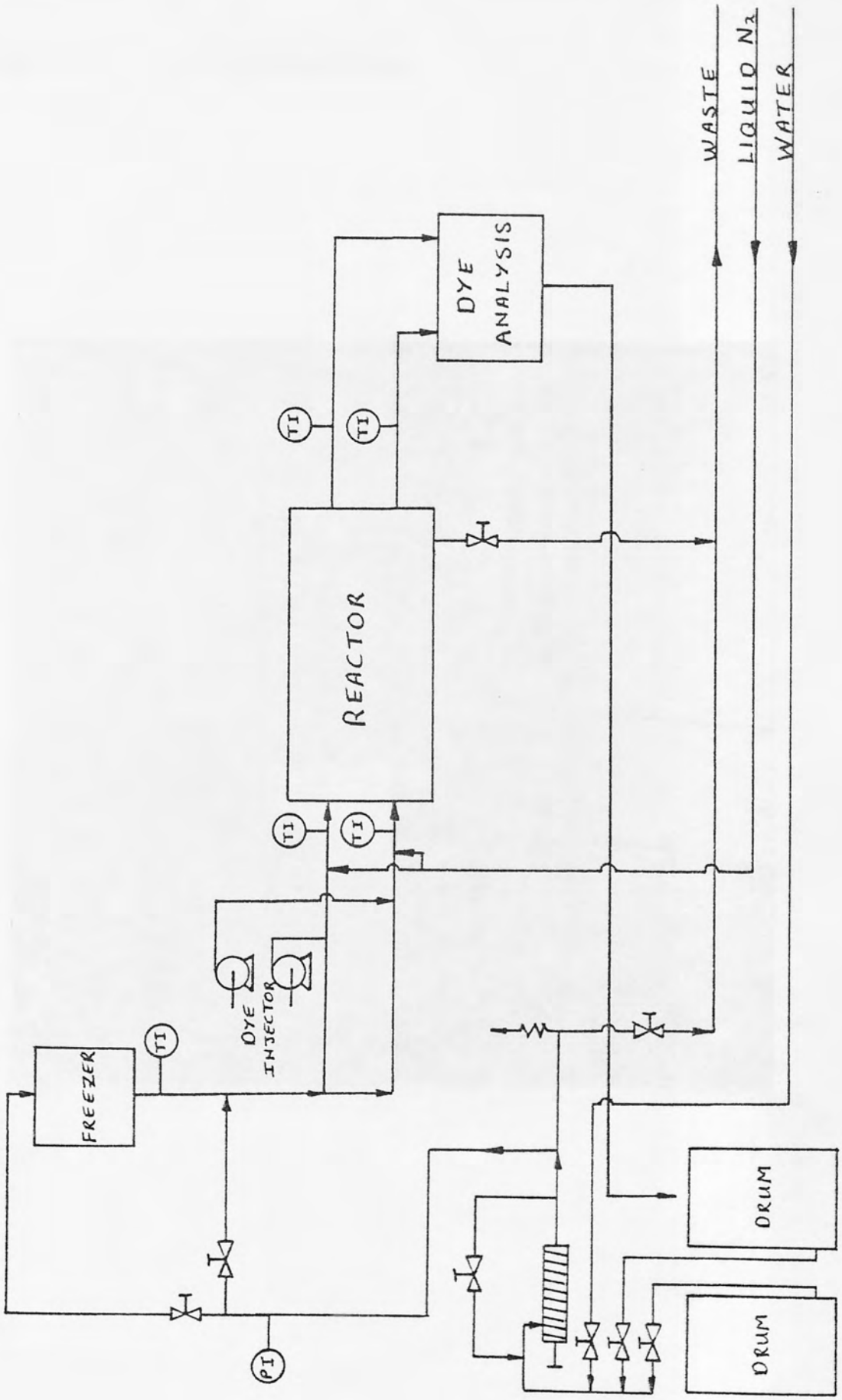

Figure 3.6: Schematic flow
Diagram of Experimental Model

FIGURE 3.7 The Experimental Rig

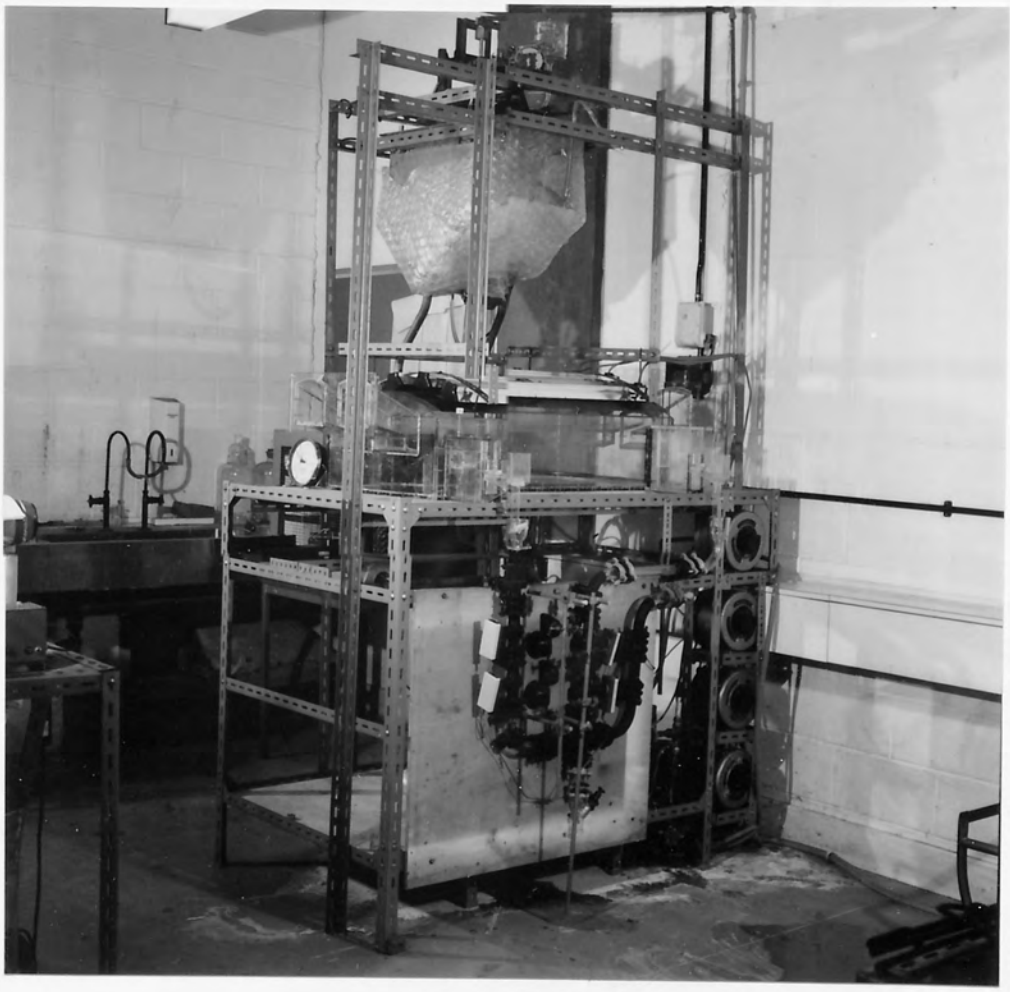

CHAPTER 4

PHYSICAL PROPERTIES

4.1 INTRODUCTION

The design and operation of physical models which operate within the constraints of dynamic similarity requires detail of physical properties of both the glass melt and modelling solution. The variety of glass melt compositions is almost infinite and although Sodium Silicate is one of the most commonly used glasses, data on physical properties is often sparce and inconsistent. In addition most workers measuring physical properties use samples of glass which are refined - that is to say all suspended solids and gases are removed. In a Sodium Silicate furnace refining is never carried to completion since it is thought that suspended gas bubbles assist in the breakup and dissolution of the solid glass.

The laws of similarity predict which physical properties are desirable for the modelling solution but it must have certain other qualities. For example it must be non-toxic, cheap, clear and be compatible with the tracer and the tank materials of construction. Glycerine is commonly used (1,23), but liquid phenolic polymers, chloride salts and slightly polymerised polyisobutylenes are said to possess superior qualities (4). The initial investigation examined the more common model liquids and solutions of Sodium Silicate (Water Glass). It was found that the Water Glass was superior to the others as a modelling liquid. The following sections detail the physical property data which was found in the literature, and how this was supplemented, were necessary, with measured data.

4.2 SODIUM SILICATE GLASS PHYSICAL PROPERTIES

The variation with temperature of density, viscosity, specific heat, thermal conductivity and coefficient of expansion are required. In the future the furnace route is likely to be used for the production of neutral glass only and therefore only Sodium Silicate with a silica to sodium oxide ratio of 3.36 : 1.0 will be considered here.

4.2.1 Viscosity

The variation of viscosity with temperature is the single most important factor when considering glass flow. The viscosity of glass melts is extremely high and falls by approximately two orders of magnitude on increasing the temperature from 800 to 1400°C. The methods of viscosity measurement applicable to glass are limited by the experimental difficulties resulting from the high temperature and the corrosive character of the glass, and so great is the range of viscosities that different methods must be used in the various portions of the viscosity - temperature curve. The literature search revealed two sources of data due to HEIDTKAMP and ENDELL (5), and ENGLISH (6). ENGLISH used a stormer type viscometer at high temperatures, and at low temperatures measured the rate of elongation of glass rods. HEIDTKAMP and ENDELL on the other hand, measured the time required for a constant force to pull a platinum ball 1cm through the liquid, at viscosities greater than 6 poises, and lower viscosities were measured by an apparatus depending on the damping of the oscillations of a suspended platinum ball. Both methods required calibration, for which purpose castor oil was used. However, there appears to be considerable disagreement between these various reports. In order to establish some confidence in any one set of data, it was decided to measure the glass viscosity directly.

An experimental rig of the stormer type viscometer was constructed and used to analyse the viscosity of glass samples taken directly from the Crosfield furnace. The main features of the rig are shown in Figure 4.1.

The following analysis provides some of the theoretical background for this technique. In vertical cylindrical co-ordinates a modified Navier-Stokes equation, which can be applied to Newtonian liquids, may be written as:-

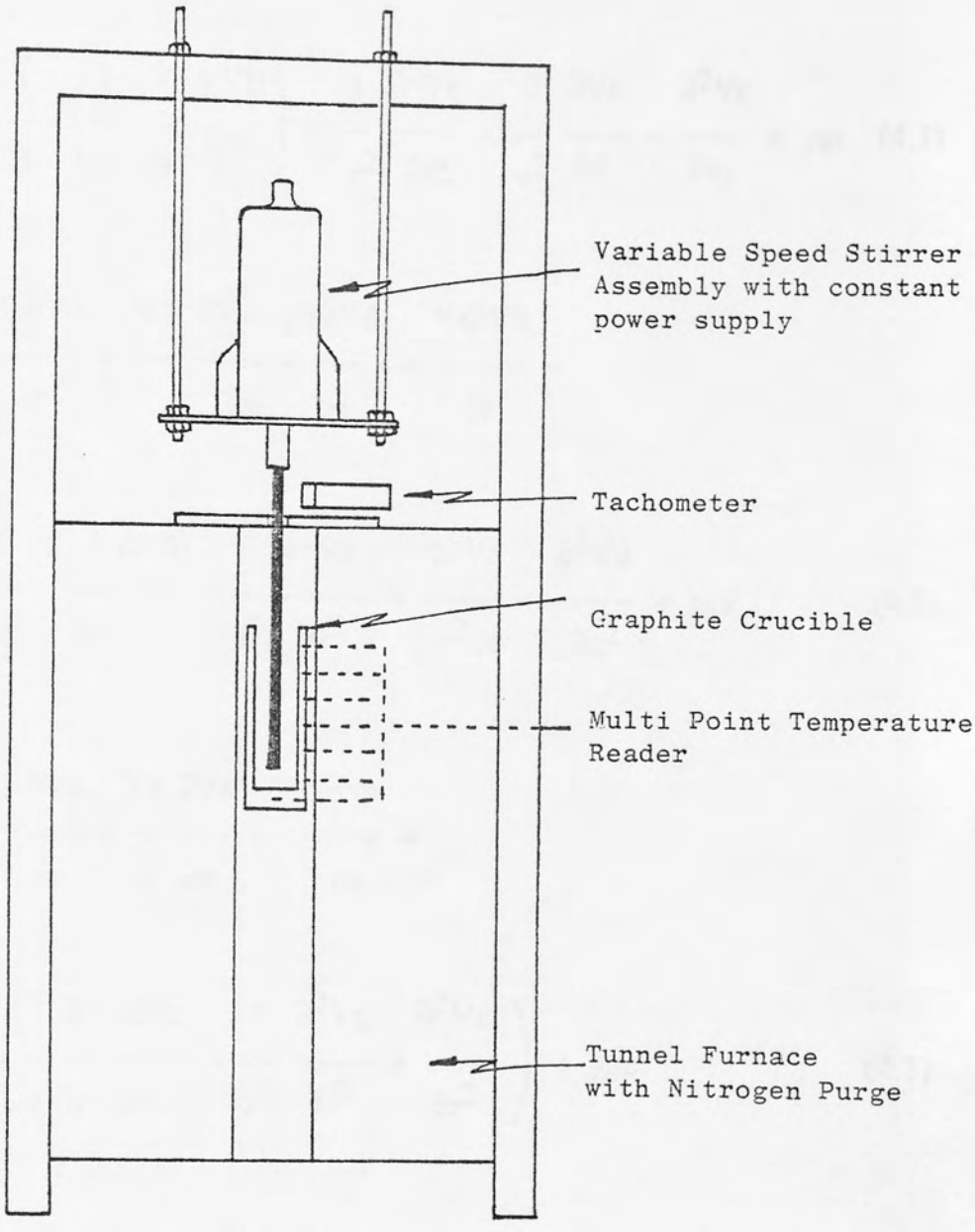

Figure 4.1: Simplified Outline of High Temperature Viscosity Measurement Rig

$$\rho\left(\frac{\partial V_r}{\partial t}+\frac{V_r\partial V_r}{\partial r}+\frac{V_\theta}{r}\frac{\partial V_r}{\partial \theta}-\frac{V_\theta^2}{r}+\frac{V_z\partial V_r}{\delta z}\right)=$$

$$-\frac{\partial P}{\partial r}+\mu\frac{\partial}{\partial r}\left(\frac{1}{r}\frac{\partial}{\partial r}(rV_r)\right)+\frac{1}{r^2}\frac{\partial^2 V_r}{\partial \theta 2}-\frac{2}{r^2}\frac{\partial V_\theta}{\partial \theta}+\frac{\partial^2 V_r}{\partial z_2}+\rho g r \quad (4.1)$$

$$\rho\left(\frac{\partial V_\theta}{\partial t}+\frac{V_r\partial V_\theta}{\partial r}+\frac{V_\theta}{r}\frac{\partial V_\theta}{\partial \theta}+\frac{V_r V_\theta}{r}+\frac{V_z\partial V_\theta}{\partial z}\right)=$$

$$-\frac{1}{r}\frac{\partial P}{\partial \theta}+\mu\left(\frac{\partial}{\partial r}\frac{1}{r}\frac{\partial}{\partial r}(rV_\theta)+\frac{1}{r^2}\frac{\partial^2 V_\theta}{\partial \theta^2}+\frac{2\partial V_r}{r^2\partial \theta}+\frac{\partial^2 V_\theta}{\partial z^2}\right)+\rho g_\theta \quad (4.2)$$

$$\rho\left(\frac{\partial V_z}{\partial t}+V_r\frac{\partial V_z}{\partial r}+\frac{V_\theta}{r}\frac{\partial V_z}{\partial \theta}+V_z\frac{\partial V_z}{\partial z}\right)=$$

$$-\frac{\partial P}{\partial z}+\mu\left(\frac{1}{r}\frac{\partial}{\partial r}\frac{r\partial V_z}{\partial r}+\frac{1}{r^2}\frac{\partial^2 V_z}{\partial \theta^2}+\frac{\partial^2 V_z}{\partial z^2}\right)+\rho g_z \quad (4.3)$$

where r is the radial distance from the vertical axis in the z direction, θ is the angle the radius r makes with a fixed line perpendicular to the z axis.

For the situation where steady laminar rotational flow exists, with no vertical or radial velocity, you can write:-

For gravitational acceleration:-

$$g_r = 0 \qquad g_\theta = 0 \qquad g_z = g$$

For velocity:-

$$V_r = 0 \qquad V_\theta = V_\theta(r) \qquad V_z = 0$$

$$\frac{\partial V_\theta}{\partial \theta} = 0 \qquad \frac{\partial V_\theta}{\partial z} = 0$$

For steady flow:-

$$\frac{\partial V_\theta}{\partial t} = 0$$

For pressure gradient:-

$$\frac{\partial P}{\partial j} = 0$$

Equations (4.1), (4.2) and (4.3) reduce to:-

$$\rho \frac{V_\theta^2}{r} = \frac{\partial P}{\partial r} \tag{4.4}$$

$$0 = \frac{\partial}{\partial r}\left(\frac{1}{r}\frac{\partial}{\partial r}(rV_\theta)\right) \tag{4.5}$$

$$0 = \frac{\partial P}{\partial z} + \rho g \tag{4.6}$$

Integrate equation (4.5) to give:-

$$\frac{1}{r}\frac{d}{dr}(r V\theta) = C_1$$

and then to:-

$$V\theta = \frac{C_1 r}{2} + \frac{C_2}{r} \qquad (4.7)$$

where C_1 and C_2 are constants.

Consider a vertical annulus of inner diameter Y_{di} and outer diameter d_i. Let the inner and outer walls move with steady rotational velocity of w_1 and w_2 radians per second respectively.

Solve equation 4.7 according to these boundary conditions:-

At $r = \frac{d_i}{2}$ $\qquad Vj = \frac{w_2 d_i}{2}$

$r = \frac{Yd_i}{2}$ $\qquad Vj = \frac{w_1 Yd_i}{2}$

to give:-

$$C_1 = \frac{2(w_2 - Y^2 w_2)}{(1 - Y^2)}$$

$$C_2 = \frac{Y^2 d_i^2 (w_2 - w_1)}{4(1 - Y^2)}$$

Substitute for C_1 and C_2 into 4.7.

$$V\theta = \frac{(w_2 - Y^2 w_1)r}{(1 - y^2)} - \frac{Y^2 d_i^2 (w_2 - w_1)}{4r\,(1 - Y^2)} \qquad (4.8)$$

Equation 4.8 gives the point linear velocity $V\theta$ in the angular θ direction in terms of position r. It can be shown that the shear stress $R_{r\theta}$ at a position r is given by:-

$$R_{r\theta} = -\mu r \frac{\partial}{\partial r}\left(\frac{V_\theta}{r}\right) \qquad (4.9)$$

where μ is the viscosity.

Differentiating 4.8 gives:-

$$\frac{d}{dr}\left(\frac{V_\theta}{r}\right) = \frac{Y^2 d_i^2 (w_2 - w_1)}{2r^3 (1 - Y^2)}$$

combining with 4.9 gives:-

$$R_{r\theta} = \frac{-\mu Y^2 d_i^2 (w_2 - w_1)}{2r^2 (1 - Y^2)} \qquad (4.10)$$

If the outer cylinder is stationary, equation 4.10 can be reduced to:-

$$R r\theta = \frac{\mu Y^2 d_i^2 (w1)}{2r^2 (1 - Y^2)}$$

Thus shear stress on the inner cylinder will be:-

$$R_{r\theta} \quad \left(r = \frac{Yd_i}{2}\right) = \frac{2\mu d_i^2 w_1}{(1 - Y^2)} \tag{4.11}$$

The torque required to turn such a cylinder will be :-

$$\tau = \pi Yd_i L + R_r\theta \,|\, r = \frac{Yd_i}{2} \quad \frac{Yd_i}{2} \tag{4.12}$$

or combining 4.11 and 4.12 to give:-

$$\tau = \pi \mu L d_i^2 w_1 \frac{Y^2}{1 - Y^2}$$

$$\mu = \frac{\tau}{\pi L d_i^2 w_1} \quad \frac{1 - Y^2}{Y^2} \tag{4.13}$$

The torque cannot be measured directly with any great accuracy, but by rewriting equation 4.13 in the form:

$$\mu = \frac{K}{w_1}$$

where K is a constant, an experimental calibration curve of μ versus w_1 can be evaluated.

A solution of sodium silicate was made up by dissolving powdered glass in boiling water at high pressure until saturation was achieved. This highly viscous solution was divided into a series of samples which were then diluted to obtain less viscous solutions. The viscosity of these was then evaluated using a Haake Rotovisco viscometer. The solutions were then used in the experimental

furance viscometer for calibration. Values of μ, w, and hence K (which was shown to remain essentially constant) are given in Table 4.1. The furnace was then set up with a melt of glass in the same crucible. Careful attention was needed in maintaining the value of L and measuring the melt temperature. Data for w, with temperature and hence viscosity with temperature are given in Table 4.2.

Considerable errors were anticipated, but the results clearly support the data due to HEIDTKAMP and ENDELL (Figure 4.2).

For convenience an expression relating viscosity and temperature is desirable. In general a plot of ln viscosity vs the reciprical of the temperature forms a straight line. The experimental data is plotted in this form as figure 4.3. The gradient of the line is 21186.44 and the intercept occurs at $\ln\mu = -8.44$. Thus the expression may be written as:-

$$\ln\mu = \frac{21186.44}{T} - 8.44$$

Table 4.1: Rotational Speed as a Function of Sodium Silicate Solution Viscosity

Viscosity (Poise)	Rotational Speed (Radians/Second)	K
4028	0.0116	46.72
3538	0.0150	53.07
2307	0.0210	48.44
1748	0.0236	41.25
1122	0.0420	47.12
500	0.0945	47.29
244	0.2048	49.96
114	0.4050	46.37
27	1.7682	48.42

Figure 4.2: Variation of Viscosity with Temperature for a Sodium Silicate Melt, Na_2O : 3.35 $Si O_2$

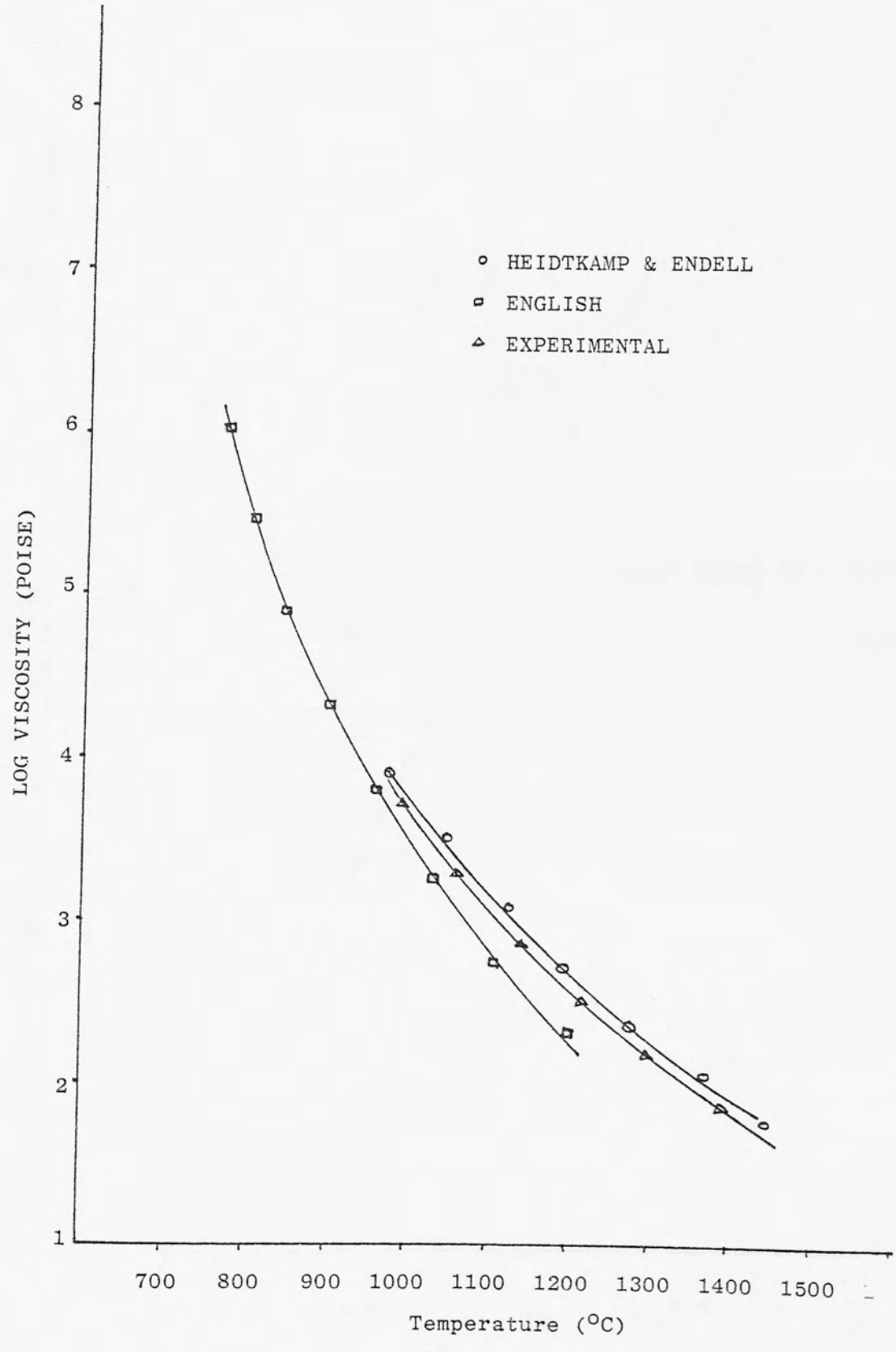

Figure 4.3: Plot of lnμ vs 1/T

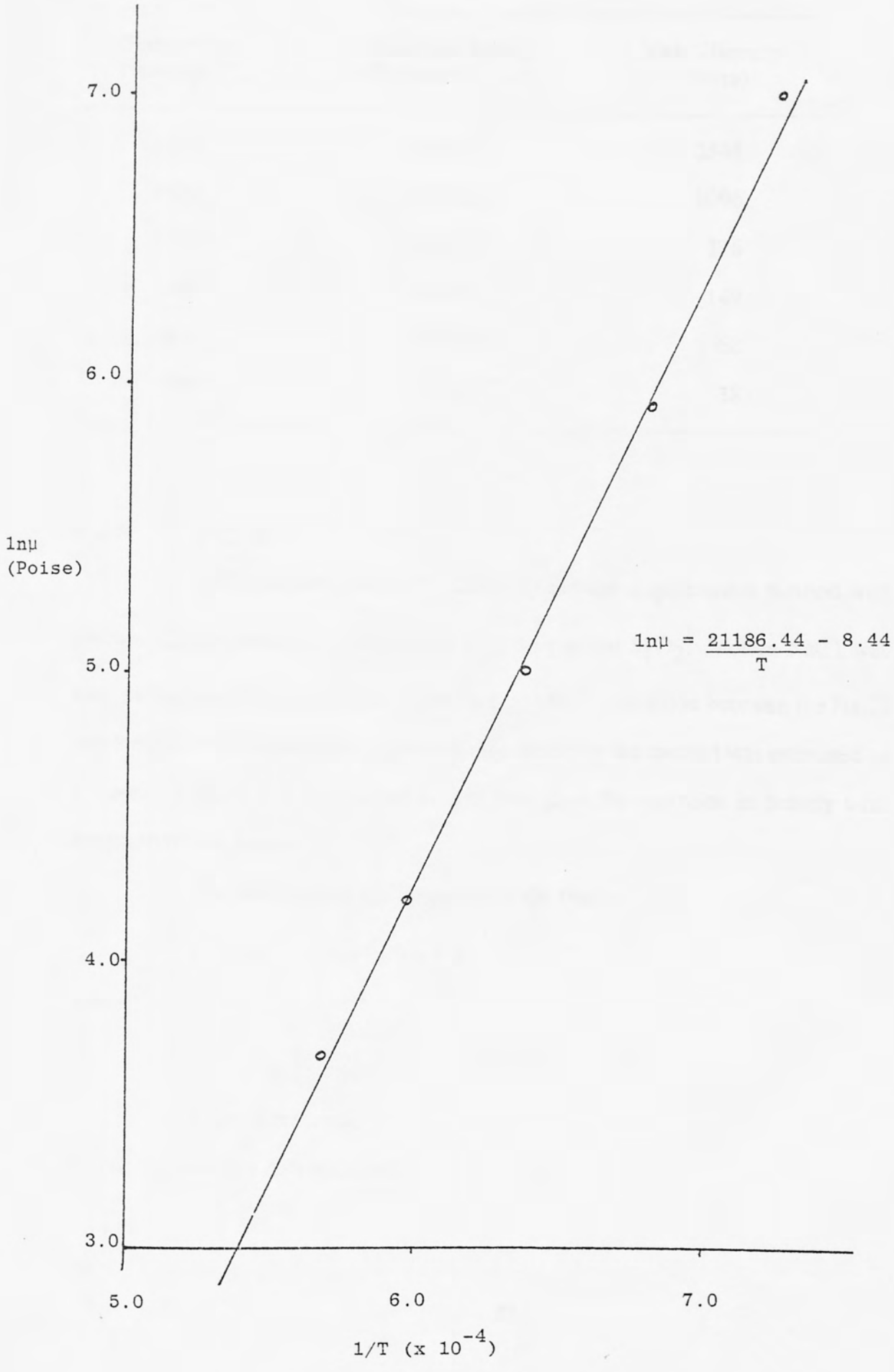

Table 4.2: Sodium Silicate Melt Viscosity as a Function of Rotational Speed

Temperature (Average ^{o}C)	Rotational Speed (Radians/Second)	Melt Viscosity (Poise)
1000	0.0149	3548
1100	0.0450	1096
1200	0.1275	376
1300	0.3032	149
1400	0.5938	68
1500	1.0510	38

4.2.2. Density

HEIDTKAMP and ENDELL (3) used the displacement method with sodium silicate melts containing more than 65 percent SiO_2. Molten NaC1 was used as buoyancy liquid and they found no appreciable reaction between the NaC1 and the Sodium Silicate melts. The maximum error for the method was estimated as 1.3 percent and it was found that for any one glass the variation in density with temperature was linear.

For neutral glass an expression of the form:-

$$\rho = 2.26 - 1.24 \times 10^{-4} T$$

where:

ρ : density (g/cm^3)

T : temperature (C)

fits the experimental data accurately.

4.2.3 Coefficient of Expansion

Generally the coefficient of expansion refers to solid materials, and hence no expression or data could be found for the variation of the coefficient of expansion with temperature in glass melts. However an expression for the variation of density with temperature is available, and this can be related to the coefficient of expansion as follows:-

The coefficient of Expansion, β, is defined as:

$$\frac{dx}{x.\Delta T} \qquad (4.14)$$

dx is the change in sample length

x is the original length

ΔT is the temperature change.

Original volume, $V_1 = x^3$ (4.15)

New volume, $V_2 = (x + dX)^3$ (4.16)

for a given mass.

$$\frac{V_1}{V_2} = \frac{\rho_2}{\rho_1} \qquad (4.17)$$

Substituting 4.15, 4.16 and density expressions into 4.17 gives,

$$\therefore \quad \frac{x^3}{(x+dx)^3} = \frac{2.268 - 1.2469 \times 10^{-4}T_2}{2.268 - 1.2469 \times 10^{-4}T_1}$$

$$\frac{x + dx}{x} = \frac{[\text{----------}T_1]^{1/3}}{[\text{----------}T_2]^{1/3}}$$

$$\therefore \quad \frac{dx}{x} = \frac{[\text{----------}T_1]^{1/3}}{[\text{----------}T_2]^{1/3}} - 1$$

from 4.14:

$$\beta = \frac{\dfrac{[\text{----------}T_1]^{1/3}}{[\text{----------}T_2]^{1/3}} - 1}{T_2 - T_1} \qquad (-^{o}C)$$

Thus the coefficient of expansion may be evaluated at some mean temperature between T_1 and T_2.

4.2.4. Specific Heat

Heat capacity is generally assumed to be approximately additive for liquid mixtures, and although it is well known that precise measurements show considerable departures from this additive relationship, the specific heat of glasses is more nearly additive than any other quantity. Sharp and Ginther (7) reviewed the literature and postulated the following expression:

$$Cm = \frac{a.T + Co}{0.00146.T + 1} \qquad cal/g^{o}C$$

where,

	a	Co
S_iO_2	0.000468	0.1657
Na_2O	0.000829	0.2229

Thus the true specific heat of the glass melt can be expressed in the form:

$$Cm = \frac{0.000468.T + 0.1657}{0.00146.T + 1.0} + 3.35 \left(\frac{0.000829.T + 0.2229}{0.00146.T + 1.0} \right)$$

4.2.5 Thermal Conductivity

The thermal conductivity of glass melts is extremely difficult to determine accurately, because of the importance of internal melt radiation. Van - Zee and Babcock (8) have developed a technique for measuring the total heat transferred through a cylindrical sample by both conduction and radiation. The thermal diffusivity so evaluated gives a direct value for thermal conductivity after multiplying with the density and true specific heat. They concluded that an exponential relationship between the glass thermal diffusivity and temperature existed:

$\log 1000\ h^2 = 0.04752 + 0.0016074.T$ h^2 - thermal diffusivity (cm^2/sec). This relationship shows the rapid rate of increase of thermal diffusivity at high temperature and illustrates the importance of melt radiation when considering heat transfer within the melt. The thermal conductivity is given by:

$$K = h^2.\ r.\ C$$

K - Thermal Conductivity cal/cm. $^oC.S$

r - Density g/cm^3

C - True Specific Heat $cal/g/^oC$

4.3 SODIUM SILICATE LIQUOR PHYSICAL PROPERTIES

In order to satisfy the laws of similarity which are applied to the model and furnace, a considerable quantity of physical property data for the modelling

solution is required. At present Crosfield manufacture a wide range of clear filtered sodium silicate liquors, and for modelling purposes a range of liquors covering high and low viscosity ranges was supplied.

At the outset it was decided that experimental runs should be carried out over two alternative mean residence times corresponding to mean times equal to that of the real furnace and to one tenth of that in the real furnace. The laws of similarity can be satisfied in both cases, but an investigation of the effects of flow impulse (which is controlled by the feed rate/residence time) was desirable. This requirement meant that two modelling solutions with different physical properties are required.

4.3.1 Viscosity

A good knowledge of the variation of viscosity with temperature is essential when operating models of glass furnaces. The standard silicate liquors provided required modification prior to use, and it was therefore necessary to measure the variation of viscosity with temperature and match this to the model requirements. The Reynolds number is the most important dimensionless group in this situation and it was noted that the specific gravities of modelling solutions were approximately 80% and 74% of the glass melt specific gravity for the long and short residence times respectively. With this in mind and noting the linear dimensions of the model, the viscosities should be 0.8% and 7.4% of the glass melt viscosity for the long and short residence times respectively.

A Haake Rotovisco RV12 viscometer was used to measure viscosity over the whole range of operating temperatures. A type MVII head was used to form a coaxial cylinder located within a temperature controlled vessel. The vessel temperature can be controlled accurately in the range -5^{o}C to 60^{o}C. Figure 4.4 highlights the main features of the viscometer.

It was noted that at temperatures above 40^{o}C water evaporation led to the formation of a 'skin' on the surface of the liquor. This would obviously affect

the results and therefore a model outlet temperature well below this limit was set. The viscosity of the glass melt at the furnace outlet is largely dependant on the temperature, which is in turn determined by the operating conditions. Over an extensive series of visits this temperature was measured in the range 1060 to 1098°C which corresponds to a product viscosity of 1111.3 to 1726.4 Poise. Under average operating conditions the mean model outlet viscosity would be 11.3 and 105.1 Poise for the long and short residence times respectively. A series of liquor samples were prepared and the variation of viscosity with temperature was measured using the Haake. The final data for the two modelling solutions is given in Table 4.3. A plot of Ln viscosity vs the reciprical of the temperature can be seen to approximate to a straight line in both cases (Fig. 4.5), and therefore the equation relating viscosity and temperature can be written:-

$$\ln\mu = \frac{11916.}{T} - 35.0 \qquad \text{(High viscosity solution)}$$

$$\ln\mu = \frac{11333.}{T} - 35.0 \qquad \text{(Low viscosity solution)}$$

where

μ : viscosity (Poise)

T : temperature (K)

FIGURE 4.4 Haake Rotovisco RV12 Viscometer

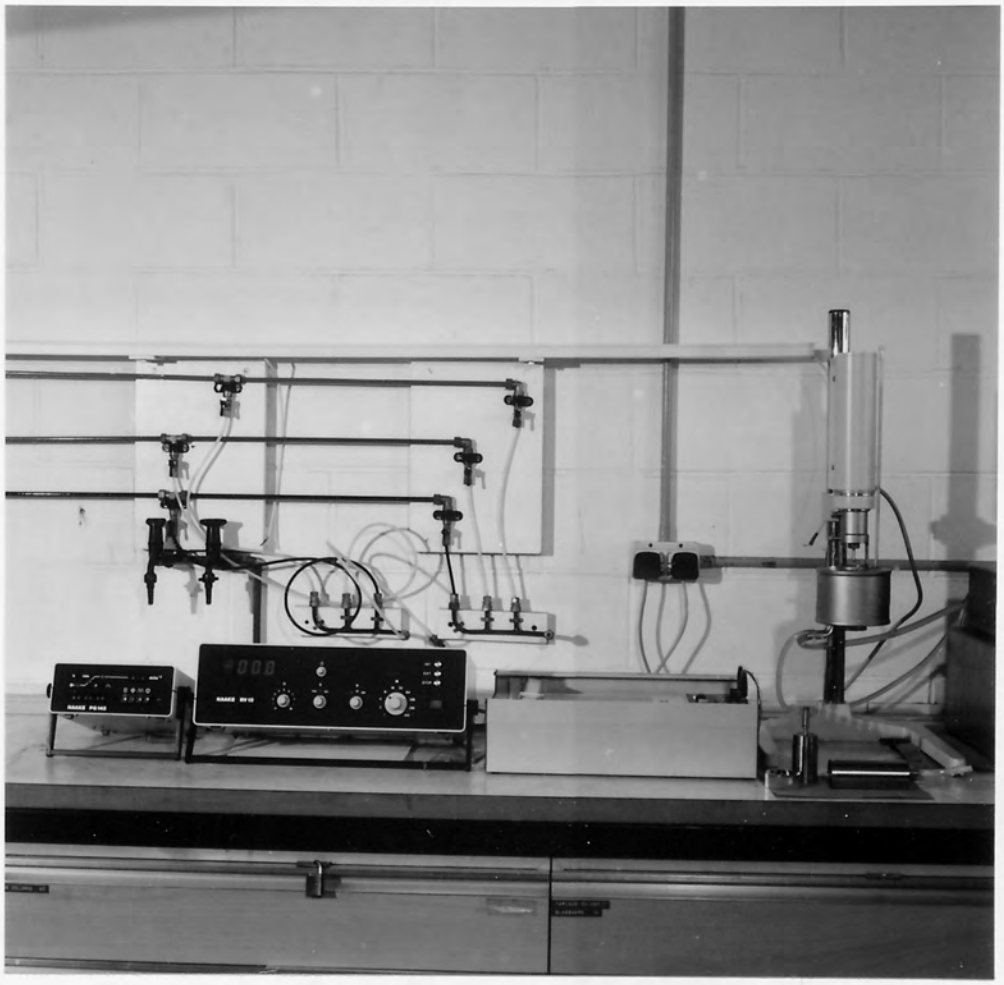

Table 4.3: Variation of Viscosity with Temperatures for Both Modelling Solutions

T(^{o}C)	($x^{1/T}$ 10^{-3}) (k^{-1})	High Viscosity μ (poise)	Low Viscosity μ (poise)	High Viscosity 1nμ	Low Viscosity 1nμ
-4	3.7175	10509.1	1255.1	9.260	7.135
-2	3.6900	8103.1	916.9	9.000	6.821
0	3.6630	6126.2	667.8	8.720	6.504
2	3.6364	4822.7	493.2	8.481	6.201
4	3.6101	3388.9	363.94	8.129	5.897
6	3.5842	2346.2	265.9	7.761	5.583
8	3.5587	1609.7	195.6	7.384	5.276
10	3.5336	1124.2	147.1	7.025	4.991
12	3.5088	814.6	106.7	6.703	4.670
14	3.4843	583.3	81.6	6.369	4.402
16	3.4602	427.7	60.15	6.058	4.102
18	3.4364	314.5	47.7	5.751	3.865
20	3.4130	238.9	33.4	5.475	3.509
22	3.3898	182.8	27.8	5.208	3.325
24	3.3670	141.2	22.1	4.950	3.096
26	3.3445	108.7	17.3	4.688	2.850
28	3.3223	85.2	13.0	4.445	2.565
30	3.3003	67.6	10.3	4.214	2.328
32	3.2787	55.4	7.9	4.015	2.073
34	3.2573	45.9	6.1	3.828	1.808
36	3.2362	33.3	4.5	3.506	1.509
38	3.2154	27.4	3.9	3.310	1.353
40	3.1949	20.2	3.2	3.006	1.160

4.3.2 Density

The variation of specific gravity with temperature is linear over the range of temperatures involved in the model, and is given by:-

S.G. = $- 7.2 \times 10^{-4}.T + 1.629$ (low viscosity solution)

S.G. = $- 4.1 \times 10^{-4}.T + 1.693$ (high viscosity solution)

4.3.3 Coefficient of Expansion

No data was available for the coefficient of expansion of the liquor. However it may be related to temperature by considering the changes in density of

Figure 4.5: Plot of lnμ vs 1/T for Two Model Solutions

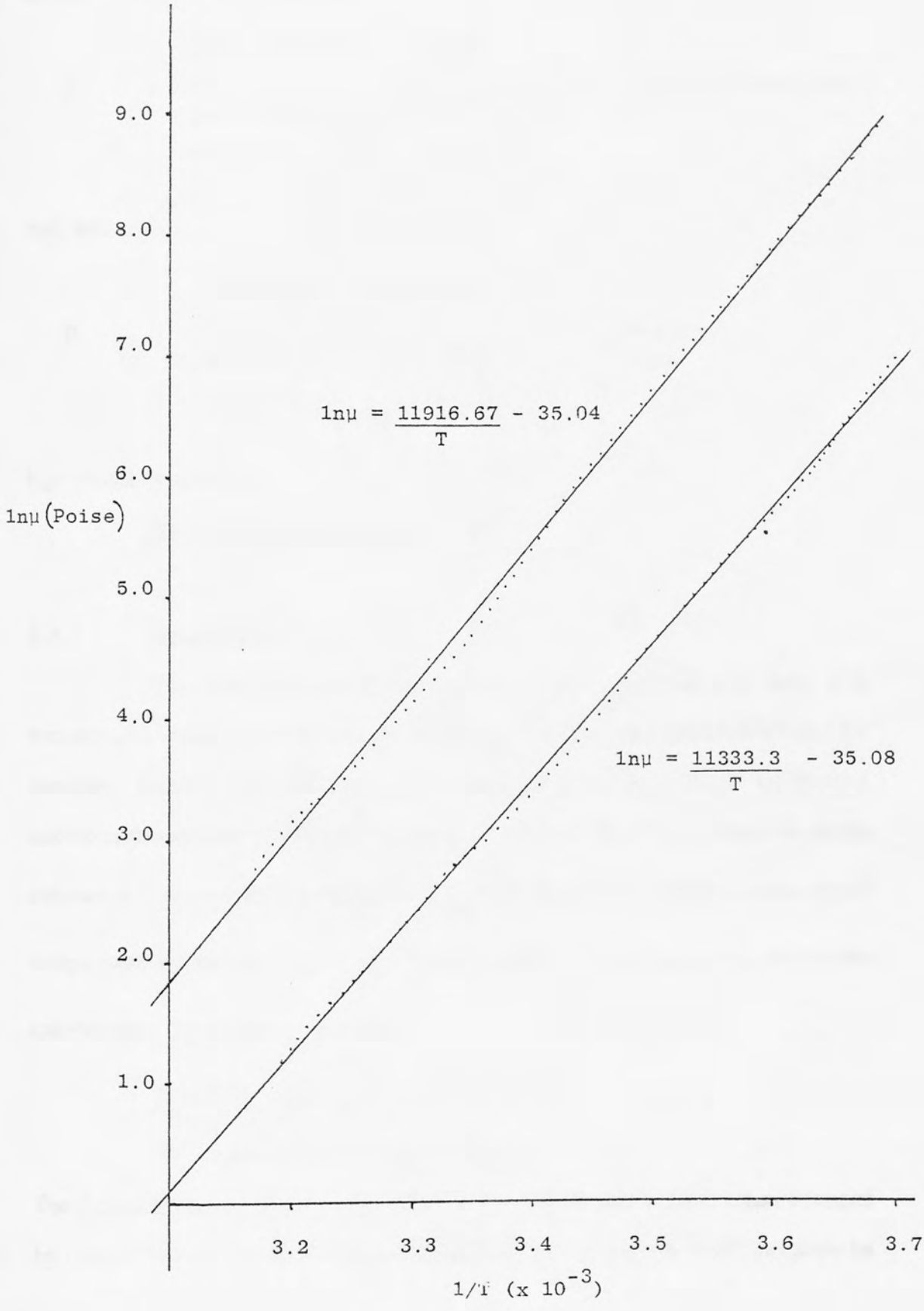

the two solutions. Section 4.2.3 detailed this technique, and gave expressions of the form,

$$\beta = \frac{\dfrac{[-7.2 \times 10^{-4}(T_1) + 1.629]^{1/3}}{[-7.2 \times 10^{-4}(T_2) + 1.629]^{1/3}} - 1}{T_2 - T_1}$$

for the low viscosity solution, and

$$\beta = \frac{\dfrac{[-4.1 \times 10^{-4}.(T_1) + 1.693]^{1/3}}{[-4.1 \times 10^{-4}.(T_2) + 1.693]^{1/3}} - 1}{T_2 - T_1}$$

for the high viscosity solutions.

β : Coefficient of Expansion (^{-o}C).

4.3.4 Specific Heat

The specific heat of the two modelling solutions will vary with temperature, and since the solutions were non-standard no data was available in the literature. Because of this the specific heat needed to be measured and a technique known as the method of mixtures was used. This states that where a mass m, of the substance is heated to a temperature T_1, then placed in a mass of water m_2 at temperature T_2 contained in a calorimeter with stirrer of mass m_3 specific heat of the calorimeter c, T_3 the final temperature

$$m_1 s (T_1 - T_3) = (m_3 C + m_2) (T_3 - T_2)$$

S : specific heat of solution cal/g^{o}C.

The data obtained by this technique showed that the solutions specific heat changed by only 0.7% over the operating temperature of the model, and could therefore be

considered a constant. The relative values are:-

$S = 0.79$ cal/g^{o}C for the high viscosity solution, and

$S = 0.74$ cal/g^{o}C for the low viscosity solution.

4.3.5 Thermal Conductivity

Thermal conductivity is defined as the time rate of transfer of heat by conduction, through unit thickness, across unit area for unit difference of temperature. Thus for two opposite faces of a rectangular solid maintained at temperatures T_1 and T_2 the heat conducted across the material of section a and thickness d in a time t will be:

$$Q = \frac{K (T_2 - T_1) at}{d}$$

K : thermal conductivity.

For the glass melt a thermal conductivity which included an allowance for internal melt radiation was used. At the low temperatures used in the model radiation is not significant. No data was available for the unique model solutions, and therefore it had to be measured. The apparatus used consists of a heat source located above the sample to be tested, a cell for the sample, and temperature probes for measuring the temperature gradients. The heat input is evaluated by measuring the electrical current consumed. For the operational temperature range, no significant variation in thermal conductivity could be found, and a value of:-

$K = 12.9$ cal. hr^{-1}. C^{-1} is considered sufficiently accurate.

4.4 SIMILARITY

The analysis carried out in Chapter 2 identified four dimensionless groups which govern the design and operation of both the furnace and model if similarity is to be preserved. These four groups are:

$$\frac{\rho V L}{\mu} \qquad \text{Reynolds}$$

$$\frac{L^3.g.\rho^2.\beta.\delta T}{\mu^2} \qquad \text{Grashof}$$

$$\frac{C\mu}{\lambda} \qquad \text{Prandtl}$$

$$\frac{M\mu}{\rho^2.g.\beta.\delta T.L^4} \qquad \text{Pull}$$

Sections 4.2 and 4.3 outline the relationships which predict values for μ, ρ, β, C and λ under the normal range of operational temperatures. The length, L, is fixed by the size of the furnace and model, and the time rate of withdrawal of mass, M, is fixed in the real furnace but can adopt two alternative values in the model depending on whether operation adopts equal liquid linear velocity, V, or equal residence time.

The temperature difference between corresponding points, λT, is more difficult to define. However it was decided that the difference between the softening point (Liquidus temperature) and the outlet temperature was a satisfactory measure. The liquidus curve for a sodium silicate melt (11), shows that this temperature is approximately 950^{o}C, and δT is therefore approximately 110^{o}C. For the model the frozen liquor becomes liquid at approximately -5^{o}C and leaves the furnace at approximately 25^{o}C, giving a temperature difference of 30^{o}C.

For convenience all data and relationships were incorporated in a computer program which evaluates each of the dimensionless groups and plots out

comparitive curves as functions of temperature. A listing of the program together with the comparitive graphs and logic diagrams are presented in Appendix 2.

CHAPTER 5

RESIDENCE TIME DISTRIBUTION

5.1 INTRODUCTION

Residence time information, which describes the macroscopic aspects of the mixing of fluids (macromixing), is essential for the study and interpretation of systems where, by channelling or recycling of fluid, or by the creation of stagnant zones, flow through the system is non-ideal. The age distribution describes the distribution of lengths of time spent by the inflow of material before reaching the exit. It concerns only the total period of time a molecule has spent in the system, rather than the way it distributed its time in the various portions of the reactor. Hence, systems with different flow patterns may give rise to the same age-distribution; the age distribution analysis should be regarded as only supporting evidence on the validity of the proposed reactor flow model.

The current furnace design adopts two feed points and only one exit. Previous work on the furnace (9) has adopted a Potash tracer, which was used to analyse the response to an 'impulse' disturbance in the batch at each of the feed points separately. This meant that two complete experiments under identical operating conditions were required to analyse the total furnace flow patterns. In order to avoid this time consuming process it was desirable to feed two independent delineators whose concentration could be analysed independently at the furnace outlet, as outlined in the following sections.

5.2 DELINEATOR

A dye solution was thought to be ideal but the two dyes must be compatible and give good colour density with light absorption spectra which do not overlap significantly. An extensive literature and practical review of the dyes available indicated that a very limited number were suitable. However a combination of Methylene Blue and Sulphacid Brill Pink (3B QUAD (B)) were found to possess very good and compatible properties. The absorption spectra of each, when dispersed in the modelling solution, is shown in figure 5.1. This was obtained using a UNICAM

Figure 5.1: Absorbtion Spectra for Sulphacid Brill Pink 3B Quad (B) and Methylene Blue

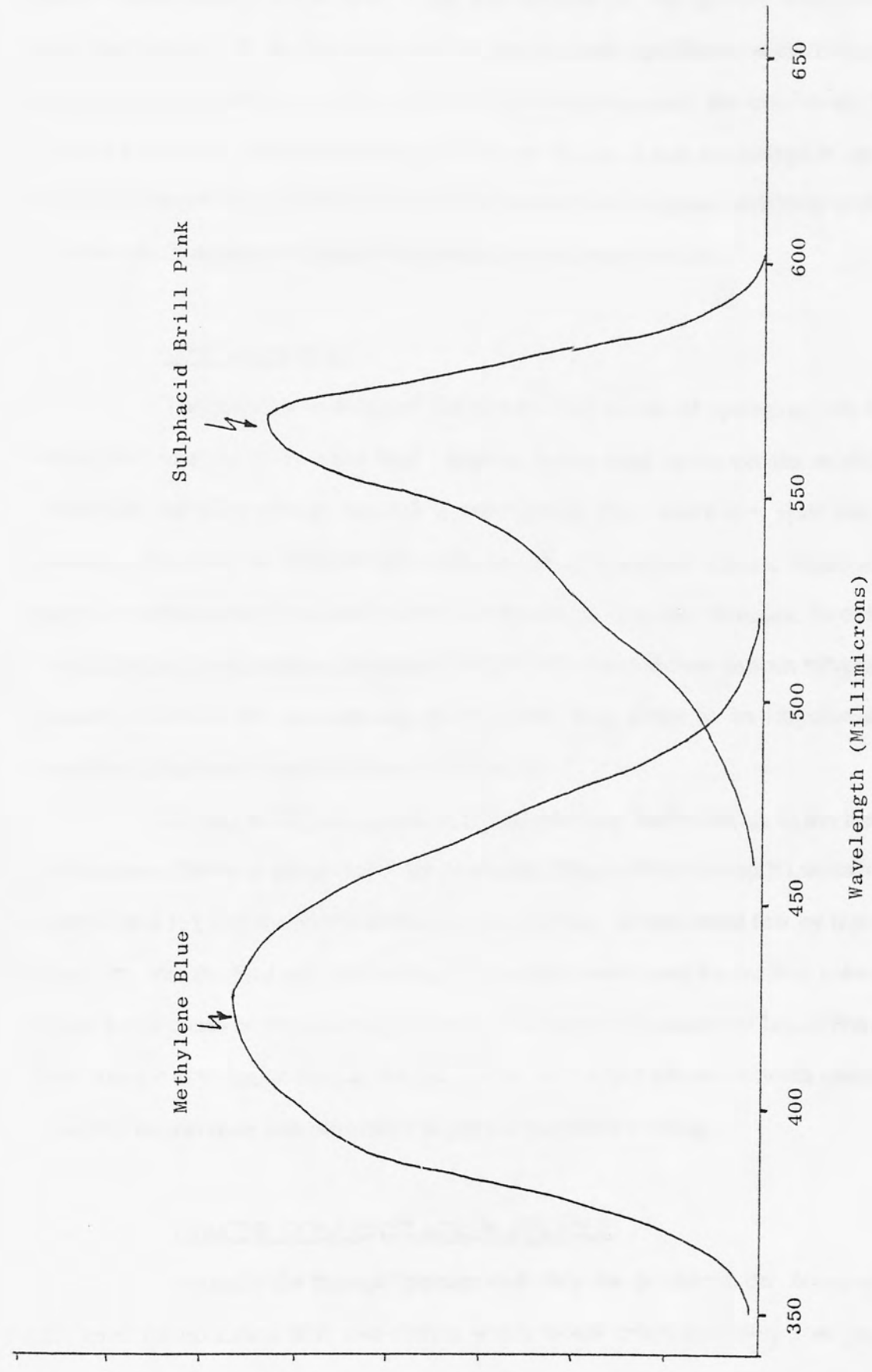

S.P. 1800 ultraviolet spectrophotometer. The colour density of each was such that a tracer containing only 0.6% w/w of dye was suitable for flow pattern and residence time observations. At this concentration the dye does not significantly alter the specific gravity of the modelling solution and will therefore represent the true model flow patterns accurately. Another advantage of the use of dyes is that any change in specific gravity of the solution, is followed by the delineator unlike some modelling systems, for example those adopting aluminium coated polystyrene particles.

5.3 DYE ADDITION

The model was designed for two distinct modes of operation, one being liquid feed and the other solid feed. During liquid feed operation the modelling solution is fed from storage through a mono-pump after which it is split into two streams. Dye may be injected into each stream as a sodium silicate solution. In general a syringe pump was used to feed the dye as an 'impulse' stimulus. In order to avoid altering the flowrate significantly the dye was injected over periods of upto one minute, and this was considering to be sufficiently close to an impulse when considering the mean residence time of the model.

During solid feed operation the mono-pump feeds silicate to the freezer, where frozen flakes at about -10^{o}C are produced. This solid is then split into two feed streams and fed into the model through screw feeders. It was found that by injecting liquid dye into the feed streams blockages could be formed, and the melting behaviour of the batch could be modified significantly. However if a stream of liquid Nitrogen was injected at the same time as the dye, the cooling effect allowed smooth operation. The feed temperature was monitored to prevent excessive cooling.

5.4 TRACER CONCENTRATION PROFILE

Normally the furnace operates with only one product outlet, however it is designed for operation with two outlets which would entail analysing four product

streams; that is two streams with two dyes in each. It is both convenient and beneficial if the dye concentration can be monitored instantaneously. The use of a micro computer for data acquisition and storage was the obvious answer.

5.4.1 Dye Concentration

The stream leaving the model contains a mixture of two dyes. The most convenient and accurate method of dye density measurement is to measure the change in light density across a cell containing the dyed solution, by using some form of photoelectric cell. In this case the absorption spectrum of the two dyes does not overlap significantely, and so if the light is first passed through a cell containing a concentrated dye solution and then through the actual measuring cell a measure of the dye density may be obtained. This is illustrated in Figure 5.2.

The light source covers the full waveband of the blue and red dyes, and a cell containing dye of concentration equal to the stimulus dye was used to modify this waveband. The light detector utilised a light dependent resistor containing a Cadmium Sulphide photo-conductive cell with a spectral response similar to that of the human eye. The cell resistance falls with increasing light intensity and follows a logarithmic law. This logarithmic variation is modified electronically to give a linear 0 to 1.8 volt output according to the light density. These signals can then be fed directly in the micro computer for analysis.

Figure 5.2: Dye Density Metering System

5.4.2 Micro Computer

Most micro computers require expensive "Analogue to Digital" convertors to monitor on line measuring devices. Fortunately the B.B.C. Model B is supplied with the capacity to take up to four analogue inputs in the range 0 to 1.8 Volts. Each analogue input is converted into it s digital equivalent in the range 0 to 65520. The series of digital numbers produced in this way can be processed with any of the normal computer techniques to produce stored data, tables, graphs etc.

The auxillary equipment purchased with the micro included a monitor, a dual disc drive allowing 400K of storage capacity, a printer and chips which assisted in various functions such as obtaining graphics dump facilities.

A computer program was written to accept the incoming data and process it to produce a simultaneous concentration vs time graph for each product stream. This data could then be stored for future reference, or converted into a hard copy by the printer. A listing of that program and logic diagram is given in Appendix 2, and typical outputs are given in Appendix 1.

CHAPTER 6

COMPUTER MODEL

6.1 INTRODUCTION

When a fluid flows through a vessel in plug flow or well mixed flow then the performance of the vessel as a reactor can be predicted in a straightforward manner. However when flow deviates from either of these two ideal patterns, performance predictions cannot be made simply. In the latter case one approach is to represent the real vessel by a flow model, determine the parameters of this model, and then predict the performance of the real vessel from the model. The relatively small deviations from plug flow which occur in packed beds and tubes of sufficient length are satisfactorily represented by the tanks in series model, and the dispersion models. When deviation from plug flow is great, neither of these models satisfactorily characterise the actual flow patterns. In this case the most fruitful approach is to view the real vessel consisting of interconnected flow regions with various modes of flow possible between and around these regions. Models such as these are called mixed models.

The furnace is a unique reactor in its mode of operation and practical observations have indicated that it is far from an idealised system. The influence of batch cover, the unknown condition of the melt close to the tank walls and the dispersion of solid and gas in the melt are a few of the factors which complicate the situation. Mixed models are ideal in this sort of application and can give a clear insight into the likely flow systems.

6.2 COMPONENTS OF MIXED MODELS

The following kind of regions may be used when developing mixed models:

i) Plug flow regions

ii) Stirred tank regions - where fluid is completely mixed and of uniform composition.

iii) Dispersed plug flow regions, where a diffusion-like process is

superimposed on plug flow.

iv) Deadwater regions, where fluid is completely stagnant.

The following kinds of flow are also visualised:

i) Bypass flow, where a portion of the fluid bypasses the vessel, or a particular flow region; This may be the same as a plug flow.

ii) Recycle flow, where a portion of the fluid leaving the vessel or leaving a flow region is recirculated and returned to mix with fresh fluid.

iii) Cross flow, where interchange of fluid occurs between two streams flowing in parallel through different flow regions.

Obviously a mixed model applied to a complex situation will give rise to a large number of parameters, and in some ways this indicates the flexibility of the model in fitting a wide variety of situations. However this gain in flexibility must be balanced against the unwieldiness of the model and the lack of clear understanding associated with the results. Hence, in fitting a real situation, one should aim for the simplest model which fits the facts and whose various regions are suggested by the real vessel.

6.3 INTERPRETATION OF DEADWATER REGIONS

The existance of stagnant zones can cause problems in interpreting the results from residence time analysis. If the literal definition of a stagnant zone was applied then the mean residence time would be infinite. Fortunately completely stagnant zones do not occur, in real reactors these regions have long residence times and exchange material slowly with the flowing stream. Thus in a real situation the deadwater regions are relatively slow moving portions of the fluid which you choose to be completely stagnant. (10) The cut off point in residence time between what is chosen as active and as stagnant depends on the shape an accuracy of available Concentration/Time curve for the system under consideration. Levenspiel (10)

suggests that material which stays in the vessel for more than twice the mean residence time can be taken to be stagnant. Reference to data taken from an operational furnace, and illustrated in Figures 6.3 and 6.4 supports this general rule of thumb.

For convenience, time will be expressed in dimensionless time within the vessel, j. Calling the mean residence time, t, one then has:

$$\theta = \frac{t}{t} = \frac{t}{V/v}$$

V is the vessel volume

v is the volumetric flowrate.

Usingθas o measure of time the output corresponding to a pulse input of unit area is called the C-curve. The C-curve represents directly the residence time distribution of fluid passing through the vessel (or the age distribution of fluid in the exit stream). To identify the existance of deadwater regions a reasonable cut off point, such as $\theta = 2$, is selected and the mean of the C-curve up to that point is then found. The C-curve has unit area, and a mean equal to unity, so that if no deadwater regions are present the mean of the residence distribution curve occurs at $\theta = 1.0$. If deadwater regions are present:

$$\theta < 1.0$$

The fraction of vessel consisting of deadwater regions is given by the deviation of j from unity. Hence:

$$\frac{dV}{V} = 1 - \theta$$

Figure 6.1 summarises these results.

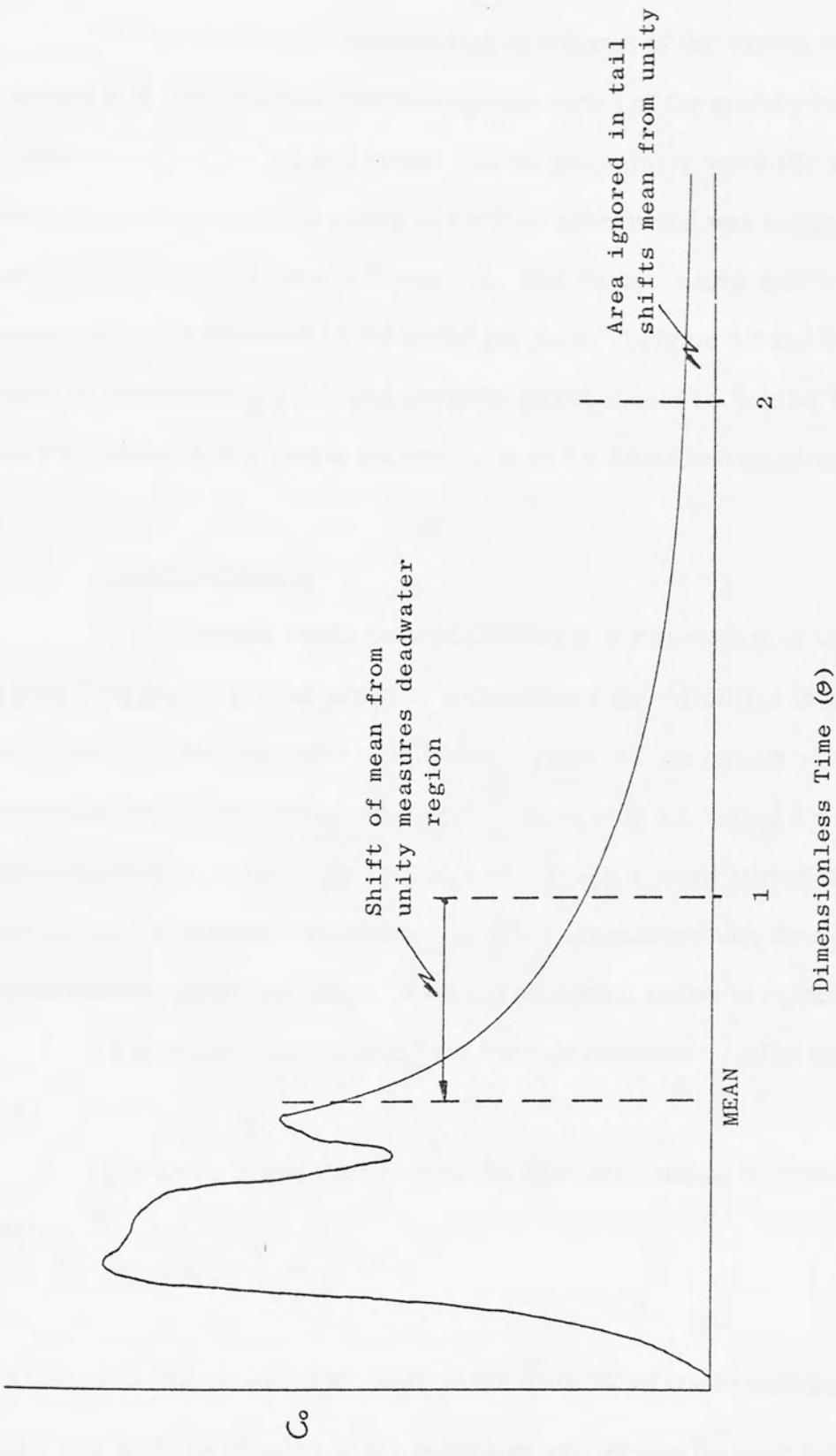

Figure 6.1: The Identification of Dead-Space

6.4 FITTING MIXED MODELS

The problem is to find the relative volumes of the various regions and the various types of flow such that the response curves of the model closely match the response curves for the real vessel. Some preliminary work (9) on the real furnace gave a insight into the nature of the flow patterns and was analysed using a Mixed Model network shown in Figure 6.2. The residence time distribution, and the comparable one predicted by the model are shown in Figure 6.3 and 6.4. As can be seen the agreement is good, and since the model should be 'similar' to the real furnace this network was used as the starting point for the experimental work.

6.5 Computer Model

The computer model network consists of a combination of stirred tanks and plug flow reactors. The stimulus to the system is 0.5g of dye in $100cm^3$ of model solution. This is injected steadily over a period of one minute. The fact that this stimulus cannot be considered a perfect impulse is accounted for within the computer model by passing the feed stream through a small stirred tank. This stream is then divided and can take any one of five alternative routes through a series of stirred tanks or plug flow delays. A typical network is shown in Appendix 1.

The equations controlling the concentration/time profile are outlined below:-

For a single well stirred vessel the transient equation on introduction of tracer is:

$$QC + V\frac{dC}{dt} = QC_o \qquad 6.1$$

In this instance, the product QC_o will be the mass 'm' of tracer introduced as an impulse and will therefore have the transform 'm'. Hence for zero tracer in the vessel at time t = 0, the transform of equation 6.1 is:-

$$QC(s) + Vs\,C(s) = m \qquad 6.2$$

Hence

$$C(s) = \frac{m}{V[s + (Q/V)]} \qquad 6.3$$

and inversion gives

$$c(t) = \frac{m}{V} e^{-Qt/V} \qquad 6.4$$

The concentration diagram for a single well mixed reactor is thus an exponentially decreasing function of time.

A single plug flow vessel acts as a time delay on the concentration/time profile according to the residence time of the vessel. The delay, t_D, is given by:

$$t_D = V/Q \qquad 6.5$$

The computer model holds a concentration array consisting of 300 elements. Each element represents a small time band and equation 6.4 and 6.5 are used to act upon each element according to the type of flow occurring.

Listings and logic diagrams of the computer model and the program used for plotting the experimental and computed data are given in Appendix 2. Typical results can be seen in Appendix 1.

FIGURE 6.2 Computer Mixed Model Network

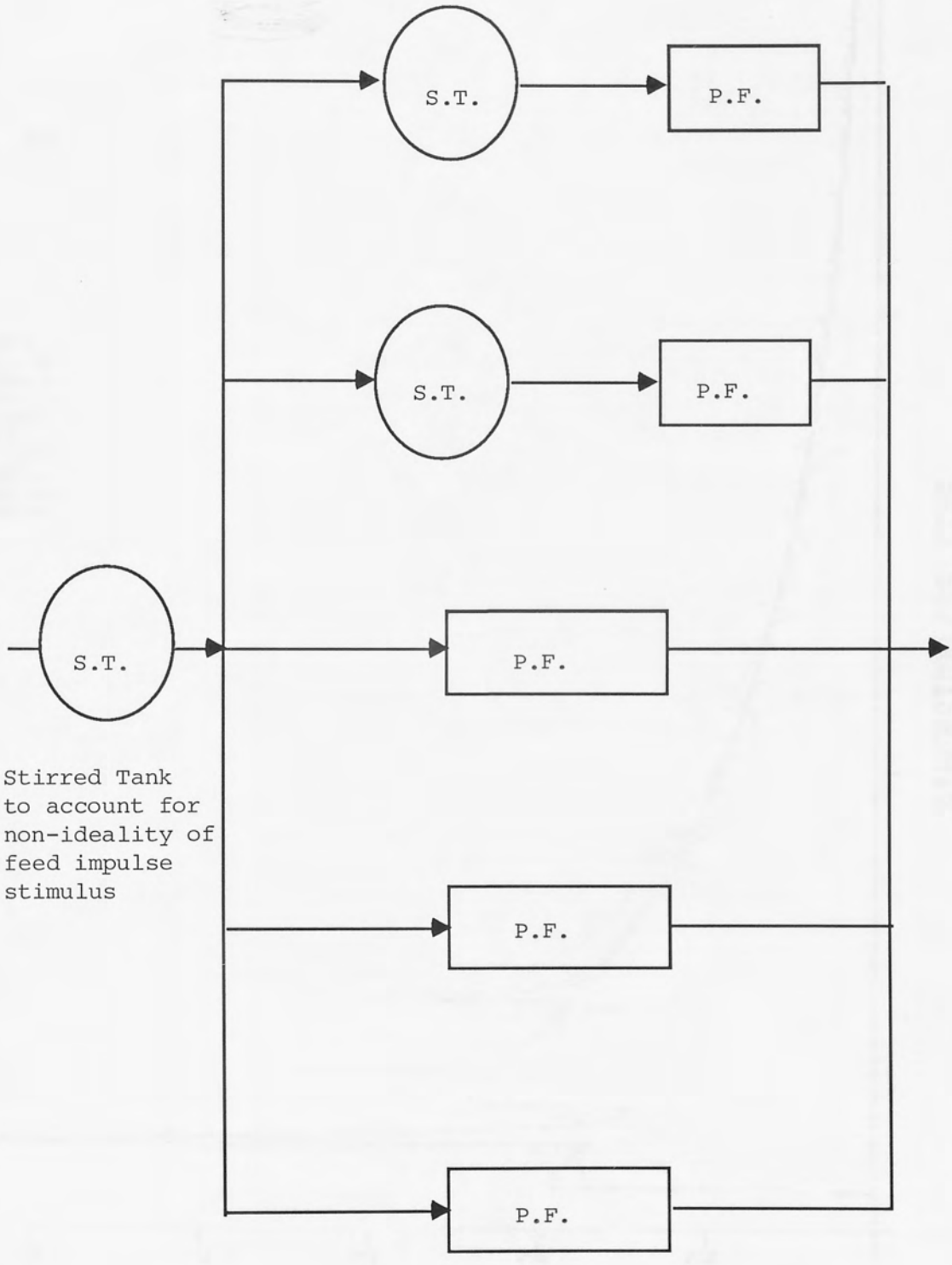

S.T. = Stirred tank

P.F. = Plug flow

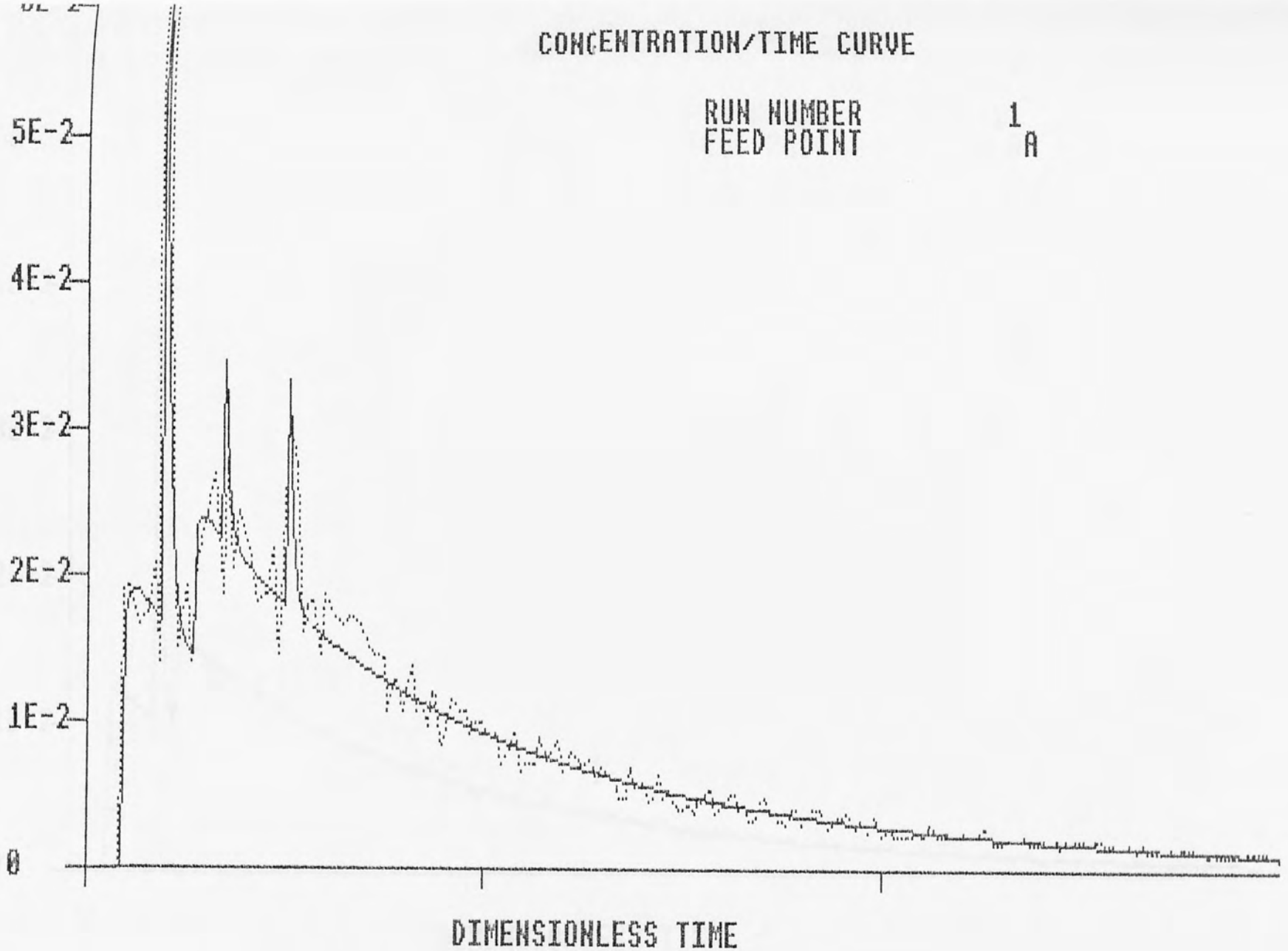

FIGURE 6.3 Residence/Time Distribution for Plant Trial

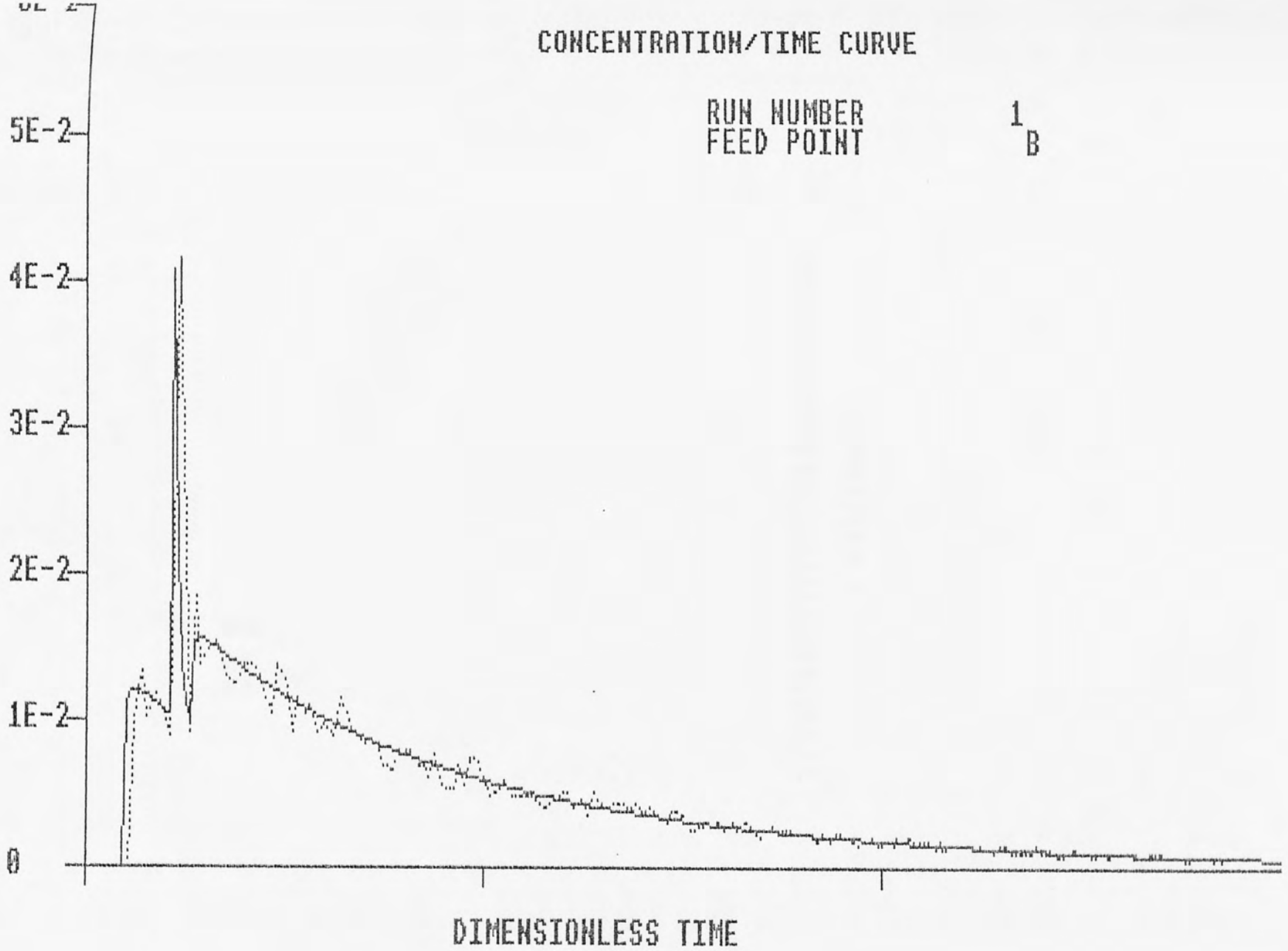

FIGURE 5.4 Residence/Time Distribution for Plant Trial

CHAPTER 7

EXPERIMENTAL PROGRAM AND RESULTS

7.1 INTRODUCTION

An experimental program was planned to investigate furnace operating characteristics on both long and short residence times and with liquid or solid feed. The program was not intended to be rigid and the results from previous runs were used in an on going manner to predict potentially interesting experiments. The experimental data was logged by computer and a mixed model computer simulation outlined in section 6.5 was used to interpret the results.

The concentration/time curves for both the practical and computer model and the computer network simulation results are given in Appendix 1. A summary of results is presented as tables 7.1 and 7.2, which should be read in conjunction with the notes in section 7.2.

7.2 NOTES FOR RESULTS TABLES

As can be seen tables 7.1 and 7.2 summarise the results given in Appendix 1, and these notes define the table column headings in order to assist in the interpretation of results :-

Run Number: The run reference number.

Feed Point: Two alternative furnace feed points were available. The one denoted by an 'A' is closest to the furnace offtake, while the one denoted by a 'B' is furthest from the offtake.

Flow Rate: The liquid or solid feed rate (L/Hr) fed to either feed point A or B.

Fraction Dead Space: The fraction of the total furnace volume occupied by the melt which can be considered stagnant (6.3).

Run No.	Feed Point	Flow Rate L/Hr	Fract^{n} Dead Space	Fract^{n} Avail. Volume	Experimental Conditions	FRACTION FLOW Stream 1	Stream 2	C.S.T.R. / P.F. FRACTION VOLUME Stream 3	Stream 4	Stream 5	Comments
Plant Trial	A	172.0	0.4	0.39	On plant trial - typical operating conditions and neutral glass						Results obtained from plant trials using Potash Tracer
Plant Trial	B	172.0	0.4	0.61	"						
003	A	17.2	0.2	0.37	Short residence time liquid feed						Very poor match on short residence time with liquid feed only.
003	B	17.2	0.2	0.63	"						"
005	A	0.172	0.3	0.35	Long residence time liquid feed						Large plug flow through tank probably caused by the absence of batch cover
005	B	0.172	0.3	0.65	"						"
006	A	0.172	0.4	0.38	Long residence time simulated batch of semi-expanded polystyrene						Reasonable results indicating that solids feed may give good match.
006	B	0.172	0.4	0.62	"						"
012	A	0.344	0.5	0.37	Simulated batch and double flow to both feedpoints						Dead space increases by 10%, no apparant advantages
012	B	0.344	0.5	0.63	"						Volume of large stirred tank decreases by 17% with 8% drop in flow
016	A	0.086	0.25	0.38	Half normal feedrate at each point						Significant reduction in dead space stirred tank flow predominates
016	B	0.086	0.25	0.62	"						"
030	A	0.172	0.4	0.38	Granulated frozen sodium silicate liquor simulated furnace feed						Good match with standard furnace operation. Solid feed may move well away from feedpoints before melting.
030	B	0.172	0.4	0.62	"						"
032	A	0.172	0.6	0.38	Solids feeding liquid level reduced by 20%						Low surface temperature. Increases surface viscosity and reduces plug flow streams.
032	B	0.172	0.6	0.62	"						Small volume P.F. slipstream develops
037	A	0.172	0.25	0.38	Feed below melt surface						Dead space reduced to 25% flow through S.T. zones fell by 24%.

TABLE 7.1 Summary of Results

Run No.	Feed Point	Flow Rate L/Hr	Frac^{n} Dead Space	Frac^{n} Avail. Volume	Experimental Conditions	FRACTION FLOW: Stream 1	Stream 2	Stream 3	Stream 4	Stream 5	FRACTION VOLUME: C.S.T.R.	P.F.	Comments
037	B	0.172	0.25	0.62	Feed below melt surface								Dead space reduced to 25% flow through S.T. zones fell by 27%. Increased plug flow.
038	A	0.344	0.37	0.56	High flow to Point A.								High feed impulse gives feed a 56% of the available volume.
038	B	0.172	0.37	0.44	Normal flow.								Slight increase in plug flow. No obvious operational advantages.
040	A	0.172	0.35	0.35	Normal flow.								3% decrease in volume occupied by stream A.
040	B	0.344	0.35	0.65	High flow to point B.								No significant change from normal.
041	A	0.172	0.22	0.38	Insulate tank base.								Dead space falls to 22% of total increase in volume and flow through stirred tank zone.
041	B	0.172	0.22	0.62	"								"
044	A	0.172	0.6	0.38	False tank base 20% higher than normal								Significant reduction in flow through and volume of stirred tank and corresponding increase with plug flows.
044	B	0.172	0.6	0.62	"								"
0.45	A	0.172	0.32	0.38	Increase heat flux by approximately 20%								Dead space falls by 8% with plug flow predominating over stirred tank flow.
045	B	0.172	0.32	0.62	"								Third plug flow stream develops.
047	A	0.172	0.36	0.38	Feed temperature increased to just below melting point								Preheated feed at 400-600°C is simulated. Increased plug flow. 40% of total is plug flow.
047	B	0.172	0.36	0.62	"								31% of total is plug flow and dead space is reduced to 36%.
049	A	0.172	0.38	0.5	Open second offtake.								12% increase in volume and flow through large stirred tank. Similar reduction with small stirred tank.
049	B	0.172	0.38	0.5	"								Results identical to feed point A. No interchange of liquid between feedpoints. Results similar to No.3 furnace.
050	A	0.172	0.55	0.5	Two offtakes and central weir.								Attempt to improve heat absorption, fail because of different modes of heat transfer between furnace and model.
050	B	0.172	0.55	0.5	"								"

TABLE 7.2 Summary of Results

Fraction Available Volume: The fraction of the available volume, taking into account dead space, which was utilised by this feed stream.

Experimental Conclusions: General operating conditions such as liquid or solid feed or modifications to the tank model are noted in this section.

Stream Column: These five columns summarise the results of the computer simulation, which uses five streams of liquid passing through combinations of ideal Continuous Stirred Tank Reactors (C.S.T.R.) and Plug Flow Reactors (P.F.R). The columns for each run are divided into two sections by a horizontal line. The shaded areas (marked) above the line represents the fraction of flow through that stream. Thus if a column is completely cross hatched 100% of the total flow passes through that stream. The total fraction through all the streams must total 1.0. The shaded area (marked) below the line represents the fraction of the available volume occupied by a C.S.T.R. while the shaded area (marked) represents the fraction occupied by a P.F. reactor. The total fraction occupied by all the reactors must total 1.0.

Comments: This section highlights any significant results and comments on any conclusions which can be drawn.

7.3 DISCUSSION

An operational furnace is a very complex chemical reactor to simulate. The problems associated with a three phase mixture and high temperature reactions are difficult to overcome. However the results obtained illustrate clearly that the

model does behave in a similar way to the real furnace. The first reported run (003) was carried out within the constraints of similarity, but utilised a high liquid feedrate, giving a residence time one-tenth of that in the real furnace. The high impulse of the liquid feed meant that 40% of the flow passed through a plug flow reactor occupying 31% of the available volume, close to the liquid surface. The flowrate is approximately four times the expected while the reactor volume is almost ten times. This significant deviation from the norm was considerably improved with the second run (005). In this case a feedrate of 0.172 L/hr was adopted giving a model residence time equal to that of the real furnace. This reduced both the flow through and the volume of the plug flow reactors to 24% and 7% respectively, compared to 13% and 3% in the real situation. This relatively small error was caused by the absence of any batch cover of solid reactants which also influenced the relative volumes of the stirred tank zones reducing the flow through and volume of the second smaller stirred tank. However the results from this run confirmed that the use of equal residence times and a simulated solid surface layer are essential.

The conclusions drawn from these two runs were applied to run 006 where semi-expanded polystyrene beads were used to simulate the solid surface batch layer. The density of the beads was such that 3/5 of the beads were below the liquid surface and an uneven batch similar to the real furnace was achieved. The results indicated a reasonable match with the norm., the surface plug flow being reduced to 12% and the volume only 2% compared with the corresponding figures of 13% and 3% in the real situation. However it was interesting to note that the stream containing the smaller stirred tank passed through the furnace very quickly with a plug flow delay occupying only 1% of the total volume compared to 5% in the real situation. This significant and important deviation may be explained by the intransient solid/liquid boundary formed by the simulated batch.

Despite the limitations of the simulated solid surface further experiments (012 and 016) were carried out using liquid feed. The first, used a feedrate of twice

the normal to both feed points, and the second used half the normal feedrate. It can be noted that with the first experiment the volume of the three plug flow streams increases by 3% to 5% of the total, while the flowrate through them remains essentially constant. In addition the volume of the large stirred tank falls by 10%, to 46% while the flowrate increases by 5%, to 54% of the total. This together with the fact that the dead space apparently increases by 10% to 50% of the available volume suggest that no operational advantages can be achieved by a straightforward increase in flowrate. By contrast the effect of halving the liquid feedrate is to slightly increase the flow through and volume of the two stirred tanks while reducing the flow through and volume of the plug flow zones. This result was anticipated but what was not was the fact that the dead space fell by 15% to only 25% of the total.

Although the work using a simulated solid surface layer of semi-expanded polystyrene was successful the model could be made more versatile by the adoption of solids feeding. A freezer was constructed and perfected to produce and store a granulated frozen solid. The first run with solid feed (030) used screw feeders to feed the granulated solid into the model. The results compare well with the real furnace and no significant deviations from the normal exit, although it is interesting to note that the source of liquid can no longer be considered to be the feed points. The frozen solid is forced into the model and forms batch piles which move slowly away from the feedpoint following the surface liquid plug flow streams. The solid slowly melts but some almost reaches the outlet before it passes into the liquid phase.

Once reliable solids feeding had been developed and shown to represent the real situation a series of experiments to investigate operational or design changes could be carried out. For run (032) a 20% reduction in liquid level was produced by redesigning the model lip and setting the charges to feed at the new liquid surface. With radiant heat transfer predominating in the real furnace, the increase in beam length and exposed area of tank wall lead to a reduced solid surface

temperature. The exact reduction cannot be predicted from the physical model but the results will be comparible in the real situation.

The most significant effect is the considerable reduction in flow through the three surface plug flow zones from 13% to 2% of the total, although the volume actually increases by 1.5%, to 4.5%. The most likely cause of this is the increase in liquid viscosity close to the surface caused by the reduction in temperature. The extra flow was largely taken up by the smaller stirred tank stream with a 10% increase in flow and an insignificant change in volume. The small stirred tank is located immediately in front of the feeders and is warmed largely by melt conduction and is therefore almost unaffected by changes in the gas phase radiant heat transfer. The efficiency of radiant heat transfer is directly related to the square of the beam length and the results of run 032 clearly show that the level of melt must not be reduced in the operational furnace.

If the raw material feed is well mixed and then granulated or pelletised, to prevent subsequent segregation, before feeding into the furnace, a good quality product will be produced when plug flow predominates. The range of residence times within the furnace will be small and since the feed was well mixed no further homogenisation is necessary. In run 037 this situation was created by setting the screw feeders at an incline of 25^{o} to the horizontal to force the frozen feed into the melt below the liquid surface. The buoyancy of the solid means that it rises to the surface but is reaonably well coated and mixed with warm liquid. This reduces the volume of the two stirred tanks by approximately 25%, with a 5% reduction in flow through the corresponding streams. The extra volume is shared between all five plug flow zones. In addition this approach reduces the dead space to only 25% of the total, and in a real furnace will allow improvements in heat transfer because of the higher absorbtivity of the 'wetted' batch.

The current furnace design utilises two feed points and only one offtake, located close to the corner of the tank opposite the feed points. This

unsymmetrical design can lead to inefficient use of the reactor, and one approach to improve this situation is to vary the relative flowrates to each feedpoint. Runs 030 and 040 investigated this possibility. It was found that although the relative sizes of the stirred tank zones changed, no benefit for operating efficiency could be identified. A later experiment (049) introduced a second liquid offtake symmetrical with the first. Virtually no crossover of tracer occurred and flow through the large stirred tank rose by 12% with a 11% increase in reactor volume. This extra flow and volume came mainly from the second smaller stirred tank which was located close to the furnace outlet, and no significant change in the plug flow region was observed. Operating with a second offtake will promote macro-mixing but product inconsistency caused by batch segregation during melting requires micro-mixing and is unlikely to be improved in this situation.

When operating with two offtakes the dead space within the furnace is only 2% below the normal at 38% of the total. This dead space is generally located close to the tank bottom where the liquid is comparatively cool and highly viscous. Although the relatively stagnant liquid does act as an insulator and heat store it makes no other contribution to effioent operation of the furnace. By insulating the tank bottom both the dead space and heat losses will be reduced. Run 041 adopted this approach by insulating the model base with a 2.5 cm thick slab of polystyrene. In practice the dead space was reduced to only 22% of the total and an increase of 5% was observed in the flow passing through the stirred tank zones. The extra useful reactor volume could be used to allow an increased throughput with no reduction in the average residence time. This assumes that the heat balance can be maintained, but it should be noted that insulating the tank bottom will reduce heat losses and therefore improve thermal efficiency.

In run 032 the depth of the melt was reduced by altering the liquid level, but an alternative approach is to raise the tank base, thus overcoming the heat transfer problems of the former situation. Run 044 adopted this approach by the

addition of a false base thereby reducing the liquid depth by 20% but at the same time maintaining the normal tank base temperature. The results are dramatic with the volumes of the large and small stirred tanks been reduced by 19% and 7% respectively, while the corresponding flowrates fell by 7% and 8%. The extra volume is shared fairly equally among the plug flow zones with the notable addition of a third plug flow stream from feed point B. The dead space of the reactor unfortunately increased by exactly the same amount as the reduced volume (20%), but this is unlikely to be the same in the real furnace where in-melt heat transfer is significantly better than in the model.

An improved understanding of the flow profiles within an operational furnace under certain conditions is essential in developing and improving the operating efficiency. However if higher production rates are required it is unlikely that any improvement in thermal efficiency brought about by changes in the flow patterns will be sufficient to offset the requirements for a greater heat input. With this in mind two runs to investigate possible changes in operating technique were investigated. The first (045) increased the crown temperature by 20% (even though at present this is not possible), and the second (047) preheated the batch to a temperature just below its melting point. Unfortunately the relative importance of the different modes of heat transfer in the model and furnace mean that the results can only be seen as representative of what is likely to happen. However in the first case the volume of the two stirred tanks fell by approximately 20% with a corresponding 9% reduction in flow. This situation is obviously created by the reduced viscosity of liquid close to the surface and the plug flow zones. The effective tank volume increase by 8% to 68% of the total. The temperature of the batch in the second run gave results similar to those which would be obtained in the real furnace with the batch preheated to between 400^{o}C and 600^{o}C. The results indicate a fall of 10% and 20% in the flowrates of the two streams containing stirred tanks while their volumes fall by 18% and 6% respectively. Under these

circumstances 41% of the flow from feedeer A and 31% from feeder B passes through as plug flow.

When operating the furnace it is necessary to maintain a heat balance, and as previously stated the improvements in thermal efficiency are unlikely to give the necessary increase in heat input. Howeveer it has also been noted that the glass batch is an extremely good thermal insulator aand poor absorber of radiant energy by comparison to other glass. Run 050 attemptped to exploit this by introducing a double weir as indicated in the figure below:-

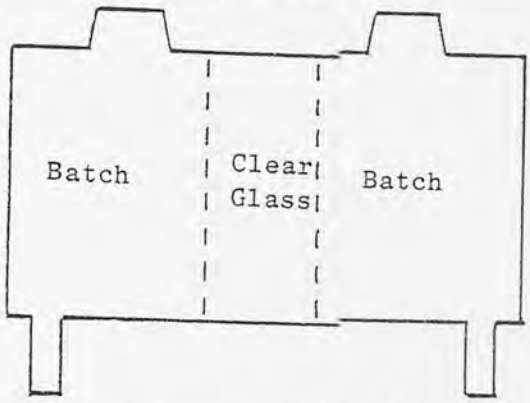

The clear glass area acts as a goood absorber of incident energy which would then be transmitted through the melt to the underside of the batch. Since heat transfer within the model solution takes place largely by conduction and convection the results can only be seen as guidelines. When compared to 049 there is a considerable fall in the flow through the smallder stirred tank from 31% to 25% with only a 2% reduction in reactor volume. In adddition the flow through the plug flow zones almost doubles while the volume increasses by 5% to 8% of the total.

The results from runs 044, 045, 047 and 049 all show an increase in volume of, and flow through the plug flow streams. As outlined earlier this can be of benefit if the batch is pretreated to prevent suubsequent segregation, and this is also necessary if the batch is preheated as outlined i in run 047. Although pretreatment is expensive, the batch will be more efficiently heated in some form of preheater than in the actual furnace and significant improvvements in throughput and thermal efficiency could be obtained.

CHAPTER 8

CONCLUSIONS AND RECOMMENDATIONS FOR FURTHER WORK

8.1 CONCLUSIONS

A series of sixteen successful physical modelling experiments were carried out to investigate the flow performance of a sodium silicate furnace. The constraints of similarity have been identified and within practical limits the model may be operated to comply with them. Early work using liquid feed highlighted the need to control the feedrate to maintain a mean residence time similar to that of the real furnace. The effects of feed impulse and withdrawal rate, and the interaction of liquid and solids within the tank can only be regarded as similar when the mean residence times of the model and furnace are the same. The concept of energy input per unit volume as a control of similar operation was not found to be applicable in this situation. However the use of a long residence time and a simulated batch was found to give reasonable results, although further improvement was found with the use of frozen sodium silicate liquor feed.

Once an acceptable operating regime had been established (Run 030) a series of experiments to investigate the effects of various operating and design changes were carried out. These included:-

i) the reduction in liquid melt level (and therefore temperature),

ii) feeding batch below the melt surface,

iii) adopting a high feed to feed point A,

iv) adopting a high feed to feed point B,

v) insulating the tank bottom,

vi) installing a false tank bottom,

vii) increasing the heat flux by 20%,

viii) increasing the batch feed temperature,

ix) introducing a second liquid offtake,

x) and installing two central tank weirs to create a batch free zone.

These runs have led to a series of predictions for how changes affect the furnace operation in terms of volume of tank used and whether plug flow or stirred

tank flow predominates in each situation. It is interesting to note that stirred tank flow and therefore relatively good mixing is promoted by reducing the liquid level. insulating the tank bottom or introducing a second offtake whereas plug flow is promoted by feeding below the liquid surface, raising the tank bottom, increasing the heat flux, pre-heating the feed or increasing the feedrate. The actual volume of tank utilised is improved by increasing the feedrate, insulating the tank bottom, increasing the heat flux, and to a small extent pre-heating the feed and introducing a second offtake. Tables of general results are presented as tables 7.1. and 7.2.

It should also be noted that the batch is an extremely good insulator and is a relatively poor absorber of radiant energy by comparison to molten glass. Because of this it is recommended that the batch should be preheated even if pelletising or other pretreatment is necessary. It may also be advantageous to modify the feeding technique to feed a batch blanket, similar to that common to most of the flat glass industry. This would minimise the depth of batch which should reduce the melting time. However the situation is complicated by the fact that a flat surface will absorb and re-emit energy in a different way to a uneven surface. It is not known whether the scattering of incident radiation will give a net increase or reduction in energy absorbed and energy losses. In addition a flat blanket will tend to hold up molten glass which will in turn absorb more energy and will reduce the buoyancy of the batch blanket.

A flat batch blanket will also pose less resistance to surface flow of molten glass, and early work using liquid model feed and a simulated batch cover of semi-expanded polystyrene showed visually that surface plug flow would increase significantly in such a situation.

Run 050 uses two feed points and offtakes and a central weir which held back batch and maintained a batch free zone. This experiment was an attempt to highlight the advantages obtained when using some batch free surface. Unfortunately the theory of operation relies on two factors which cannot be

simulated in the physical model. These are:-

i) Heat transfer within the model solution occurs largely by conduction and convection, whereas at the high temperature found in an operating furnace the effective thermal conductivity is upto 50 times the normal because of inter melt radiation.

ii) The furnace is heated by burning gas or oil above the batch. The temperature distribution of the flame can be controlled to some extent, to give a 'hot spot', which in practice could be located above the batch free zone.

These two factors prevented a representative experiment from been carried out, and this technique is still believed to be of considerable value for improved operation.

8.2 RECOMMENDATIONS FOR FURTHER WORK

The physical model has been developed and thoroughly tested for various modes of operation. The results are adequate in predicting what is likely to happen for any reasonable change of operating procedure or design. The author believes that the modelling work gives confidence in predicting the likely effect of higher production rates and goes some way to suggesting improvements in operation. However the problem is two-fold; the prediction and control of flow patterns is essential for safe and reliable operation, but if increased production rates are required then the extra energy or energy efficiency must be found and this is the area for further work. The potential for improvement in batch pre-treatment and heating and for the investigation of heat transfer in the batch/crown zone is enormous and allows great scope for development.

APPENDIX 1

RESIDENCE TIME DISTRIBUTION AND COMPUTER SIMULATION RESULTS

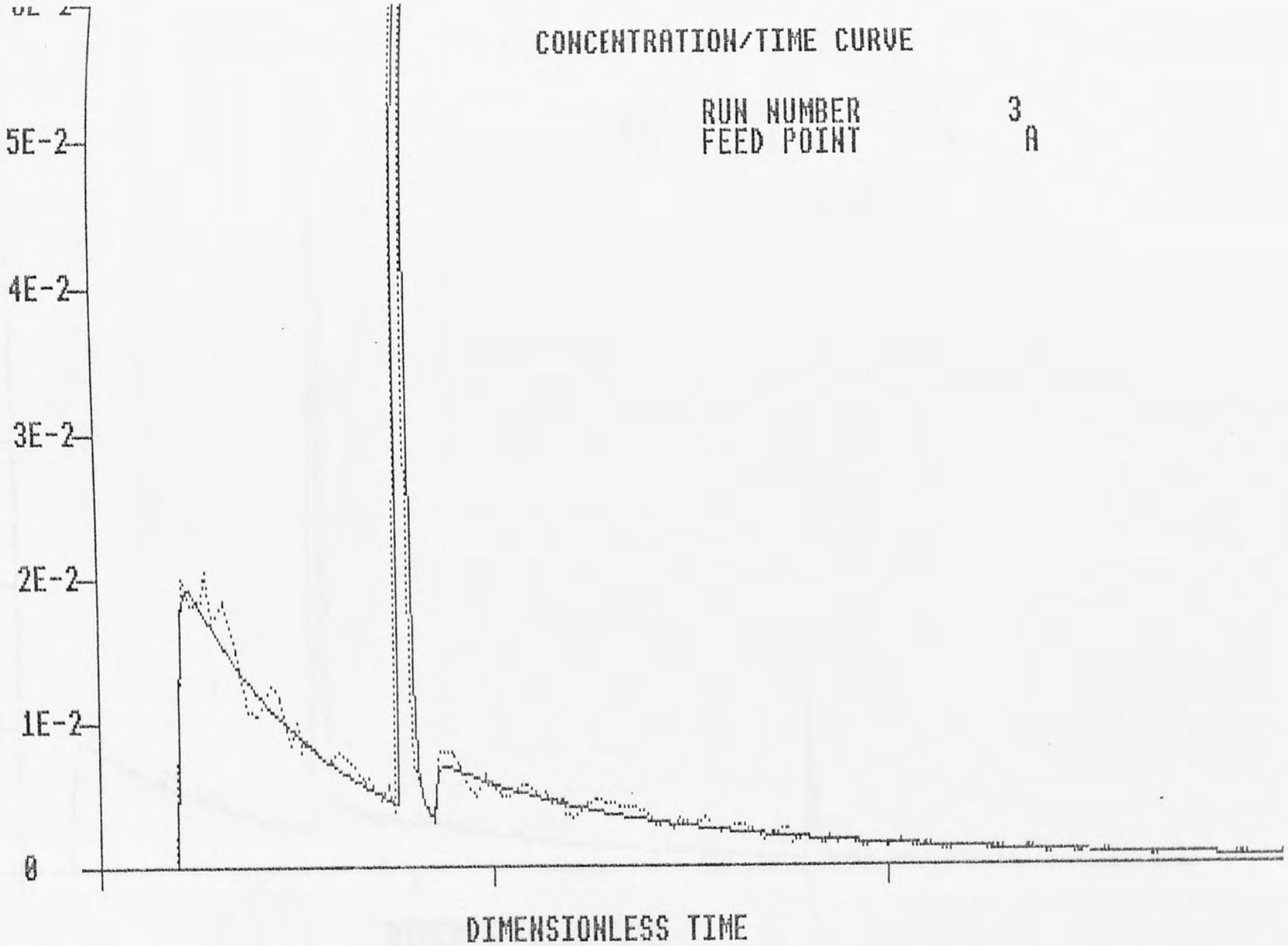

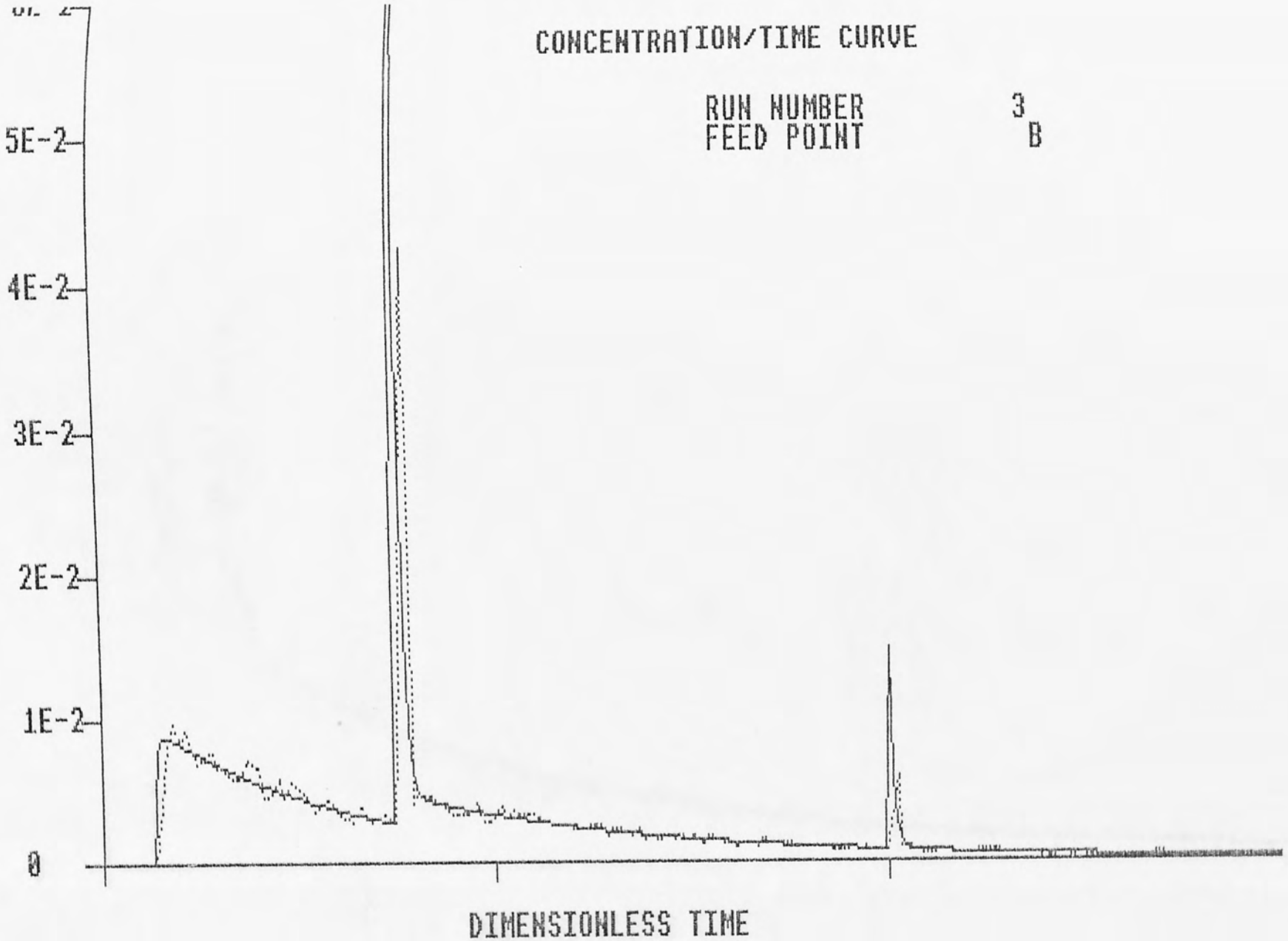

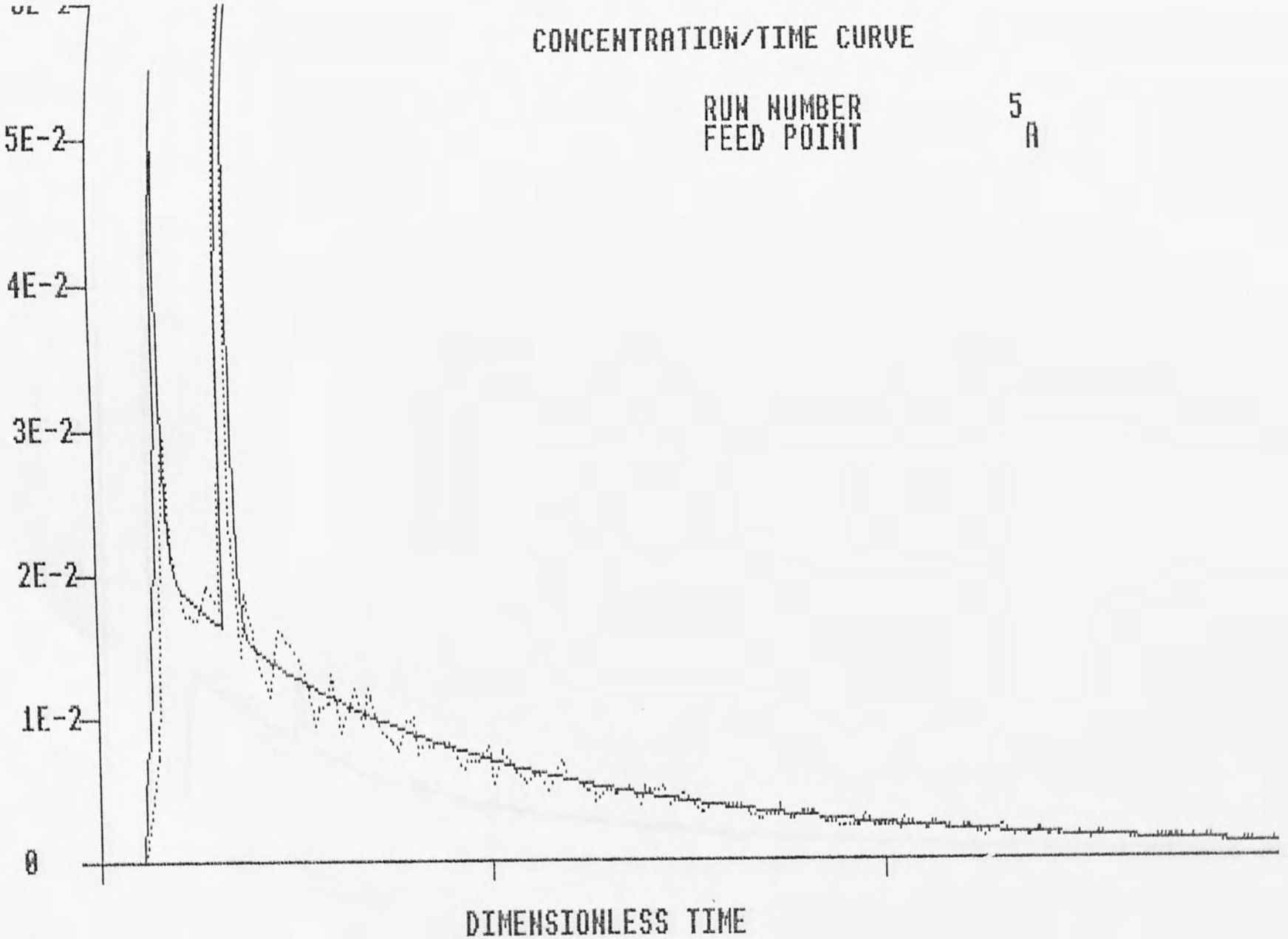

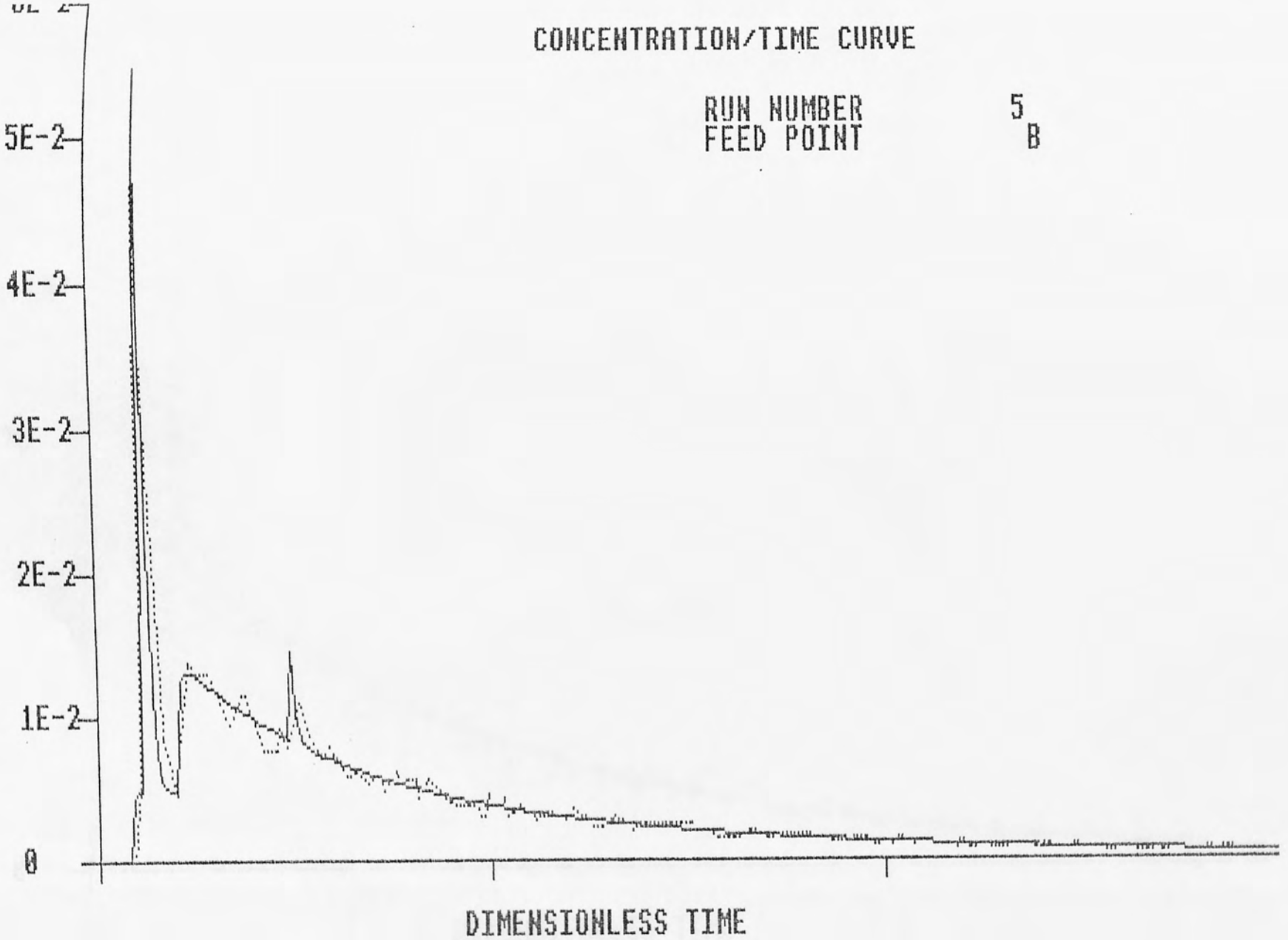

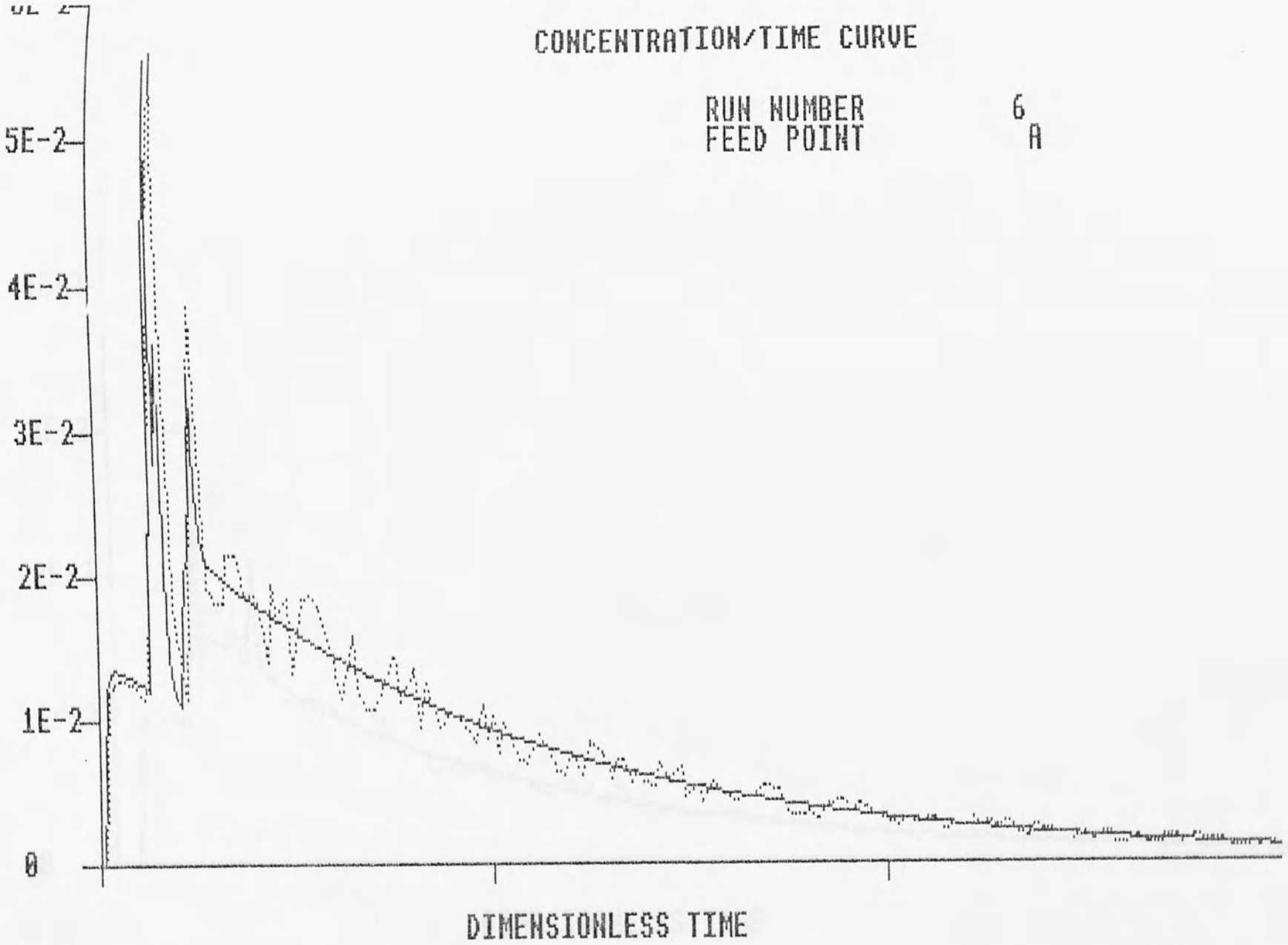

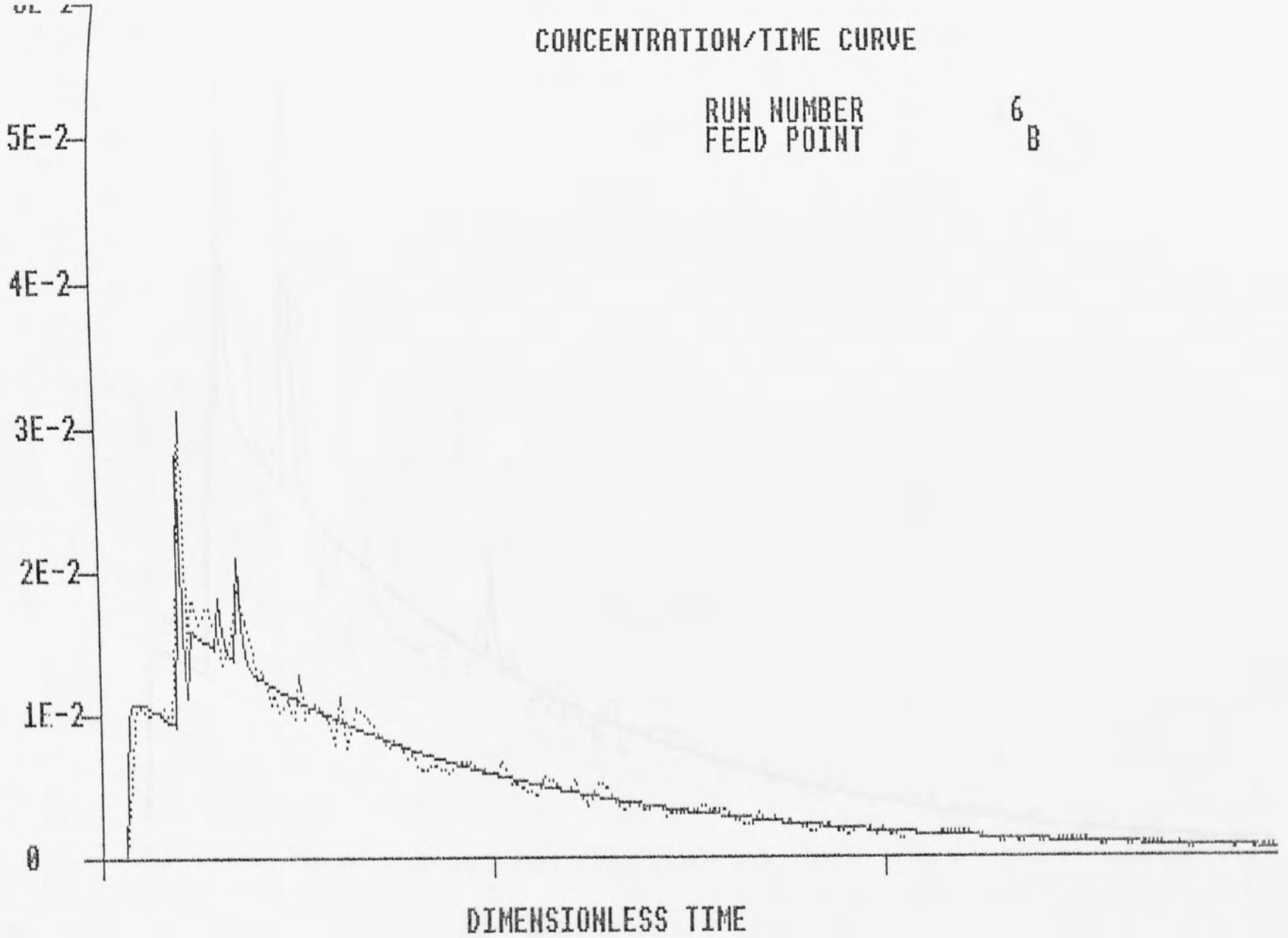

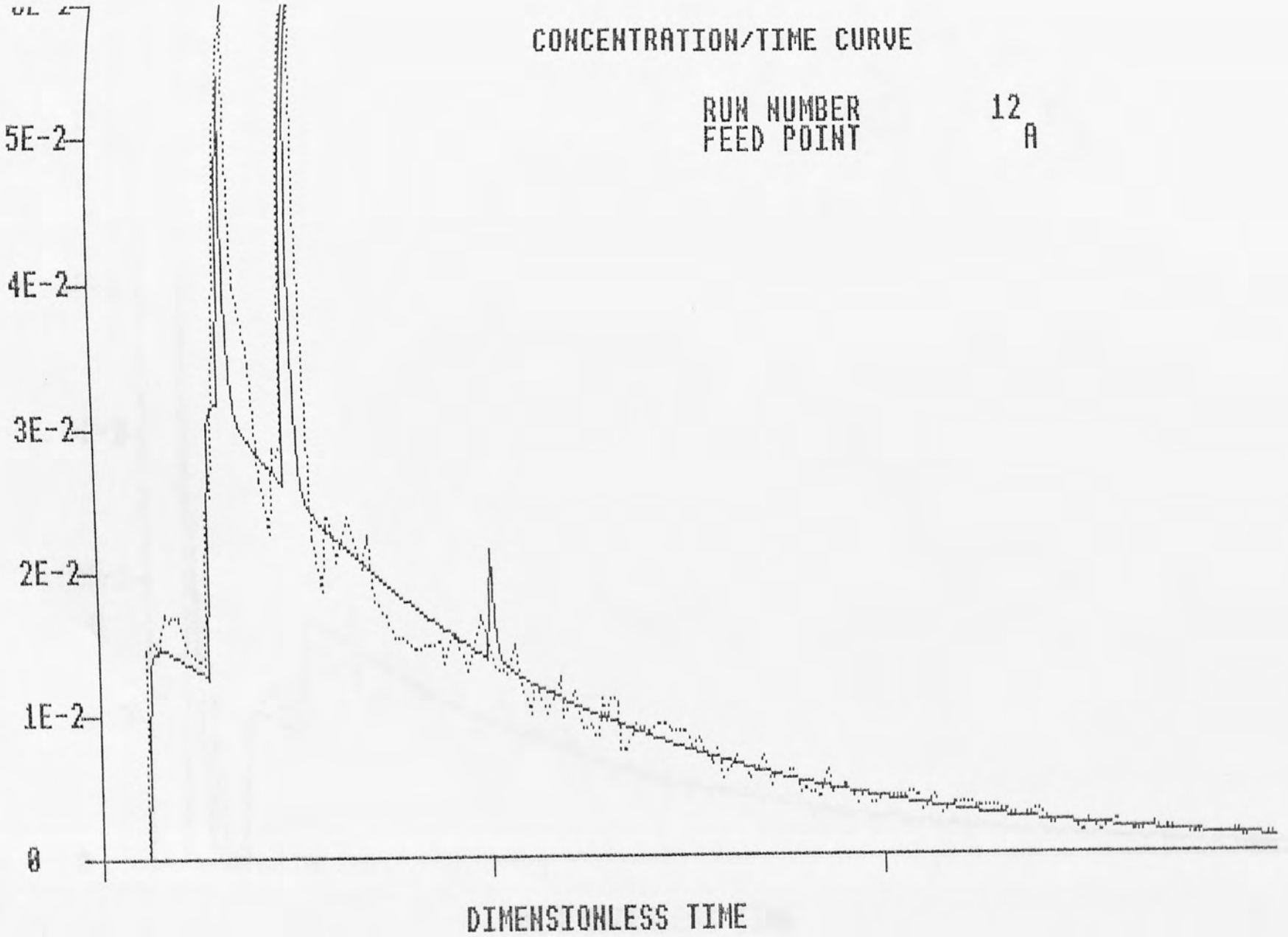

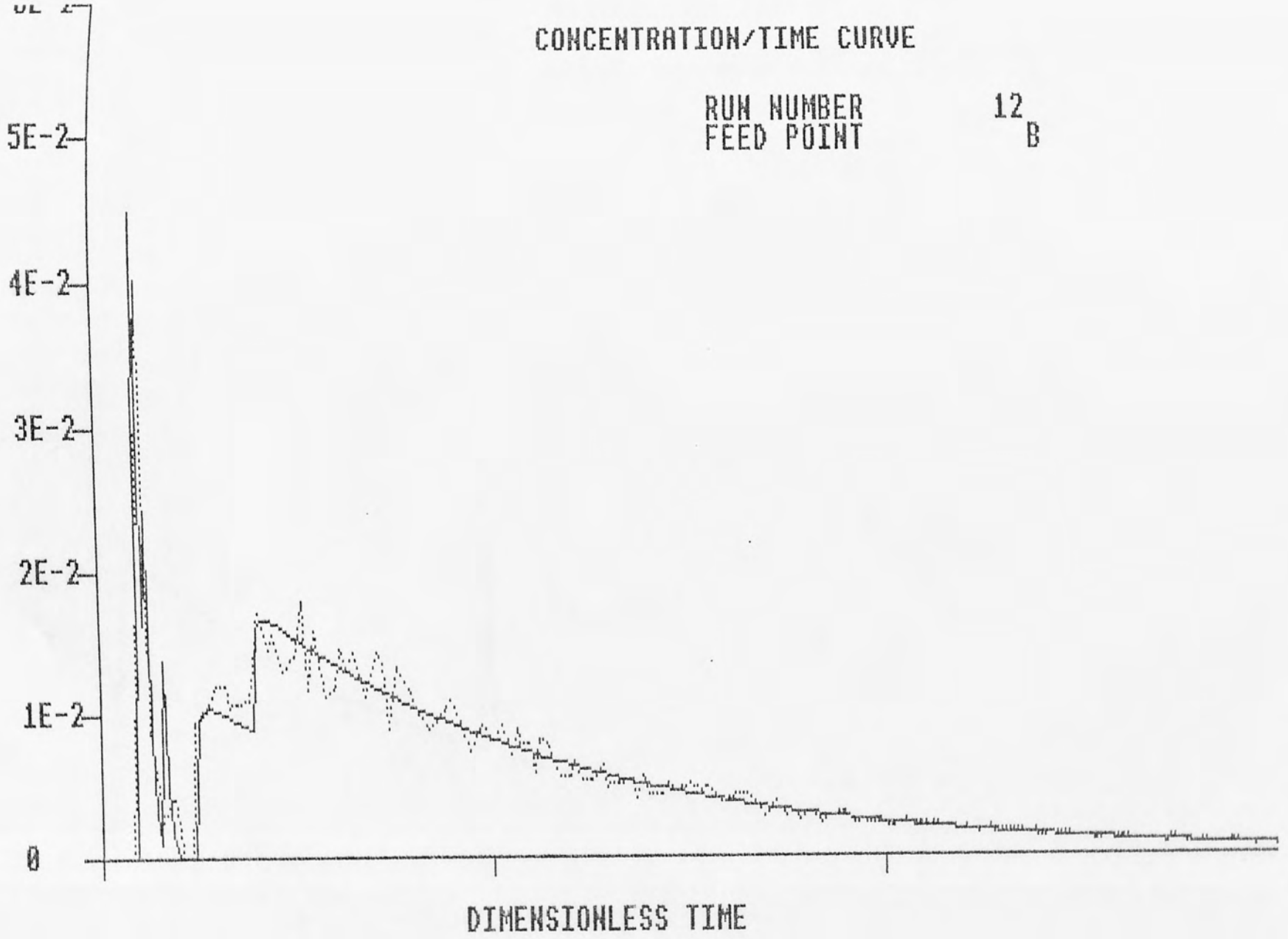

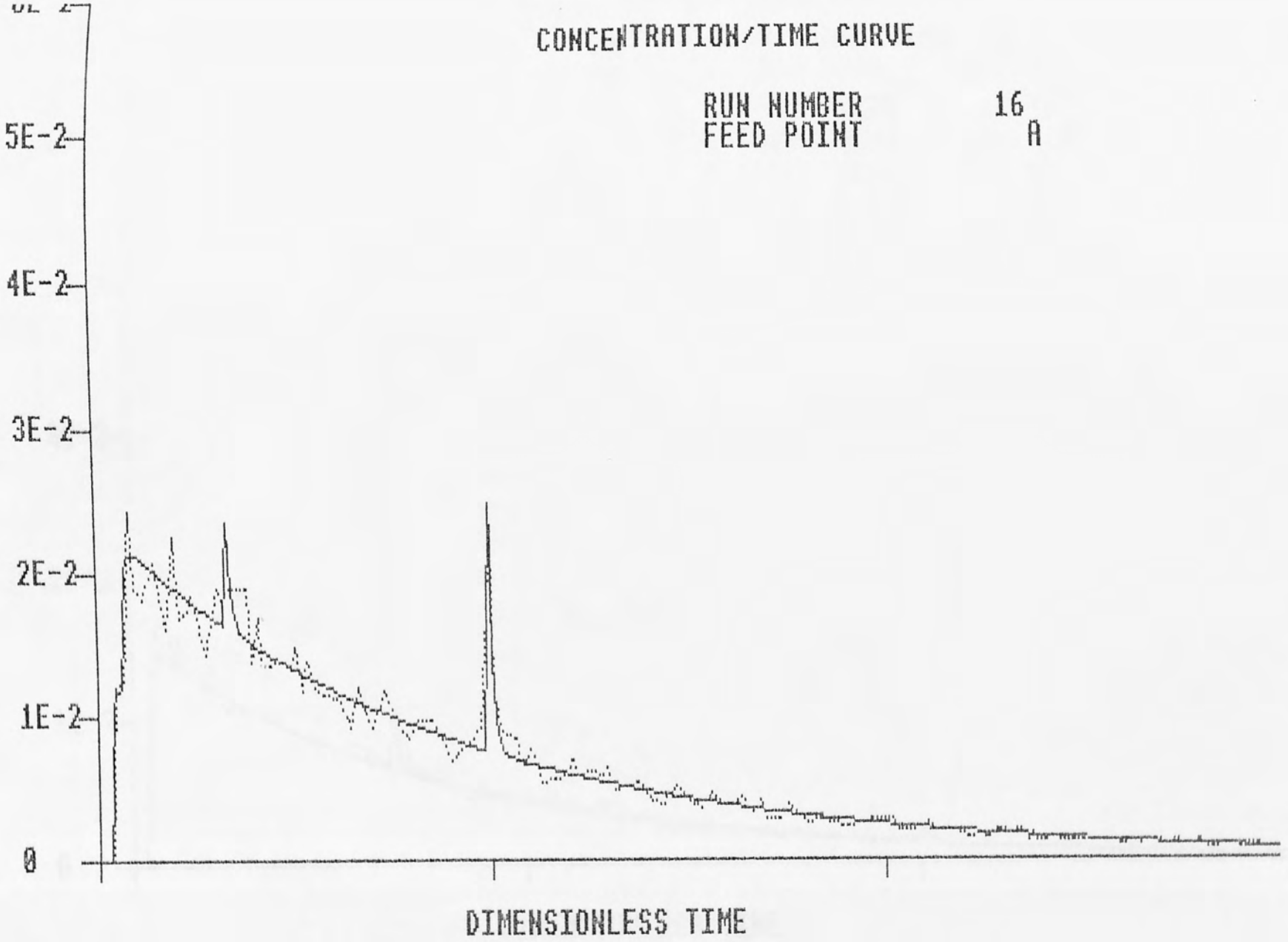

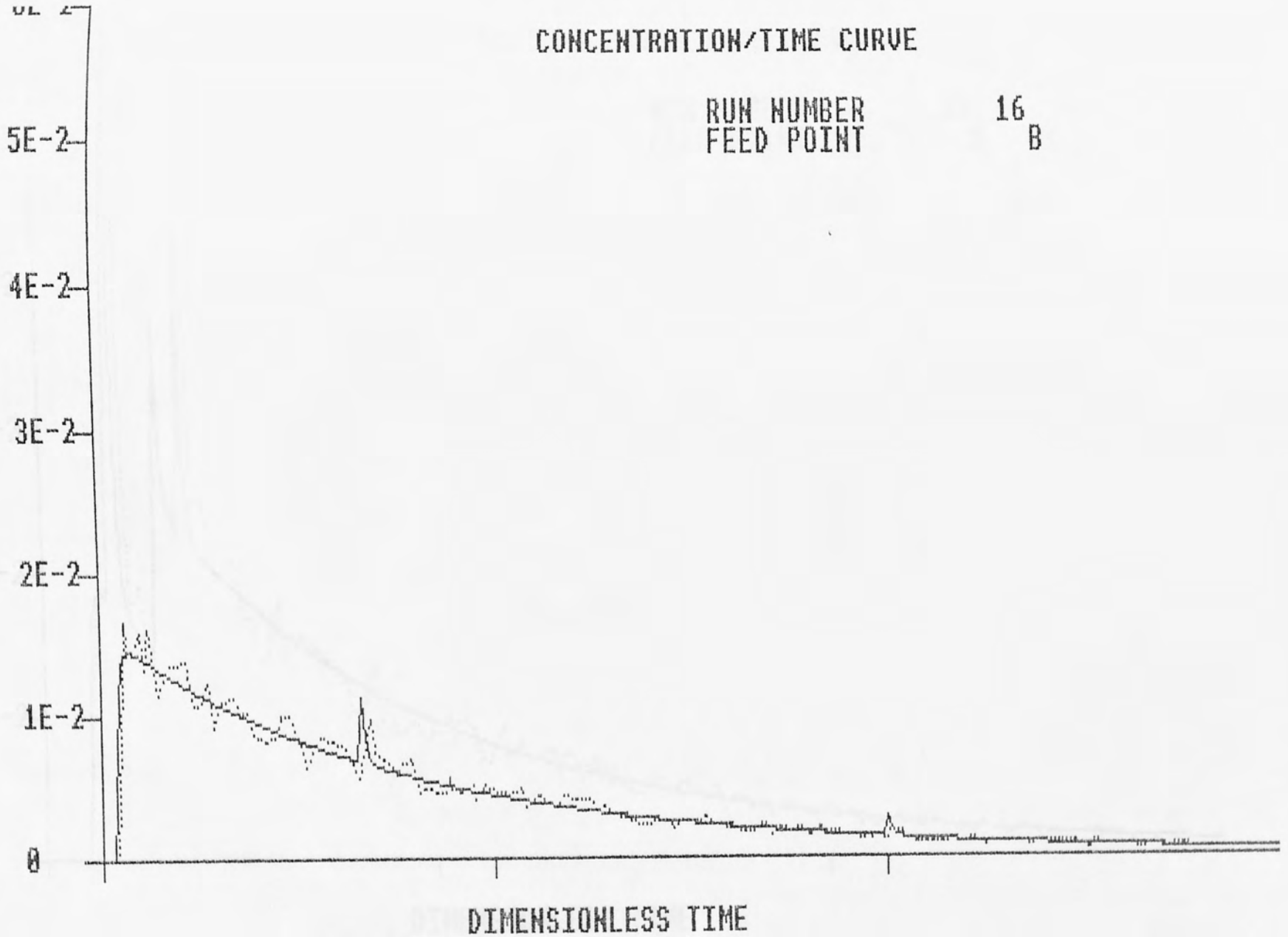

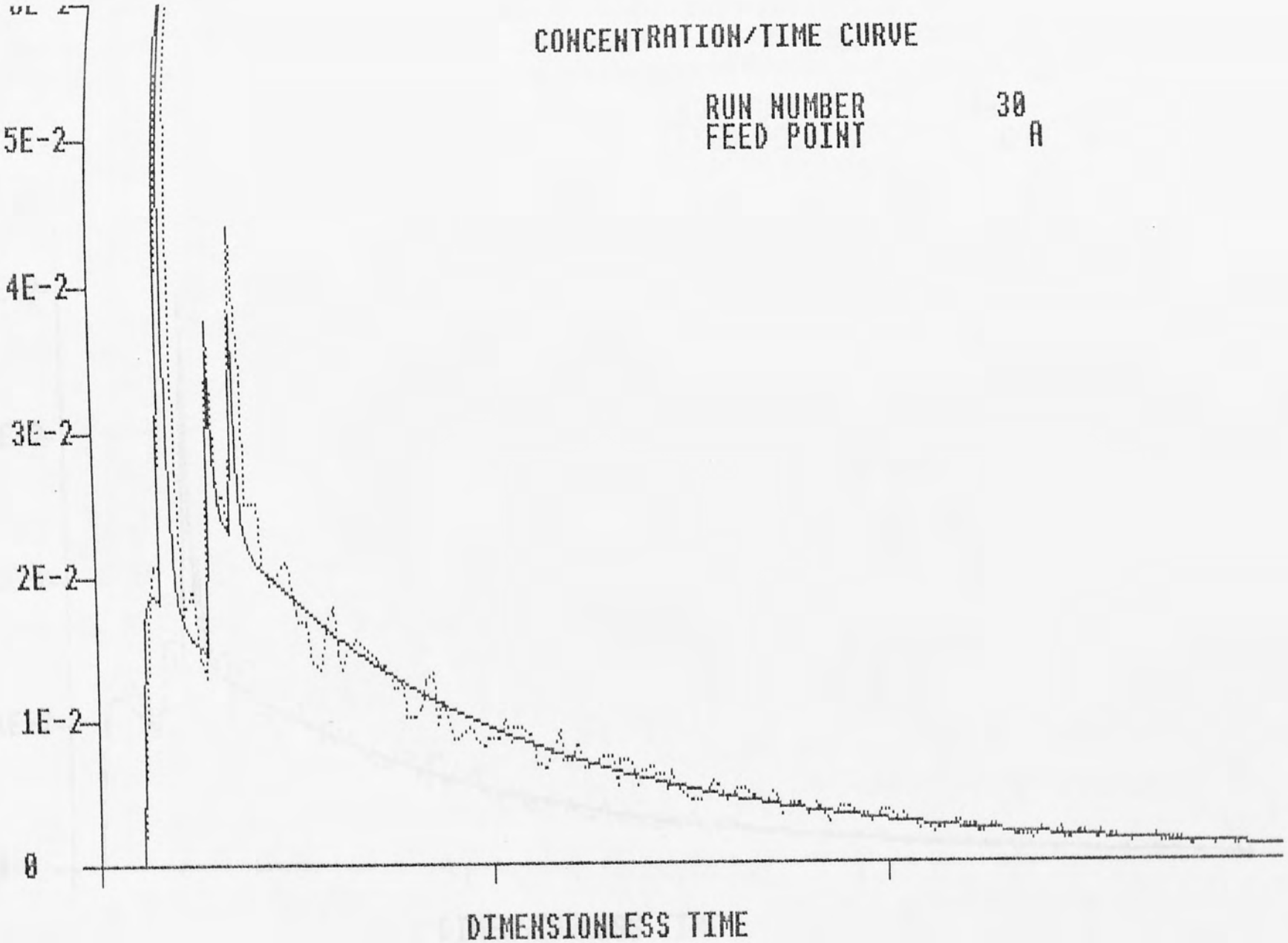

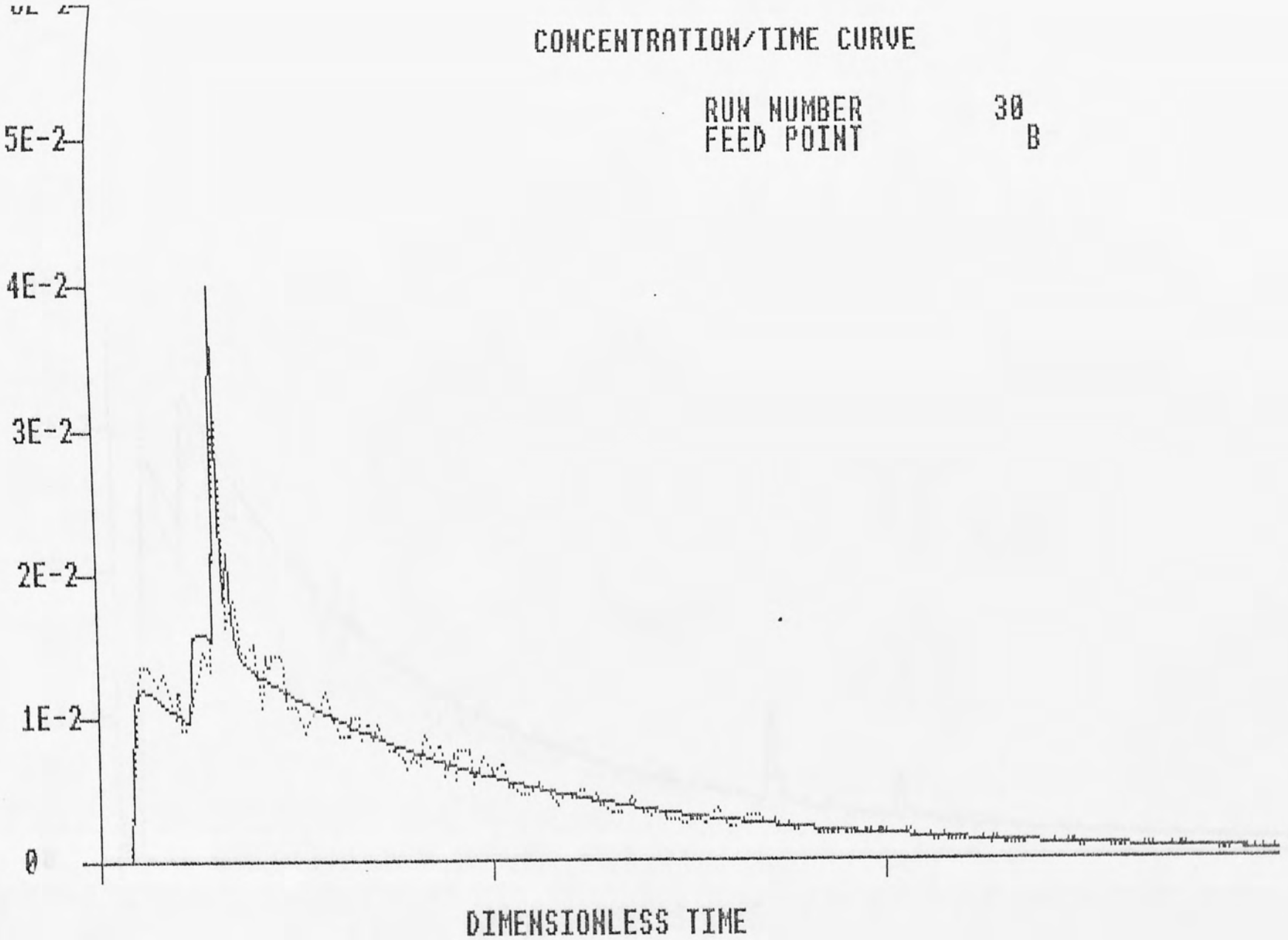

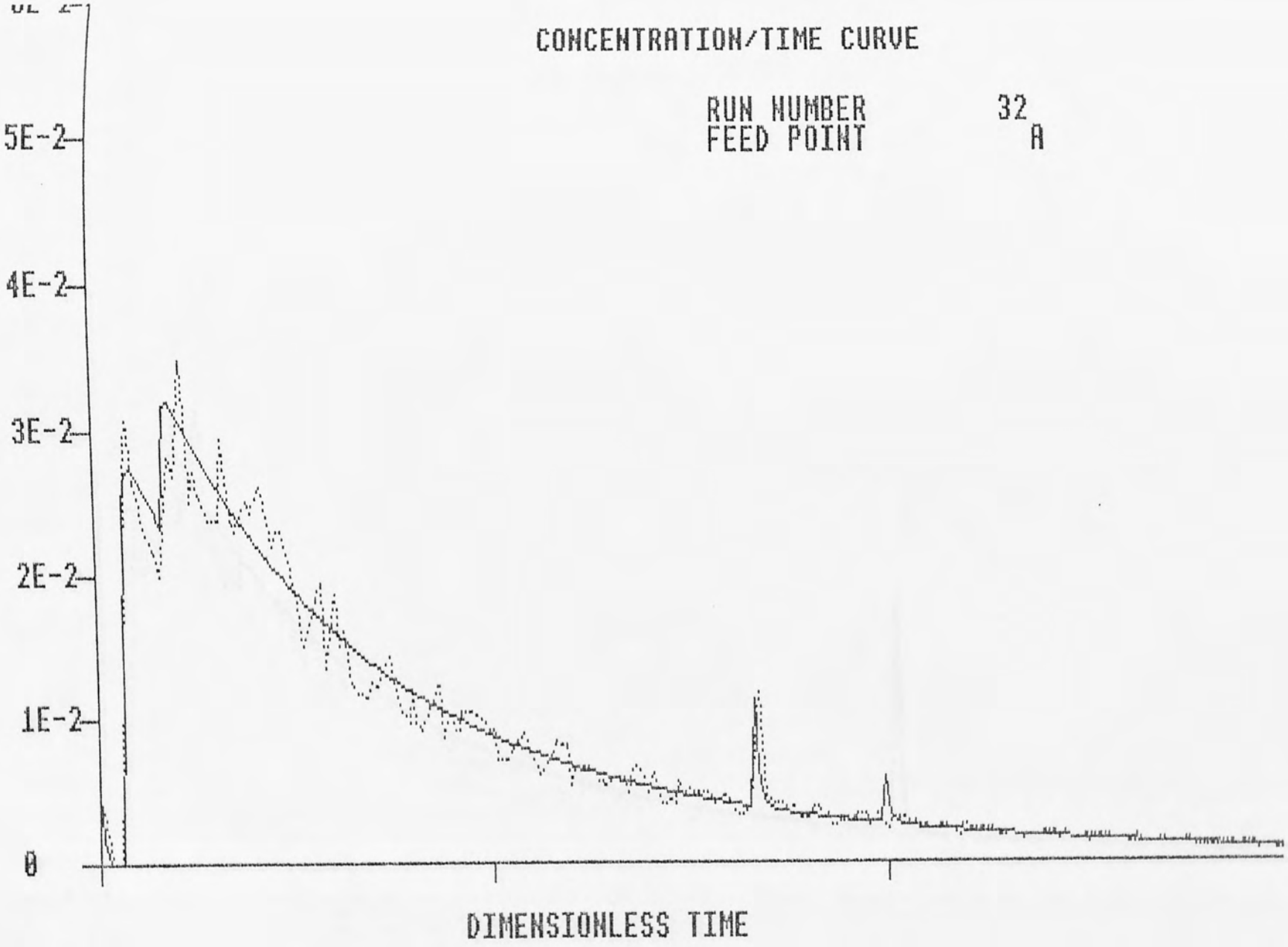

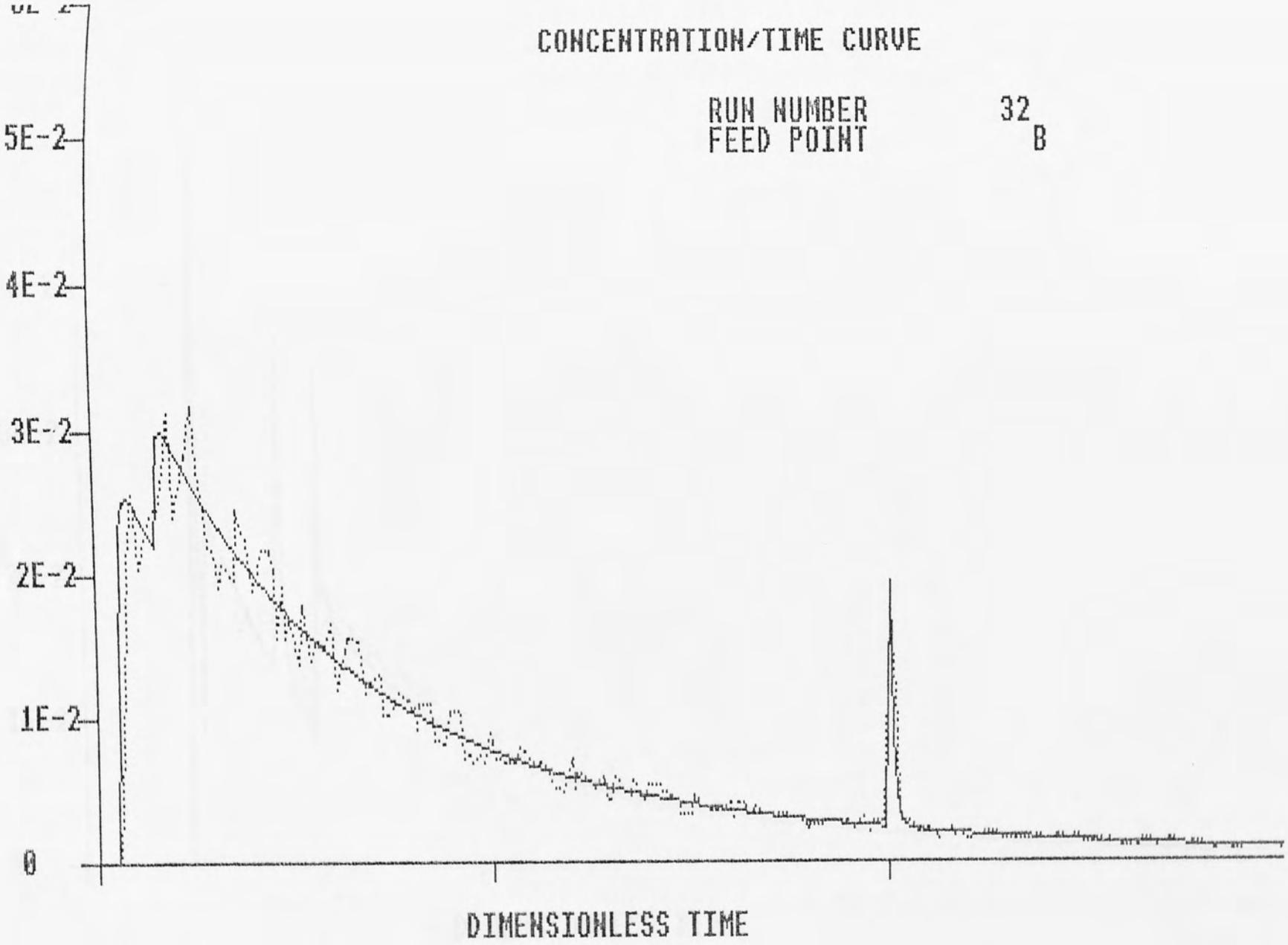

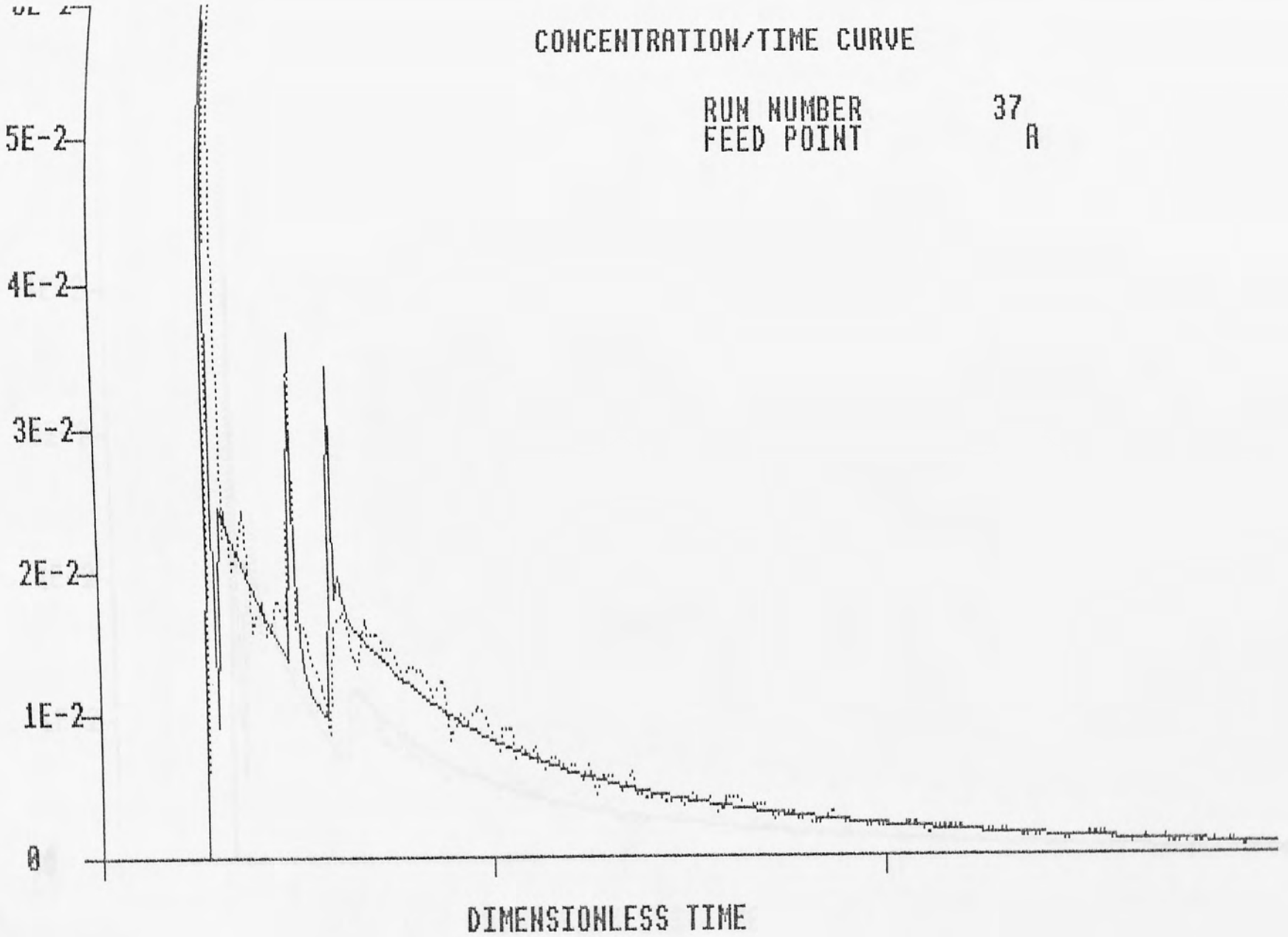

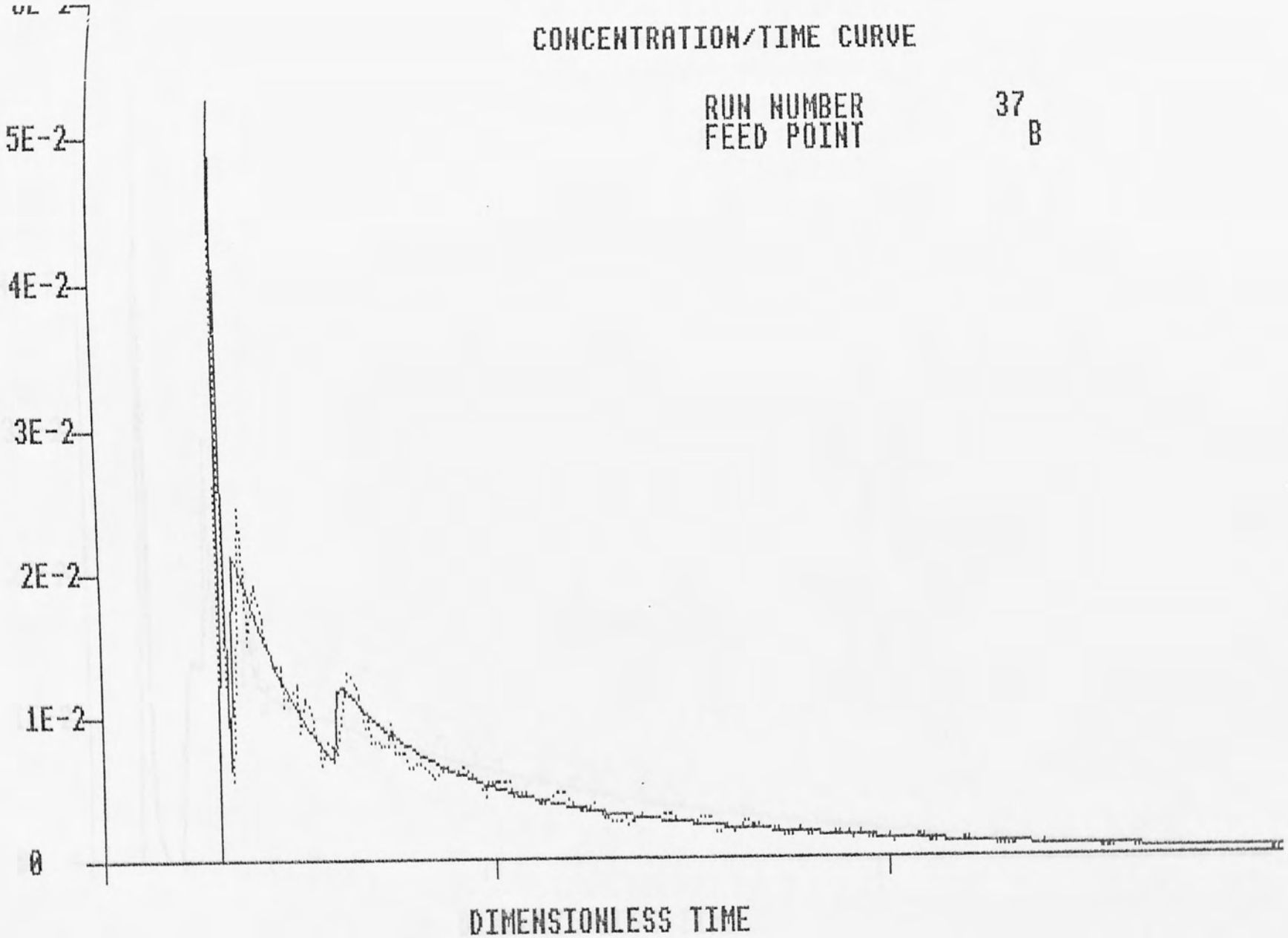

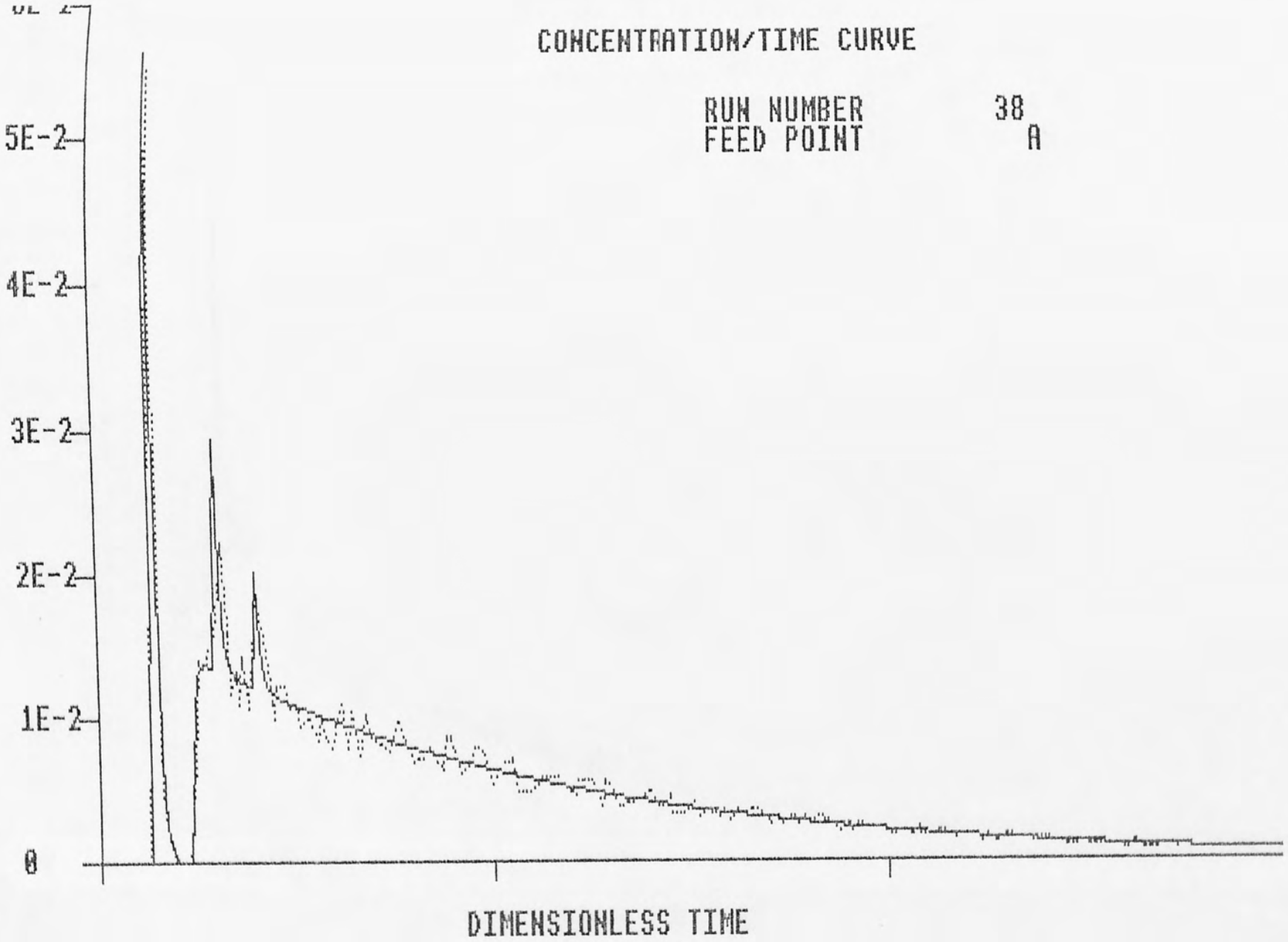

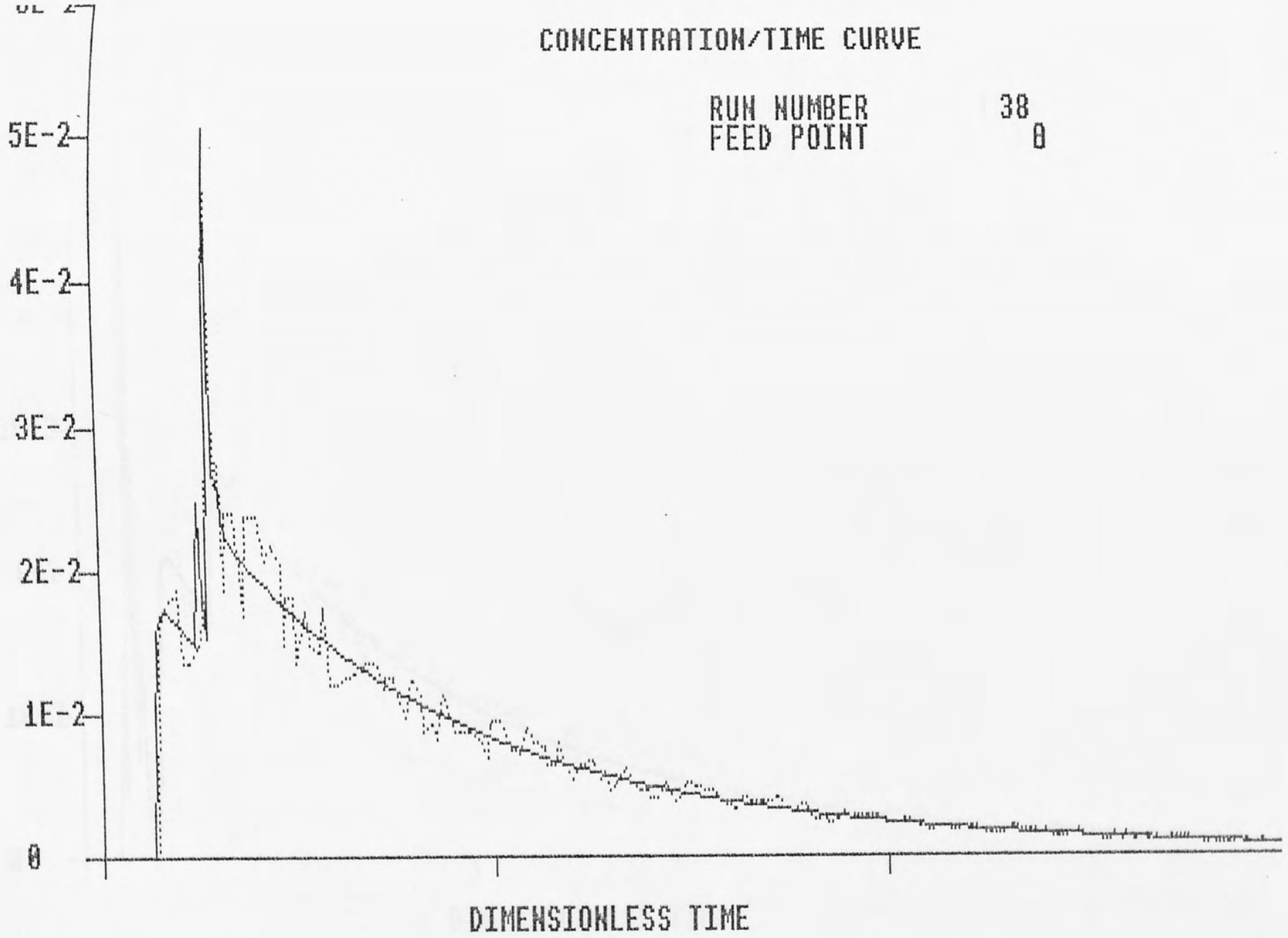

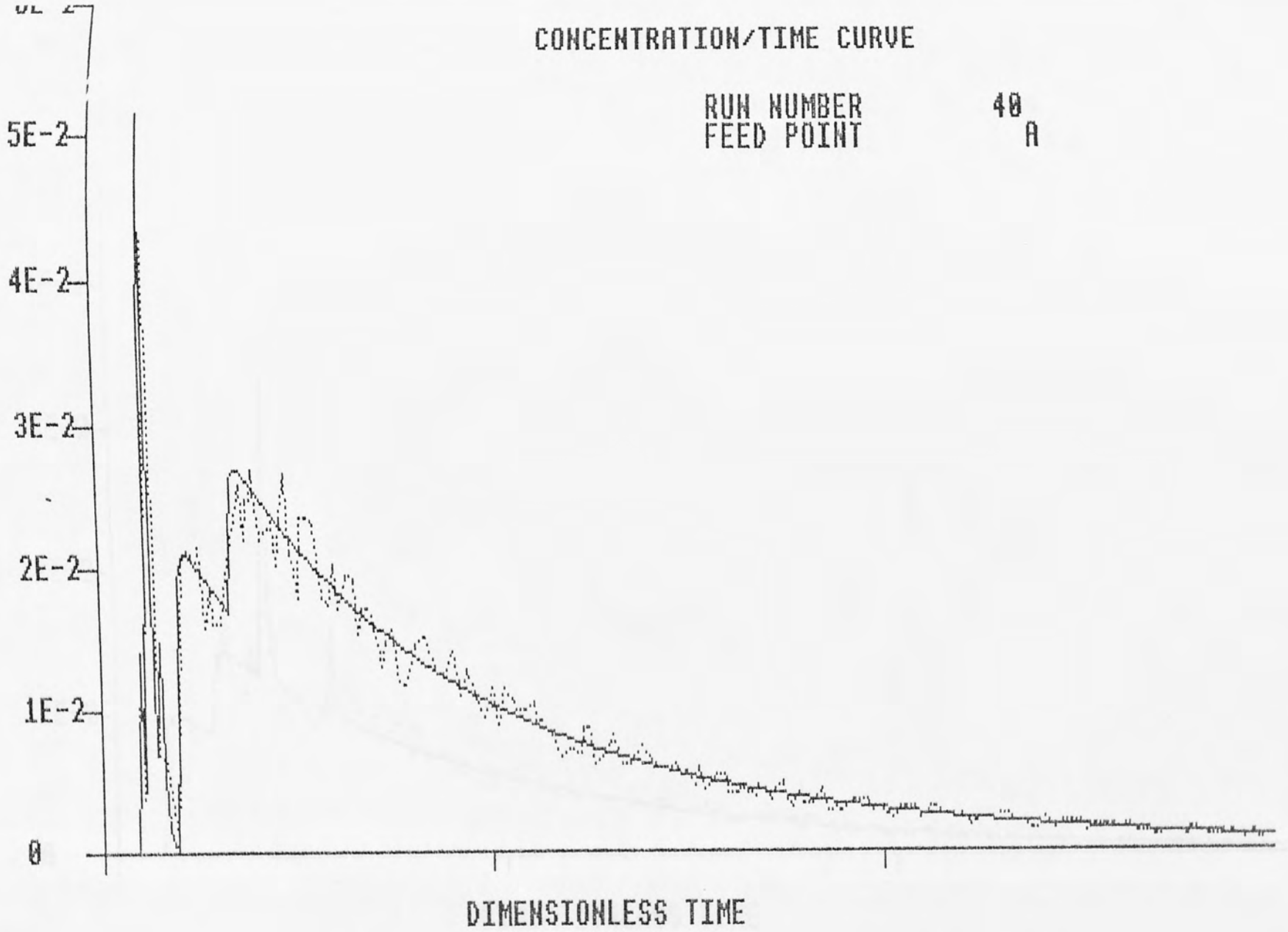

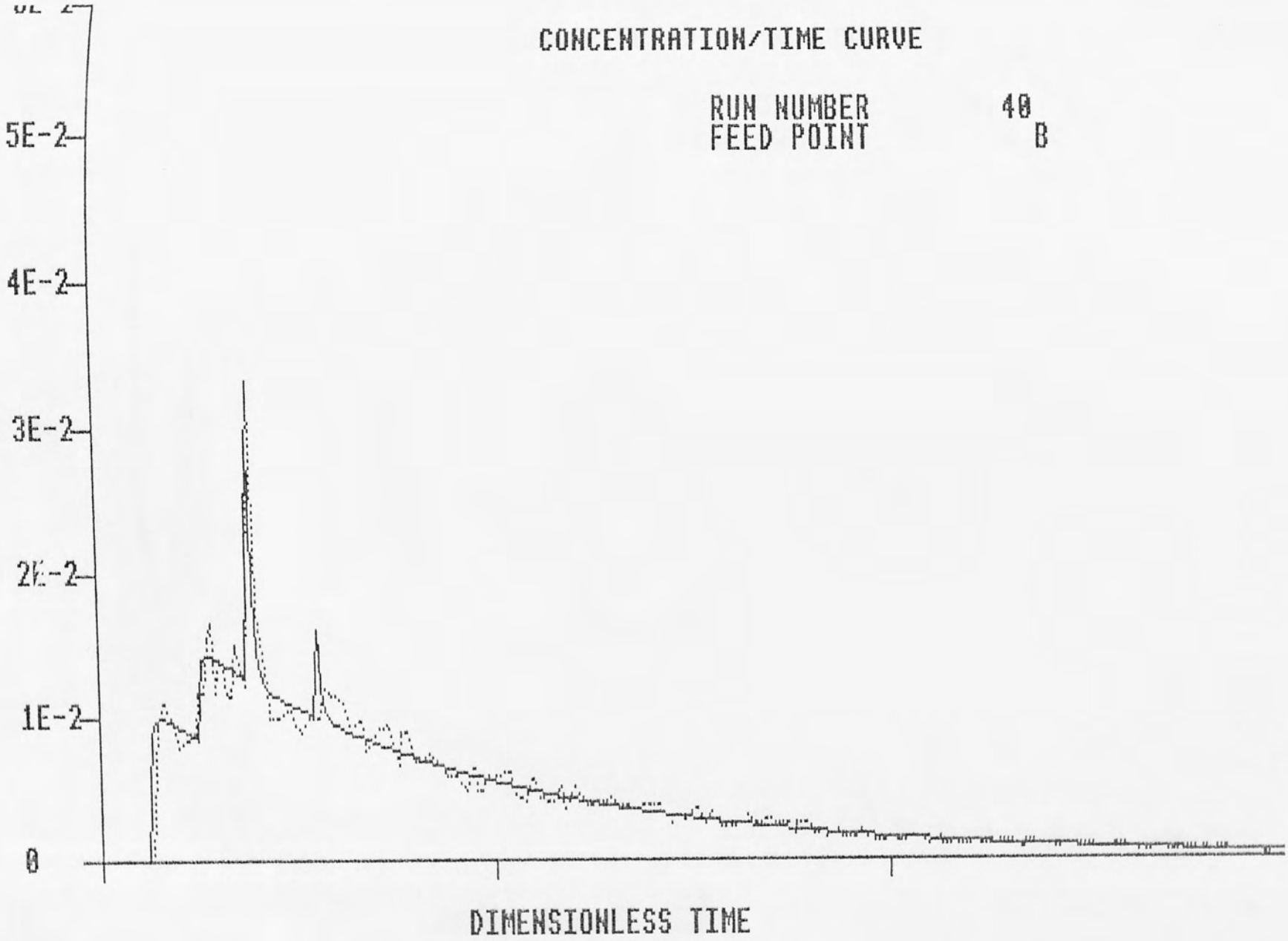
CONCENTRATION/TIME CURVE
RUN NUMBER 40
FEED POINT B
5E-2
4E-2
3E-2
2E-2
1E-2
0
DIMENSIONLESS TIME

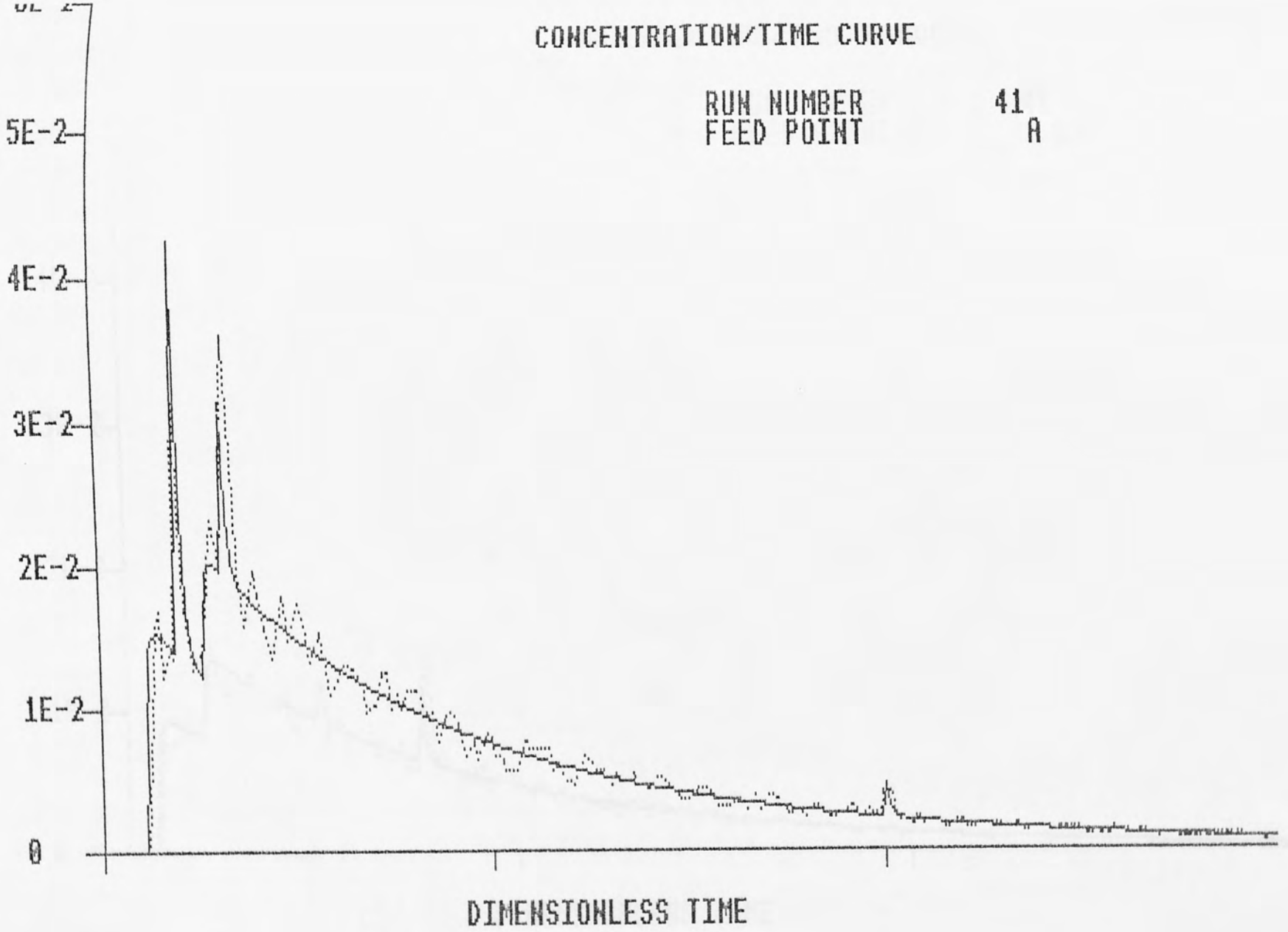
CONCENTRATION/TIME CURVE
RUN NUMBER 41
FEED POINT A
5E-2
4E-2
3E-2
2E-2
1E-2
0
DIMENSIONLESS TIME

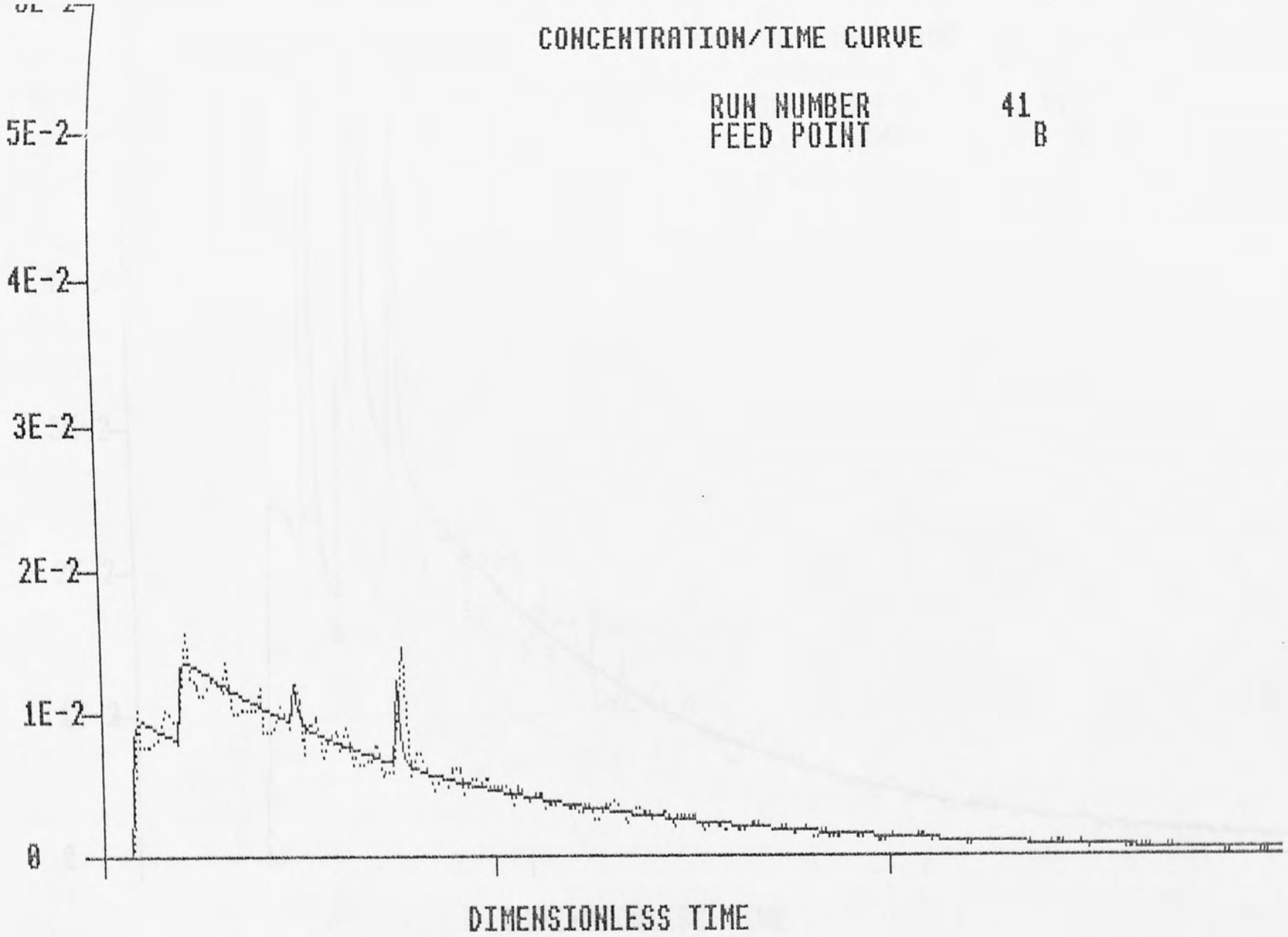

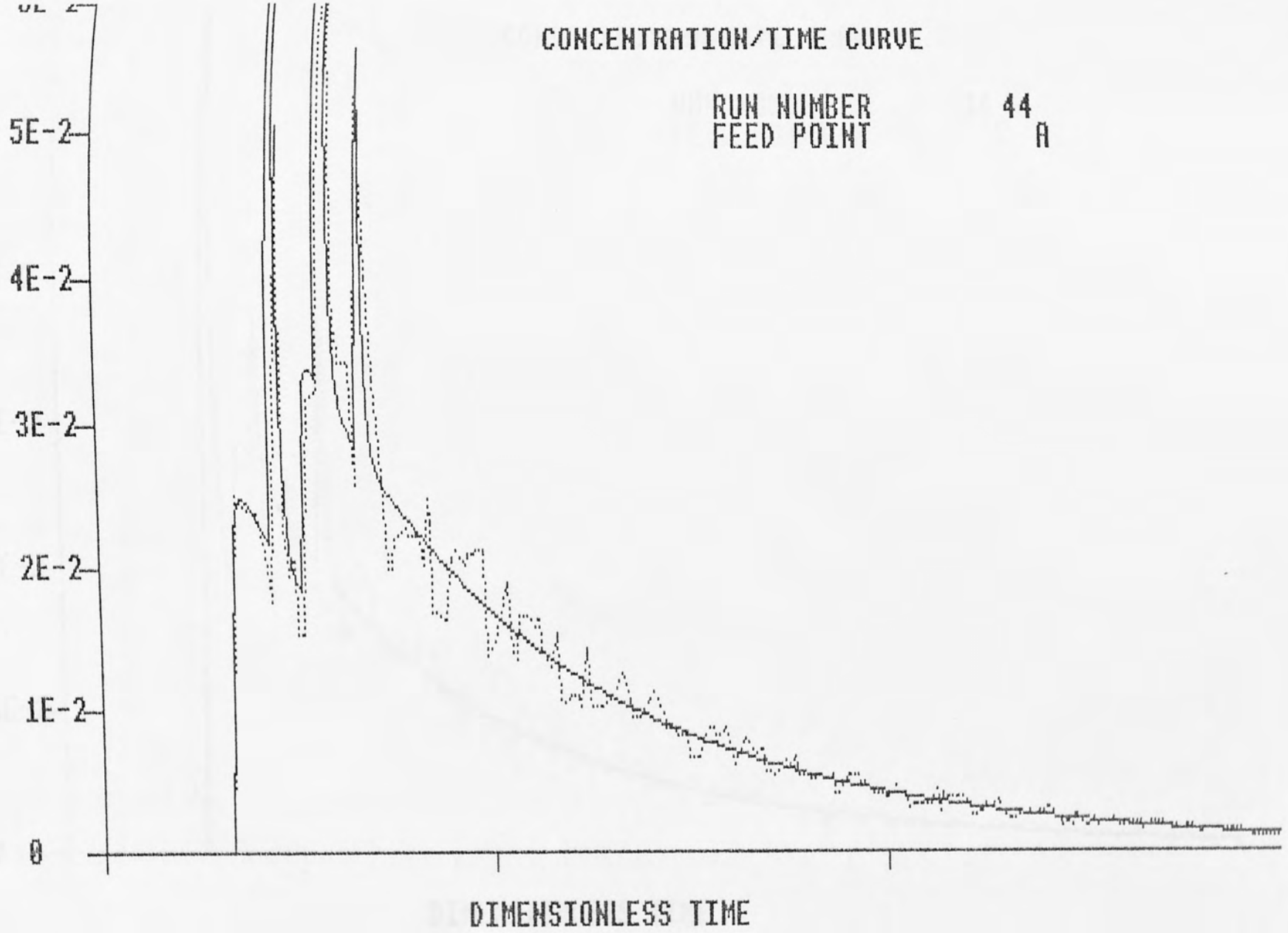
CONCENTRATION/TIME CURVE
RUN NUMBER 44
FEED POINT A
5E-2
4E-2
3E-2
2E-2
1E-2
0
DIMENSIONLESS TIME

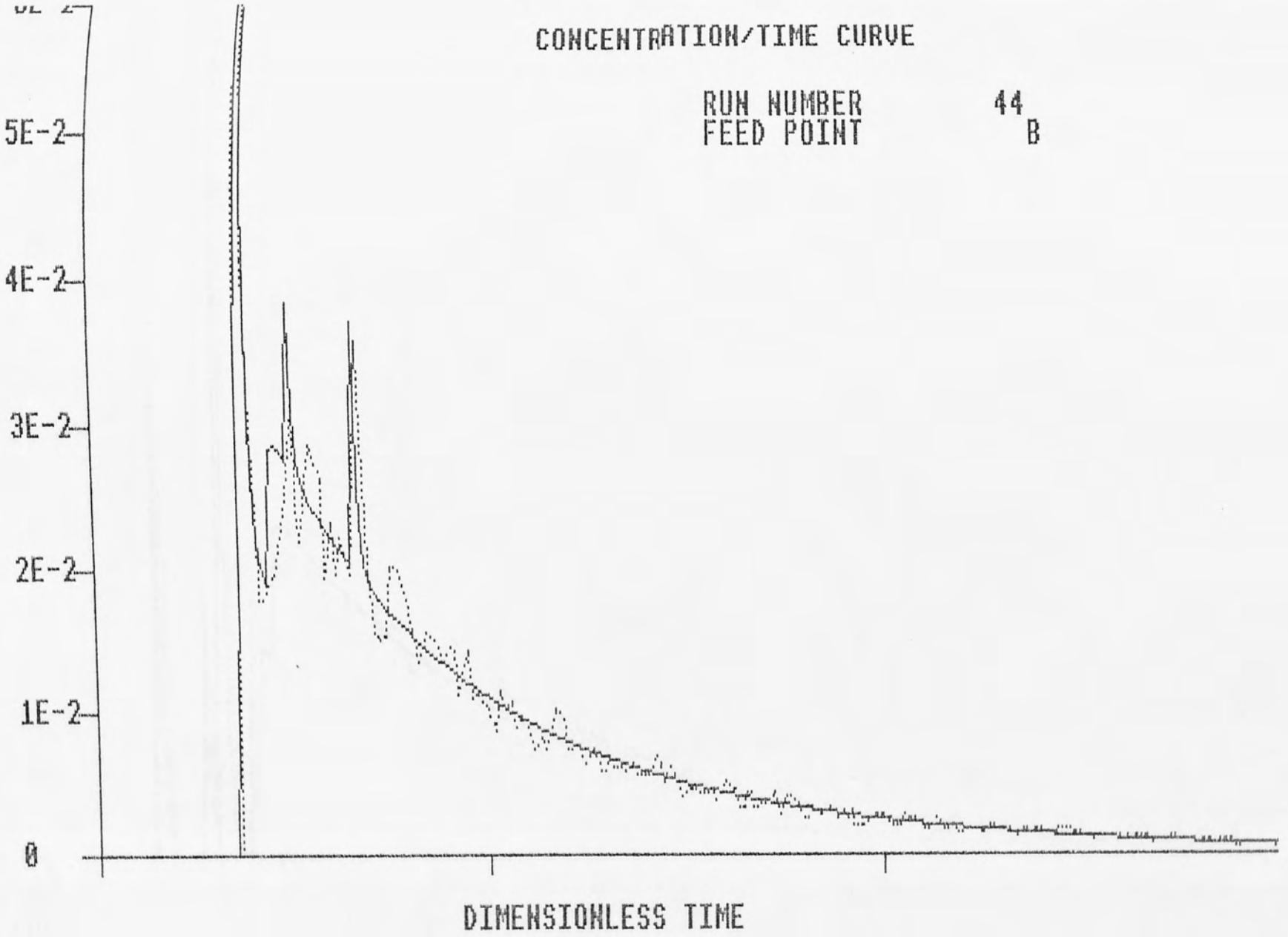
CONCENTRATION/TIME CURVE
RUN NUMBER 44
FEED POINT B
5E-2
4E-2
3E-2
2E-2
1E-2
0
DIMENSIONLESS TIME

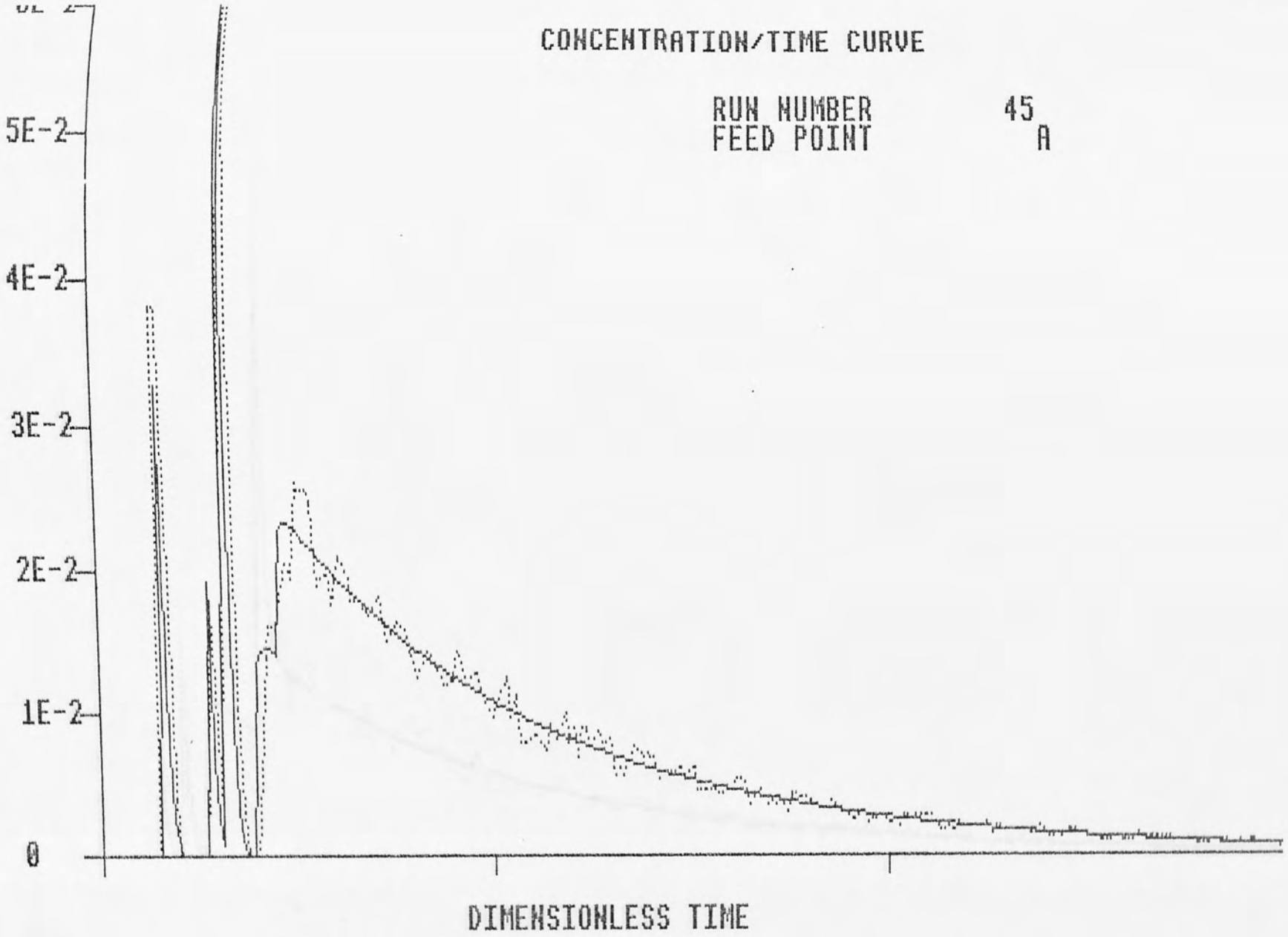
CONCENTRATION/TIME CURVE
RUN NUMBER 45
FEED POINT A
5E-2
4E-2
3E-2
2E-2
1E-2
0
DIMENSIONLESS TIME

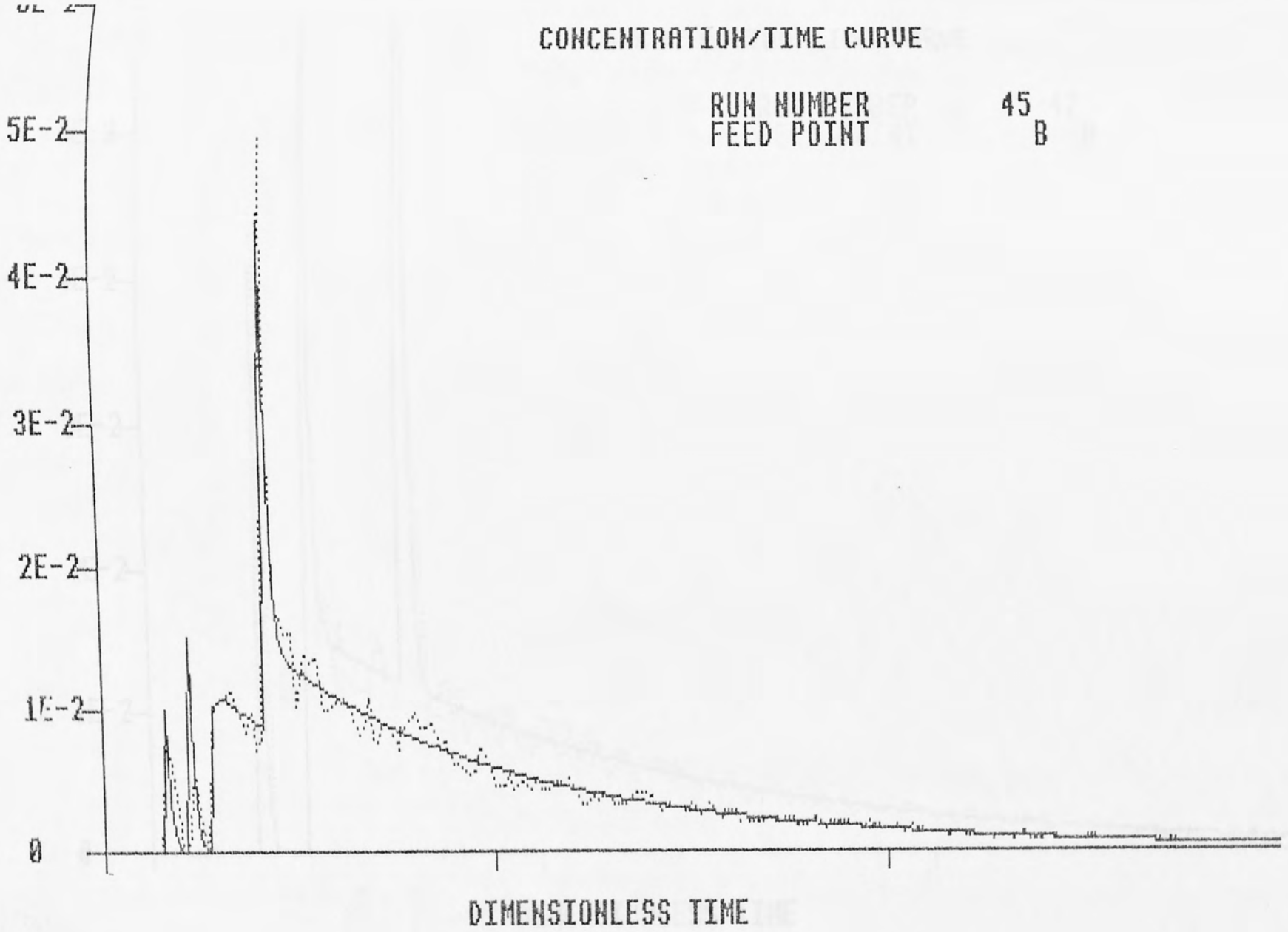
CONCENTRATION/TIME CURVE
RUN NUMBER 45
FEED POINT B
5E-2
4E-2
3E-2
2E-2
0
DIMENSIONLESS TIME

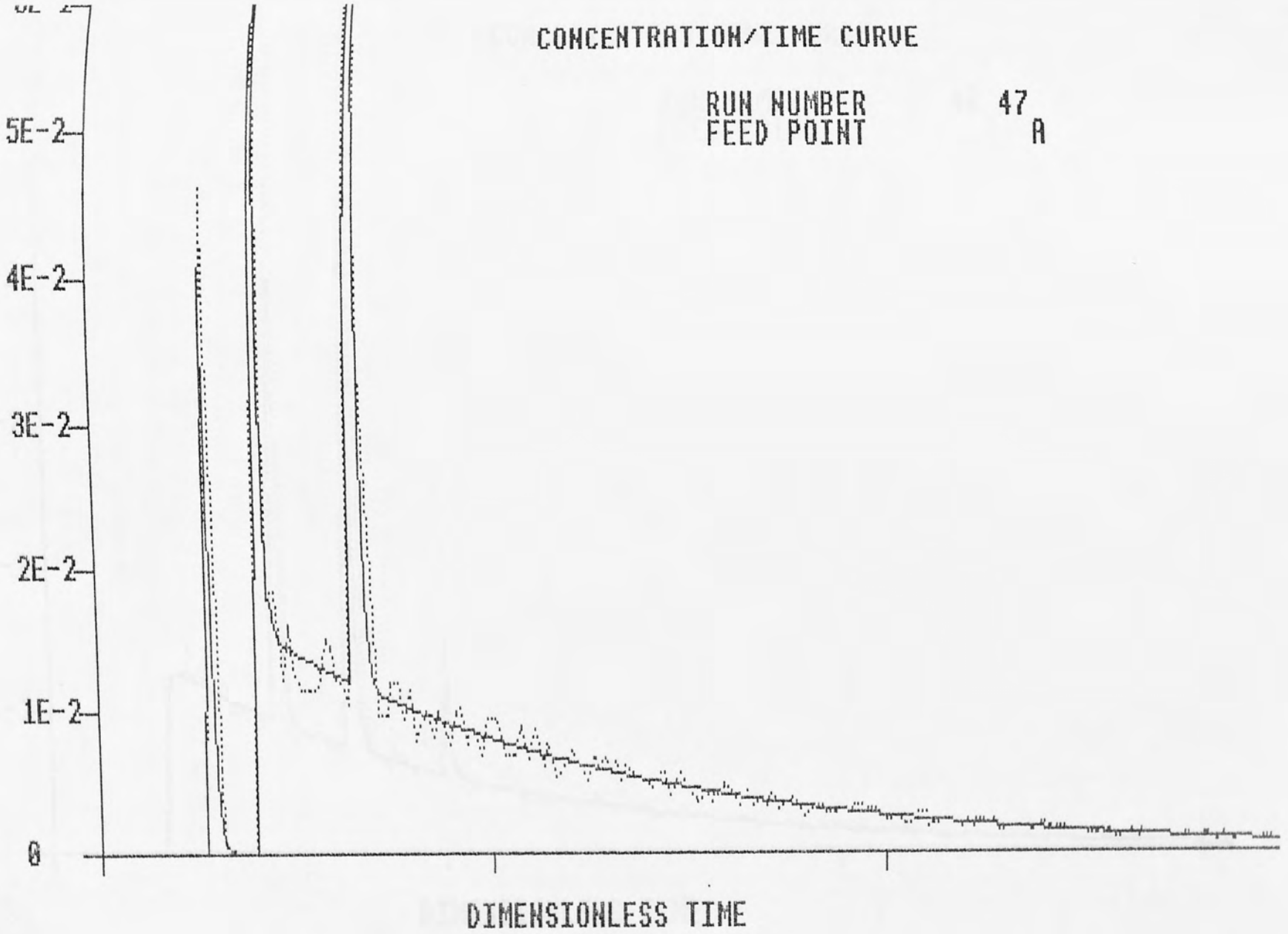
CONCENTRATION/TIME CURVE
RUN NUMBER 47
FEED POINT A
5E-2
4E-2
3E-2
2E-2
1E-2
0
DIMENSIONLESS TIME

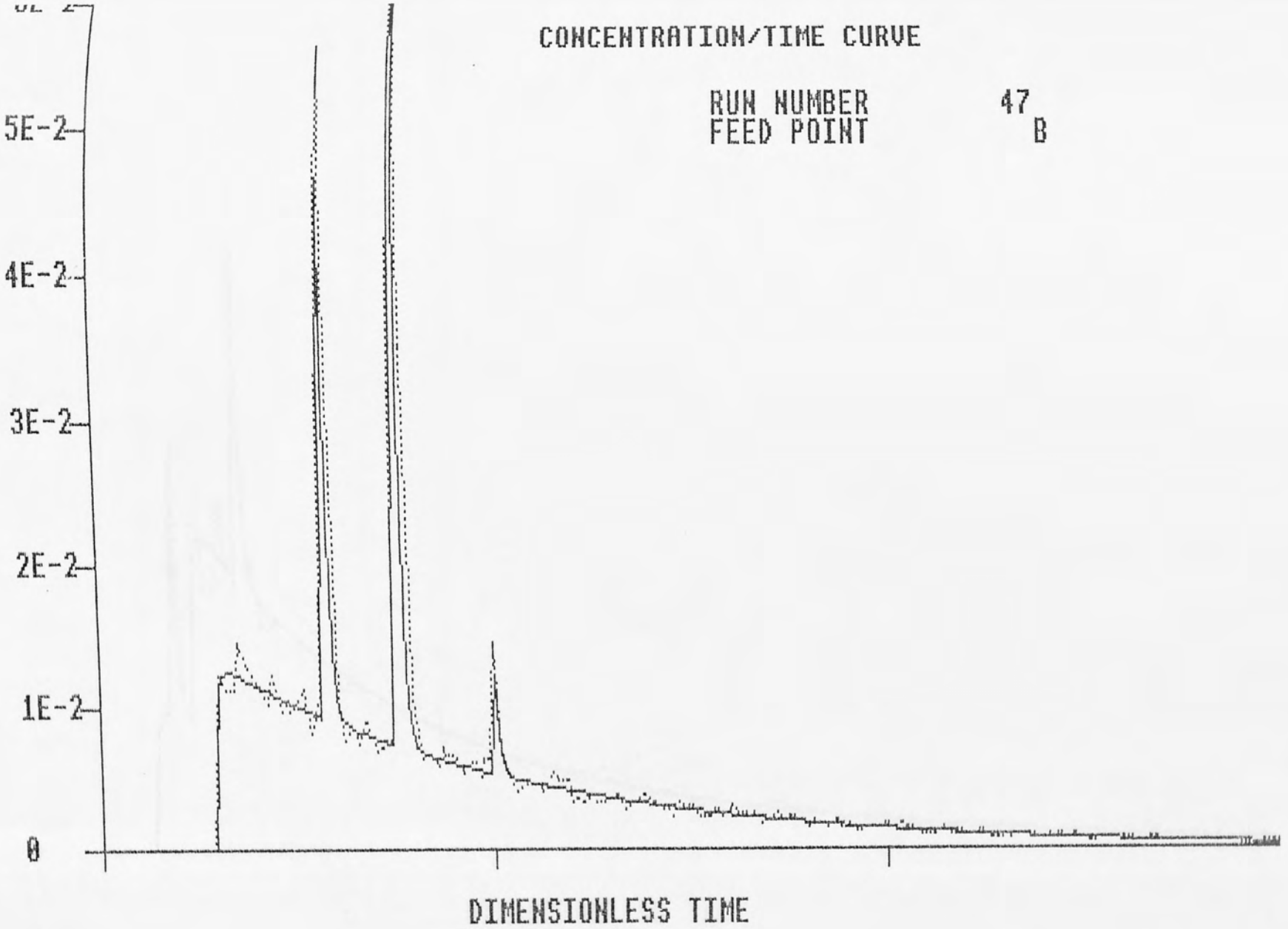
CONCENTRATION/TIME CURVE
RUN NUMBER 47
FEED POINT B
5E-2
4E-2
3E-2
2E-2
1E-2
0
DIMENSIONLESS TIME

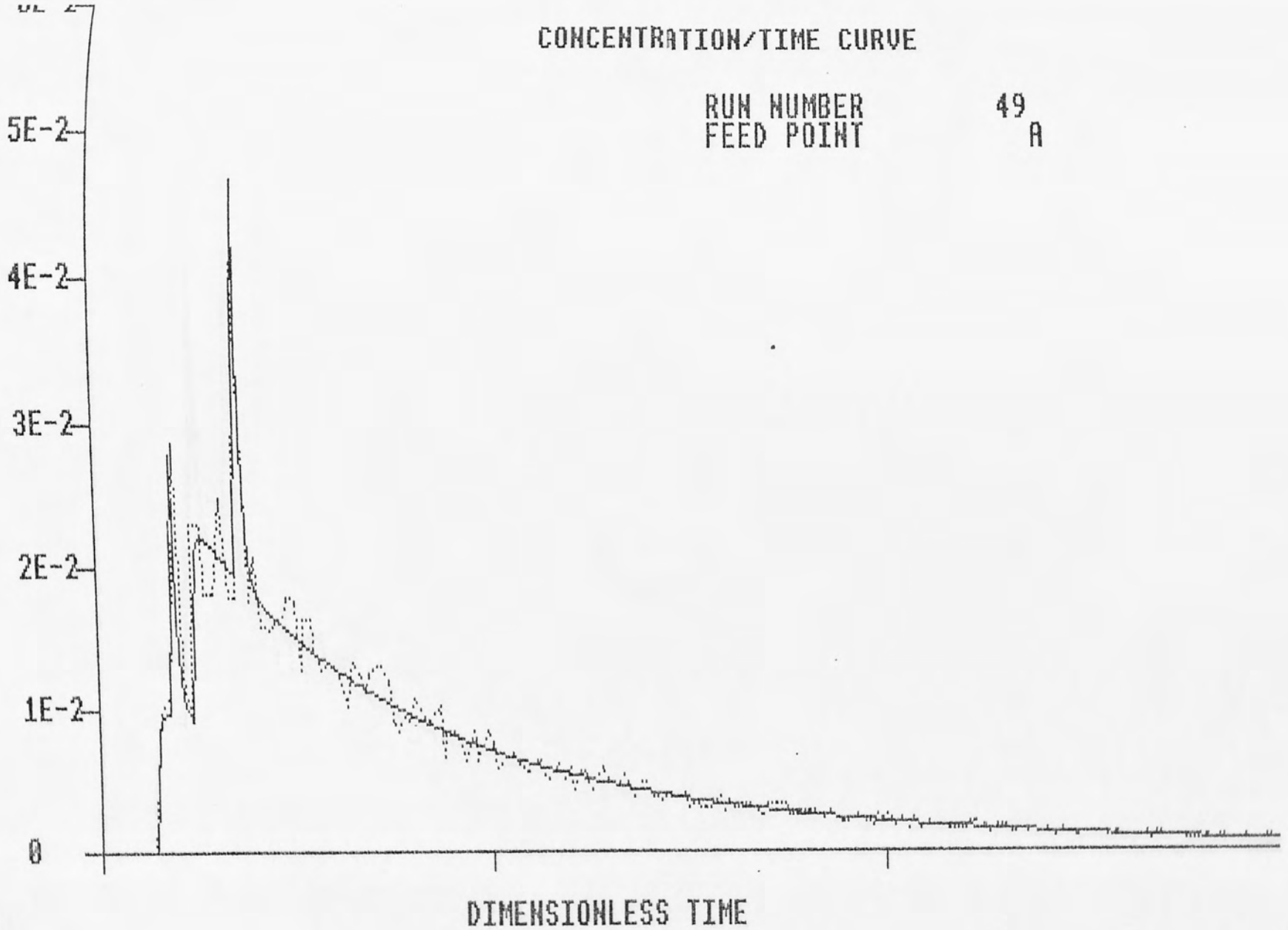

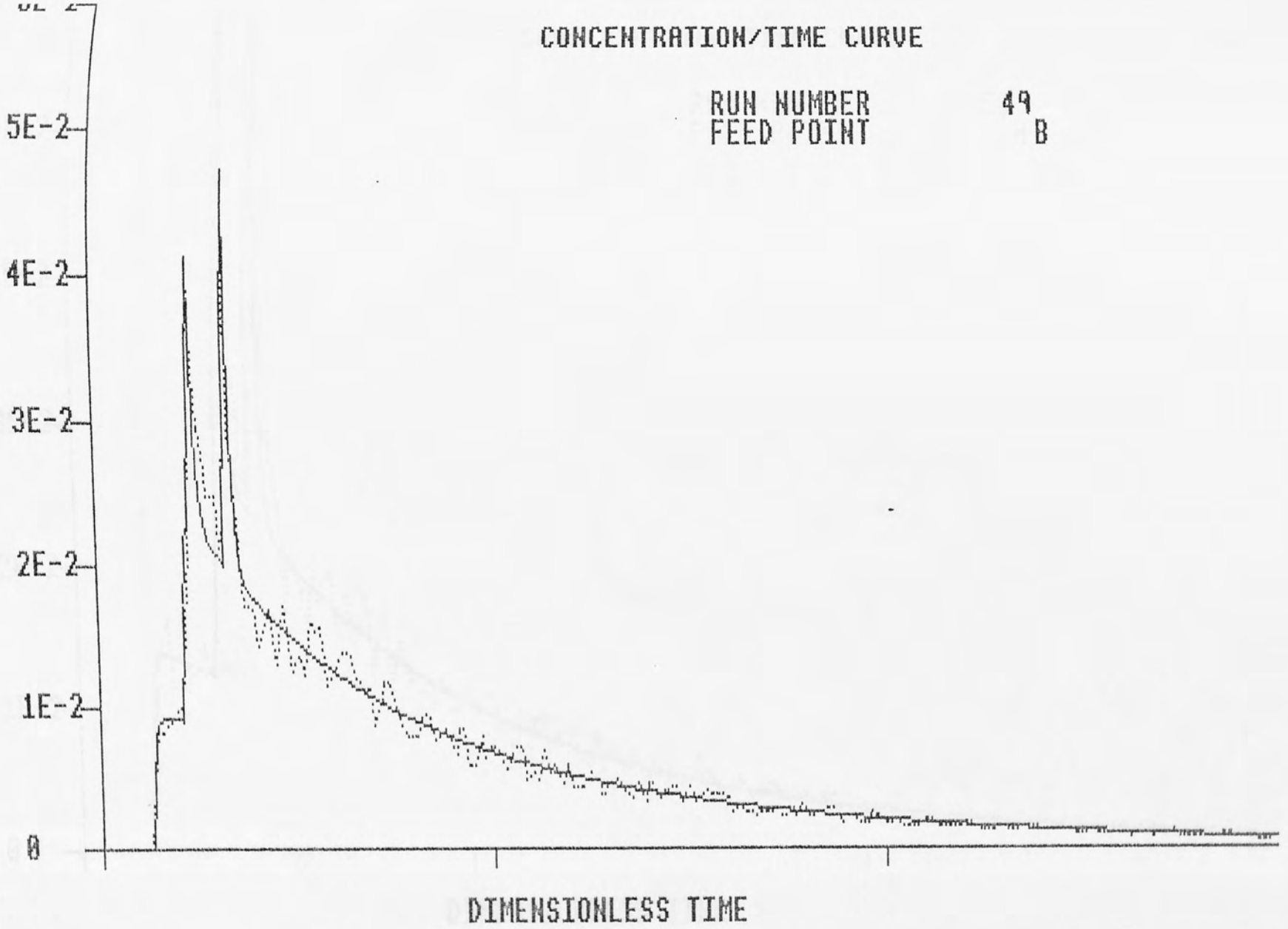
CONCENTRATION/TIME CURVE
RUN NUMBER 49
FEED POINT B
5E-2
4E-2
3E-2
2E-2
1E-2
0
DIMENSIONLESS TIME

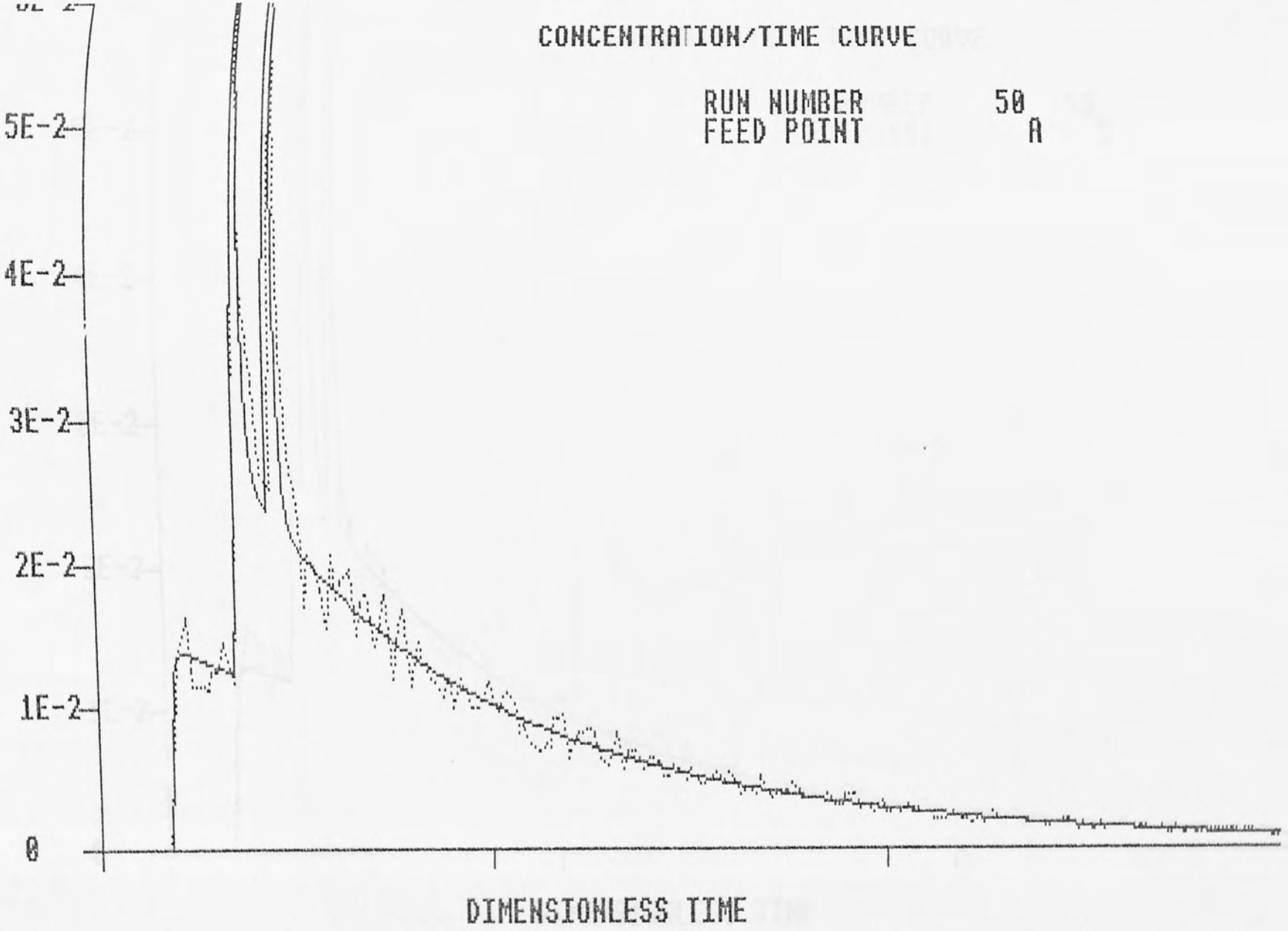
CONCENTRATION/TIME CURVE
RUN NUMBER 50
FEED POINT A
5E-2
4E-2
3E-2
2E-2
1E-2
0
DIMENSIONLESS TIME

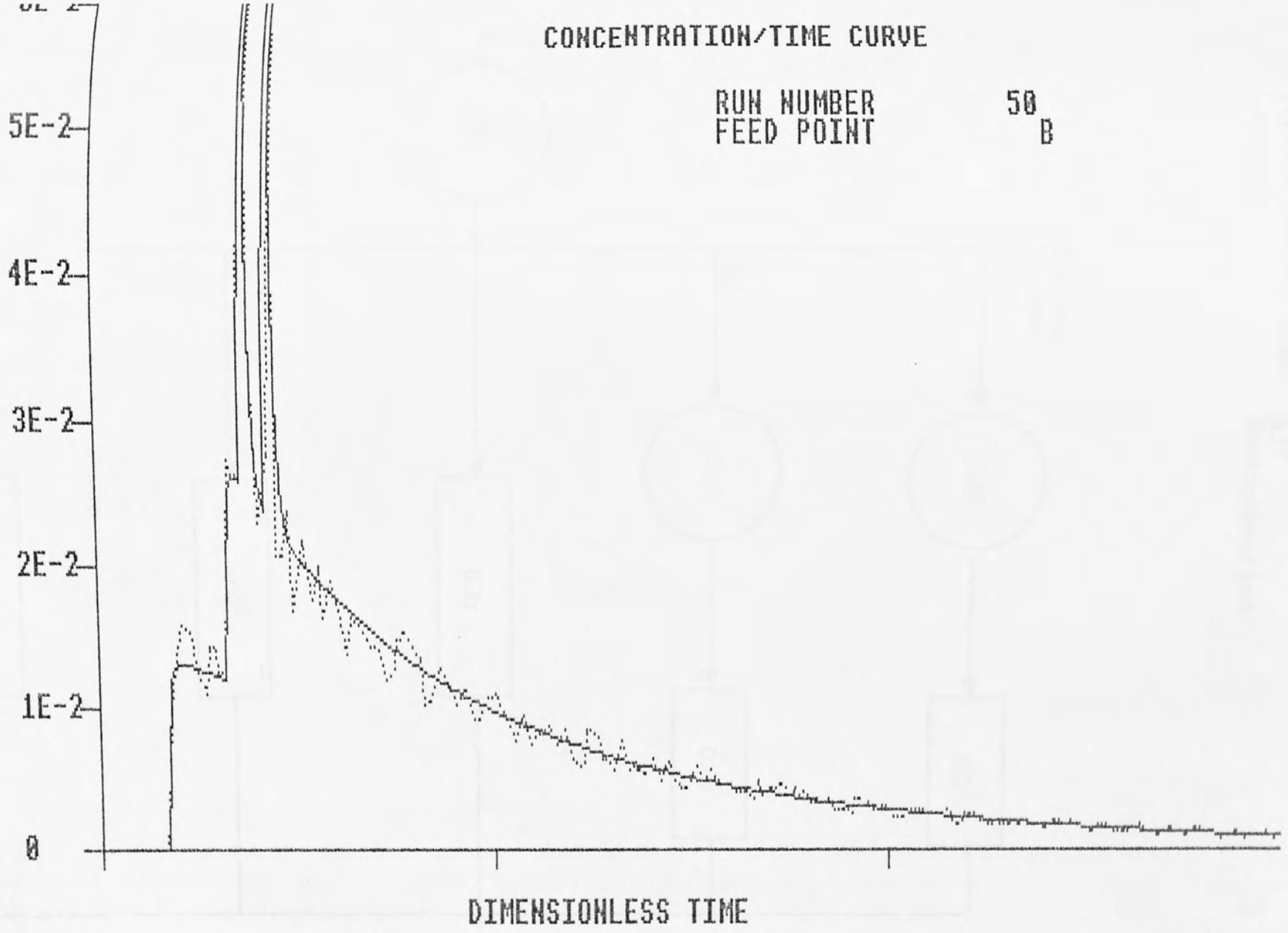
CONCENTRATION/TIME CURVE
RUN NUMBER 50
FEED POINT B
5E-2
4E-2
3E-2
2E-2
1E-2
0
DIMENSIONLESS TIME

Run Number: 003
Flowrate: 17.2 L/Hr
Feed Point: A
Dead Space: 0.2
Fraction Stream Volume: 0.37
Comments: Short residence time

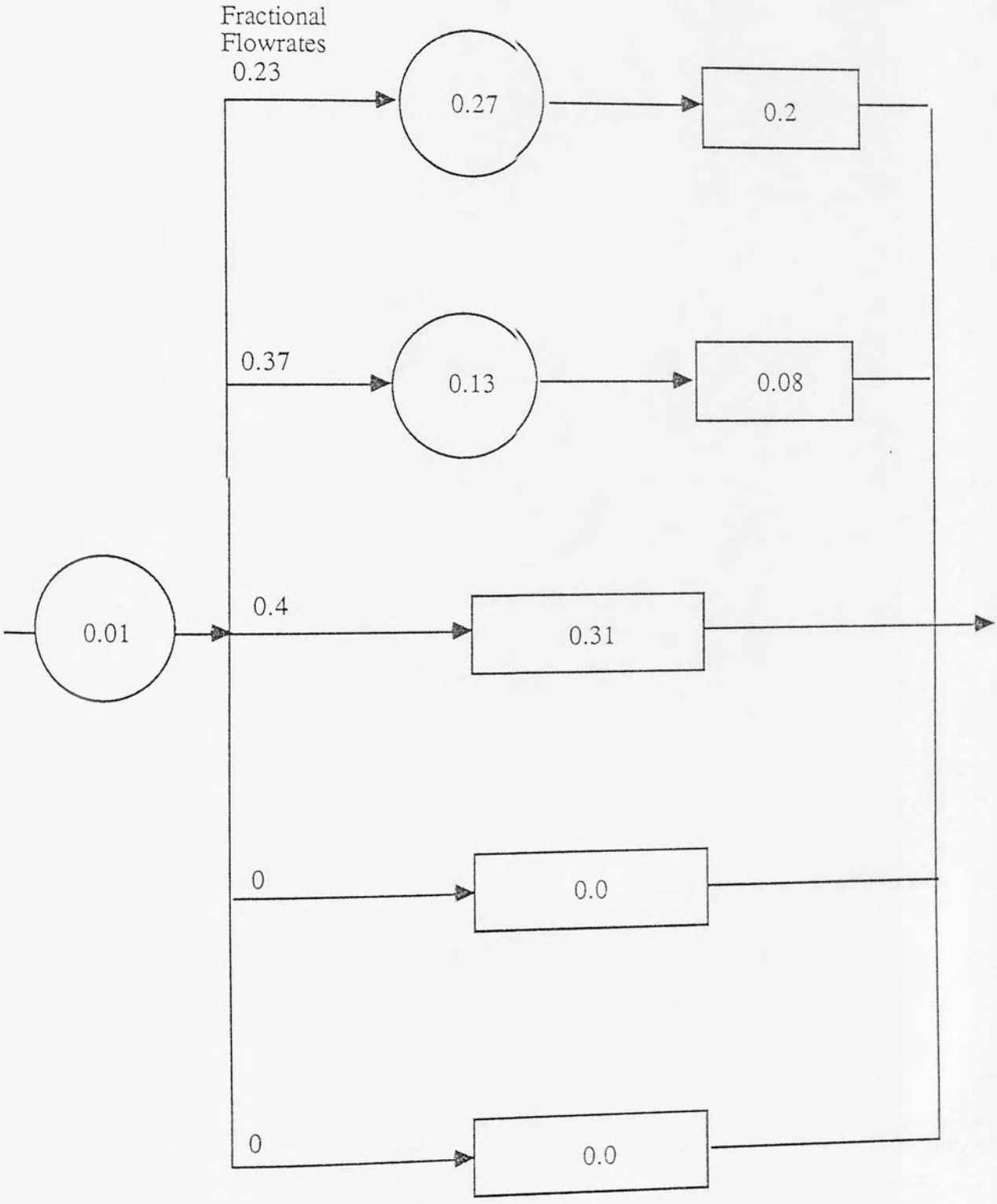

Run Number: 003
Flowrate: 17.2 L/Hr
Feed Point: B
Dead Space: 0.2
Fraction Stream Volume: 0.63
Comments: Short residence time.

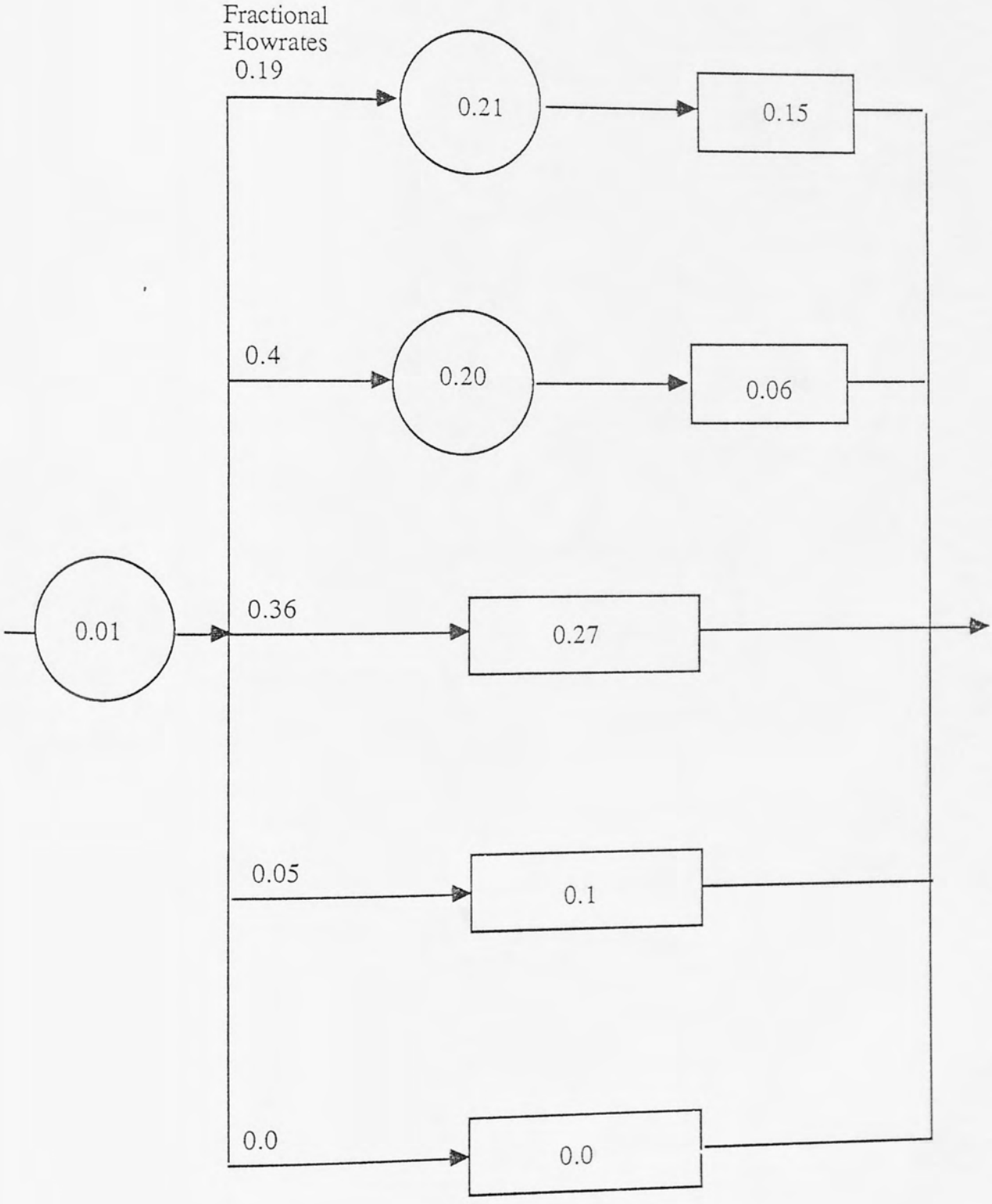

Run Number: 005
Flowrate: 0.172 L/Hr
Feed Point: A
Dead Space: 0.3
Fraction Stream Volume: 0.35
Comments: Long residence time.

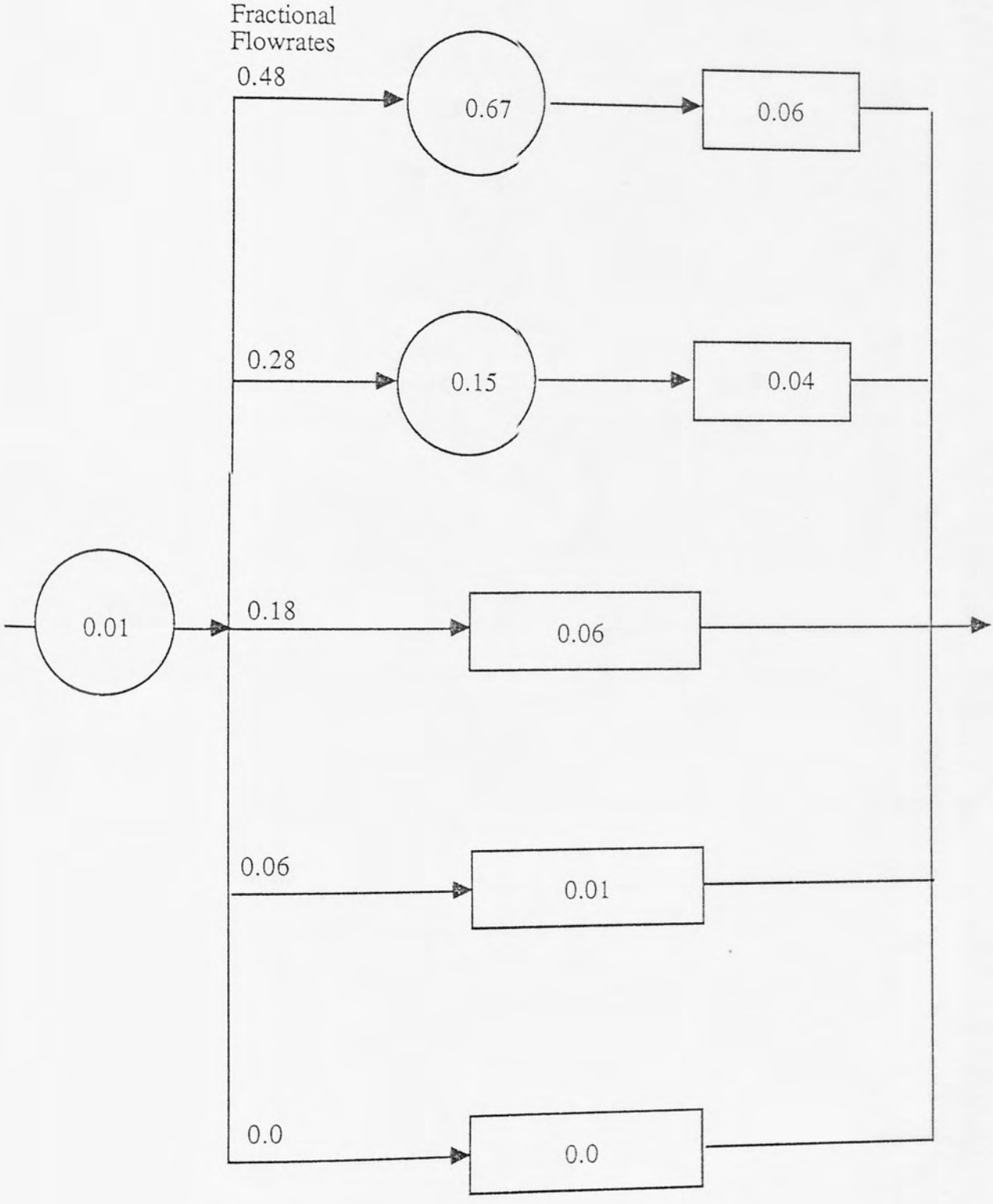

Run Number: 005
Flowrate: 0.172 L/Hr
Feed Point: B
Dead Space: 0.3
Fraction Stream Volume: 0.65
Comments: Long residence time

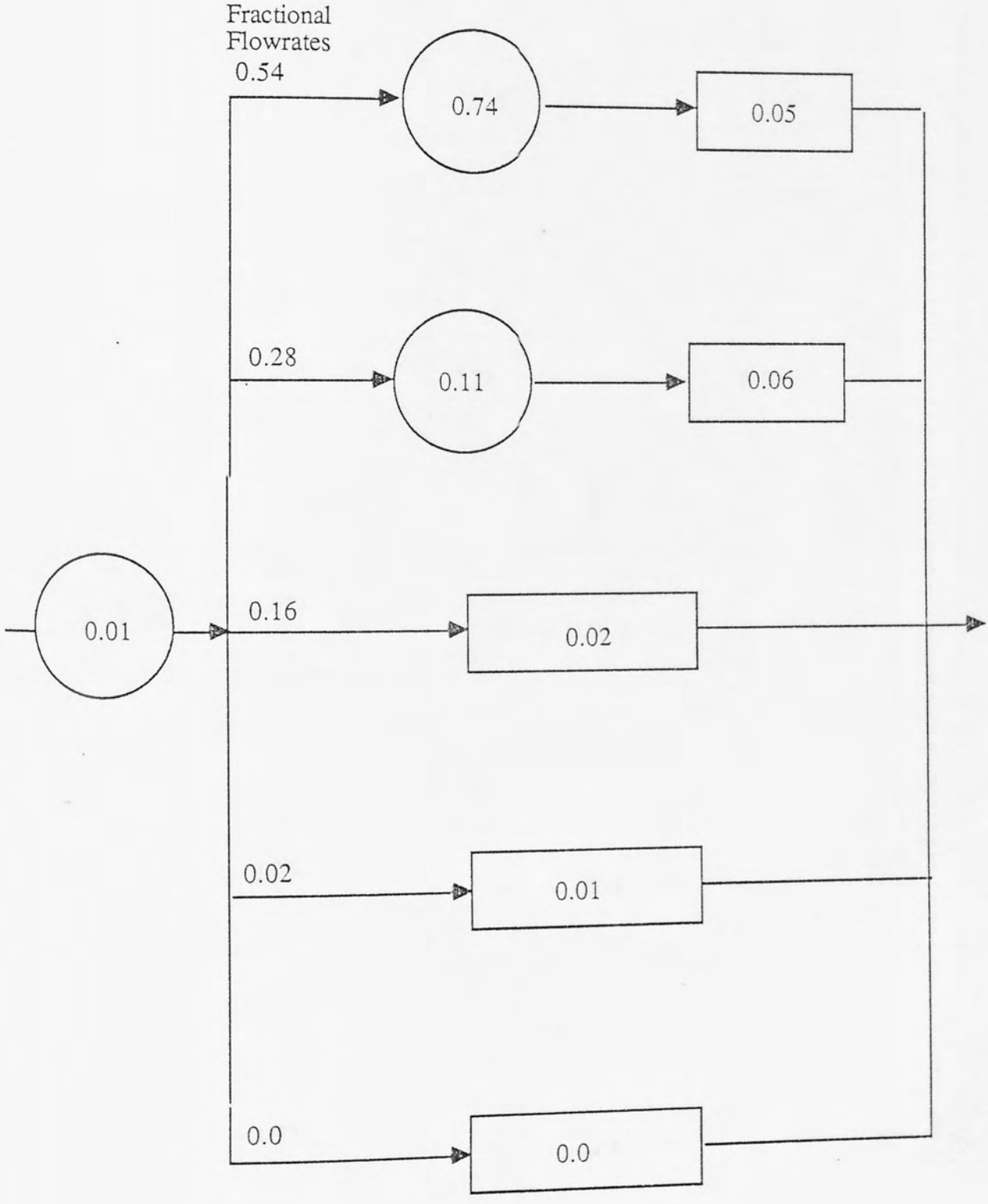

Run Number:	006
Flowrate:	0.172 L/Hr
Feed Point:	A
Dead Space:	0.4
Fraction Stream Volume:	0.38
Comments:	Batch cover simulated by semi-expanded polystyrene beads

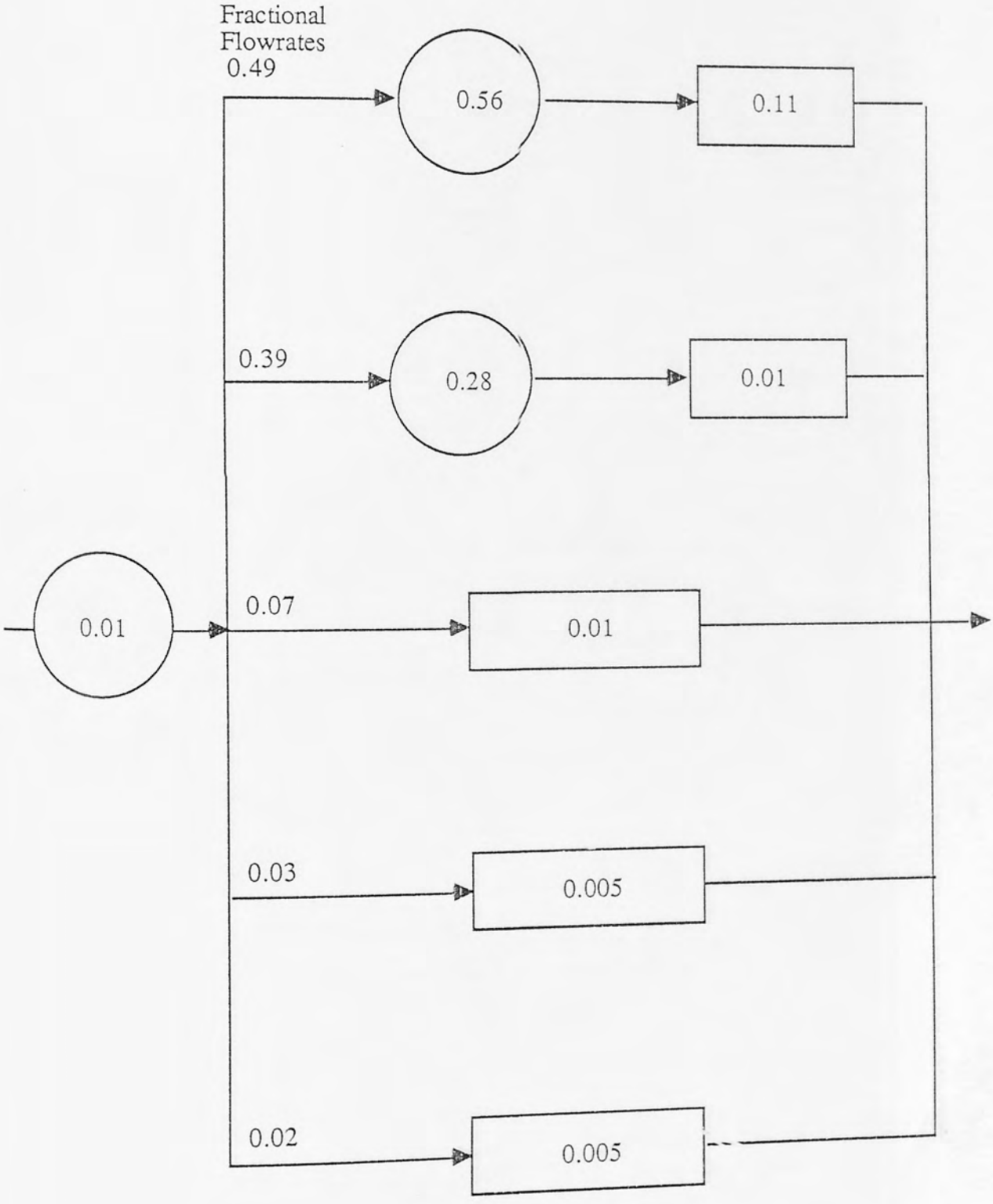

Run Number: 006
Flowrate: 0.172 L/Hr
Feed Point: B
Dead Space: 0.4
Fraction Stream Volume: 0.62
Comments: Batch cover simulated by semi-expanded polystyrene beads.

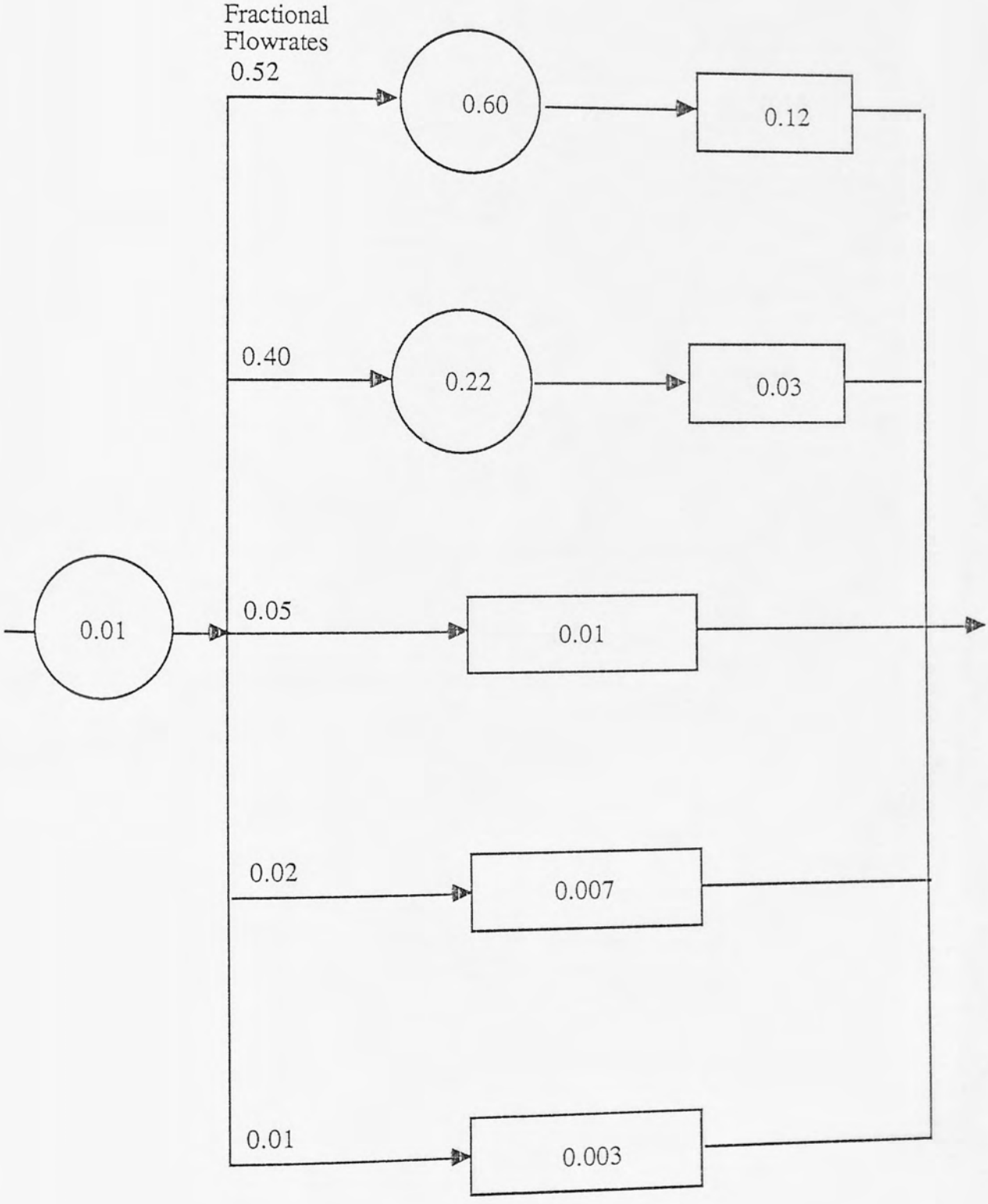

Run Number: 012
Flowrate: 0.344 L/H
Feed Point: A
Dead Space: 0.5
Fraction Stream Volume: 0.37
Comments: Double flowrate

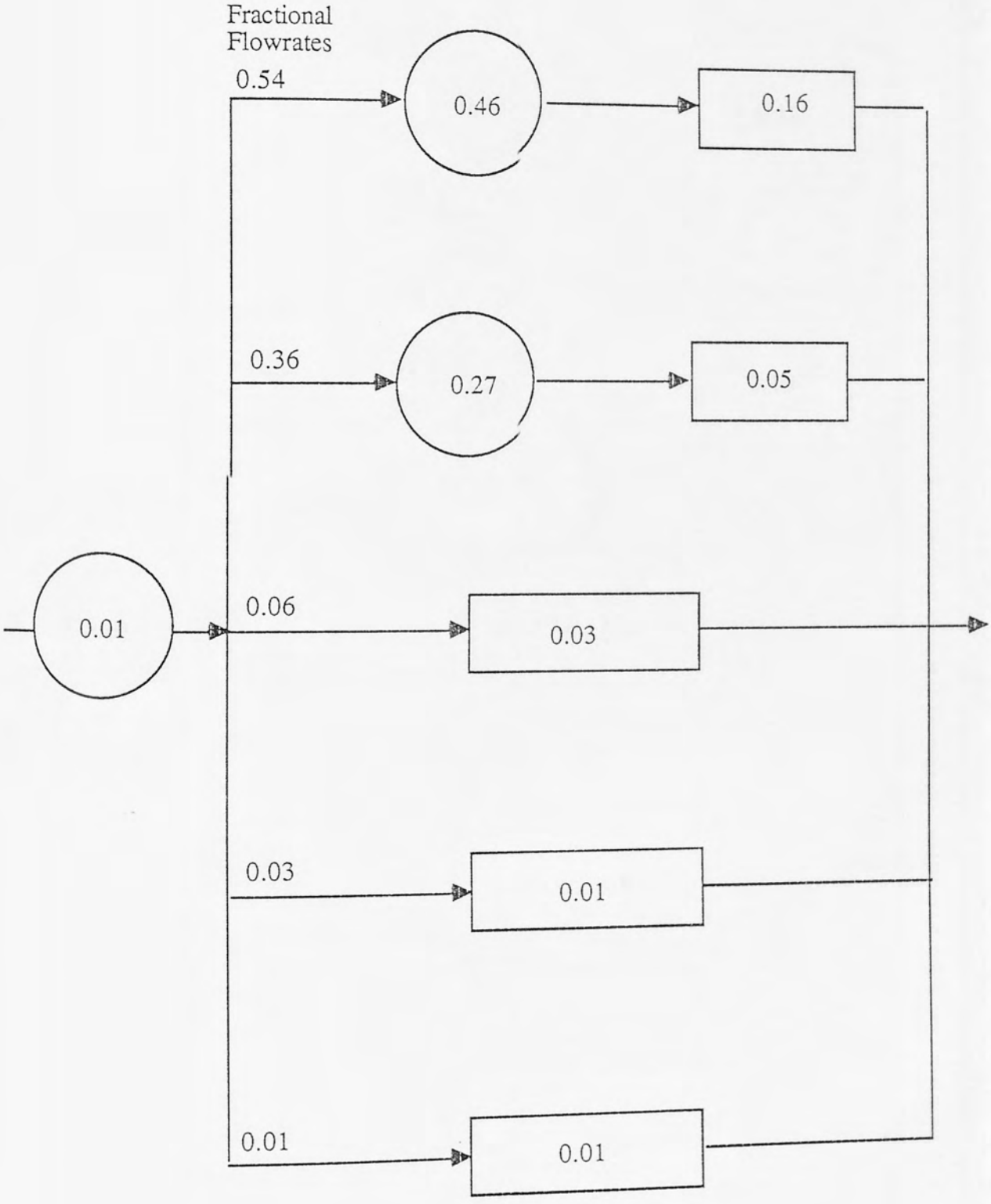

Run Number: 012
Flowrate: 0.344 L/Hr
Feed Point: B
Dead Space: 0.5
Fraction Stream Volume: 0.63
Comments: Double Flowrate

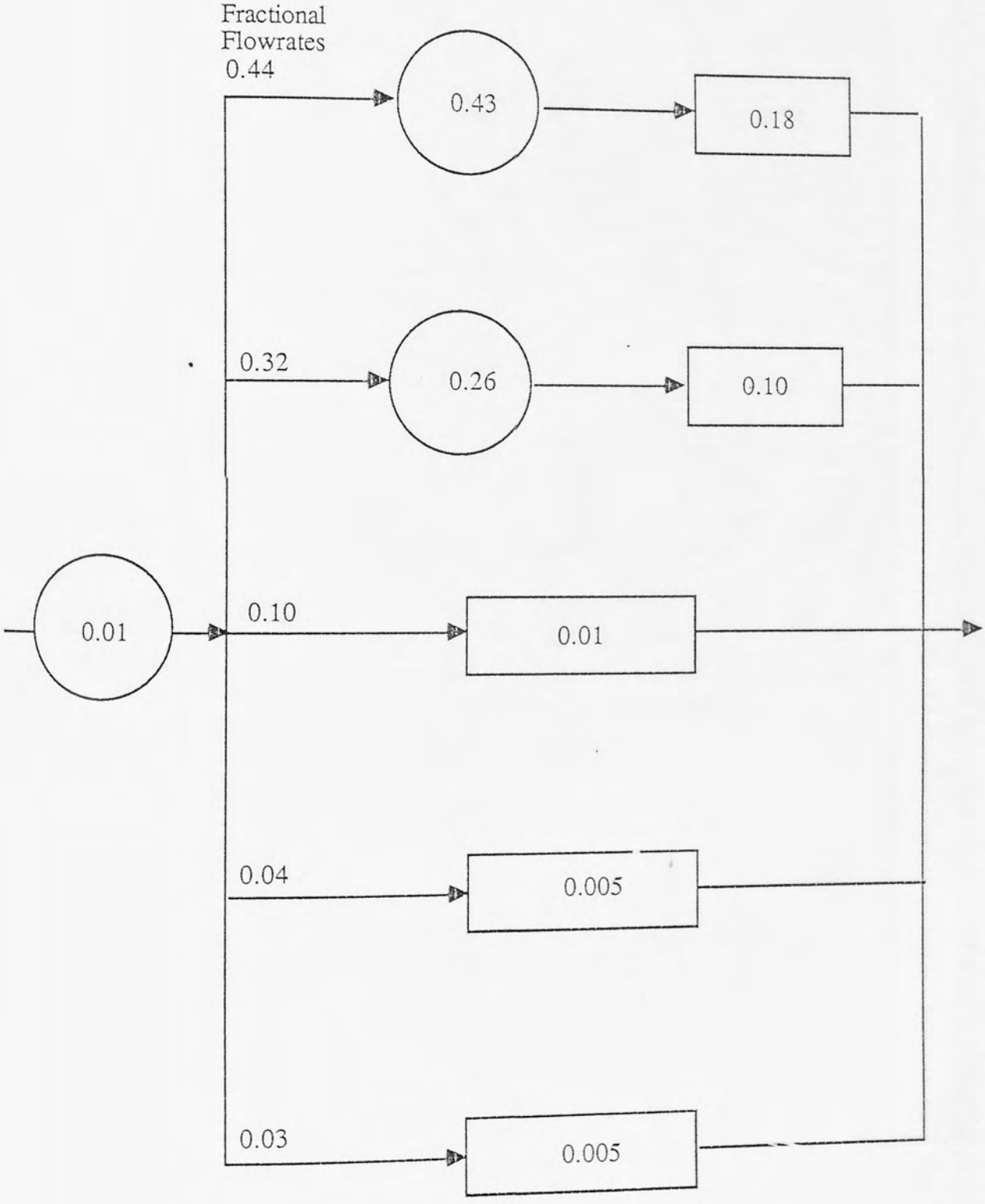

Run Number: 016
Flowrate: 0.086 L/Hr
Feed Point: A
Dead Space: 0.25
Fraction Stream Volume: 0.38
Comments: Liquid feed half normal flow

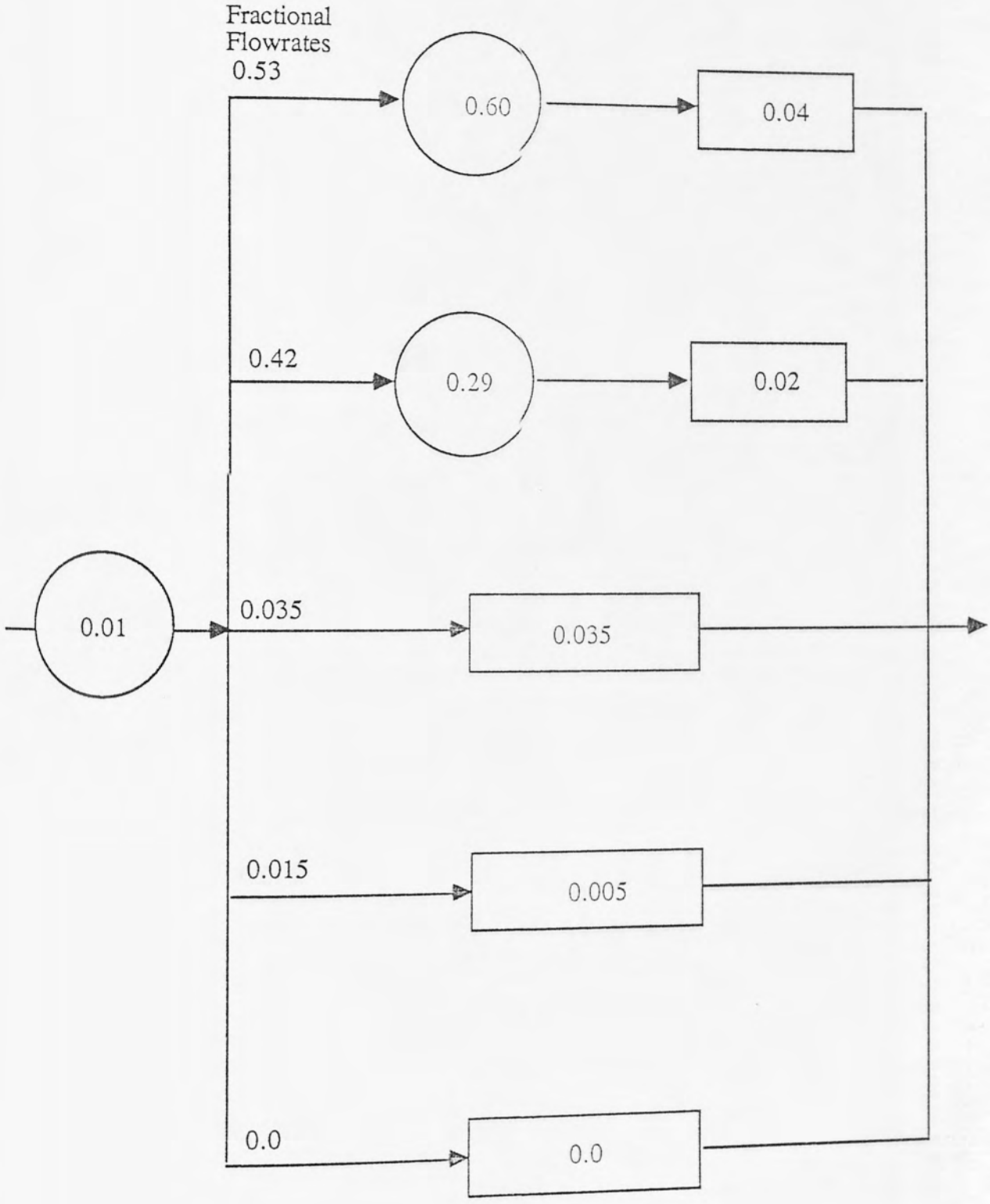

Run Number: 016
Flowrate: 0.086 L/Hr
Feed Point: B
Dead Space: 0.25
Fraction Stream Volume: 0.62
Comments: Liquid feed half normal flow

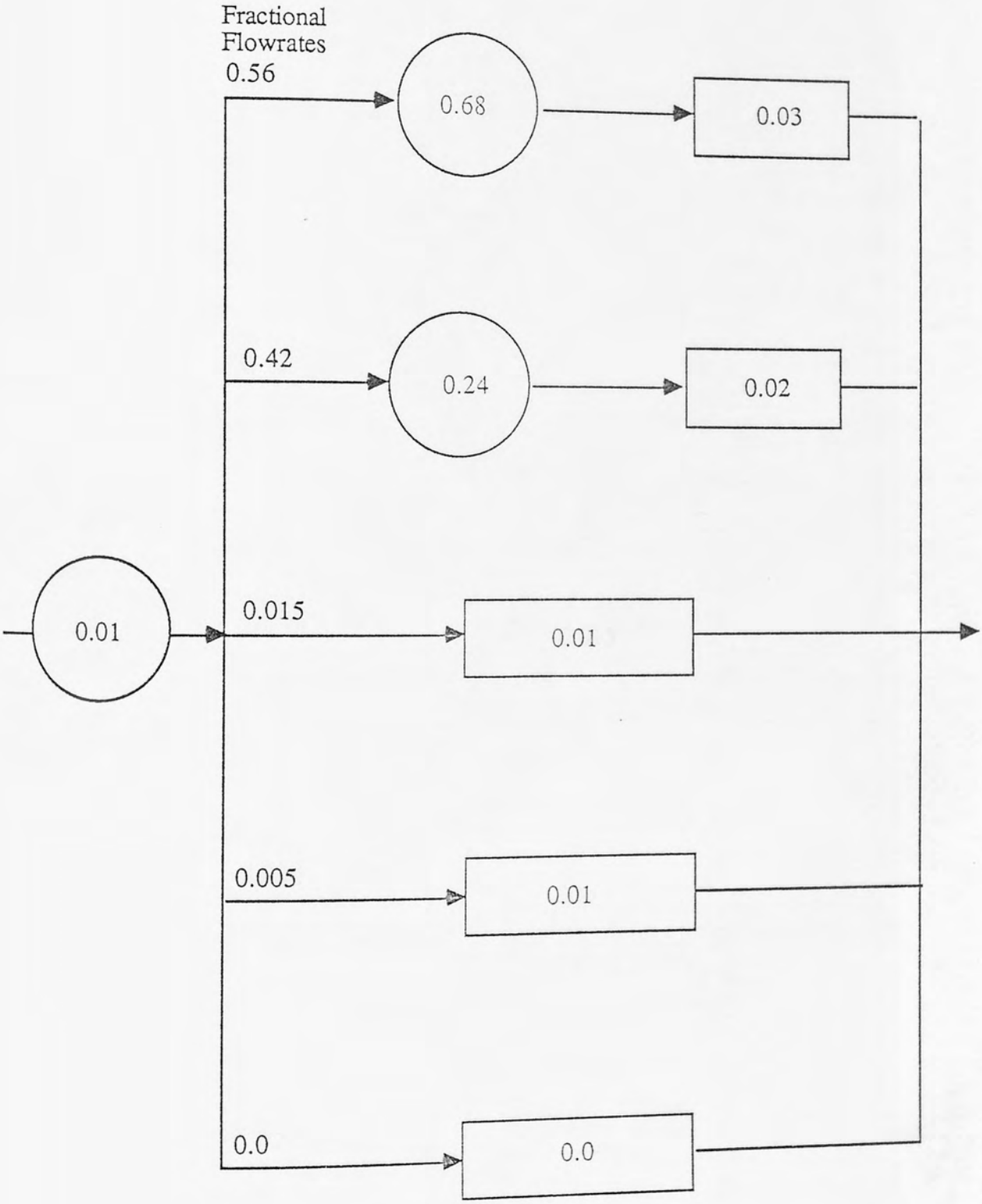

Run Number: 030
Flowrate: 0.172
Feed Point: A
Dead Space: 0.4
Fraction Stream Volume: 0.38
Comments: Solids feeding

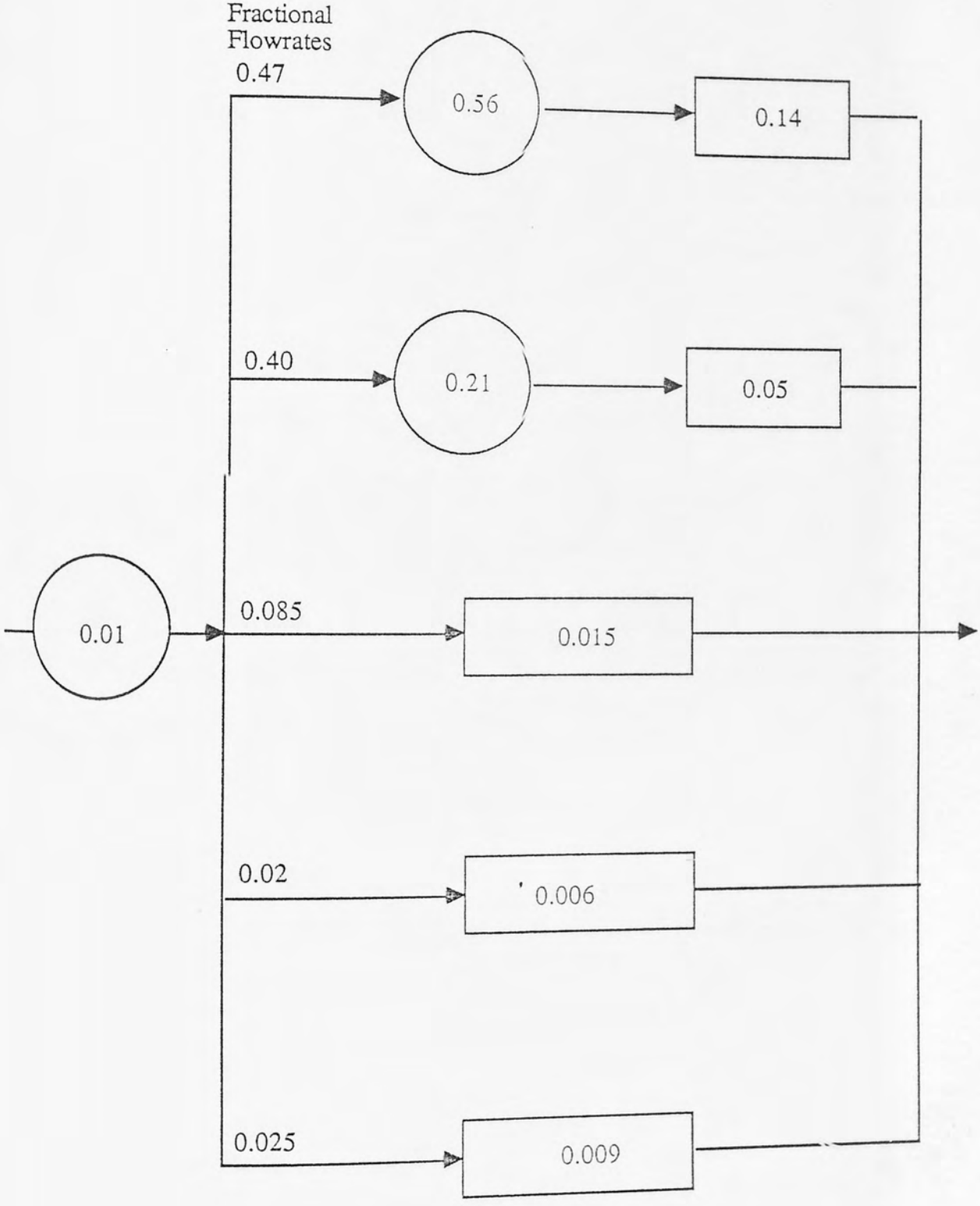

Run Number:	030
Flowrate:	0.172 L/Hr
Feed Point:	B
Dead Space:	0.4
Fraction Stream Volume:	0.62
Comments:	Solids feeding

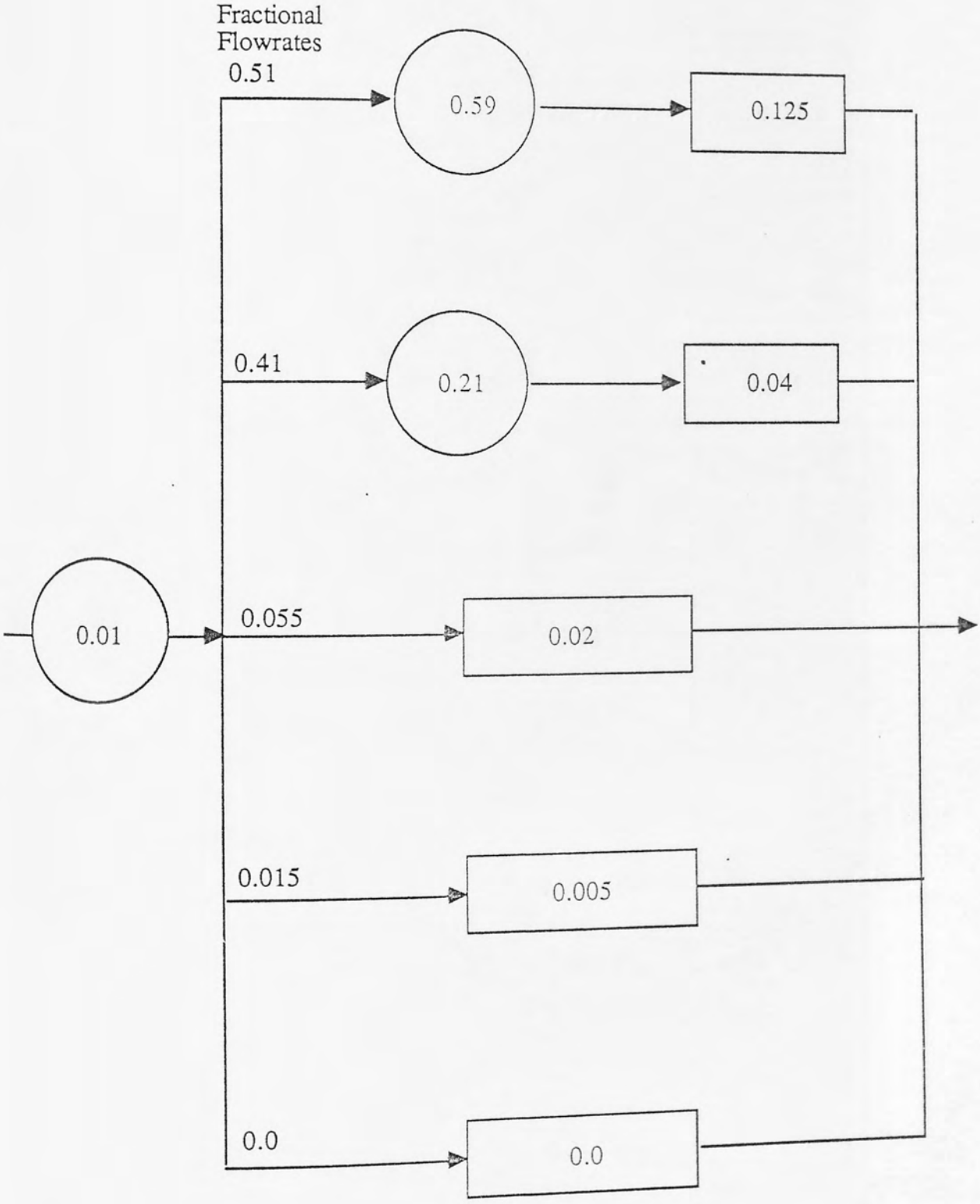

Run Number:	032
Flowrate:	0.172 L/Hr
Feed Point:	A
Dead Space:	0.6
Fraction Stream Volume:	0.38
Comments:	Liquid level reduced by 20% (low temp.)

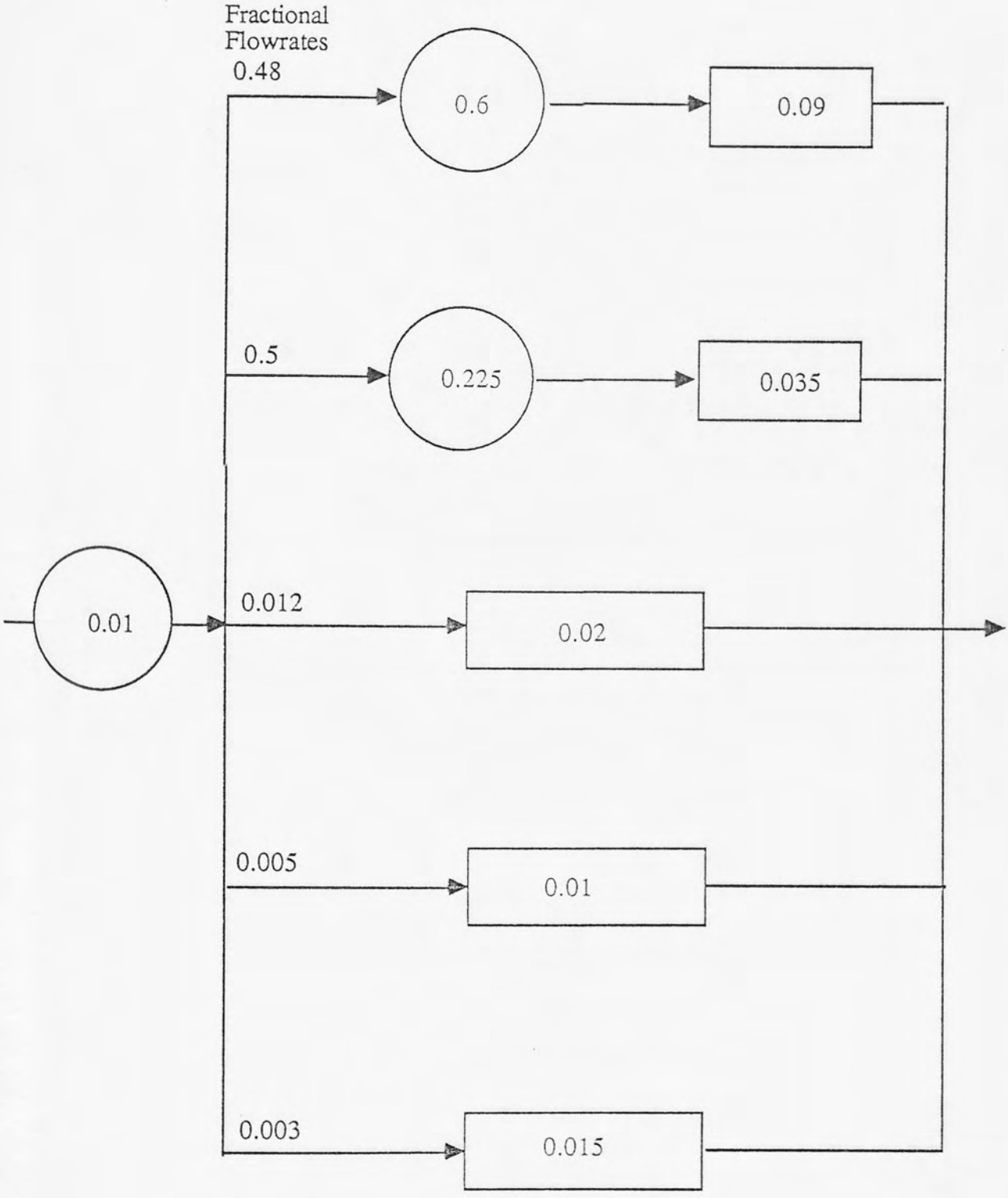

Run Number:	032
Flowrate:	0.172 L/Hr
Feed Point:	B
Dead Space:	0.6
Fraction Stream Volume:	0.62
Comments:	Liquid Level Reduced by 20% (low temp.)

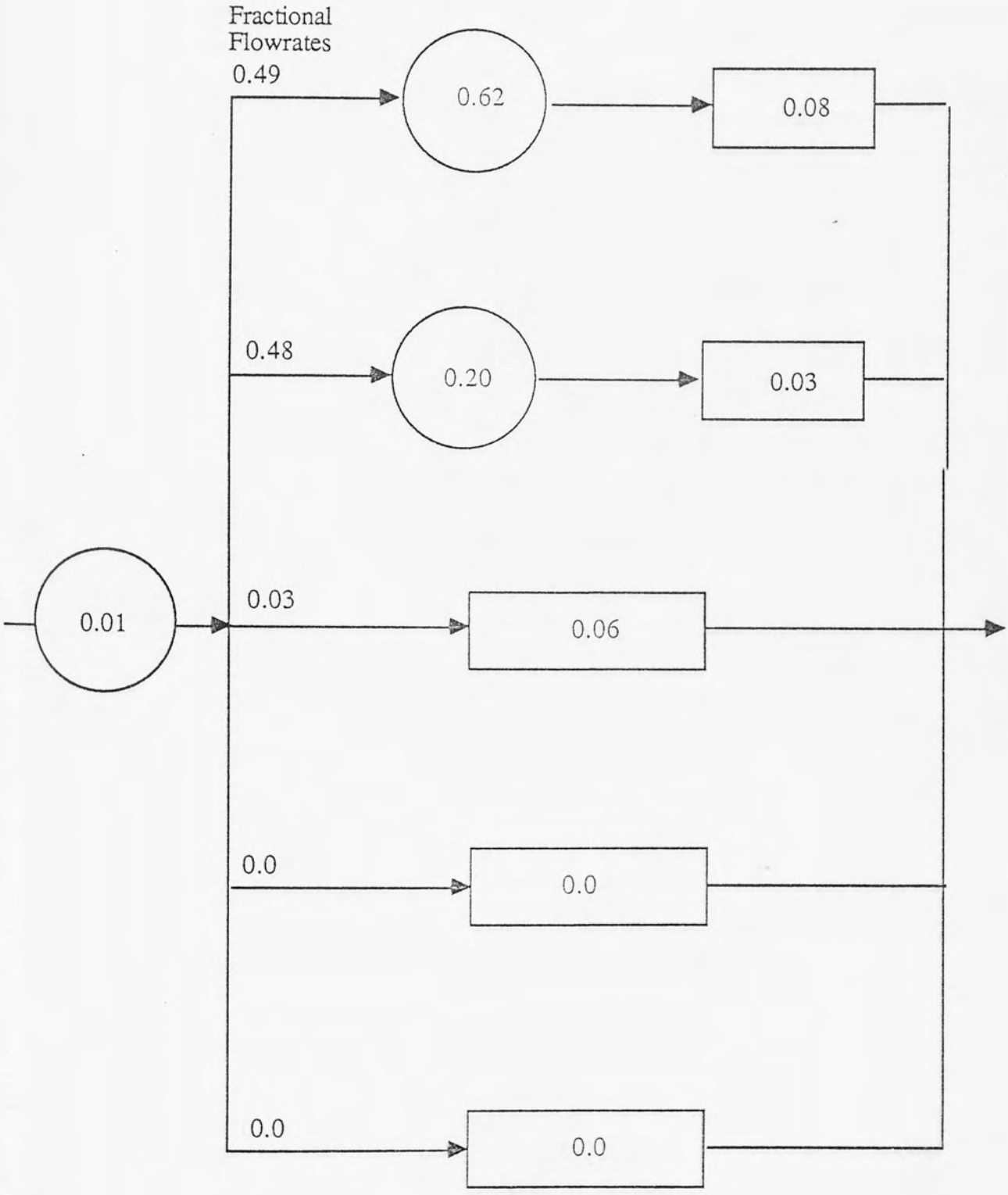

Run Number:	037
Flowrate:	0.172 L/Hr
Feed Point:	A
Dead Space:	0.25
Fraction Stream Volume:	0.38
Comments:	Feed below melt surface

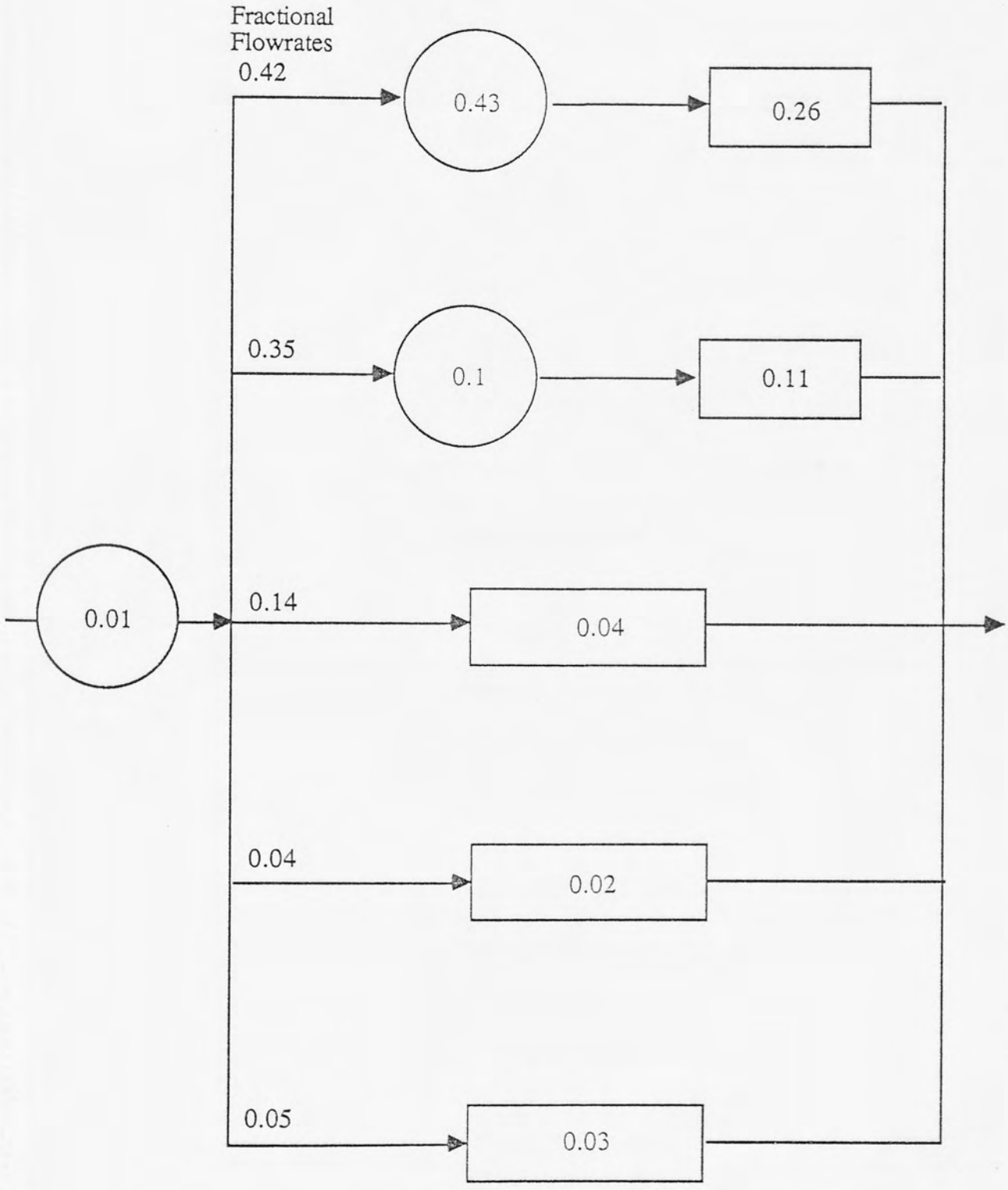

Run Number:	037
Flowrate:	0.172 L/Hr
Feed Point:	B
Dead Space:	0.25
Fraction Stream Volume:	0.62
Comments:	Feed below melt surface.

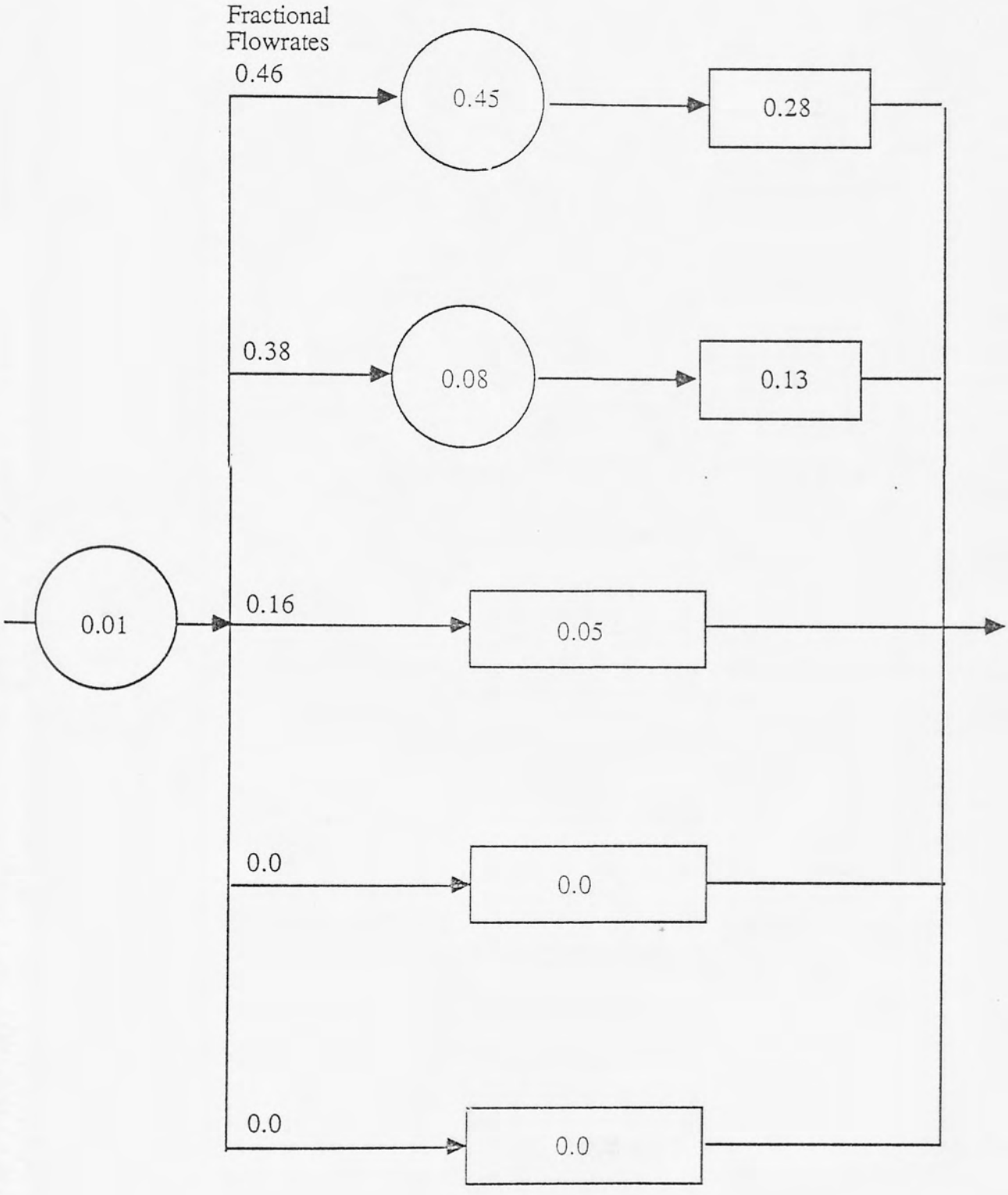

Run Number:	038
Flowrate:	0.344 L/Hr
Feed Point:	A
Dead Space:	0.37
Fraction Stream Volume:	0.56
Comments:	High flow to feed A.

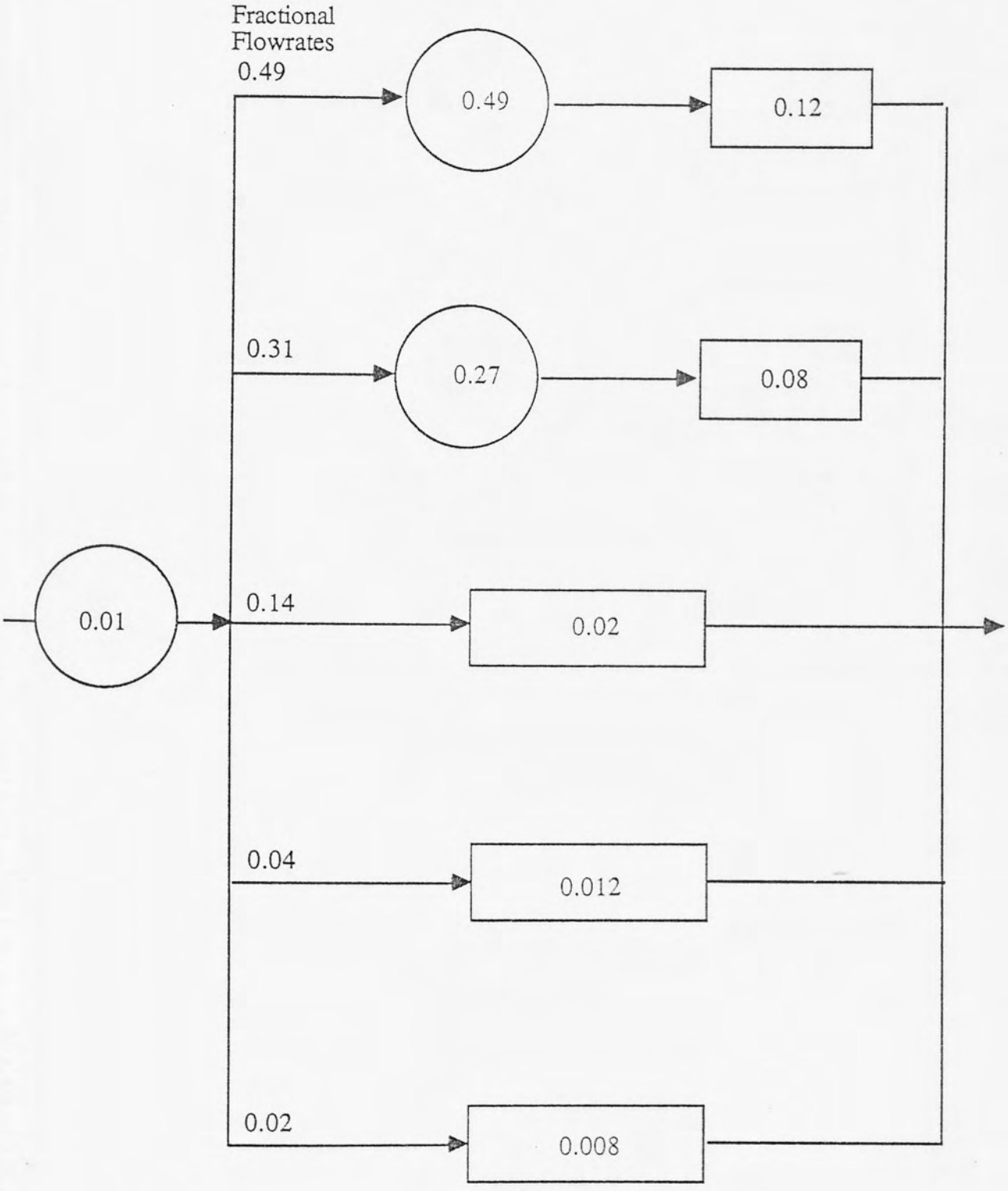

Run Number:	038
Flowrate:	0.172 L/Hr
Feed Point:	B
Dead Space:	0.37
Fraction Stream Volume:	0.44
Comments:	High flow to feed point A.

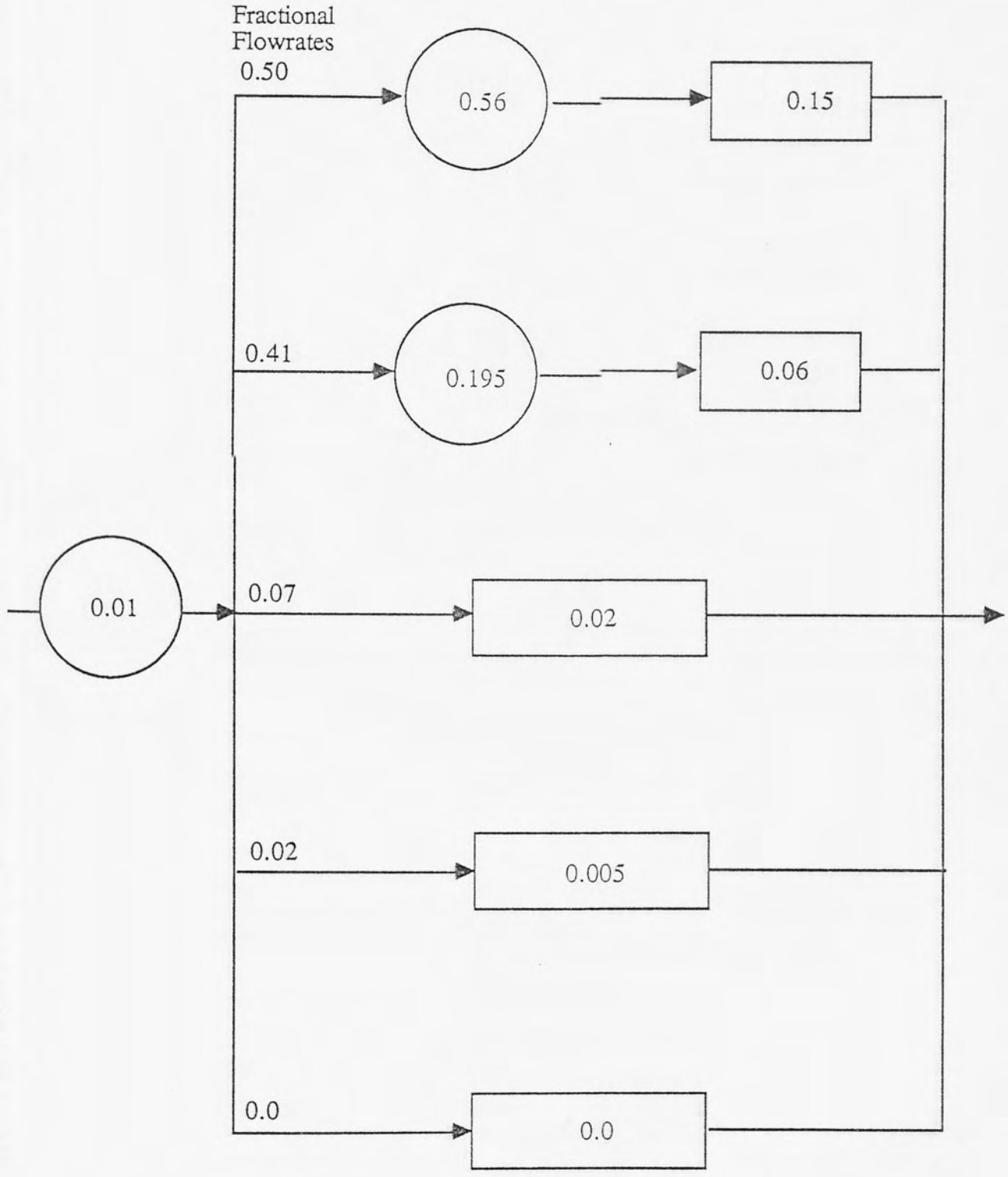

Run Number:	040
Flowrate:	0.172 L/Hr
Feed Point:	A
Dead Space:	0.35
Fraction Stream Volume:	0.35
Comments:	High flow to feed point B.

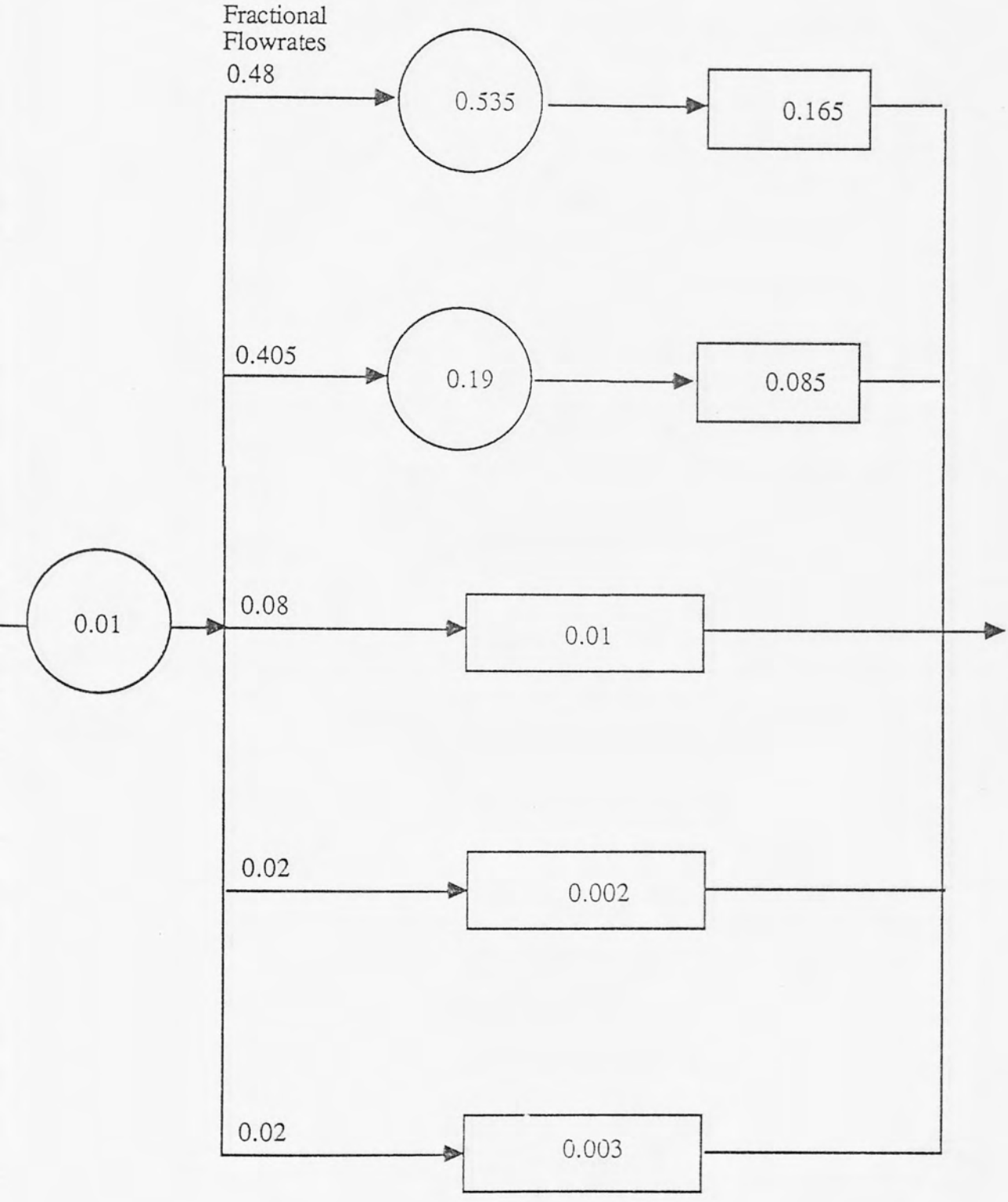

Run Number:	040
Flowrate:	0.344 L/Hr
Feed Point:	B
Dead Space:	0.35
Fraction Stream Volume:	0.65
Comments:	High flow to feed point B

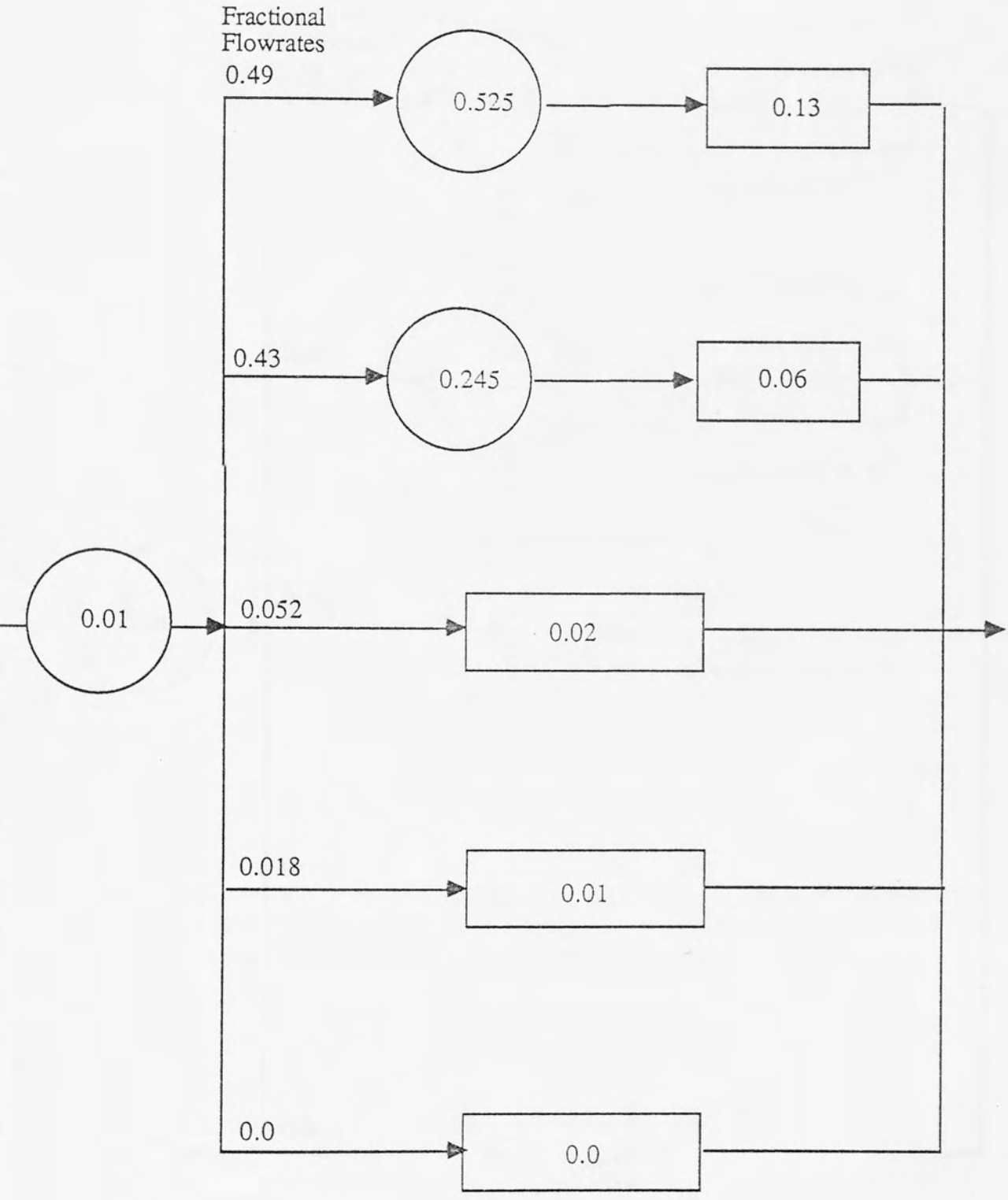

Run Number:	041
Flowrate:	0.172
Feed Point:	A
Dead Space:	0.22
Fraction Stream Volume:	0.38
Comments:	Tank bottom well insulated

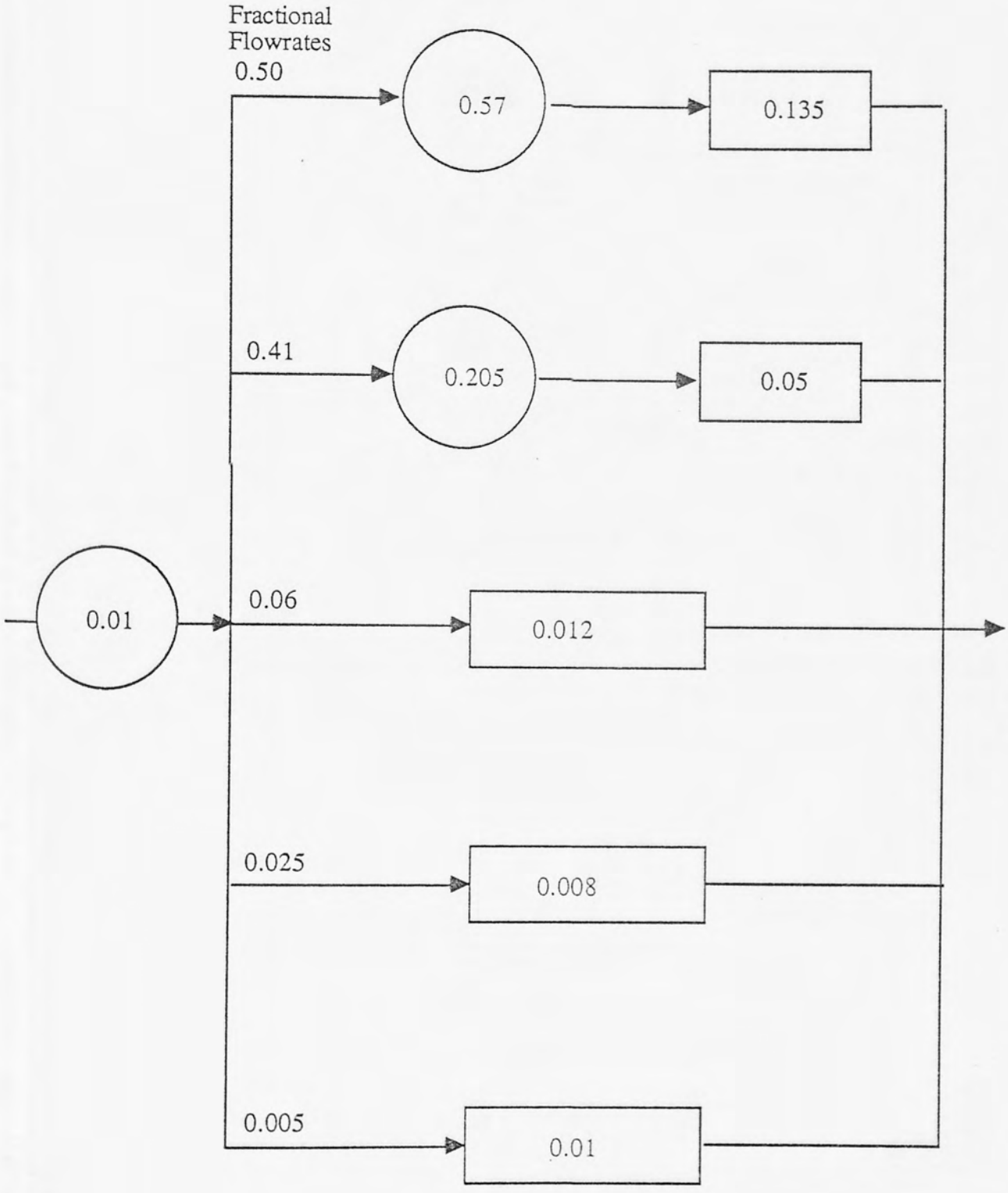

Run Number: 041
Flowrate: 0.172 L/Hr
Feed Point: B
Dead Space: 0.22
Fraction Stream Volume: 0.62
Comments: Tank bottom well insulated

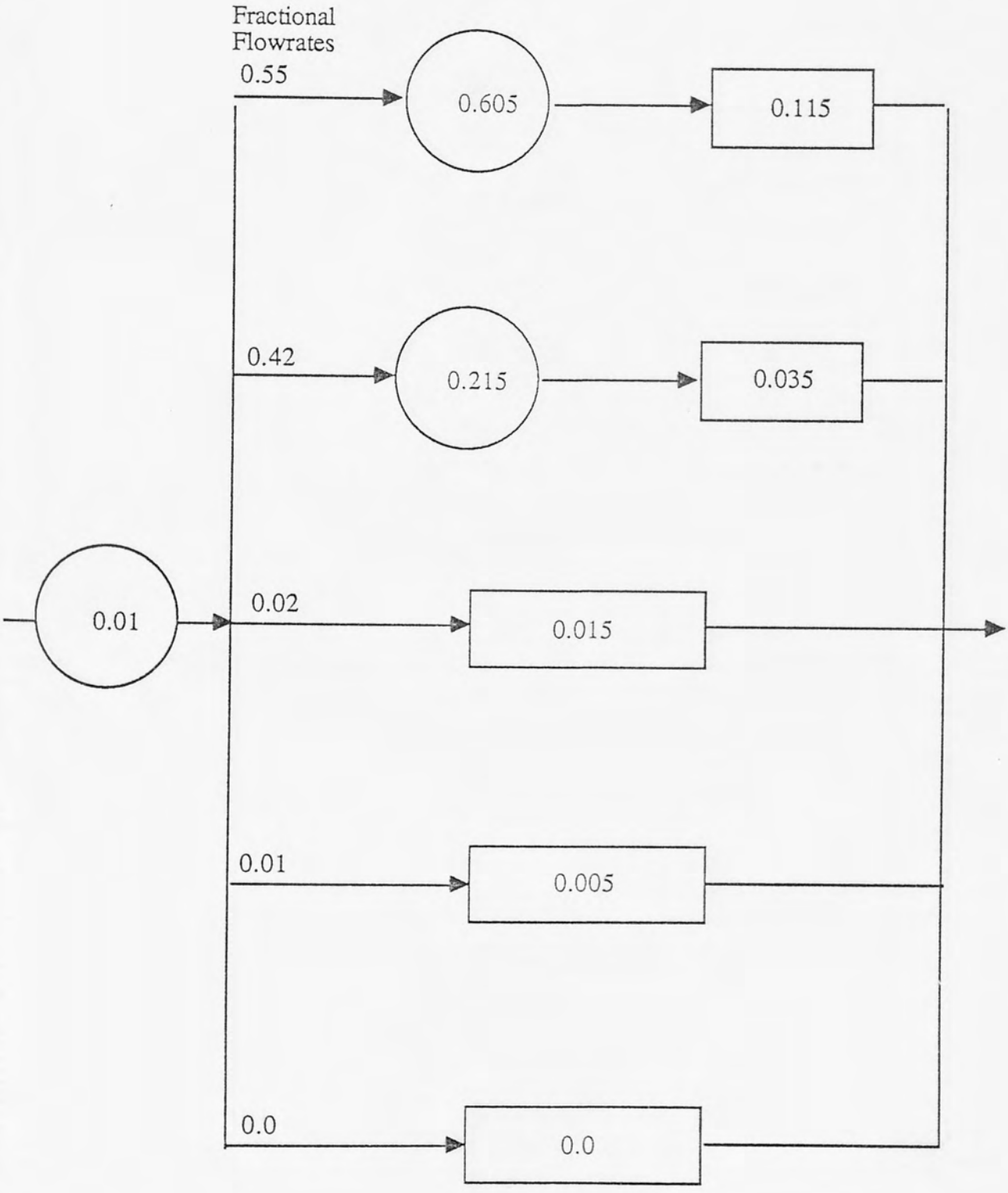

Run Number:	044
Flowrate:	0.172 L/Hr
Feed Point:	A
Dead Space:	0.6
Fraction Stream Volume:	0.38
Comments:	Tank bottom raised 20%

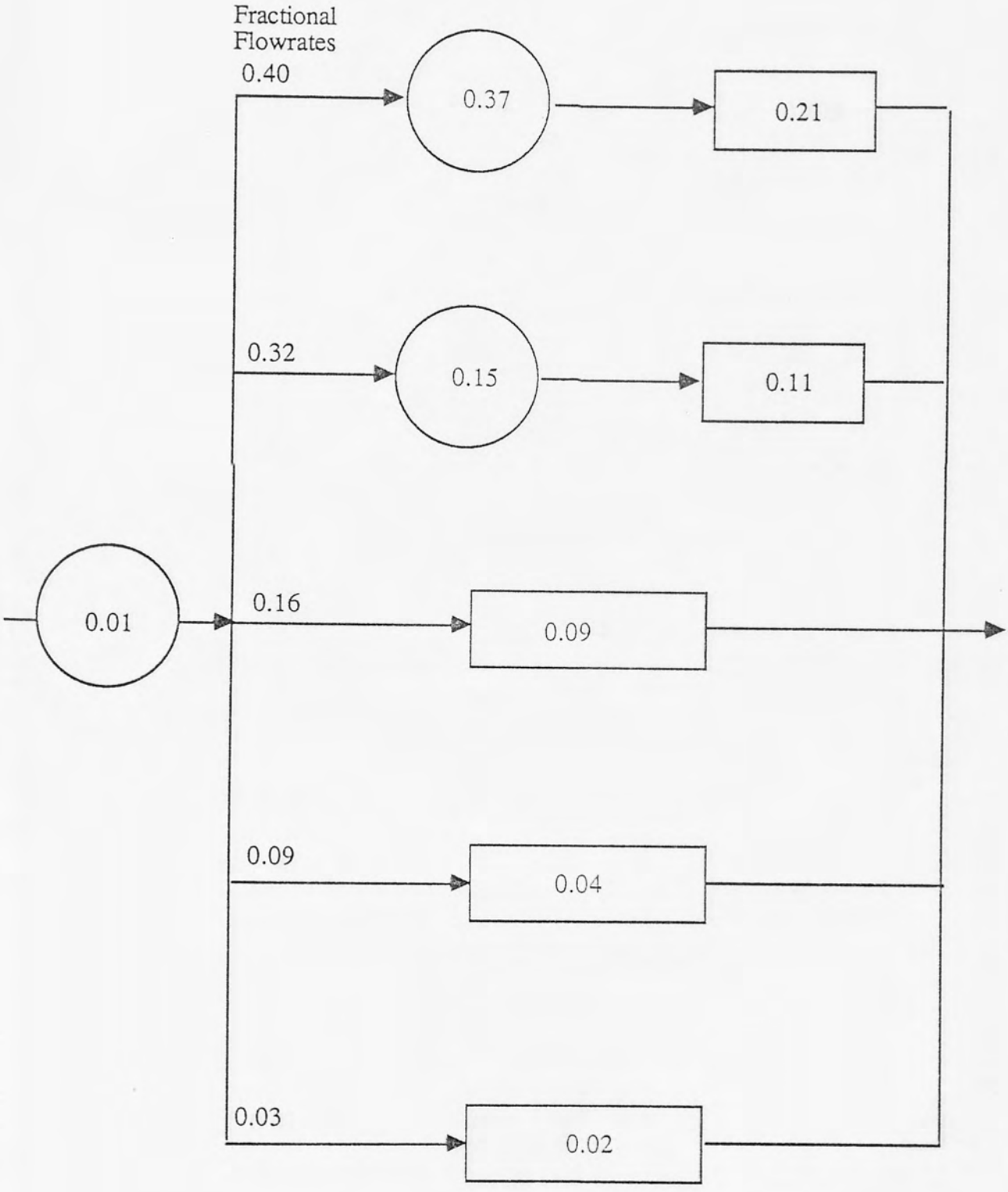

Run Number:	044
Flowrate:	0.172 L/Hr
Feed Point:	B
Dead Space:	0.6
Fraction Stream Volume:	0.62
Comments:	Tank bottom raised 20%

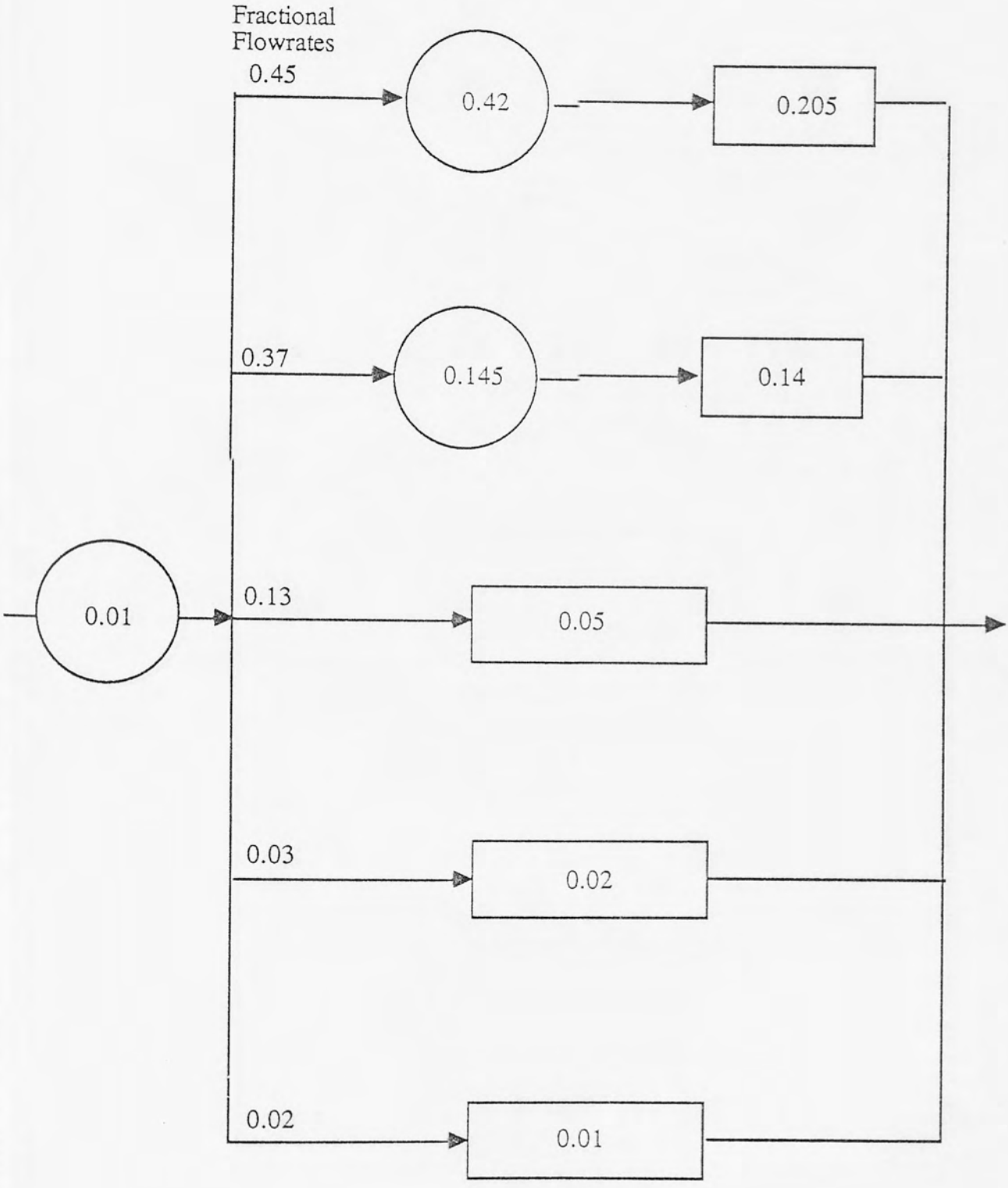

Run Number:	045
Flowrate:	0.172 L/Hr
Feed Point:	A
Dead Space:	0.32
Fraction Stream Volume:	0.38
Comments:	Increase heat flux by approximately 20%.

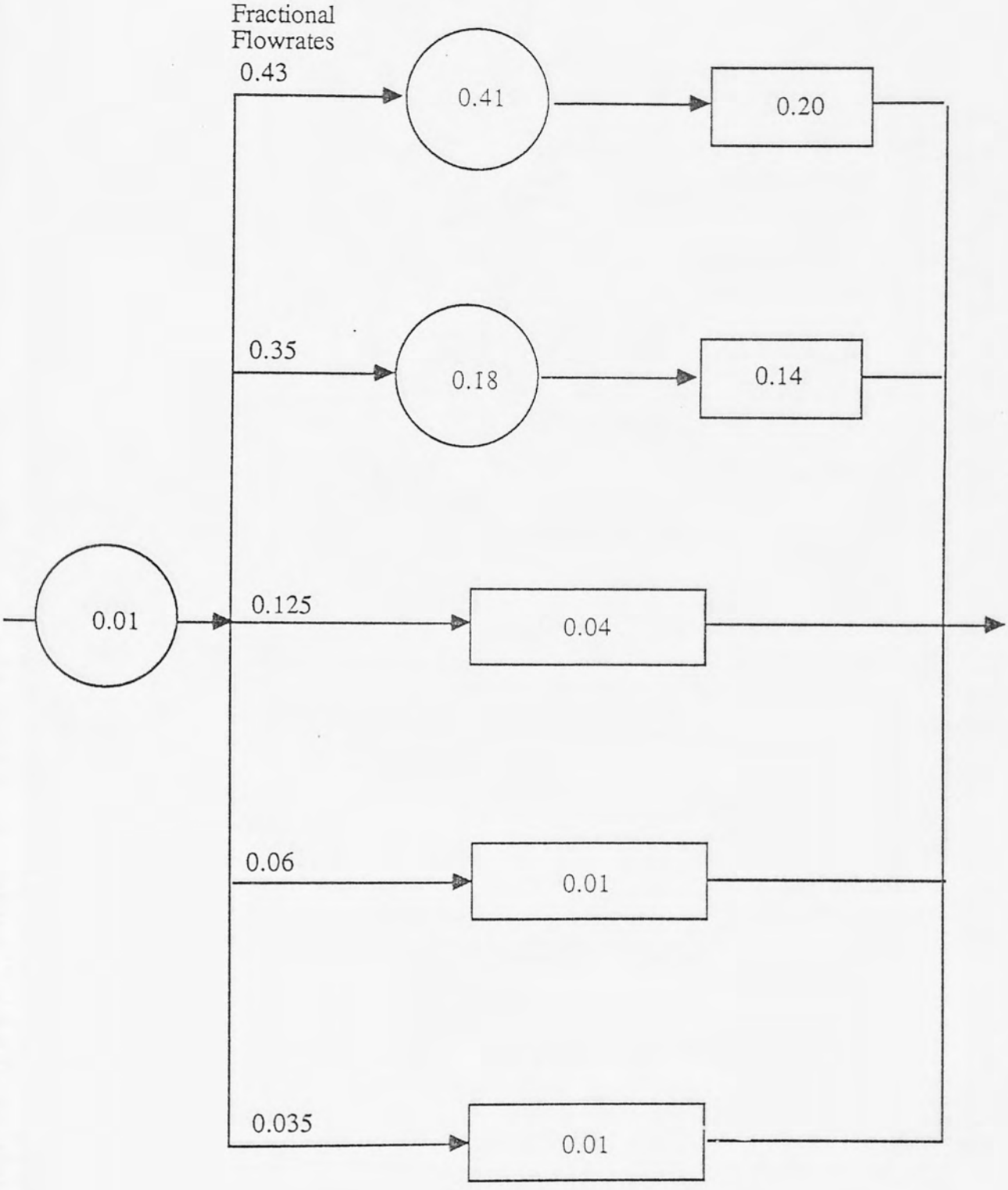

Run Number: 045
Flowrate: 0.172 L/Hr
Feed Point: B
Dead Space: 0.32
Fraction Stream Volume: 0.62
Comments: Increase heat flux by approximately 20%.

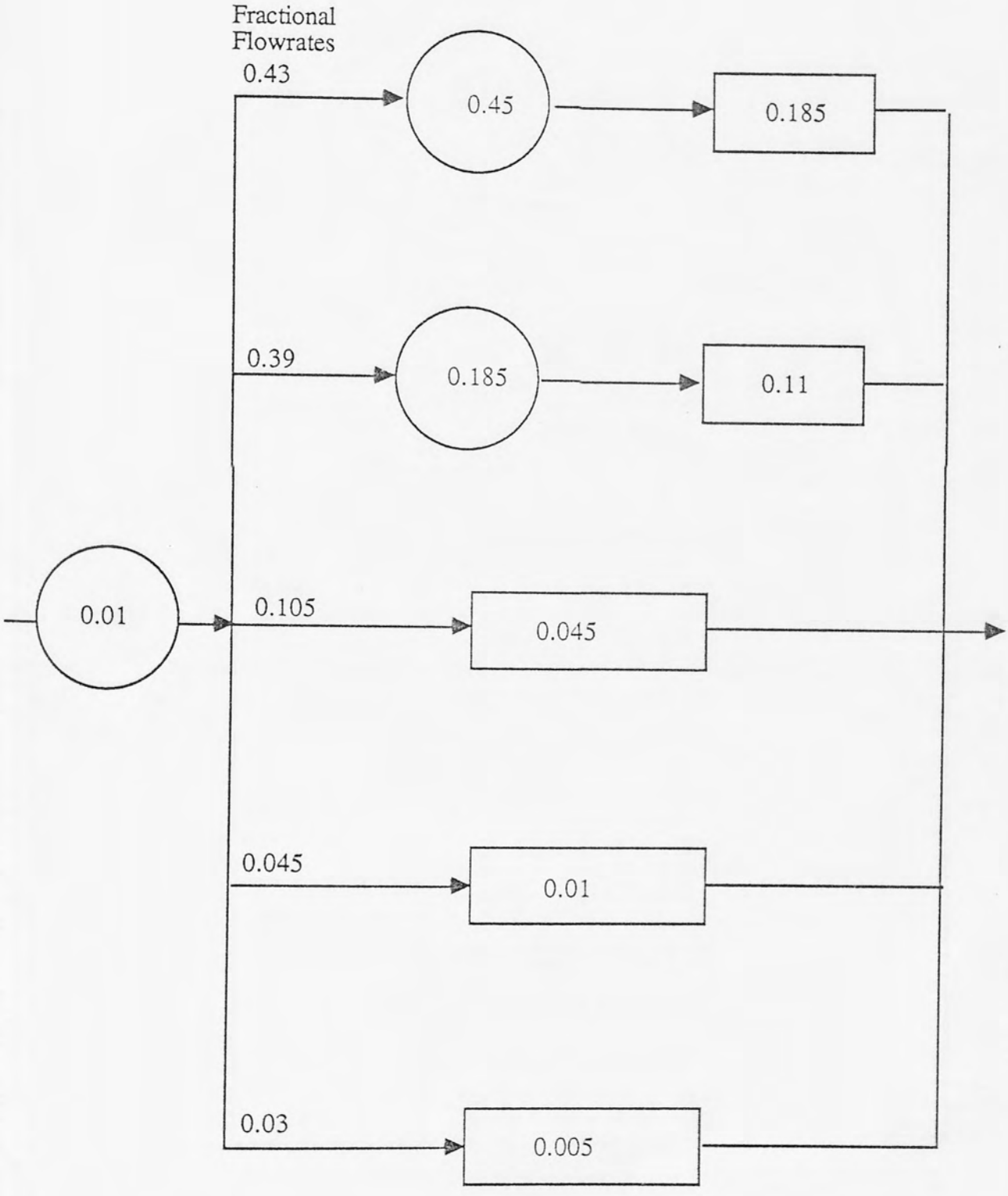

Run Number:	047
Flowrate:	0.172 L/Hr
Feed Point:	A
Dead Space:	0.36
Fraction Stream Volume:	0.38
Comments:	Feed temp. increased to just below melting point.

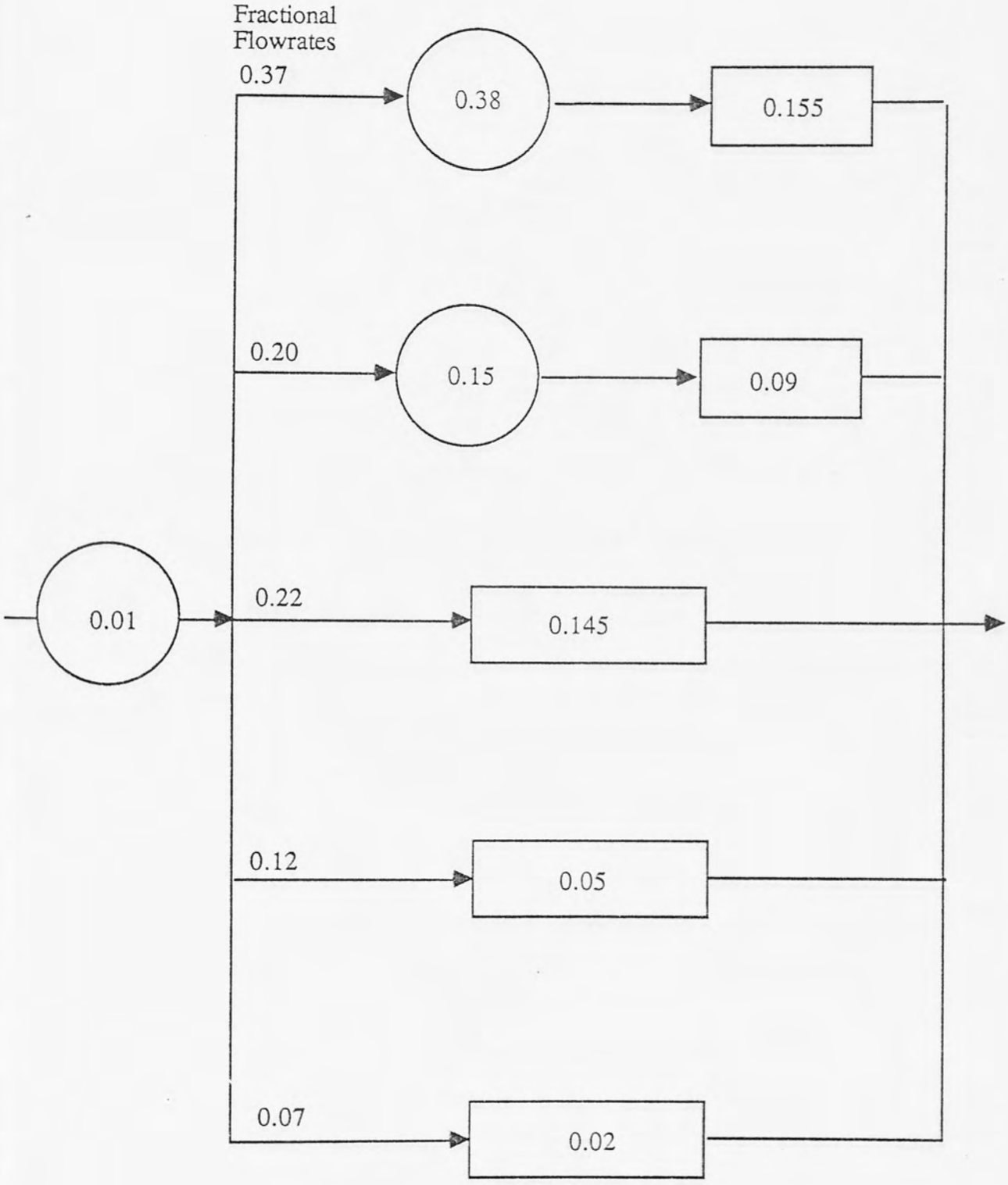

Run Number:	047
Flowrate:	0.172 L/Hr
Feed Point:	B
Dead Space:	0.36
Fraction Stream Volume:	0.62
Comments:	Feed temp. increased to just below melting point

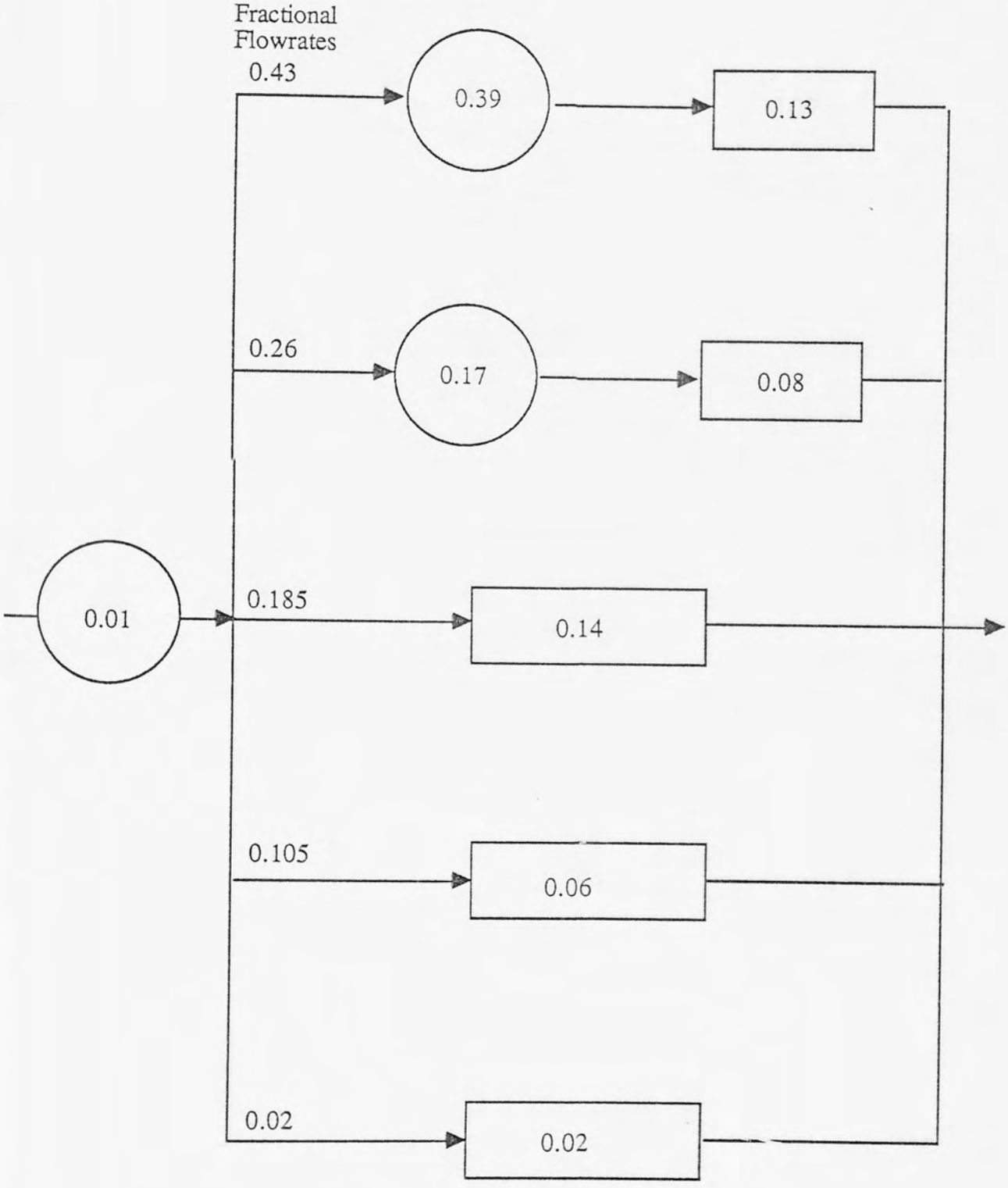

Run Number: 049
Flowrate: 0.172 L/Hr
Feed Point: A
Dead Space: 0.38
Fraction Stream Volume: 0.5
Comments: Open second offtake

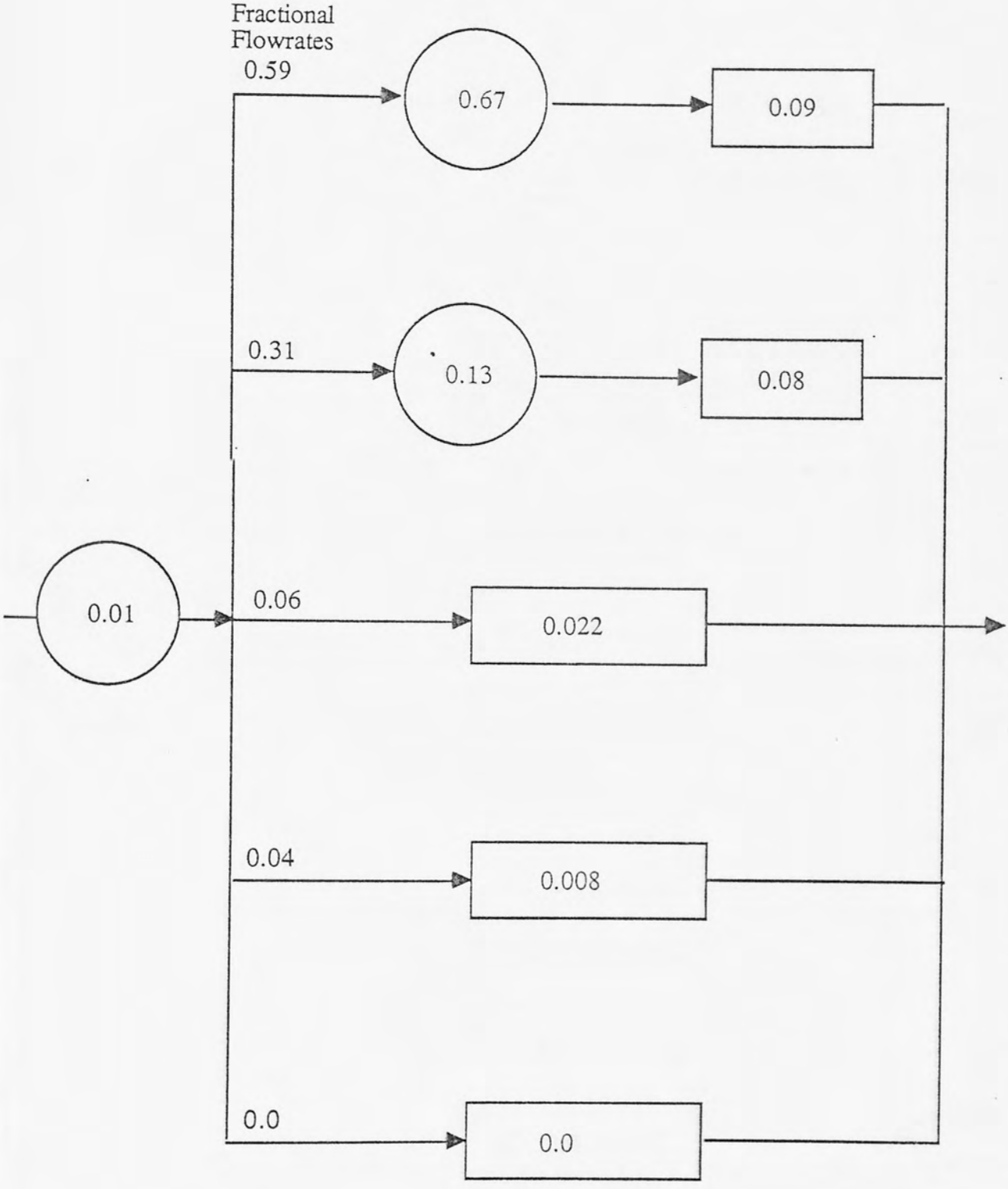

Run Number: 049
Flowrate: 0.172 L/Hr
Feed Point: B
Dead Space: 0.38
Fraction Stream Volume: 0.5
Comments: Open second offtake

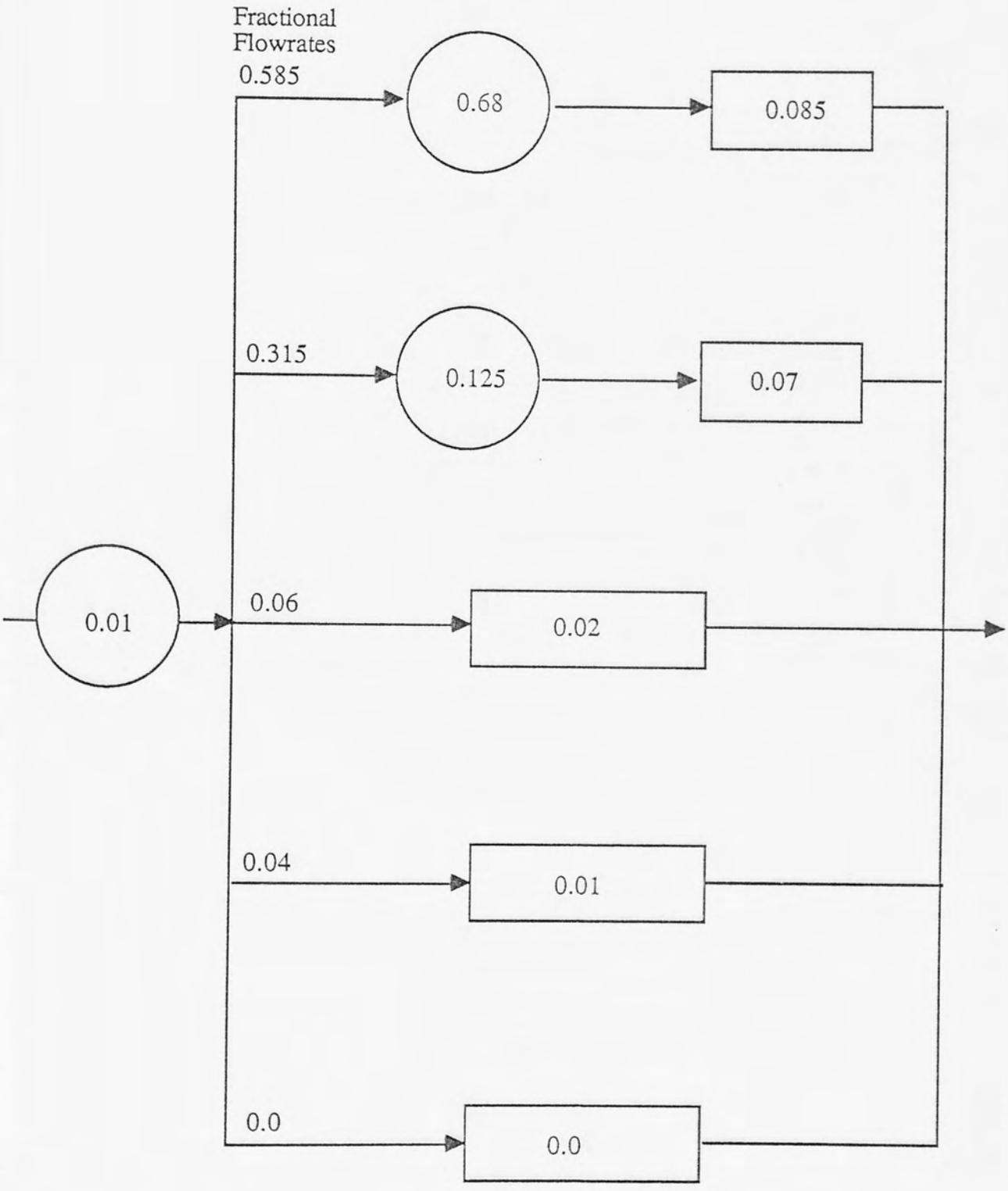

Run Number: 050
Flowrate: 0.172 L/Hr
Feed Point: A
Dead Space: 0.55
Fraction Stream Volume: 0.5
Comments: Two offtakes and central weir

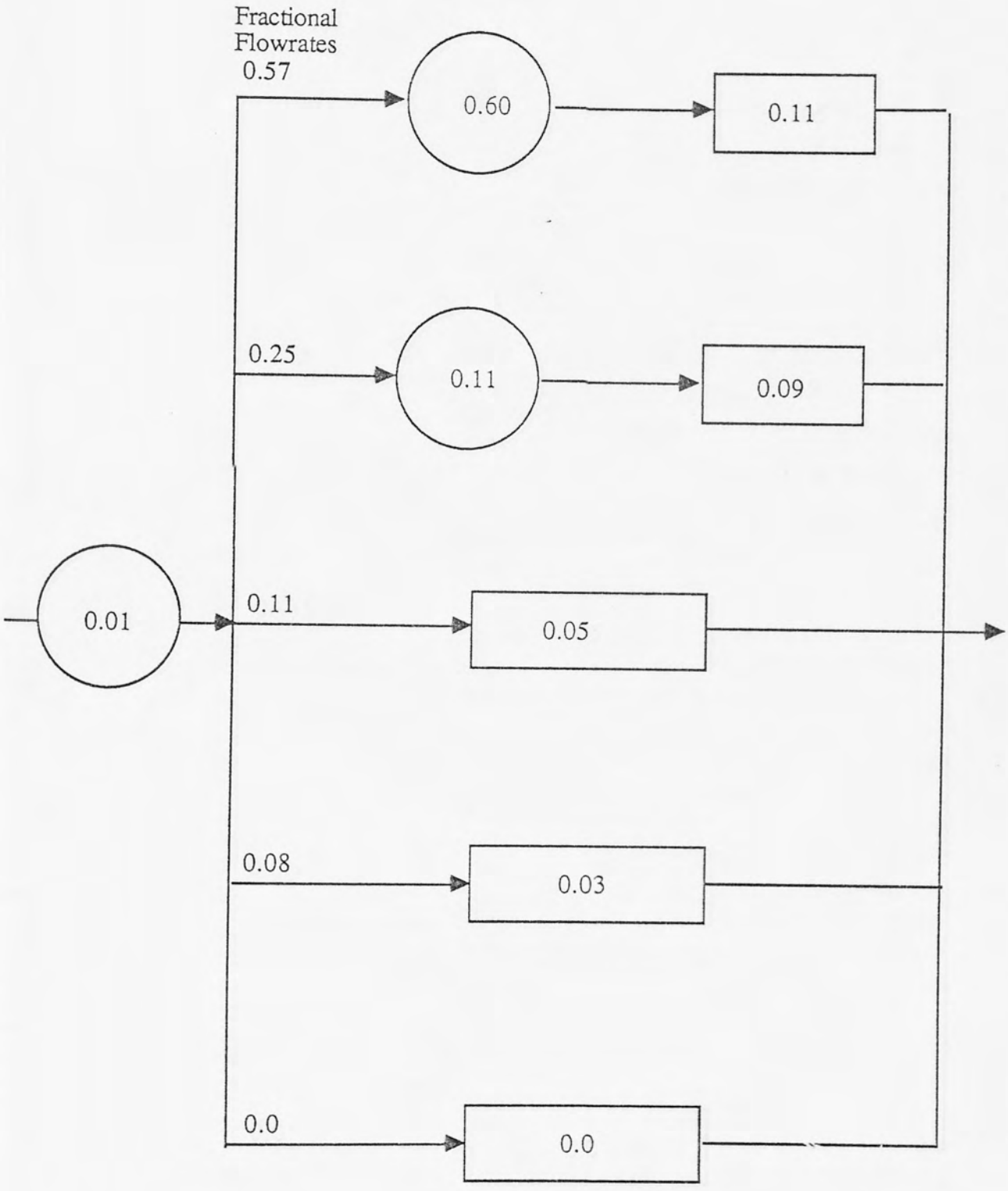

Run Number:	050
Flowrate:	0.172 L/Hr
Feed Point:	B
Dead Space:	0.55
Fraction Stream Volume:	0.5
Comments:	Two offtakes and central weir

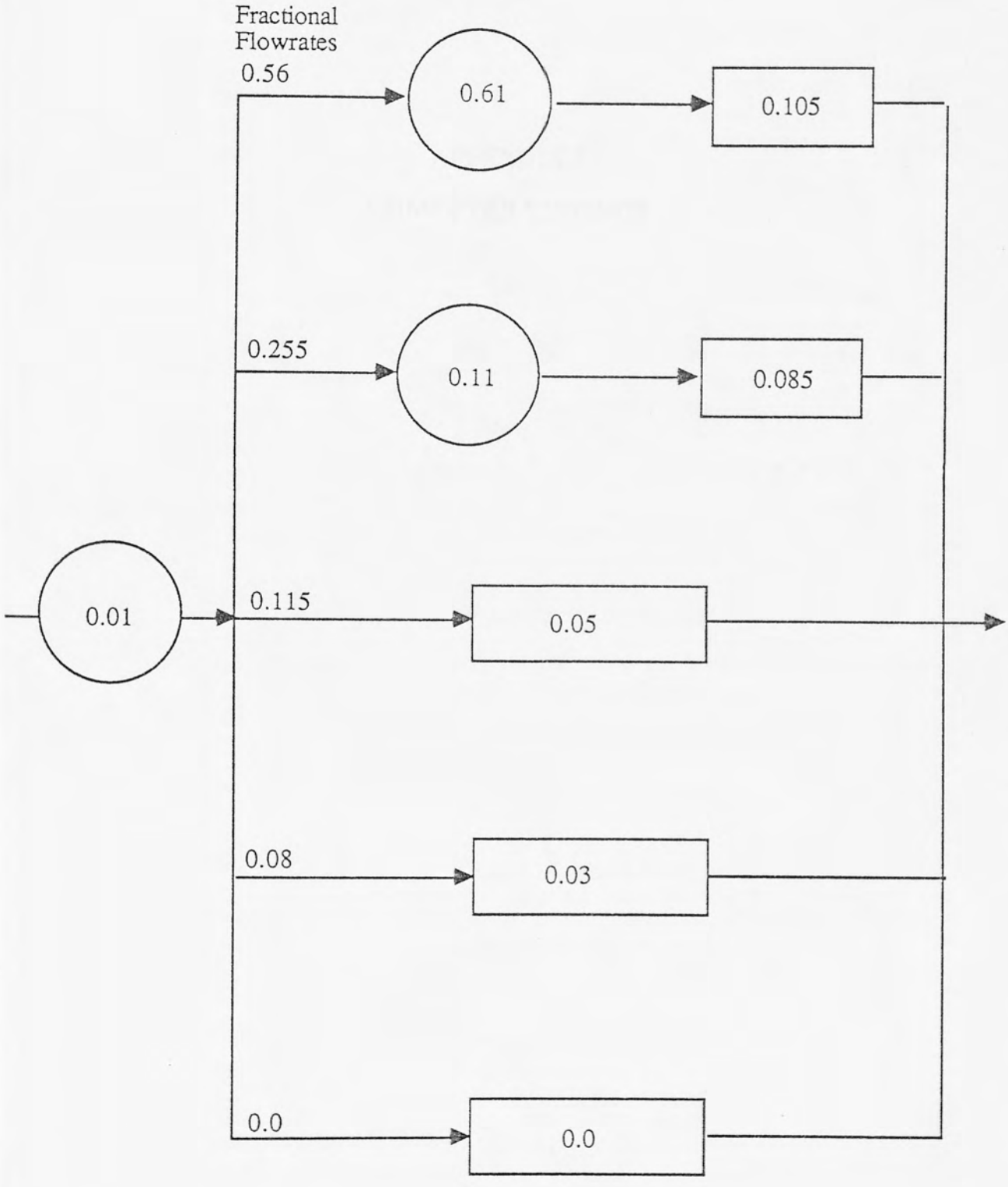

APPENDIX 2

COMPUTER LISTINGS

i) SAME : Evaluation of values for four dimensionless groups for the furnace and model within specified temperature ranges.

ii) PLTSAM : Plotting routines for four dimensionless groups, together with four similarity plots.

iii) PLOTTA! : Processes Analogue inputs and plots concentration/time curves for upto four channels.

iv) MODEL : Constructs a concentration/time array based on a particular mixed model network and input parameters.

v) PLOT : Plots out practical and theoretical concentration/ time graphs.

SAME

```
IN 10,70 70
   >L. 0,450
     10 DIM RE(40),GR(40),PR(40),PU(40),RE1(40),RE2(40),GR1(40
  ),GR2(40),PR1(40),PR2(40),PU1(40),PU2(40)
     20 FOR I = 1 TO 40
     30 T = 685+(I*15)
     40 REM EVALUATE REYNOLD NUMBER(RE)
     50
     60 REM MELT VELOCITY (3.60M^3/HR)
     70 V=(3.6*(10^6))/(3600*945*100)
     80 VI = EXP((21186.44/(T+273))-8.44)
     90 RE(I) = ((2.268-(1.2469*(10^-4))*T)*V*945)/VI
    100 REM EVALUATE GRASHOF NUMBER(GR)
    110 D=2.268-(1.2469*(10^-4)*T)
    120 B=((((2.268-(1.2469*(10^-4)*(T-1.0)))^0.333)/((2.268-(
  1.2469*(10^-4)*(T+1.0)))^0.33))-1.0)/2.0
    130GR(I)=945^3*981*D^2*B*110/VI^2
    140 REM EVALUATE PRANDTL NUMBER(PR)
    150 C=((0.000468*T+0.1657)/(0.00146*T+1.0))+3.35*((0.00082
  9*T+0.229)/(0.00146*T+1.0))
    160 DIFF=10^(0.04752+(0.0016074*T))/1000
    170 K=DIFF*D*C
    180 PR(I)= C*VI/K
    190 REM EVALUATE PULL(PU)
    200 PU(I)=882*VI/(D^2*981*B*110*945^4)
    210 NEXT I
    220 Y1 = OPENOUT"RE"
    230 FOR J = 1 TO 40
    240 PRINT£Y1,RE(J)
    250 NEXT
    260 CLOSE£Y1
    270 Y2 = OPENOUT"GR"
    280 FOR J = 1 TO 40
    290 PRINT£Y2,GR(J)
    300 NEXT
    310 CLOSE£Y2
    320 Y3 = OPENOUT"PR"
    330 FOR J = 1 TO 40
    340 PRINT£Y3,PR(J)
    350 NEXT
    360 CLOSE£Y3
    370 Y4 = OPENOUT"PU"
    380 FOR J = 1 TO 40
    390 PRINT£Y4,PU(J)
    400 NEXT
    410 CLOSE£Y4
    420 FOR I = 1 TO 40
    430 T = -1.0 + I
    440 REM EVALUATE REYNOLDS NUMBERS
    450 V1 = (3.6*(10^6))/(3600*10000*945)
```

SAME

```
BIN 10 70
   >L. 0460,900
    460 VI1 = EXP((11916.7/(T+273))-35.04)
    470 D1 = 1.693 -(4.1*(10^-4)*T)
    480 V2 = (3.6*(10^6))/(3600*100000*945)
    490 VI2 = EXP((11333.3/(T+273))-35.08)
    500 D2 = 1.629 - (7.2*(10^-4)*T)
    510 RE1(I) = D1*V1*94.5/VI1
    520 RE2(I) = D2*V2*94.5/VI2
    530 REM EVALUATE GRASHOF NUMBERS
    540 B2 = (((1.629-(7.2*(10^-4)*(T-1.0)))^0.333/((1.629-(7.
  2*(10^-4)*(T+1.0)))^0.333))-1.0)/2.0
    550 B1 = (((1.693-(4.1*(10^-4)*(T-1.0)))^0.333/((1.693-(4.
  1*(10^-4)*(T+1.0)))^0.333))-1.0)/2.0
    560 GR1(I) = 94.5^3*981*D1^2*B1*30/VI1^2
    570 GR2(I) = 94.5^3*981*D2^2*B2*30/VI2^2
    580 REM EVALUATE PRANDTL NUMBERS
    590 PR1(I) = 0.79 * VI1/12.9
    600 PR2(I) = 0.74 * VI2/12.9
    610 REM EVALUATE PULL
    620 PU1(I) = 8.82*VI1/(D1^2*981*B1*30*(94.5^4))
    630 PU2(I) = 0.882*VI2/(D2^2*981*B2*30*(94.5^4))
    640 NEXT I
    650 X1 = OPENOUT"RE1"
    660 FOR J = 1 TO 40
    670 PRINT£X1,RE1(J)
    680 NEXT
    690 CLOSE£X1
    700 X2 = OPENOUT"RE2"
    710 FOR J = 1 TO 40
    720 PRINT£X2,RE2(J)
    730 NEXT
    740 CLOSE£X2
    750 X3 = OPENOUT"GR1"
    760 FOR J = 1 TO 40
    770 PRINT£X3,GR1(J)
    780 NEXT
    790 CLOSE£X3
    800 X4 = OPENOUT"GR2"
    810 FOR J = 1 TO 40
    820 PRINT£X4,GR2(J)
    830 NEXT
    840 CLOSE£X4
    850 X5 = OPENOUT"PR1"
    860 FOR J = 1 TO 40
    870 PRINT£X5,PR1(J)
    880 NEXT
    890 CLOSE£X5
    900 X6 = OPENOUT"PR2"
```

```
ABIN 10 70
    >L.910,1100
     910 FOR J = 1 TO 40
     920 PRINT£X6,PR2(J)
     930 NEXT
     940 CLOSE£X6
     950 X7 = OPENOUT"PU1"
     960 FOR J = 1 TO 40
     970 PRINT£X7,PU1(J)
     980 NEXT
     990 CLOSE£X7
    1000 X8 = OPENOUT"PU2"
    1010 FOR J = 1 TO 40
    1020 PRINT£X8,PU2(J)
    1030 NEXT
    1040 CLOSE£X8
    1050 END
```

PLTSAM 2

```
L.0, 450
   10 *TV255,1
   20 MODE 0
   30 DIM RE(40),RE1(40),RE2(40),GR(40),GR1(40),GR2(40),PR(4
0),PR1(40),PR2(40),PU(40),PU1(40),PU2(40)
   40 INPUT "RE1:1,RE2:2,GR1:3,GR2:4,PR1:5,PR2:6,PU1:7,PU2:8
";I
   50 IF I = 1 THEN PROCRE1
   60 IF I = 2 THEN PROCRE2
   70 IF I = 3 THEN PROCGR1
   80 IF I = 4 THEN PROCGR2
   90 IF I = 5 THEN PROCPR1
  100 IF I = 6 THEN PROCPR2
  110 IF I = 7 THEN PROCPU1
  120 IF I = 8 THEN PROCPU2
  130 INPUT "Y_AXIS FULL SCALE(FURNACE)"YF
  140 INPUT "Y_AXIS FULL SCALE(MODEL)"YM
  150 VDU19,128,132,0,0,0
  160 VDU5
  170 PROCAXIS
  180 PROCPLOT
  190 REPEAT
  200 IF INKEY(-1)THEN PROCDUMP
  210 UNTIL FALSE
  220 VDU4
  230 END
  240 DEF PROCAXIS
  250 CLS
  260 VDU29,0;0;
  270 FOR I = 0 TO 40 STEP 4
  280 INC = I *30
  290 MOVE (80+INC),94
  300 DRAW (80+INC),99
  310 MOVE (80+INC),84
  320 PRINT;I
  330 MOVE (80+INC),55
  340 PRINT;INT(700+(I*15))
  350 NEXT
  360 MOVE 300,950
  370 PRINT"REYNOLDS vs TEMPERATURE";
  380 VDU29,80;99;
  390 MOVE 0,0
  400 DRAW 0,235*4
  410 MOVE 0,0
  420 DRAW 300*4,0
  430 ENDPROC
  440 DEF PROCPLOT
  450 LET PREVX=0:PREVY1=0:PREVY2=0
```

```
L.460,900
  460 FOR X=0TO 40*30 STEP 30
  470 YPIXEL = YF/235
  480 YPIXEL1 = YM/235
  490 I = ((X/30)+1)
  500 IF I = 41 THEN I = 40
  510 Y1 = (RE(I)/YPIXEL)*4
  520 Y2 = (RE2(I)/YPIXEL1)*4
  530 MOVE PREVX,PREVY1
  540 PLOT5,X,Y1
  550 MOVE PREVX,PREVY2
  560 PLOT21,X,Y2
  570 LET PREVX=X:PREVY1=Y1:PREVY2=Y2
  580 NEXT X
  590 MOVE (X-180),Y1
  600 PRINT"FURNACE"
  610 MOVE (X-180),Y2
  620 PRINT"MODEL"
  630 ENDPROC
  640 DEF PROCDUMP
  650 VDU19,132,128,0,0,0
  660 *GDUMP 1,1,3,1,15
  670 VDU19,128,132,0,0,0
  680 ENDPROC
  690 DEF PROCRE1
  700 Y1 = OPENIN"RE"
  710 FOR J = 1 TO 40
  720 INPUT£Y1,RE(J)
  740 NEXT
  750 CLOSE£Y1
  760 X1 = OPENIN"RE1"
  770FOR J = 1 TO 40
  780 INPUT£X1,RE1(J)
  800 NEXT
  810 CLOSE£X1
  820 ENDPROC
  830 DEF PROCRE2
  840 Y1 = OPENIN"RE"
  850 FOR J = 1 TO 40
  860 INPUT£Y1,RE(J)
  880 NEXT
  890 CLOSE£Y1
  900 X2 = OPENIN"RE2"
```

```
L. 910,1350
  910 FOR J = 1 TO 40
  920 INPUT£X2,RE2(J)
  940 NEXT
  950 CLOSE£X2
  960 ENDPROC
  970 DEF PROCGR1
  980 Y2 = OPENIN"GR"
  990 FOR J = 1 TO 40
 1000 INPUT£Y2,GR(J)
 1010 RE(J) = GR(J)
 1020 NEXT
 1030 CLOSE£Y2
 1040 X3 = OPENIN"GR1"
 1050 FOR J = 1 TO 40
 1060 INPUT£X3,GR1(J)
 1070 RE2(J) = GR1(J)
 1080 NEXT
 1090 CLOSE£X3
 1100 ENDPROC
 1110 DEF PROCGR2
 1120 Y2 = OPENIN"GR"
 1130 FOR J = 1 TO 40
 1140 INPUT£Y2,GR(J)
 1150 RE(J) = GR(J)
 1160 NEXT
 1170 CLOSE£Y2
 1180 X4 = OPENIN"GR2"
 1190 FOR J = 1 TO 40
 1200 INPUT£X4,GR2(J)
 1210 RE2(J) = GR2(J)
 1220 NEXT
 1230 CLOSE£X4
 1240 ENDPROC
 1250 DEF PROCPR1
 1260 Y3 = OPENIN"PR"
 1270 FOR J = 1 TO 40
 1280 INPUT£Y3,PR(J)
 1290 RE(J) = PR(J)
 1300 NEXT
 1310 CLOSE£Y3
 1320 X5 = OPENIN"PR1"
 1330 FOR J = 1 TO 40
 1340 INPUT£X5,PR1(J)
 1350 RE2(J) = PR1(J)
```

```
L. 1360,1800
 1360 NEXT
 1370 CLOSE£X5
 1380 ENDPROC
 1390 DEF PROCPR2
 1400 Y3 = OPENIN"PR"
 1410 FOR J = 1 TO 40
 1420 INPUT£Y3,PR(J)
 1430 RE(J) = PR(J)
 1440 NEXT
 1450 CLOSE£Y3
 1460 X6 = OPENIN"PR2"
 1470 FOR J = 1 TO 40
 1480 INPUT£X6,PR2(J)
 1490 RE2(J) = PR2(J)
 1500 NEXT
 1510 CLOSE£X6
 1520 ENDPROC
 1530 DEF PROCPU1
 1540 Y4 = OPENIN"PU"
 1550 FOR J = 1 TO 40
 1560 INPUT£Y4,PU(J)
 1570 RE(J) = PU(J)
 1580 NEXT
 1590 CLOSE£Y4
 1600 X7 = OPENIN"PU1"
 1610 FOR J = 1 TO 40
 1620 INPUT£X7,PU1(J)
 1630 RE2(J) = PU1(J)
 1640 NEXT
 1650 CLOSE£X7
 1660 ENDPROC
 1670 DEF PROCPU2
 1680 Y4 = OPENIN"PU2"
 1690 FOR J = 1 TO 40
 1700 INPUT£Y4,PU(J)
 1710 RE(J) = PU(J)
 1720 NEXT
 1730 CLOSE£Y4
 1740 X8 = OPENIN"PU2"
 1750 FOR J = 1 TO 40
 1760 INPUT£X8,PU2(J)
 1770 RE2(J) = PU2(J)
 1780 NEXT
 1790 CLOSE£X8
 1800 ENDPROC
```

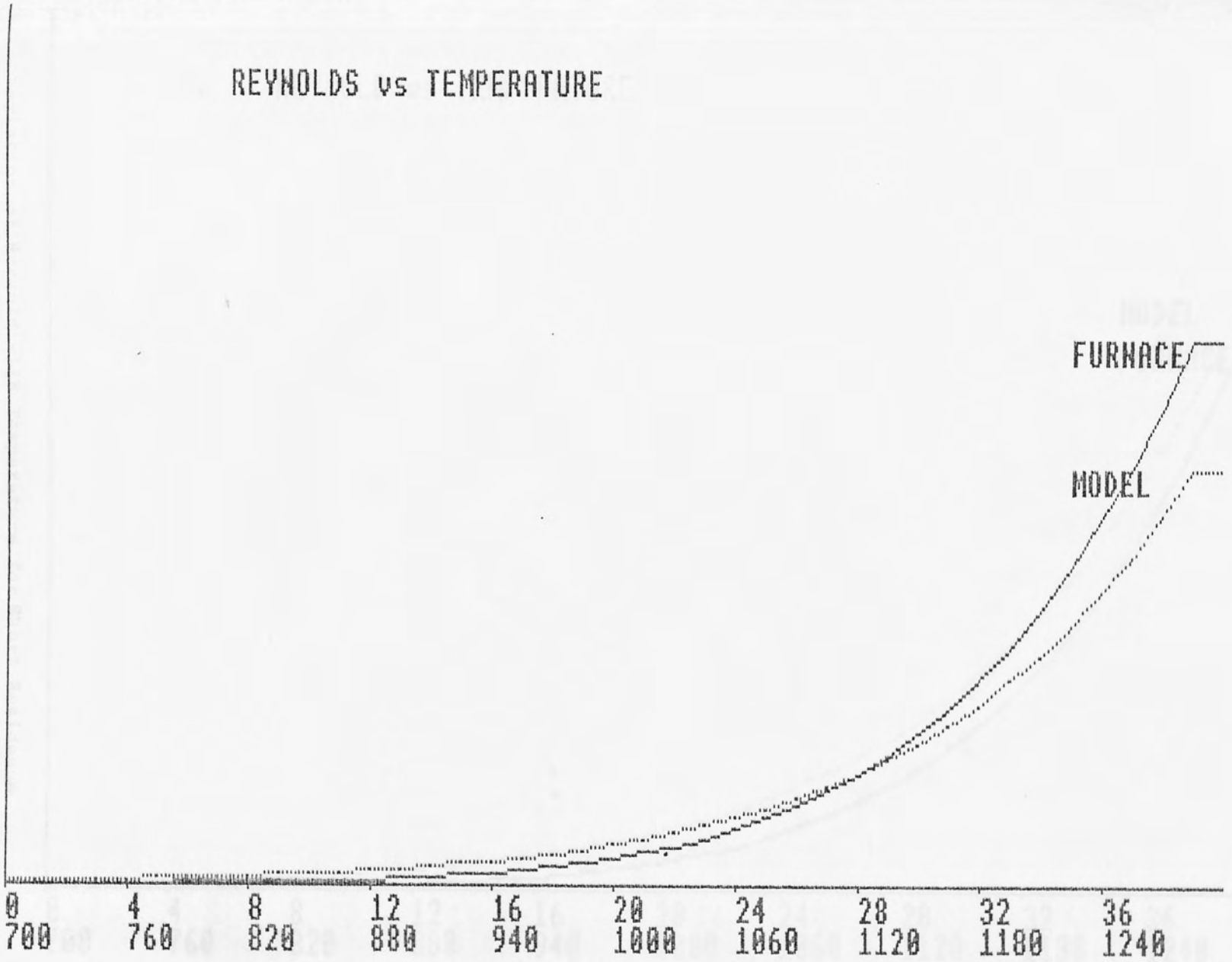

Variation of Reynold with Temperature for Long Residence Time Experiment

Variation of Reynold with Temperature for Short Residence Time Experiment

Variation of Prandtl with Temperature for Long Residence Time Experiments

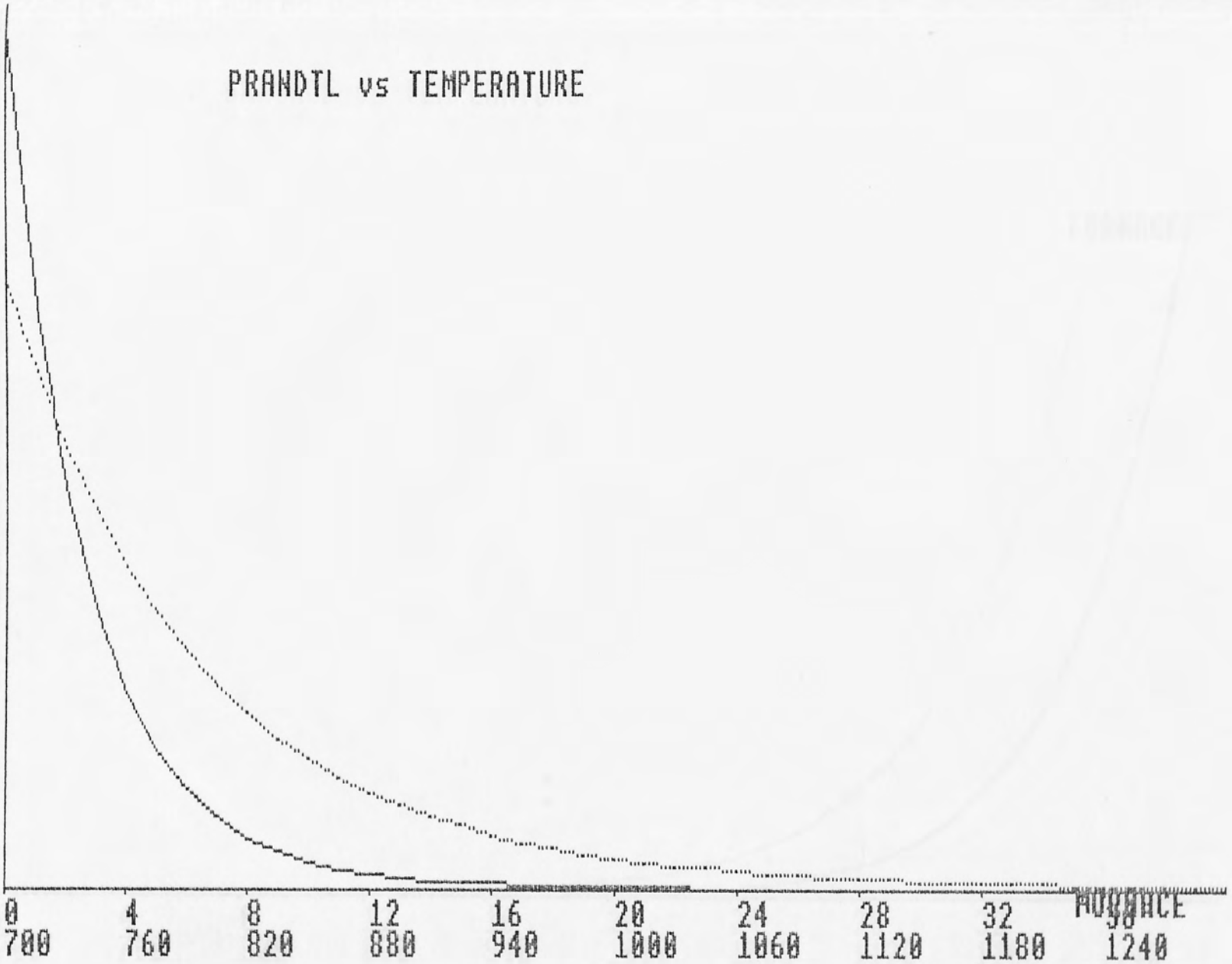

Variation of Prandtl with Temperature for Short Residence Time Experiments

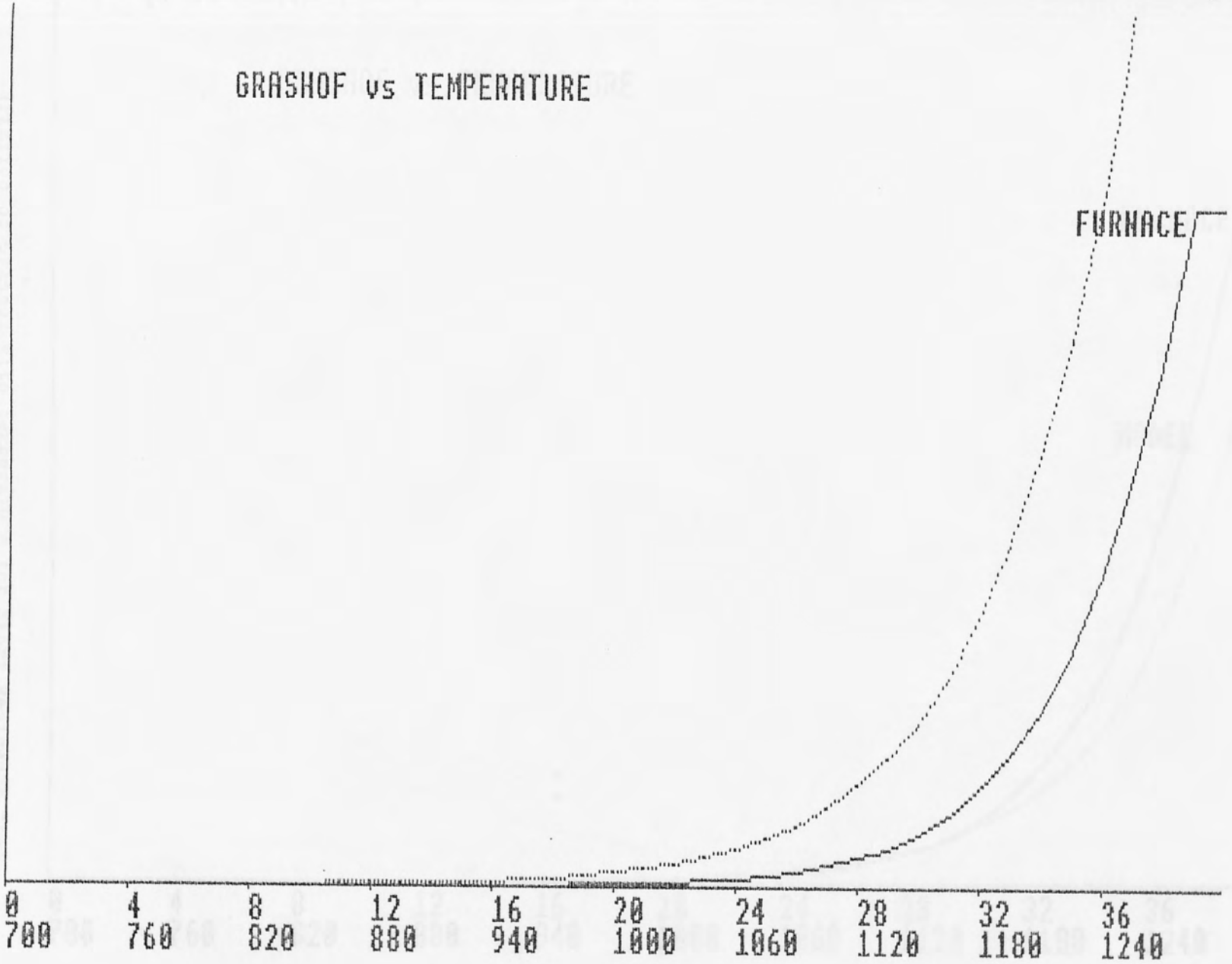

Variation of Grashof with Temperature for Long Residence Time Experiment

Variation of Grashof with Temperature for Short Residence Time Experiment

Variation of 'Pull' with Temperature for Long Residence Time Experiment

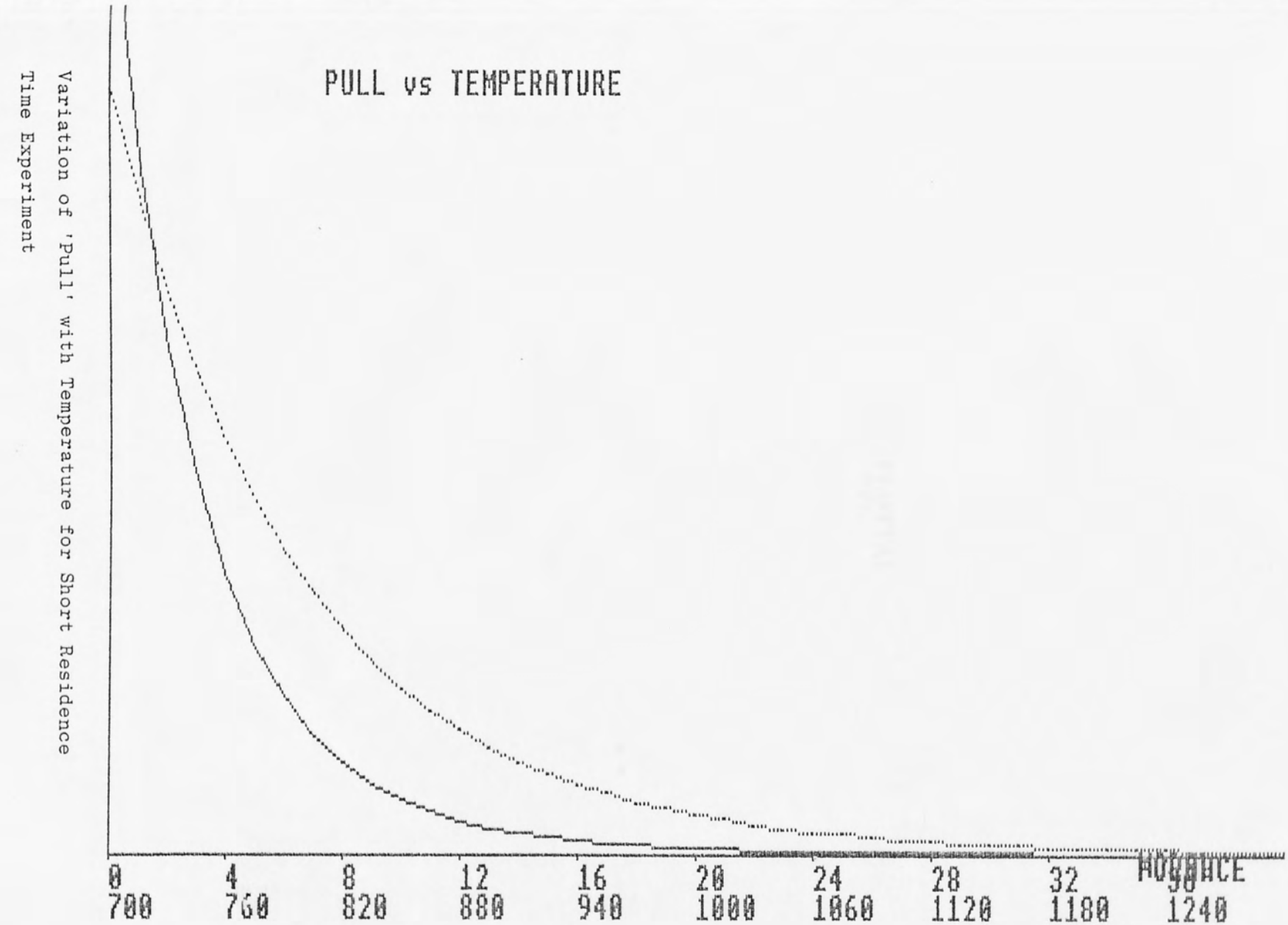
PULL vs TEMPERATURE
Variation of 'Pull' with Temperature for Short Residence Time Experiment
0
700
4
760
8
820
12
880
16
940
20
1000
24
1060
28
1120
32
1180
1240

PLOTTA!

```
L. 0, 450
   10 *TV255,1
   20 MODE 0
   30 VDU19,1,3,0,0,0
   40 DIM C$(4)
   50 ENVELOPE 1,1,0,0,0,0,0,0,126,-10,0,-1,126,100
   60 ON ERROR GOTO 1340
   70 PROCINPARAMETERS
   80 @%=&20209
   90 PROCAXIS
  100 VDU28,60,4,79,0
  110 VDU23,1,0;0;0;0;
  120 PrevX=0:PrevY1=0:PrevY2=0:PrevY3=0:PrevY4=0:X=0
  130 Totaltime=0
  140 TIME=0
  150 REPEAT
  160 PROCTIME
  170 PROCVOLT
  180 PROCPLOT
  190 Totaltime=Totaltime+Samptime
  200 UNTIL Totaltime > Xfullscale
  210 REPEAT
  220 IF INKEY(-1) THEN PROCDUMP
  230 UNTIL FALSE
  240 END
  250 :
  260 :
  270 DEF PROCINPARAMETERS
  280 CLS
  290 INPUT TAB(5,3)"Y.AXIS full scale voltage (volts) " Yfu
llscale
  300 INPUT TAB(5,5)"Y.AXIS offset voltage (volts) " Yoffset
  310 LET Ypixel=(Yfullscale-Yoffset)/235
  320 INPUT TAB(5,7)"Y.AXIS divisional markings (volts) " Yd
ivmarks
  330 LET Ydivpixel=INT(Ydivmarks/Ypixel)
  340 INPUT TAB(5,9)"X.AXIS full scale (minutes) " Xfullscal
e
  350 Xfullscale=Xfullscale*60 : Xpixelsec=Xfullscale/600
  360 INPUT TAB(5,11)"X.AXIS divisional markings (minutes) "
 Xdivmarks
  370 Xdivmarks=Xdivmarks*60 : Xdivpixel=(Xdivmarks/Xpixelse
c)
  380 INPUT TAB(5,13)"Sampling Time (minutes) "Samptime
  390 Samptime=Samptime*60 : Samppixel=(Samptime/Xpixelsec)
  400 PRINT TAB(5,15)"Input (Y)yes or (N)no for channel requ
ired"
  410 FOR N%=1 TO 4
  420 PRINT TAB(5,16+N%)"Channel ";N%;"  ";
  430 INPUT C$(N%)
  440 NEXT N%
  450 ENDPROC
```

PLOTTA:
(i)

```
L. 460,900
  460 :
  470 :
  480 DEF PROCAXIS
  490 CLG
  500 VDU5
  510 VDU29,0;0;
  520 MOVE 30,30
  530 PRINT "Div-Marks = ";Xdivmarks;" Secs.  ";
  540 PRINT "Sampling Time = ";Samptime;" Secs.  ";
  550 PRINT"Total time = ";Xfullscale/60;" Mins"
  560 VDU29,0;21*4;
  570 MOVE 0,0
  580 INC=0
  590 FOR Y=0 TO 235*4 STEP Ydivpixel*4
  600 MOVE 0,Y+17
  610 PRINT;INC+Yoffset
  620 MOVE 30*2,Y
  630 DRAW 40*2,Y
  640 INC=INC+Ydivmarks
  650 NEXT Y
  660 VDU29,40*2;16*4;
  670 MOVE 0,0
  680 FOR X=0 TO 600*2 STEP Xdivpixel*2
  690 MOVE X,0
  700 DRAW X,20
  710 NEXT X
  720 VDU29,40*2;21*4;
  730 MOVE 0,0
  740 DRAW 0,235*4
  750 MOVE 0,0
  760 DRAW 600*2,0
  770 VDU4
  780 ENDPROC
  790 :
  800 :
  810 DEF PROCPLOT
  820 Y1=((VOLT1-Yoffset)/Ypixel)*4
  830 Y2=((VOLT2-Yoffset)/Ypixel)*4
  840 Y3=((VOLT3-Yoffset)/Ypixel)*4
  850 Y4=((VOLT4-Yoffset)/Ypixel)*4
  860 IF C$(1)="N" THEN 890
  870 MOVE PrevX,PrevY1
  880 PLOT5,X,Y1
  890 IF C$(2)="N" THEN 920
  900 MOVE PrevX,PrevY2
```

```
L. 910,1350
  910 PLOT5,X,Y2
  920 IF C$(3)="N" THEN 950
  930 MOVE PrevX,PrevY3
  940 PLOT5,X,Y3
  950 IF C$(4)="N" THEN 980
  960 MOVE PrevX,PrevY4
  970 PLOT5,X,Y4
  980 LET PrevX=X:PrevY1=Y1:PrevY2=Y2:PrevY3=Y3:PrevY4=Y4
  990 X=X+(Samppixel*2)
 1000 SOUND 3,1,245,1
 1010 ENDPROC
 1020 :
 1030 :
 1040 DEF PROCVOLT
 1050 VOLT1=(ADVAL(1)/16)*(1.8/4095)
 1060 VOLT2=(ADVAL(2)/16)*(1.8/4095)
 1070 VOLT3=(ADVAL(3)/16)*(1.8/4095)
 1080 VOLT4=(ADVAL(4)/16)*(1.8/4095)
 1090 ENDPROC
 1100 :
 1110 :
 1120 DEF PROCTIME
 1130 @%=&20009
 1140 REPEAT
 1150 SEC=(TIME DIV 100)MOD 60
 1160 MIN=(TIME DIV 6000)MOD 60
 1170 HR=(TIME DIV 360000)MOD 24
 1180 PRINT TAB(0,1)"Time  ";HR;MIN;SEC
 1190 IF INKEY(-1) THEN PROCDUMP
 1200 UNTIL TIME/100 > Totaltime
 1210 @%=10
 1220 ENDPROC
 1230 :
 1240 :
 1250 DEF PROCDUMP
 1260 Time=TIME
 1270 VDU19,1,7,0,0,0
 1280 *GPRINT "ANALOGUE INPUT    VOLTS ",3,2,6,1,30
 1290 *GDUMP 1,1,3,1,15
 1300 VDU19,1,3,0,0,0
 1310 TIME=Time
 1320 ENDPROC
 1330 :
 1340 IF ERR=17 THEN 1400
 1350 ON ERROR OFF
```

```
L. 1360,1800
 1360 MODE 3
 1370 REPORT:PRINT" AT ";ERL
 1380 END
 1390 :
 1400 VDU26:CLS
 1410 INPUT TAB(5,5)"(R)repeat  (C)change  (E)end  " D$
 1420 IF D$="R" THEN 80
 1430 IF D$="C" THEN 70
 1440 IF D$="E" THEN MODE3 : END
 1450 PRINT TAB(5,5)"                              "
 1460 GOTO 1410
```

MODEL

```
L. 0,450
   10 MODE 3
   20 DIM C(310)
   30 DIM CI(310)
   40 DIM CO(310)
   50 DIM TE(310)
   60INPUT "WHAT IS FIRST ESTIMATE OF FRACTION OF TOTAL VOLU
ME WHICH IS DEADSPACE ?",DS
   70VOL = 47.85
   80 INPUT "TYPE IN FEED POINT NUMBER",N%
   90 IF N% = 2 THEN 150
  100INPUT "WHAT IS FEEDER ONE FLOWRATE,L/HR ?",Q1
  110INPUT "WHAT MASS OF TRACER IS INJECTED,G ?",M1
  120INPUT " WHAT FRACTION OF AVAILABLE REACTOR VOLUME IS US
ED BY FEED ONE ?",FV1
  130PRINT "STREAM ONE CAN BE DIVIDED INTO FIVE STREAMS,ST &
 PF,ST & PF,PF,PF,PF.THE INPUT STREAM FIRST PASSES THROUGH A
 ST.DEFINE THE FRACTION FLOW THROUGH EACH STREAM,AND THEN TH
E FRACTION VOLUME OF EACH REACTOR"
  140 GOTO 190
  150 INPUT"WHAT IS FEEDER TWO FLOWRATE L/HR",Q1
  160 INPUT"WHAT MASS OF TRACER IS INJECTED,G",M1
  170 INPUT "WHAT FRACTION OF AVAILABLE REACTOR VOLUME IS US
ED BY FEED TWO",FV1
  180 PRINT "STREAM TWO CAN BE DIVIDED INTO FIVE STREAMS,ST
& PF,ST & PF,PF,PF,PF.THE INPUT STREAM FIRST PASSES THROUGH
A ST.DEFINE THE FRACTION FLOW THROUGH EACH STREAM,AND THEN T
HE FRACTION VOLUME OF EACH REACTOR"
  190INPUT "FRACTION FLOWS(5)",F1,F2,F3,F4,F5
  200TF = F1+F2+F3+F4+F5
  210IF TF > 1.05 THEN PRINT "INCORRECT FLOWRATES!" THEN 190

  220INPUT "REACTOR FRACTIONS(8)",V1,V2,V3,V4,V5,V6,V7,V8
  230TV = V1+V2+V3+V4+V5+V6+V7+V8
  240IF TV > 1.050 THEN PRINT "INCORRECT VOLUMES!" THEN 220

  250VOL1 = (VOL*(1.0-DS)*FV1)
  260MEANT =VOL1 /Q1
  270TT = 3*MEANT
  280 DV = TT/300
  290T = 0.0
  300 V = VOL1*V1
  310FOR I% = 1 TO 300
  320T = T + DV
  330C(I%) = (M1/V)*EXP(-1.0*T*(Q1/V))
  340NEXT
  350 J% = 1
  360IF J% = 1 THEN 410
  370IF J% = 2 THEN 530
  380IF J% = 3 THEN 650
  390 IF J% = 4 THEN 750
  400IF J% = 5 THEN 850
  410V = V2*VOL1
  420Q = Q1*F1
  430FOR K% = 1 TO 300
  440CI(K%) = C(K%)
  450NEXT
```

MODEL
(i)

```
L. 460,00900
  460GOSUB 1300
  470V = V3*VOL1
  480GOSUB 1400
  490FOR L% = 1 TO 300
  500CO(L%) =CI(L%)*Q
  510NEXT
  520GOTO 940
  530V = V4*VOL1
  540Q = Q1*F2
  550FOR K% = 1 TO 300
  560CI(K%) = C(K%)
  570NEXT
  580GOSUB 1300
  590V = V5*VOL1
  600GOSUB 1400
  610FOR L% = 1 TO 300
  620CO(L%) =CO(L%) + (CI(L%)*Q)
  630NEXT
  640GOTO 940
  650V = V6*VOL1
  660Q = Q1*F3
  670FOR K% = 1 TO 300
  680CI(K%) =C(K%)
  690NEXT
  700GOSUB 1400
  710FOR L% = 1 TO 300
  720CO(L%) = CO(L%) + (CI(L%)*Q)
  730NEXT
  740 GOTO 940
  750V = V7*VOL1
  760Q = Q1*F4
  770FOR K% = 1 TO 300
  780CI(K%) =C(K%)
  790NEXT
  800GOSUB 1400
  810FOR L% = 1 TO 300
  820CO(L%) =CO(L%)+ (CI(L%)*Q)
  830NEXT
  840GOTO 940
  850V = V8*VOL1
  860Q = Q1 * F5
  870FOR K% = 1 TO 300
  880CI(K%) = C(K%)
  890NEXT
  900GOSUB 1400
```

```
L. 910-,135,1350
  910FOR L% = 1 TO 300
  920CO(L%) =CO(L%) +(CI(L%)*Q)
  930NEXT
  940 J% = J% + 1
  950 IF J% < 6 THEN 360
  960 AREA = 0.0
  970 FOR M% = 1 TO 200
  980 AREA = AREA + (CO(M%)*DV)
  990 NEXT
 1000 MEAN = 0.0
 1010 FOR M = 1 TO 200
 1020 MEAN = MEAN +(CO(M)*DV)
 1030 IF (MEAN - (AREA/2))>0.0 GOTO 1050
 1040 NEXT
 1050 MT = DV*M
 1056 MT = DV*M
 1100 IF N% = 1 THEN 1190
 1110 Y2 = OPENOUT"CO2"
 1120 FOR M% = 1TO 300
 1130 CO(M%) = CO(M%)/Q2
 1140 PRINT£Y2,CO(M%)
 1150 NEXT
 1160 PRINT£Y2,DS,N%,Q1,VOL1,F1,F2,F3,F4,F5,V1,V2,V3,V4,V5,V
6,V7,V8
 1170 CLOSE£Y2
 1180 GOTO 1260
 1190 Y1=OPENOUT"CO1"
 1200 FOR M% = 1 TO 300
 1210 CO(M%) = CO(M%)/Q1
 1220 PRINT£Y1,CO(M%)
 1230 NEXT
 1240 PRINT£Y1,DS,N%,Q1,VOL1,F1,F2,F3,F4,F5,V1,V2,V3,V4,V5,V
6,V7,V8
 1250 CLOSE£Y1
 1260END
 1270:
 1280:
 1290:
 1300 M = CI(1) * Q* DV
 1310 FOR I% = 1 TO 299
 1320 CI(I%) = (M/V)*EXP(-1.0*DV*(Q/V))
 1330 MO = CI(I%) * Q * DV
 1340 M = M-MO+(CI(I%+1)*Q*DV)
 1350NEXT
```

```
L. 1360,1800
 1360RETURN
 1370:
 1380:
 1390:
 1400T = V/Q
 1410NUM% = INT(T/DV)
 1420 FOR K% =1 TO 300
 1430 TE(K%) = CI(K%)
 1440 NEXT
 1450FOR A% = NUM% TO 300
 1460 B% =A% -NUM%+1
 1470 CI(A%) = TE(B%)
 1480NEXT
 1490FOR I% = 1 TO NUM%
 1500CI(I%) = 0.0
 1510NEXT
 1520RETURN
```

COMPUTER LOGIC DIAGRAM (MODEL

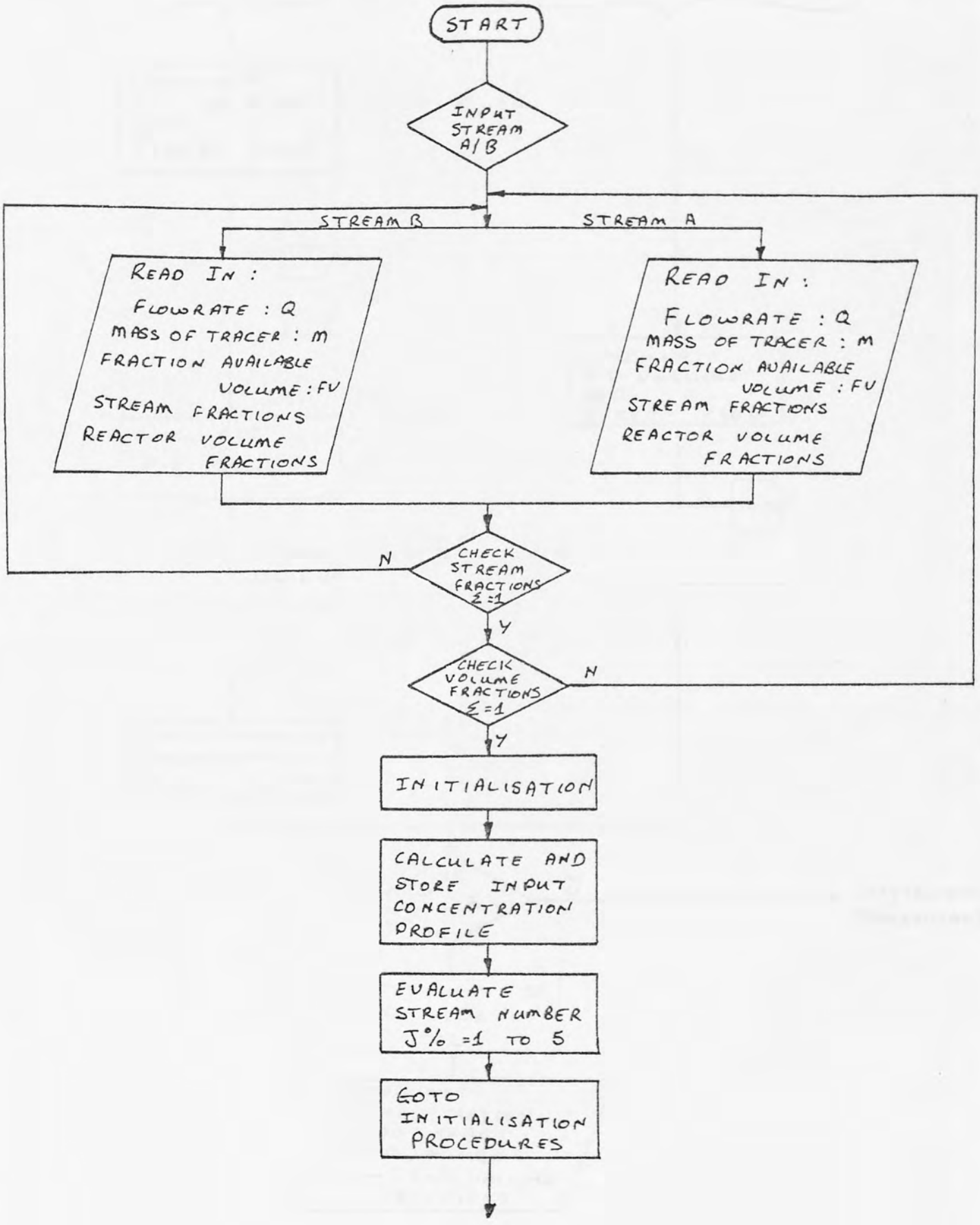

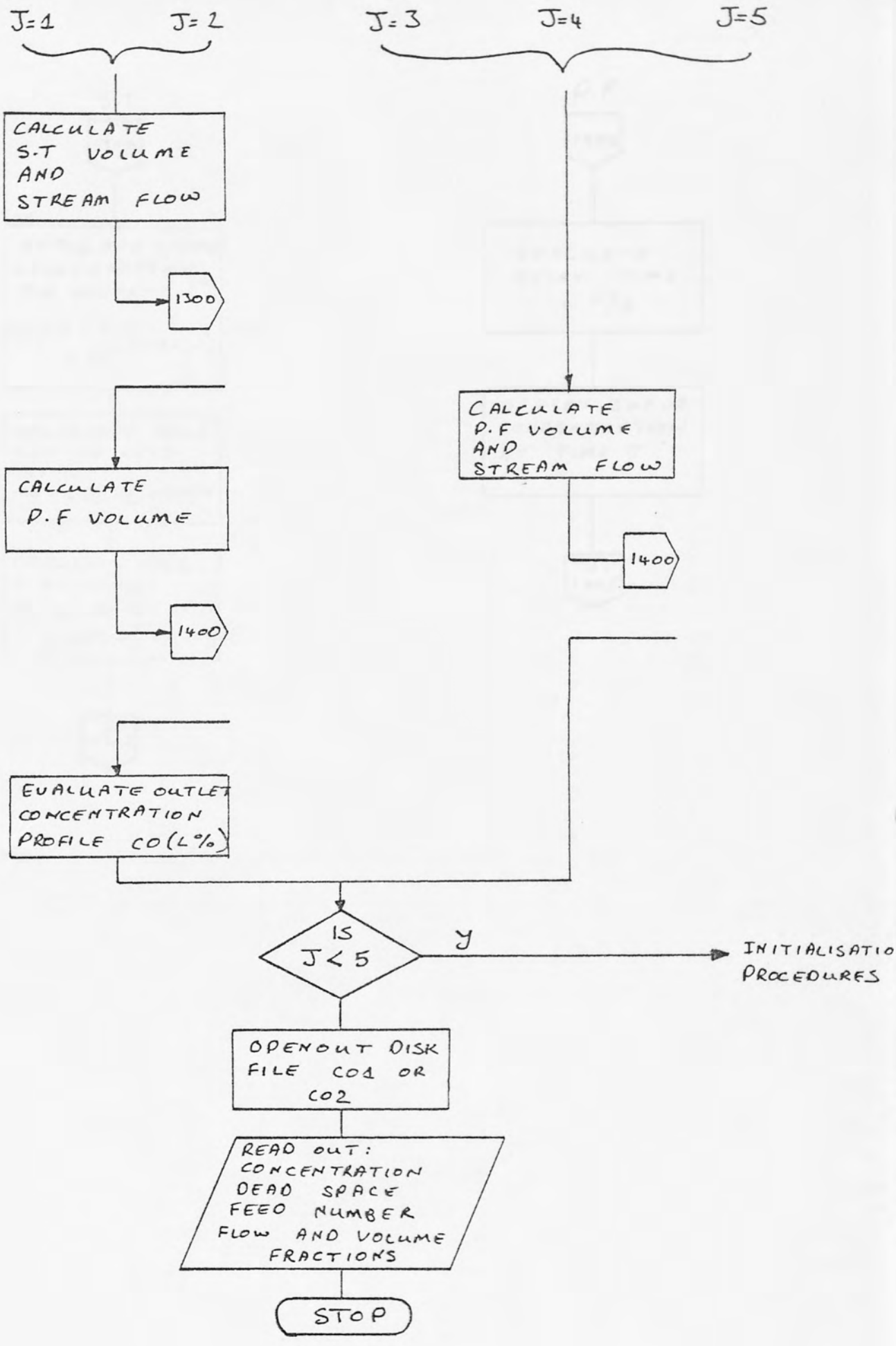
J=1
J=2
J=3
J=4
J=5
CALCULATE S.T VOLUME AND STREAM FLOW
1300
CALCULATE P.F VOLUME
1400
CALCULATE P.F VOLUME AND STREAM FLOW
1400
EVALUATE OUTLET CONCENTRATION PROFILE CO(L%)
IS J<5
y
INITIALISATIO PROCEDURES
OPENOUT DISK FILE CO1 OR CO2
READ OUT: CONCENTRATION DEAD SPACE FEED NUMBER FLOW AND VOLUME FRACTIONS
STOP

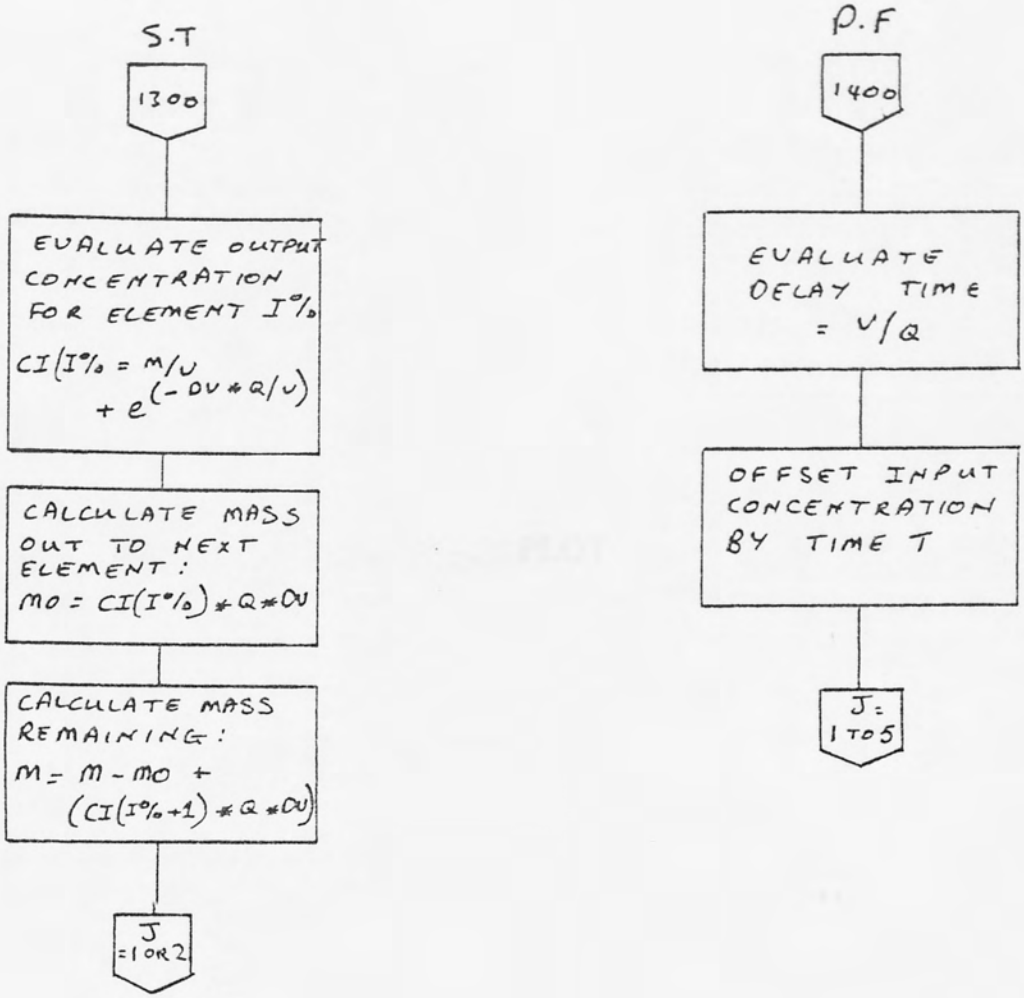
S.T
1300
EVALUATE OUTPUT CONCENTRATION FOR ELEMENT I%
CI(I% = M/V + e^(-DV*Q/V)
CALCULATE MASS OUT TO NEXT ELEMENT:
MO = CI(I%) * Q * DV
CALCULATE MASS REMAINING:
M = M - MO + (CI(I%+1) * Q * DV)
J = 1 OR 2
P.F
1400
EVALUATE DELAY TIME = V/Q
OFFSET INPUT CONCENTRATION BY TIME T
J = 1 TO 5

PLOT

```
L. 0,450
   10 *TV255,1
   20 MODE 0
   30 DIM CO(310)
   40 VDU19,128,132,0,0,0
   50 VDU5
   60 Y1 = OPENIN"CO1"
   70 FOR I% = 1 TO 300
   80 INPUT£Y1,CO(I%)
   90 NEXT
  100 CLOSE£Y1
  110 PROCAXIS
  120 PROCPLOT
  130 REPEAT
  140 IF INKEY(-1) THEN PROCDUMP
  150 UNTIL FALSE
  160 VDU4
  170 END
  180 DEF PROCAXIS
  190 CLS
  200 YPIXEL = 0.06/235
  210 YDIVPIXEL = INT(0.01/YPIXEL)
  220 TT = 3
  230 XPIXEL = TT/300
  240 XDIVPIXEL = INT(TT/(3*XPIXEL))
  250 VDU29,0;21*4;
  260 MOVE 0,0
  270 INC = 0
  280 FOR Y = 0 TO 235*4 STEP YDIVPIXEL*4
  290 MOVE 0,Y+17
  300 PRINT;INC
  310 MOVE 30*2,Y
  320 DRAW 40*2,Y
  330 INC = INC + 0.01
  340 NEXT Y
  350 VDU29,40*2;16*4;
  360 MOVE 0,0
  370 FOR X=0 TO 300*4 STEP XDIVPIXEL*4
  380 MOVE X,0
  390 DRAW X,20
  400 NEXT X
  410 VDU29,40*2;21*4;
  420 MOVE 0,0
  430 DRAW 0,235*4
  440 MOVE 0,0
  450 DRAW 300*4,0
```

```
L. 460,600
  460 ENDPROC
  470
  490 DEF PROCPLOT
  500 LET PREVX = 0:PREVY1 = 0
  510 FOR X = 0 TO 300*4 STEP 4
  520 I% = INT((X/4)+1)
  530 IF I% = 301 THEN I% = 300
  540 Y1 = (CO(I%)/YPIXEL)*4
  550 MOVE PREVX,PREVY1
  560 DRAW X,Y1
  570 LET PREVX = X:PREVY1 = Y1
  580 NEXT X
  590 ENDPROC
```

NOMENCLATURE

L	Linear dimension of tank
Δ	Mean excess of surface temp. over air
M	Time rate of withdrawal of mass
g	Gravitational constant
λT	Thermal conductivity of tank walls
ρ	Density of liquid
μ	Viscosity of liquid
C	Specific heat of liquid
λ	Thermal conductivity of liquid
β	Coefficient of expansion of liquid
δT	Temperature difference corresponding to two similar points
V	Liquid velocity as a vector
F	Force on unit volume of liquid
P	Pressure
Si	Scale factors
V	Liquid velocity
K	Thermal diffusivity
r	Radius
z	Distance
θ	Angle
w	Angular velocity
di	Diameter

R	Shear stress
τ	Torque
T	Temperature
dx	Change in length
x	Length
Vi	Volume of sample
Cm	Heat capacity
λ^2	Thermal diffusivity

REFERENCES

REFERENCES

1. SAWAI, I. and Others, The flow of glass through the throat of the bridge wall of a glass melting tank, III International Congress on Glass, 1953, 482-501.

2. VELEV, D.S., Influence of the construction of the bridge-wall on the flow of glass, Steklo i Kermika, 1959 16 (a) 13-16.

3. KUNUGI, KATSUAKI, TAKAHASHI and SAWAI, Studies on flow and mixing of glass in tank furnaces by model techniques, VI Int. Cong. on Glass, 1962, 165-174.

4. DUPERRAY, N., A method for the study of thermal currents in models of tank furnaces, Vetro & Silicati, 1959, 3, (16), July/Aug., 3-10.

5. HEIDTKAMP, G. and ENDELL, K., Glastech Ber., 14, 89, (1936).

6. ENGLISH, S., J. Soc. Glas. Technol., 7, 25 (1923); 8, 205 (1924); 9, 83 (1925), 10, 52, (1926).

7. SHARP, D.E. and GINTHER, L.B., J. Am. Ceram. Soc., 34, 260, (1951).

8. VAN ZEE, A.F. and BABCOCK, C.L., A method for the measurement of thermal diffusivity of molten glass., J. Am. Ceram. Soc., 34 (8) Aug, (1951).

9. Unilever Research Soluble Silicate Part III - Mathematical model for reactant flow in No. 2 furnace; A.L. Lovell, J.K. Potter.

10. OCTAVE LEVENSPIEL, Mixed models to represent flow of fluids through vessels, Canadian Jn. Chem. Eng., August 1962.

11. Soluble silicates & their derivatives, D. Barby, T. Griffiths, A.R. Jacques and D. Pawson, J. Crosfield & Sons Ltd., Publ^{n}.

12. MICHAELS, P.A., Representation of tank furnaces., J. Amer. Ceram. Soc., 34, pp 470-481.

13. LEGER, R., Dimensional analysis in glass furnaces models., Bulletin de l'institut du verre, 1965 (13) 15-22.

14. BUCKINGHAM, E., The use of models for studying the circulation in glass tanks., J. Amer. Ceram. Soc., 1937, 20, (1), 1-10.

15. DUPERRAY, N., A method for the study of thermal currents in models of tank furnaces, Vetro e silicati, 1959, 3, (16), July/August, 3-10.

16. KRUSEWSKI, W., Physical models for observing glass tank currents, Glastechnische Berichte, 1958, 21 (9), 218-229.

Toledo, Ohio)., Improved techniques for studying the design and operation of glass melting furnaces by means of models., Technical papers of VI Int. Cong. on Glass., July 8-14 1962, Washington D.C.

18. KONIG, W., Glasstromungen in der ziehwannenanlage, Glastechn. Ber., 5, (1927/28), H.6, , 5, 252-274.

19. JEBSEN-MARWEDEL, H., Ober stromurgen des glases in der wannenschmelze., Glastechn. Ber., 5, (1927/28), H.5, S. 202-212.

20. MOULT, A., Two and three dimensional mathematical models of glass tank furnaces., Glass Technology, Vol.23, No.2, Apr. 1982.

21. MASE, H. and ODA, K., Mathematical model of glass tank furnace with batch melting process., Int. Cong. in Glass., July 1982.

22. BUCKINGHAM, E., (1937), J. Amer. Ceram. Soc., 20, 1-10.

23. JOHNSTONE, R.E. and THRING, M.W., Pilot plants, models and scale-up methods in chemical engineering., McGraw-Hill, 1957.

24. GEFFEKEN, W., Processes of homogenization in melting drawing out of cords, and diffusion., Glastech. Ber., 1957, 30, 4 143-5, (BGIRA translation Tr/57/28).

25. JACK, H.R.S. and JACQUEST, J.A.T., Heat transfer in glass-batch materials source is not known., Private communication Mr. P. Doyle, B.G.I.R.A.

26. UNILEVER RESEARCH - Utilisation of energy in Crosfields glass making furnaces., J.K. Potter.

27. Soluble Silicates, Part I, Mathematical model for the flow of reactants in Crosfields No.3 furnace producing neutral sodium silicate : J.K. Potter; Unilever Research Internal report.

28. Improved furnace efficiency and glass quality by temperature structuring., D.H. Davies, B.G.I.R.A., June 1984.

29. Patent Application No. 763140 Republic of South Africa, Preparing alkali, metal silicate glass.

30. Investigation of the melting of pelletised glass batch., P. Costa, B.G.I.R.A., translation No. 1039.

31. Immersion pyrometry of the glass metal in the working canal., V.A. Gorokhouskii, B.G.I.R.A., translation No. 343.

32. Observations on operating tanks, F. Ellies, B.G.I.R.A., translation No. 1019.

33. Fuel economy in the melting end of glass tank furnaces - possibilities of improvement., W. Trier, B.G.I.R.A., translation No. 984.

34. Review of furnace design methods., D.A. Lihou, Trans. I. Chem. E.,

34. Review of furnace design methods., D.A. Lihou, Trans. I. Chem. E., Vol.55, 1977.

35. Chemical kinetics and reactor desiign., A.R. Cooper and G.V. Jeffreys.